Tools for Managing Intermittent Water Supplies

by

David Donald James Taylor

Submitted to the Department of Mechanical Engineering
in partial fulfillment of the requirements for the degree of

Doctor of Philosophy

at the

MASSACHUSETTS INSTITUTE OF TECHNOLOGY

June 2018

Author ....
Department of Mechanical Engineering
May 11, 2018

Certified by..
Alexander H. Slocum
Walter M. May and A. Hazel May Professor of Mechanical Engineering
Thesis Supervisor

Accepted by ....
Rohan Abeyaratne
Chairman, Department Committee on Graduate Theses

Tools for Managing Intermittent Water Supplies

by

David Donald James Taylor

Submitted to the Department of Mechanical Engineering
on May 11, 2018, in partial fulfillment of the
requirements for the degree of
Doctor of Philosophy

Abstract

Nearly one billion people receive water from piped networks that are not always pressurized. These intermittent water supplies (IWS) are more likely to recontaminate the distributed water than continuously-operated (or '24x7') water supplies. In addition, IWS may not provide customers with enough water. Improving the safety and sufficiency of IWS requires new management tools. This thesis proposes some such tools.

Specifically, this thesis develops a suite of hydraulic, financial, and water quality models that show how each is affected by a utility's operational decisions. The proposed models are simple and do not require information about a pipe network's topology. To contextualize this work, an overview of Delhi, India's IWS is provided.

The hydraulic model relates the supply pressure, supply duration, leakage rate, and volume of water received by customers. It shows that an IWS' behavior changes substantially when its customers receive the water they demand (i.e., are satisfied) and suggests why IWS exist and persist. The financial model additionally considers a utility's variable revenues and costs. It finds that low-pressure and intermittent operations maximize a utility's (short-term) gross margin and that current performance indicators encourage inequity. Where utilities are financially-motivated (e.g., performance-based contracts) the need for careful regulation and better benchmarks is demonstrated. Optimal performance penalties are proposed to ensure leak repair and high-pressure continuous water supply. The water quality model considers the conditions in which external contaminants can enter a pipe network. It shows that IWS have opposite effects on water quality during steady-state and non-steady-state operations. Both states should be regulated, modeled, and sampled.

These models show that knowing the point at which customers become satisfied is crucial to managing and optimizing IWS. To better measure this point, a more accurate multi-jet water meter, which does not measure air, is designed and tested for use in IWS.

The tools presented in this thesis support measuring and making progress towards global efforts such as the Sustainable Development Goals and the human right to water, promoting "safe" water supplies that are "available when needed."

Doctoral Committee

Alexander H. Slocum, Ph.D.
Thesis Supervisor and Committee Chair
Walter M. May and A. Hazel May Professor of Mechanical Engineering
Massachusetts Institute of Technology

Andrew J. Whittle, Sc.D.
Professor of Civil Engineering
Massachusetts Institute of Technology

Amos G. Winter, V, Ph.D.
Assistant Professor of Mechanical Engineering
Massachusetts Institute of Technology

Kara L. Nelson, Ph.D.
Professor of Civil and Environmental Engineering
University of California, Berkeley

James L. Wescoat, Ph.D.
Professor of Landscape Architecture
Massachusetts Institute of Technology

Acknowledgments

I must begin by acknowledging my deep gratitude to my family. I am indebted to parents who push me to do things I love and share their earned wisdom gently. I love my siblings who keep me humble and whose friendships I treasure.

I am also grateful for the Stroup family, Chris, Amy, Micah, Livia, and Calvin, who became my family in Boston. Thank you for bringing me into your family, for feeding me, for playing Ninja with me, and for consistently demonstrating the joy and meaning of life outside of the lab.

I want to express my special gratitude to Prof. Alex Slocum who has been my advisor for six years. I am so grateful for your consistent support of me as an individual and researcher. Your design advice, unquenchable enthusiasm, creativity, and patience have been essential to the shaping of this thesis. From thanksgiving at your farm to dinner in Delhi, your friendship and advising have encouraged and inspired me as a problem solver and researcher. Thank you.

Prof. Andrew Whittle, you have been my unofficial co-advisor over the past three years. Thank you for your patient perspectives, considered advice, and affirming support. Your feedback and role modeling have shaped how I hope to pursue research (and structure sentences).

I have treasured the diverse perspectives of my committee members. Prof. Amos Winter, thank you for your encouragement and support – from 2.007 to pushing me to step back and ask the hard questions. Prof. Kara Nelson, you brought substantive domain expertise and kind support. Your encouragement to pursue my modeling ideas has shaped the focus of my research and the contents of this thesis. And last, but not least, I am grateful for the quiet and meaningful support of Prof. Jim Wescoat. Your wide-ranging perspectives have encouraged my explorations into the broader context of this work, which I have really enjoyed.

To my lab mates past and present, your friendship, comradery, and thought partnership were crucial to the shape of this work. Kevin Simon, I am especially grateful for our friendship, banter, and the ways we were able to push each other towards better research. To Dr. Tyler Wortan, Anthony Wong, Dr. Nevan Hanumara, Hilary Johnson, Megan O'Brien, Dr. Douglas Jonart, Dr. Maha Haji, Jacob Bayless, Julia Canning, Andrew Duenner, Justin Carrus, Will Sawyer, and to all my lab-mates; thank you. Outside of our lab, I am also grateful for the friendship and support of Natasha Wright, Mark Jeunnette, Albert Wang, and many others. Thank you also to Xin Zhang, for all your hard work on the transient models. And finally, thank you to my many, many friends who helped edit and strengthen this document.

Irina Gaziyeva and Deborah Alibrandi, thank you for working so hard to keep our lab running smoothly. To Leslie Regan, I am grateful for your consistently-kind and patient advice amidst the inevitable hiccups of graduate school. Thanks also to Joan Kravit, Una Sheehan, and the many people who keep the Department of Mechanical Engineering running smoothly.

This work would not have been possible without fantastic counterparts. At the Delhi Jal Board, I am especially grateful to Mr. Vijar Kumar Babbar who was my initial contact and encouraged me to keep exploring and experimenting. I also want to thank Manish Kumar, formerly of Tata Consulting Engineers; thank you for teaching me what an intermittent water supply was. To my many friends and colleagues in the private sector: thank you so very much for your time and kindness, AJM, JK, AB, PM, AM, and JML. Thank you also to the team at Honeywell (Elster) in Brazil and especially Gabriel Cardoso.

To Prof. Emily Kumpel, you are a fantastic, albeit unofficial, mentor to me. Thank you for your patient investment and thoughtful career advice, and for blazing a trail for others like me to follow into studying intermittent water supplies.

Susan Murcott, thank you for all of your enthusiastic support. Thank you also to Aaron Bivins, who endures my rookie questions about microbiology and has helped me in the field.

To my former colleagues at HydraTek & Associates, especially Prof. Bryan Karney, Fabian Papa, and Djordje Radulj, our work together set me on this trajectory to a degree that none of us expected. This work is substantially shaped by the knowledge and confidence you imparted to me. Your support and encouragement has continued since we worked together and I am grateful for it.

I am grateful also to Prof. Gutowski, who allowed me to defer my admission to MIT so that I could work for Engineers Without Borders Canada (EWB). The perspective I gained with EWB shapes how I approach international work and this work would not have been what it is without that opportunity.

Finally, thank you so much to MIT Sailing pavilion, its great staff, and especially Stewart Craig for letting me windsurf in the craziest of winds. It has kept me healthy and happy and I will miss it.

This work was generously funded by the MIT Tata Center for Technology and design. At the Tata Center, I am especially grateful for the consistent and bantering support of Dr. Rob Stoner. I have also been supported in part by the Natural Sciences and Engineering Research Council of Canada (NSERC).

Chapter 6 and its figures are a partial reprint of an article published in PLOS ONE (Taylor et al., 2018b). Several of its figures were illustrated by Victoria Call; thank you Vik.

Contents

List of Figures

List of Tables

Nomenclature

Symbols are consistently defined throughout this thesis (except in Chapter 7) and are defined as follows:

Symbol	**Units**	**Description**
A	m^2	Cross-sectional area of a leaking orifice, or equivalent orifice area (EOA) of several orifices
a	$-$	A for a leaking network, normalized by its ideal network's EOA
a_C	$-$	Normalized EOA of the ideal network, $a_C \equiv 1$
a_{crit}	$-$	Normalized EOA above which a system cannot be satisfied
a_X	$-$	EOA at a given point X, normalized by its ideal network's EOA
C	$\$/m^3$	Variable costs of treating and delivering water to customers
C_d	$(ms^{-1})^{2\alpha-1}$	The orifice coefficient accounts for the shape of the orifice; when modeling intrusion, units adjust to β instead of α
C_{HW}	$-$	Hazen-Williams minor loss coefficient for a pipe
Cost	$	Total variable costs of a utility
c	$-$	Total variable costs, normalized by CV_T
D	m	Pipe diameter
E	m	Elevation of a customer's connection
$\Delta E_{\max}$	m	Maximum elevation of a customer's connection above the system's average E
F	$	Operators fixed fee for executing a contract
f	$	Operators fee, normalized by project revenues
f_C	$-$	The probability that an external fluid is in the vicinity of a leakage pathway
GM	$-$	Gross margin percent of a utility
g	m/s^2	Gravitational acceleration constant
H	m	Average internal water pressure head
H_C	m	Average pressure head of external contaminants
H_{equity}	m	Minimum pressure head required to provide equitable volumes of water to customers
$H_{\min}$	m	Minimum pressure head required to satisfy customer demand
H_{target}	m	Targeted pressure head
h	$-$	Pressure head, normalized by H_{target}

h_a	$-$	Normalized pressure head at point A
h_{optimal}	$-$	Gross-margin-maximizing pressure head, normalized by H_{target}
h_{p}	$-$	Normalized pressure head at which $v_P = 1$ while $t = 1$
K_C	$m^{1-\beta}/s$	Aggregated intrusion constant
K_D	m^3/d	Pipe and topography constant
K_L	$m^{1-\alpha}/d$	Aggregated leakage constant
K_R	\$	Cost required to find and fix 50% of a system's leaks
k_D	$-$	Normalized pipe and topography constant; K_D/V_T
k_m	$-$	Minor loss coefficient
k_R	$-$	Normalized cost required to find and fix 50% of a system's leaks
l	$-$	The allowable increase of leakage in a system (0=none)
m	$-$	Price margin, $m = (R - C)/R$
n	$-$	Non-revenue water (NRW)
n_A	$-$	NRW defined at operating point A
n_B	$-$	NRW defined at operating point B
n_C	$-$	NRW defined at operating point C, the ideal case
n_S	$-$	NRW defined at operating point S
n_X	$-$	NRW defined at operating point X
N	people	Number of customers aggregated at a simulation node
P	Pa	Pressure in a pipe
p	$-$	Percent of NRW that is physical leakage, i.e. $v_L = np$
p_A	$-$	Percent of NRW that is physical leakage at point A
p_B	$-$	Percent of NRW that is physical leakage at point B
p_X	$-$	Percent of NRW that is physical leakage at point X
Q_C	m^3/d	Instantaneous intrusion rate of fluids into the network during the supply stage
Q_{CF}	m^3/d	Instantaneous intrusion rate of fluids into the network during the non-supply stage
Q_D	m^3/d	Instantaneous flow rate demanded by customers (in a CWS)
Q_L	m^3/d	Instantaneous flow rate of leaks during a system's supply stage
Q_R	m^3/d	Instantaneous flow rate received by customers during the supply stage
R	$\$/m^3$	Price of water sold by the utility to customers
R_a	$\$/m^3$	Equivalent price of water, accounting for water delivered to all customers
Rev	\$	Revenue of a utility
r	$-$	Revenue, normalized by RV_T
T	d	Period of supply, 1/(supply frequency) of an IWS
t	$-$	Duty cycle (not time!); fraction of time a system is pressurized
t_A	$-$	Duty cycle at operating point A
t_B	$-$	Duty cycle at operating point B
t_C	$-$	Duty cycle at operating point C
t_{optimal}	$-$	Gross-margin-maximizing duty cycle
t_S	$-$	Minimum duty cycle required to satisfy customer demand
u	$-$	Percent of V_D that is unpaid for

u_X	$-$	Percent of V_D that is unpaid for at an operating point X
V_C	m^3/d	Daily volume of intruded fluid in the steady-state phase
V_{CF}	m^3/d	Daily volume of intruded fluid in the flushing phase
V_D	m^3/d	Daily volume of water demanded by customers
V_L	m^3/d	Daily volume of leaked water
V_{LC}	m^3/d	Daily volume of leaked water in the ideal network
V_P	m^3/d	Daily volume of water input (e.g., pumped) into a system
V_R	m^3/d	Daily volume of water received by customers
V_T	m^3/d	Daily volume of water available to be input into the system
$\boldsymbol{V_S}$	m^3	Volume of customer storage
$\boldsymbol{V_{DV}}$	m^3	Dead volume of a pipe network
v_D	$-$	Normalized daily volume of water demanded by customers; normalized by V_T
v_L	$-$	Normalized daily volume of leaked water
v_{LA}	$-$	Normalized daily volume of leaked water at operating point A
v_{LB}	$-$	Normalized daily volume of leaked water at operating point B
v_{LC}	$-$	Normalized daily volume of leaked water in the ideal network
v_P	$-$	Normalized daily volume of water input into a system
v_R	$-$	Normalized daily volume of water received by customers
$\overline{v_R}$	$-$	Average normalized daily volume of water received by customers
$v_{R,\min}$	$-$	Minimum allowable normalized daily volume of water received by customers
v_T	$-$	Normalized daily volume of input water available; $v_T \equiv 1$
w	$-$	Penalty weight, normalized by project revenues
w_F	$-$	Fixed penalty weight, applied whenever the target is missed
w_h	$-$	Penalty weight for low pressure supply
w_t	$-$	Penalty weight for intermittent supply
α	$-$	Pressure coefficient governing flow to leaks
β	$-$	Pressure coefficient governing intrusion into the network
γ_S	$-$	Difficulty of satisfying customer demand; minimum th^ϕ required to satisfy customers
$\Theta()$	$m \to m/d$	Function relating the probability distribution of internal (pipe) pressures and the average external pressure to the intrusion rate
Λ_i	$-$	Fraction of a utility's total supply volume required to satisfy subnetwork i
λ_i	$-$	Fraction of a utility's total supply volume delivered to subnetwork i
ρ	kg/m^3	A fluid's density
τ	d	Duration of an intermittent system's supply stage
Υ	$\$/m^3$	Gross margin dollars per unit of water input into the (sub)network
Υ_C	$\$/m^3$	Gross margin dollars per unit of water input into Commoners' Crescent
Υ_V	$\$/m^3$	Gross margin dollars per unit of water input into VIP Village

ϕ	$-$	Pressure coefficient governing flow to customers
Ψ	\$	Gross margin dollars of a utility

Chapter 1

Introduction

> The public interest, and more especially the welfare of the poorer classes, absolutely requires that the mode of intermittent supply should be abandoned, and that the system of constant supply at high pressure should be generally introduced.
>
> — Health of Towns Association (1846, Sec. 77)

From 2000 to 2015, 1.2 billion people gained access to piped water, out-pacing population growth and increasing access from 57% to 64% of the global population (WHO, 2017a). Unfortunately, these piped-water systems are not always filled with water (Bivins et al., 2017; Laspidou and Spyropoulou, 2017) and when filled, their water is not always safe to drink (Onda et al., 2012; Taylor et al., 2018a; Shaheed et al., 2014; WHO, 2017a). Nearly one billion people receive water from piped networks that are not always pressurized (Bivins et al., 2017; Laspidou and Spyropoulou, 2017); such networks are referred to as intermittent water supplies (IWS) and can be contrasted with Continuous Water Supplies (CWS; 24x7 systems), which are standard in most higher-income countries. Since their introduction in the nineteenth century, the health benefits of CWS have been well recognized (Health of Towns Association, 1846). Studies continue to demonstrate that IWS deliver water less equitably and are more likely to recontaminate the treated water than CWS (Solgi et al., 2015; Kumpel and

Nelson, 2013). Yet 41% of piped water systems in lower- and middle-income countries operate intermittently (Laspidou and Spyropoulou, 2017). Currently available data show that 97% of utilities in South Asia operate intermittently (Van den Berg and Danilenko, 2011). In India alone, it is estimated that at least 200 million people connect to IWS (Kumpel and Nelson, 2016). Globally, IWS are responsible for an estimated 17 million infections, 4 million cases of diarrhea, and 1560 deaths annually (Bivins et al., 2017).

Following and building on the Millennium Development Goals, the United Nations' (UN's) Sustainable Development Goals set forth 17 goals and 169 targets for global development by 2030. Target 6.1 (SDG 6.1) is to "achieve universal and equitable access to safe and affordable drinking water for all" (WHO, 2017b, p.6). To monitor this target, different classifications of water supplies are used. The highest classification requires that water supplies be "available when needed" (WHO, 2017b, p.33). Supply availability is preferentially measured using surveys in which households self-determine if their water is 'available when needed.' While subjective, household surveys have the advantage of being able to assess the equity of supply. In the absence of such surveys, supply availability is measured using utility-level data, where "a minimum of 12 hours per day" of supply is taken as the "global benchmark" for 'available when needed' (WHO, 2017b, p.33). The UN's articulation of the human right to water specifies that water supply "needs to be continuous enough to allow for the collection of sufficient amounts to satisfy all needs, without compromising the quality of water" (de Albuquerque, 2010, para.19).

So while the UN rallies the international community to ensure that everyone has access to safe drinking water that is available 'enough' and 'when needed' by 2030, in 2015, an estimated one billion people accessed water from sources that were run intermittently. Therefore, in addition to advocating for CWS, determining management strategies that maximize IWS' water availability, equity, and quality will prove key to meeting the human right to water and SDG 6.1. Accordingly, this thesis aims to contribute new models and an improved water meter to better manage intermittent water supplies.

The new models developed in this thesis will help to understand why IWS exist, persist, and how they can be optimally managed. These models will highlight that understanding when customers get enough water is critical to managing IWS. To more accurately measure the water delivered to customers in IWS, a higher-accuracy water meter is also developed in this thesis.

1.1 A taxonomy of intermittent water supplies

The operations of IWS (an acronym used in this thesis for both the singular and plural) can be sub-divided into a *supply stage*, when water is being delivered to customers; and a *non-supply stage*, when water is left to stagnate and possibly drain out of the pipes through leakage. During the non-supply stage, the lack of water pressure allows for contaminant transport (i.e., *intrusion*) into the pipe network through cracks or holes in the pipes (Kumpel and Nelson, 2014; Vairavamoorthy et al., 2007c). The supply stage can be further divided into an initial *flushing phase* and a *steady-state phase*. Flushing occurs when the water supply is connected, leading to rapid filling of the distribution network and pressurization of pipes. Fluid velocities can be high, potentially causing detachment of biofilms and transport of other accumulated contaminants (Kumpel and Nelson, 2016). Towards the end of the flushing phase, turbidity and contamination decrease over time and eventually reach a steady-state level (Kumpel and Nelson, 2016).

Intermittent water supplies vary in the duration of their supply stage, denoted *supply duration*, (i.e., how long a single supply stage lasts, τ) and the period of their supply, denoted *supply period* (i.e., the elapsed time between the start of two consecutive supply stages, T, equivalent to 1/frequency). To discuss their behavior in more general terms, it is convenient to define an IWS' *duty cycle*, t, as the average percent of time that the IWS supplies water (i.e., $t = \tau/T$).

IWS are diverse. Galaitsi et al. (2016) classify three types of IWS: *predictable*, where customers receive a predictable volume of water according to a known schedule; *irregular*, where the received volume is predictable, but the schedule is unknown; and *unreliable*, where the received volume and schedule are both uncertain. Erickson et al. (2017) classify three methods of controlling IWS: *gravity-fed*, where an intermittent (sub-)network's supply stage ends when the service reservoir that supplies it is closed or empties; *pump-fed*, where an intermittent (sub-)network's supply stage ends when the pump that supplies it is turned off (intentionally or because of absent power) or when the pump's source water is exhausted; finally, *valve-operated*, where different intermittent sub-networks are provided water on a rotational basis by operating valves throughout the distribution network.

Totsuka et al. (2004, p.507) distinguish between three causes of IWS. IWS in which CWS could be achieved through leak repair and/or different network-operating strategies are caused by *technical scarcity*. Where a network could be a CWS if its water treatment capacity or distributional capacity (e.g., pipe diameters) were augmented, it is caused by "*economic scarcity*" (Totsuka et al., 2004, p.507, emphasis added). Finally, where customer demand exceeds the available source (untreated) water, IWS is caused by "*absolute scarcity*" (Totsuka et al., 2004, p.507, emphasis added).

Intermittent networks and sub-networks vary in pressure and duty cycle. For example, of 18 surveyed utilities in India, some had supply stages lasting 20 minutes per day while others lasted 12 hours per day (i.e., $t = \tau/T \in [0.0139, 0.5]$; Asian Development Bank and Ministry of Urban Development Government of India (2007)). These utilities had similarly diverse average pressures at customer connections, ranging from 1-15 meters of pressure head (Fig 1-1; data from Asian Development Bank and Ministry of Urban Development Government of India (2007)).

For readers unfamiliar with pressure head, H, it is defined as $H = P/\rho g$, where P is the pressure, ρ is the density of water, and g is gravitational acceleration (Larock et al., 2000, p.8). In this thesis, pressure always refers to pressure head and is measured in units of meters of water column. In addition, the pressure (head) is always specified in gauge pressure (i.e., 0m is atmospheric pressure).

The pressure, water quality, (un)reliability, and duty cycle, as experienced by each customer, vary substantially, even within an intermittent sub-network (De Marchis

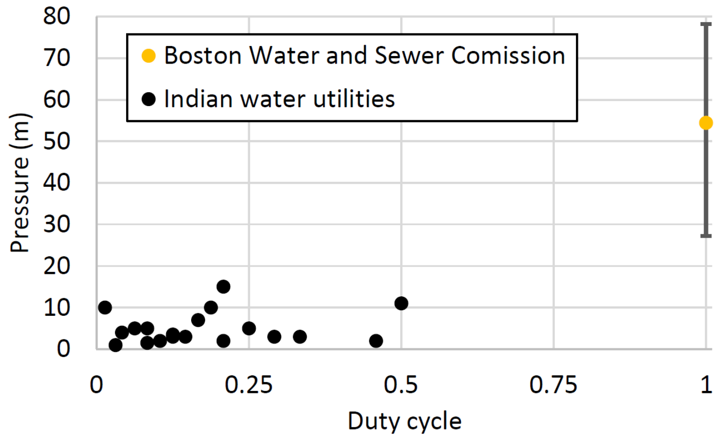

Figure 1-1: **Average pressure and duty cycle in India and Boston.** Indian utility (black dots) performance data were self-reported to Asian Development Bank and Ministry of Urban Development Government of India (2007). Data on Boston's average pressure (yellow dot) and the 99th percentile of its pressure (error bars) were from BWSC and CDM (2011).

et al., 2010; Guragai et al., 2017; Kumpel and Nelson, 2013; Erickson et al., 2017; Vairavamoorthy and Elango, 2002). In IWS with short duty cycles, high flow velocities induce high pressure losses. These pressure losses cause large pressure differences across the network that cause substantial variation in the volume and quality of water that customers can access. As a first step towards equity-focused models, this thesis considers the average performance of an intermittently-supplied network or sub-network.

1.2 Document structure

Instead of a background chapter, Kumpel and Nelson (2016) have presented a comprehensive summary of the current understanding of IWS. When needed, additional background information is provided at the beginning of the chapters that follow.

Perspectives on IWS are shaped by people's exposure to different types of IWS. The author's field work, some of which is included in this thesis, has primarily been based in Delhi, India. To frame this context, Chapter 2 provides an overview of Delhi's water supply system and situates it amidst public water distribution systems in India that are changing and sometimes privatizing.

Recent advances in the numerical modeling of specific IWS rely on network-specific information, which can be hard to acquire (McIntosh, 2014). As a compliment to such models, this thesis derives and validates a parsimonious model of an IWS in Chapter 3. Since "all models are wrong but some are useful" (Box, 1979, p.2), the model's utility is demonstrated by extending and applying it to consider three broad questions:

1. What are the main causes and effects of IWS, and how do these depend on a system's characteristics? (Chapter 4)

2. How would a utility manage an IWS if it were motivated only by short-term financial returns; and what types of penalties would ensure that such a utility would provide high-pressure, continuous water supply? (Chapter 5)

3. How does the operation of an IWS affect its water quality? (Chapter 6)

Examining the causes and effects of IWS in Chapter 4 will suggest that knowing a system's leakage level and the extent to which its customers receive all the water they desire is essential to predicting how the system will behave. Residential water meters are typically an important tool for measuring both of these parameters (McIntosh, 2014). However, meter accuracy is thwarted by IWS. When IWS refill (at the start of each supply stage), the displaced air often exits through customer meters causing them to register the air as if it were water (Walter et al., 2017; McIntosh, 2014). This not only creates a billing error, but also enrages currently-metered customers and makes unmetered customers more resistant to the installation of water meters (e.g., Delhi BJP (2016)). To help address both of these challenges, Chapter 7 presents the design and testing of a mechanical water meter that measures only water (and not air).

Finally, in Chapter 8, this thesis concludes by acknowledging the limitations of this work and highlighting the exciting opportunities for future work.

1.3 Approach: apologetically technocratic

IWS are technopolitical systems, governed as much by politics as physics (Anand, 2012). Understanding how both the political and physical components of these systems work will be essential to improving them. This thesis aims to contribute models and a better water meter that will help understand and manage the physical side of these systems. This thesis is complemented by social and political studies of intermittent water supply (e.g., Anand (2012); Björkman (2015); Sangameswaran (2014)).

Walters (2013, p.45) importantly warns that technocratic approaches to development issues, like this thesis, exclude "the poor and marginalized peoples who are less likely, due to the structural dimensions of poverty, to become the trained experts of technocratic development." In addition, Anand (2011, p.545) argues that consumers in IWS "critically compromise the authority of city engineers and other technocrats to control the system." This thesis, therefore, may contribute to re-empowering technocratic engineers who wish to exert centralized control over their water systems and further exclude the poor from formally and informally influencing their piped water supply. While not an intentional decision in the framing of this thesis, it is an acknowledged reality and stems in part from extensive collaboration with such engineers and in part from the author's technocratic background.

While Morgan (2002, p.8) argues that "knowledge and technique almost never catalyzed a dysfunctional system to reconfigure itself and move towards effectiveness," Toyama (2015, p.29) would more carefully qualify that only where human forces are aligned to reconfigure a dysfunctional system can knowledge and technique "amplify [those] human forces." With the increasing international attention to issues of water quality and water availability, social and political forces may be aligning to improve dysfunctional water systems, thereby creating an impactful opportunity for technocratic contributions to amplify these forces. This thesis aims to be one such contribution.

Chapter 2

Context: Delhi and privatization

> Case studies offer . . . more nuanced descriptions of the diverse actors and processes that are involved in any process of neoliberalisation of water.
>
> Sangameswaran (2014, p.38)

To contextualize the author's work and perspective on IWS, this section provides a brief overview of Delhi and its water supply. As Delhi is controversially experimenting with privatizing components of its water supply, this chapter also contextualizes these experiments.

2.1 Water supply in Delhi

The National Capital Territory (NCT) of Delhi, or more commonly Delhi, became India's capital city in 1911. Its administrative status is complex; it functions more like a state government than a city government, not unlike Washington, D.C.. Its metropolitan area is made up of five municipal corporations: North Delhi Municipal Corporation, South Delhi Municipal Corporation, East Delhi Municipal Corporation, New Delhi Municipal Corporation, and the Delhi Cantonment Board.

Delhi's water utility, the Delhi Jal Board (DJB), was established in 1998. It provides water and sewerage in North, South, and East Municipal Corporation areas and provides bulk water supply to the other two areas. The DJB is mandated to operate on a full cost recovery basis (Legislative Assembly of the National Capital Territory of Delhi, 1998). DBJ reports segment the city into the nine districts shown in Fig 2-1.

The DJB's water supply comes primarily (91%) from surface waters, and more than a third (41%) of its supply comes from the Yamuna River (Fig 2-2; data from Government of NCT of Delhi (2017)). The DJB network has 14000 km of pipes, some of which are 40-50 years old (Government of NCT of Delhi, 2017). It serves treated piped water to 75.2% of Delhi's 18 million inhabitants (Government of NCT of Delhi, 2017). The DJB also pipes untreated water (from tube wells) to 6.1% of Delhi's inhabitants (Government of NCT of Delhi, 2017).

2.1.1 Water supply timing

The DJB operates most of its system intermittently. Schedules of when different areas will be supplied were last updated in 2014 and are reported for 845 different zones across Delhi (DJB, 2014) (ignoring tube well schedules, inter-zonal pumping, and Dwarka's supply). The majority (75.9%) of Delhi has supply scheduled at least once per day (treating all water supply zones equally; 'Daily' in Fig 2-3e).

Supply schedules concentrate around 6:30am and 6:30pm. Almost half (45%) of all zones are supplied at 6:30am and a third (33%) at 6:30pm (Fig 2-3d). The median percent of time that each zone is scheduled for supply (i.e., duty cycle) was 8.3% (two hours per day; Fig 2-3b). In the extremes, 1% of zones (9 of 845) are scheduled to receive CWS and 2% (17 of 845) are scheduled to receive 20 minutes of supply every third day (Fig 2-3b). 9.5% of the DJB's supply zones have no set supply schedule (Fig 2-3c). Fig 2-3a visualizes the diversity and glut of supply schedules in Delhi. The distribution of supply times also varies by administrative areas of Delhi (Figs 2-4 and A-1).

Due to data limitations, supply zones were not weighted by either population or the volume they distribute. This lack of weighting may inflate the influence of areas with water shortages, as their supply schedules are typically subdivided into

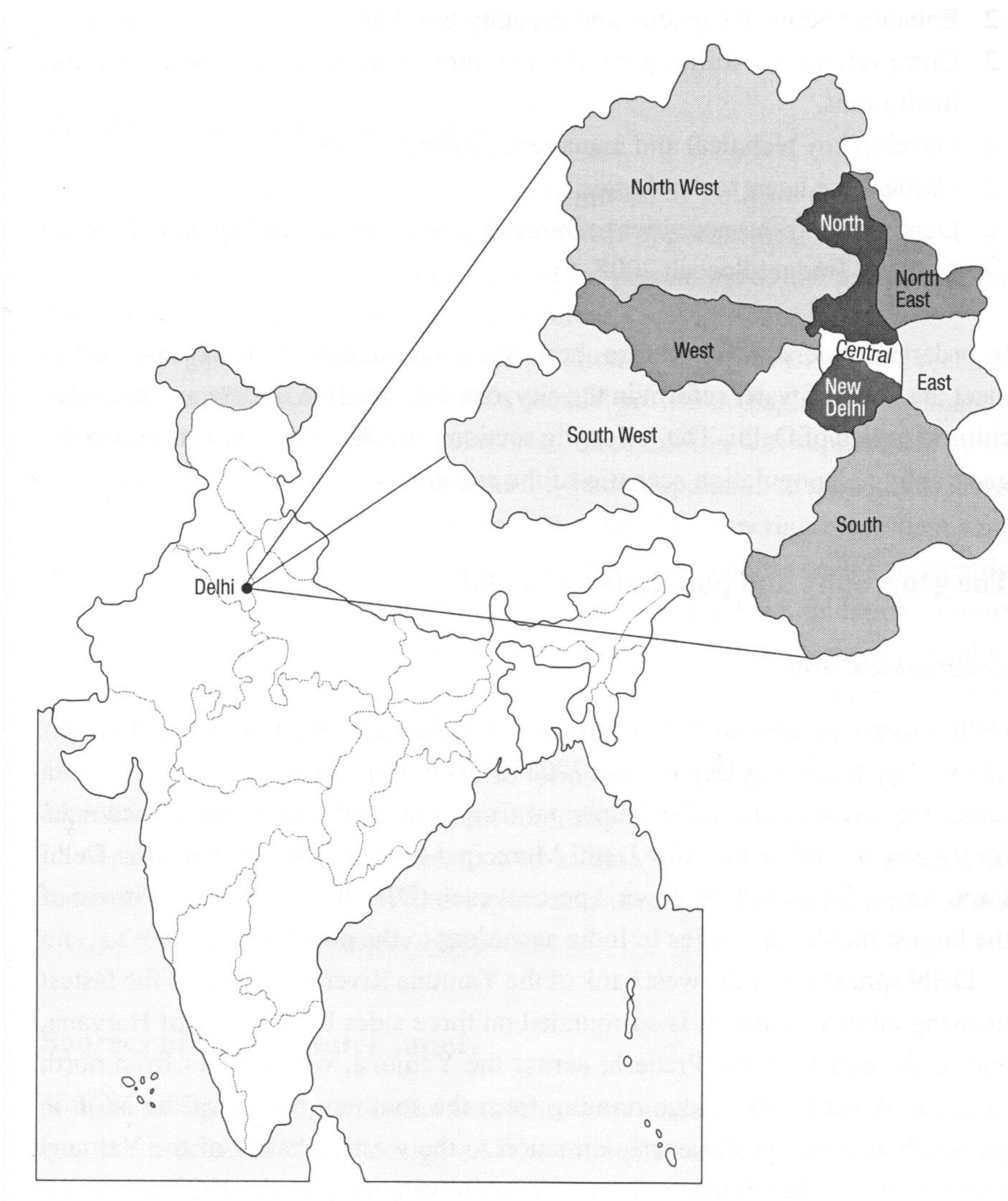

Figure 2-1: **Delhi's districts** before 2012. From Asthana (2009, p.73).

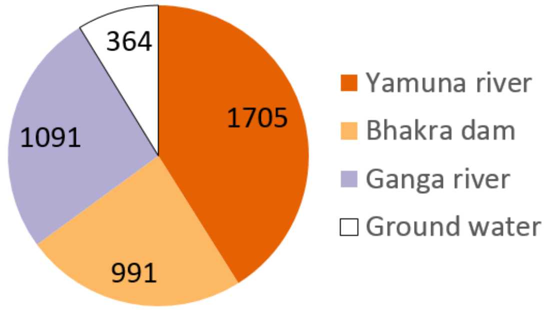

Figure 2-2: **DJB's production capacity by source.** The Yamuna river, Bhakra dam, and Ganga river are the DJB's biggest sources. Production capacities listed in $\times 10^6$L/day. Data from Government of NCT of Delhi (2017)

.

smaller zones. Another limitation of the data is that scheduled supply times differ substantially from actual supply times, especially when source water is constrained. Nevertheless, unweighted supply schedules demonstrate the functioning and complexity of Delhi's system. Fig A-1 segments Fig 2-3 by administrative area and takes the first step towards weighting zones by either population or supply volume.

2.1.2 Water volume

DJB reports quantify water production capacity instead of produced volume because not all of their treatment facilities have metered outputs. In 2017, Delhi's production capacity was 4120 million liters per day (MLD) (Government of NCT of Delhi, 2017). This corresponds to more than 210 liters per capita per day (lpcd) (Fig 2-5a). Delhi's production capacity has kept pace with population growth over the past 100 years and has remained above 190 lpcd since 1980 (Fig 2-5).

The DJB suggests that the required water for domestic consumption in Delhi is 172 lpcd plus an additional 102 lpcd for commercial and other uses (total 274 lpcd; Government of NCT of Delhi (2017)). If the DJB's estimates are correct, the DJB will need an additional 25% production capacity to meet demand (Fig 2-5). However, different Indian organizations and standards have suggested different per capita water requirements for cities like Delhi, ranging from 150-270 lpcd (Mathur et al., 2007). Amidst the range of recommendations, the standard of 150 lpcd (CPHEEO, 1999)

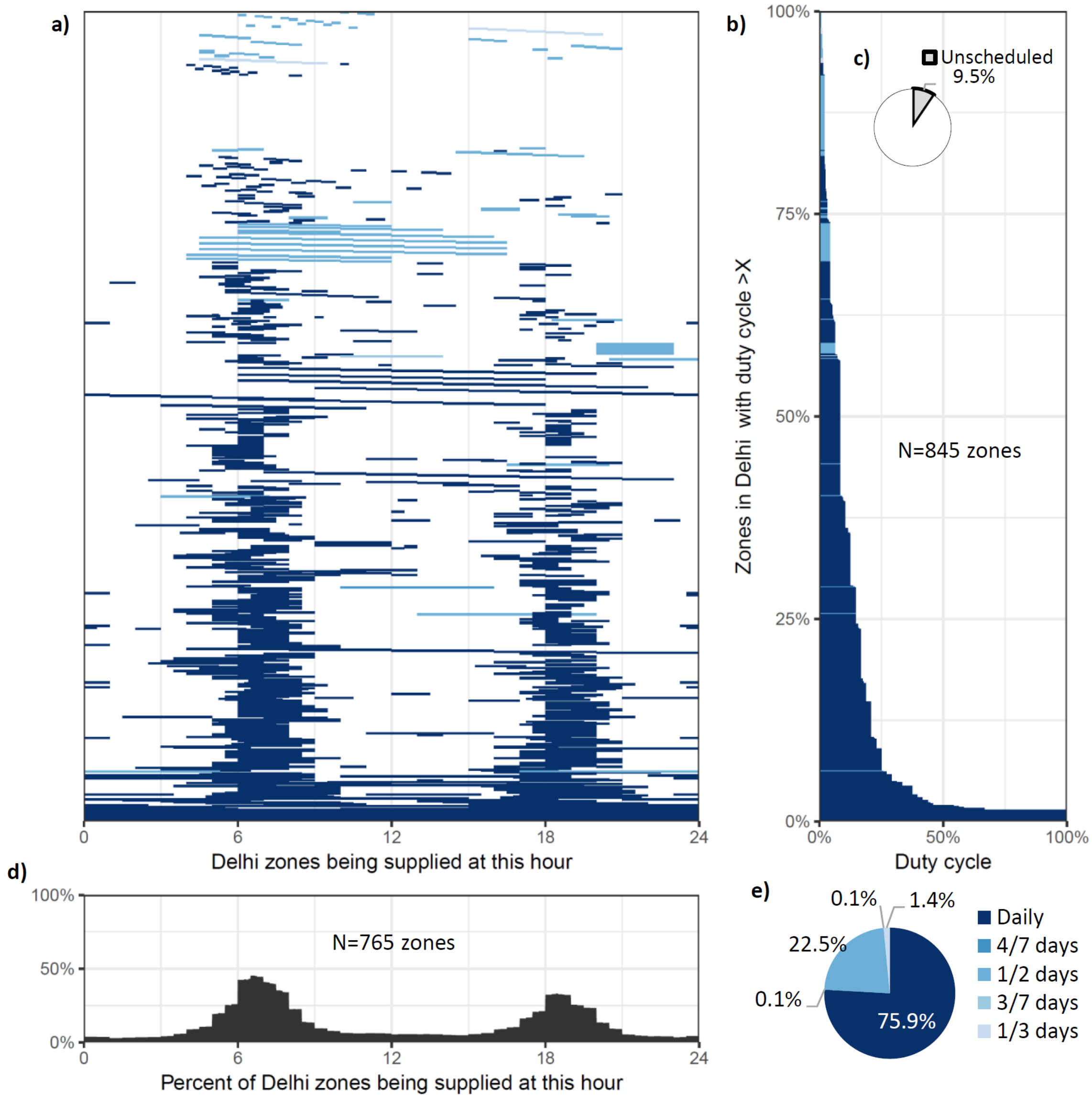

Figure 2-3: **DJB's supply timing.** The DJB describes schedules (or lack there of) for 845 different areas in Delhi. e) shows the fraction of zones scheduled to be supplied daily (darkest blue), 4/7, 1/2, 3/7, and 1/3 days (lightest blue). The prevalence of zones with fixed durations of supply but unscheduled timing is shown in c). Unscheduled zones are omitted from a) and d). From least frequently supplied to most (top to bottom in a & b), the supply schedule is shaded by time of the day in (a). b) aggregates supply schedules into a cumulative frequency plot, displaying the percent of DJB zones that are scheduled to be supplied with a duty cycle $\geq$ the x-axis value. Finally, d) shows the percent of zones that are being supplied throughout an average day. Data were aggregated from DJB (2014) and not weighted by population or supply volume.

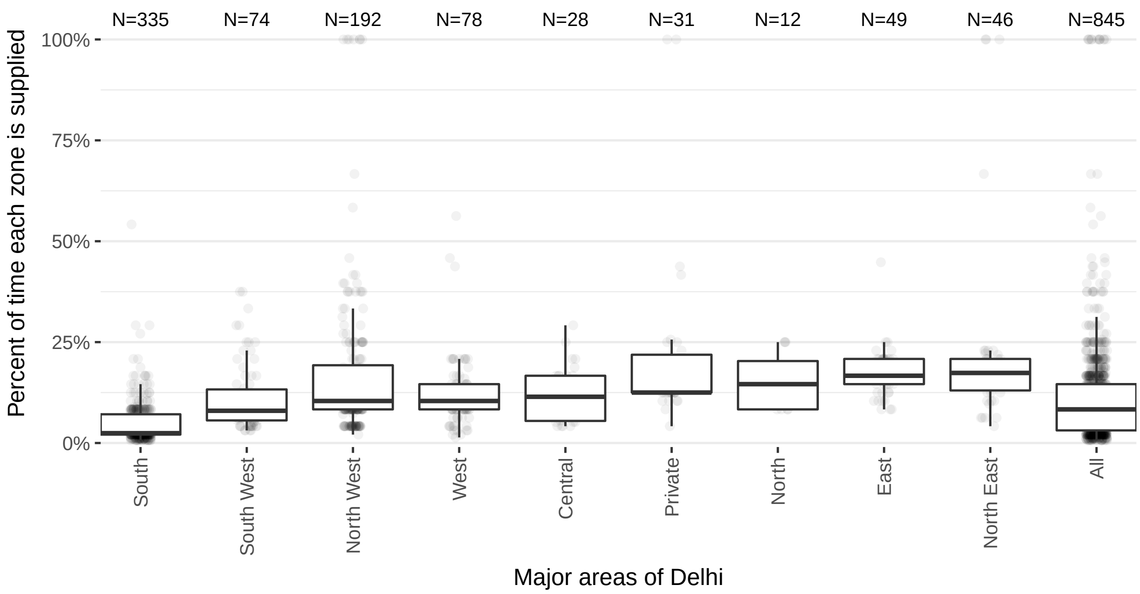

Figure 2-4: **DJB's supply timing by area.** Reducing supply schedules to the percent of time a zone is supplied (duty cycle), box plots summarize the duty cycle distributions by areas of Delhi (boxing the median and quartiles, with whiskers that extend up to 1.5x the interquartile range). Outside of the inter-quartile range, each translucent point represents the duty cycle of one zone. In addition to standard areas of Delhi, 'Private' refers to sections of the DJB network that are operated by private companies. The final category ('All') contains the aggregated data. Raw data are from DJB (2014); displayed data are unweighted.

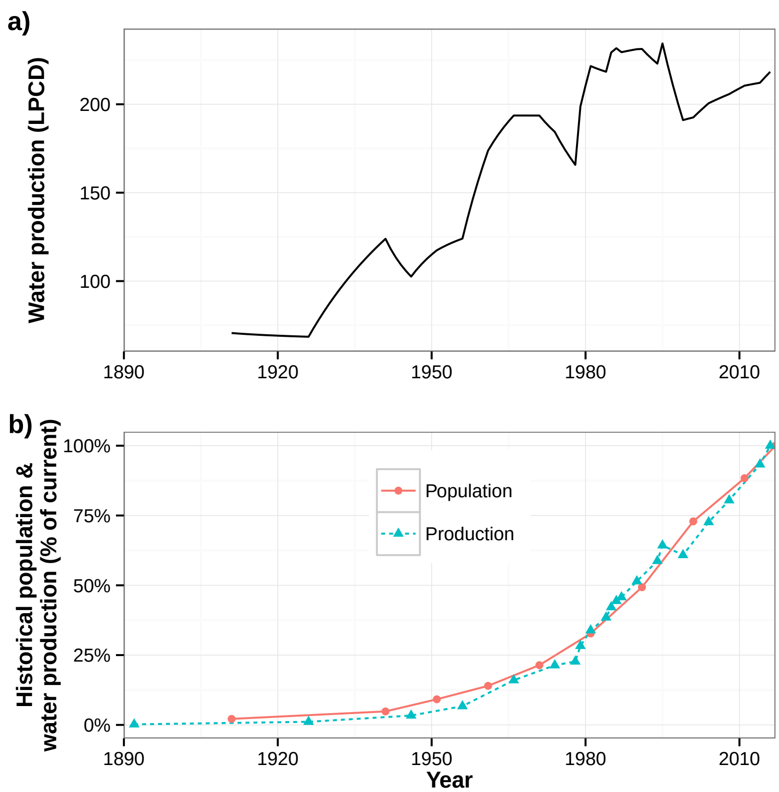

Figure 2-5: **Historical water production in Delhi.** a) interpolated per capita water production and b) population (solid red line and round dots) and water production (dashed blue line and triangle) growth over time as a percentage of current values (19 million people and 4069 MLD). Points represent actual data values, while the lines are linearly interpolated. Data and its sources are included in Tables A.1 and A.2.

seems to guide at least one of Delhi's private partnerships (see Section 4.3).

Distinguishing between customer consumption and leakage is critical to understanding Delhi's actual water demand. The measured consumption of individual connections in Delhi can range from 16-646 lpcd, with one estimate of average consumption being 67 lpcd in unplanned areas and 165 lpcd in planned areas (Dutta and Tiwari, 2005).

2.1.3 Metering and billing

71% of the DJB's 2.32 million customers have functioning water meters. 17% of customers have non-functioning meters; the remaining 11% have no meters (Government of NCT of Delhi, 2015, 2017). While these reports also claim "a majority of houses do not have working meters" (Government of NCT of Delhi, 2017, p. 193), this is likely an artifact from 2009, when only 49% of customers had working meters (Government of NCT of Delhi, 2009).

Customers with water meters who consume less than 20kL per connection per month are not charged any fees. Other customers are charged a volumetric tariff (which increases with consumption) plus a service fee. Where the DJB provides sewerage services, the bill is increased by 60% (Government of NCT of Delhi, 2017). DJB bill collection efficiency is 90%.

2.1.4 Leakage

The DJB estimates their "total distribution losses" (leaks and unauthorized consumption) to be on the "order of" 40% (Government of NCT of Delhi, 2017). Their 2017 report suggests that the pipe replacement rate (260km/year for the past five years) and the introduction of a "leak detection and investigation cell" will reduce their distribution losses to 20% "in the near future" (Government of NCT of Delhi, 2017).

Despite the DJB's optimistic self-report, their reported replacement rate (1.7%/year) will increase their average pipe age (from a reported maximum of 40-50 years to an average of 58 years old). In addition, the DJB has included these same figures and optimistic projections (i.e., length of main repairs, establishment of leak cell, current losses of 40%, and 'near-future' attainment of 20% losses) verbatim in each of their bi-annual reports from 2006 to 2017 (Government of NCT of Delhi, 2006, 2009, 2013, 2015, 2017). Clearly, any efforts to reduce leakage over the past decade have been ineffective or unreported.

2.2 Privatization of water supply

The author's Master's thesis work (Taylor, 2014) was done in partnership with the DJB. However, to fund further work, senior DJB executives suggested working with their private partners. Since then, the author has worked predominantly with one of these private partners.

Water supply privatization in Delhi is controversial and needs to be framed in light of the history of water supply in India and of global and Indian trends towards water's commodification. The articulation of this history below is indebted to the thoughtful work of Walters (2013) and Asthana (2009).

2.2.1 Historical context

Under colonial rule in British India, investment focused on centralized water works that increased state legitimation and facilitated industry, trade, commerce, and/or resource exploitation (Asthana, 2009). This centralized focus continued after Indian independence (1947) with the Nehru-government's vision of a centralized, planned, socialist state (Walters, 2013). Under the constitution of India, states have most of the responsibility for water supply, while trans-boundary river issues fall under national responsibility (Government of India, 1949).

More recently, the International Water Supply and Sanitation Decade (1980-1990) brought global focus and funding to water supply. But in 1990, still one third of the global population did not have access to adequate water and sanitation services (New Delhi Statement, 1990). The United Nation's report on the decade's achievements and lack thereof, recommended efficient and appropriate technology and additional funding sources were needed to achieve universal access to water and sanitation (New Delhi Statement, 1990).

The report's focus on technology and funding aligned with narratives about the value of privatization in other domains, which emphasized the private sector's technical expertise, cost efficiency, and investment capital. Support for privatization, therefore, quickly diffused into water policy discourses (Walters, 2013; UN-HABITAT, 2004).

In 1992, the Dublin Statement on water and sustainable development refered to water as an "economic good" (UN, 1992). By 1994, the World Bank was advocating for market forces to participate in the water sector (The World Bank, 1994). And by 1998, India's national water policy (adopted in 2002), recommended that "private sector participation should be encouraged" (Ministry of Water Resources, 2002, p.6). By 2002, India's then president said of all public sector enterprises, divestment "is no longer a matter of choice, but an imperative. The prolonged fiscal hemorrhage from the majority of these enterprises cannot be sustained any longer" (Kalam, 2002, para. 42).

Amidst this growing policy support for privatization, including in the water sector, the World Bank drew up plans for the privatization of parts of Delhi's water supply in 2001 (Delhi Jal Board, 2004). The first phase would expand Delhi's water treatment capacity and the second phase would use the additional water to supply South Delhi zones II & III so that they could be converted to CWS (Delhi Jal Board, 2004). South Delhi has pockets of Delhi's affluent, but also some of Delhi's shortest supply zones (Fig A-1). The first phase was implemented with a Suez subsidiary, Degremont, which built the Sonia Vihar water treatment facility (Asthana, 2009).

Public resistance to the project was substantial. It catalyzed around slogans such as "Our Mother Ganga is not for sale", and argued that Suez took on none of the risk and yet was guaranteed substantial reward (Asthana, 2009). However, Singh (2008) of the World Bank suggests that the populous resistance was actually engineered by groups who objected to the use of a foreign consultant for the project proposal stage in 2004, and not to privatization in general. No matter the initial motivations behind the resistance, it worked. The second phase of the project was abandoned.

By 2012, several other cities in India had tendered private partnerships in order to upgrade some zones of their networks to CWS (e.g., Mysore, Hubli-Dharwad, and Mumbai (Walters, 2013; Björkman, 2015)). With these added precedents, the DJB successfully launched partnerships with private consortia to upgrade different sections of their network to be CWS. Two projects were awarded in South Delhi: Suez and SPML Infra together formed Malvia Nagar Water Services (MNWS); and SPML Infra, Tahal Group, and Hagihon formed MVV Water (officially not an acronym). In West Delhi, Veolia, and Swach formed Nangloi Water Services (NWS).

2.2.2 Perspectives on privatization

Opinions about privatization in India's water sector continue to be passionate and polarized. Privatization has been traditionally justified for its potential to bring: i) competition-induced efficiency and ii) increased access to capital. However, Sangameswaran (2014) questions the applicability of either argument to water distribution projects. Since water distribution networks are natural monopolies, the competition-induced benefits of privatization (i) may not materialize. In addition, many projects with private participation are still predominantly funded with public funds, calling into question (ii).

Nevertheless, privatization is also advocated for iii) as a means of preventing the government from catering to special interest groups (Gómez-Ibáñez, 2006) and iv) because of the private sector's technical competency (Sangameswaran, 2014). Demonstration projects are often setup to evaluate the private sector's ability to improve water systems that public utilities were unable to improve. However, such projects typically focus on the most 'hydraulically feasible' subsets of a water supply network and require significant capital expenditures. Walters (2013), therefore, argues that the results of such demonstrations should not be contrasted with the status quo of public utilities, but with a yet-to-exist comparable project in which a public utility received the capital support and incentives to try such a demonstration project.

Hall (2004, p.4) argues that private sector involvement in water supply is fundamentally flawed because their bottom line is not public health: "eliminating the risk of dying of cholera is different from reducing the risk of an underperforming investment." However, public utilities can also overemphasize financial returns. To account for this, Sangameswaran (2014, p.223) suggests that how a utility prioritizes cholera prevention vs. financial returns is "an indicator of whether the body in question is functioning like a 'public' body or a 'private' body." By focusing more on how a utility behaves (e.g., prioritizes financial returns or cholera prevention), instead of its legal status (e.g., for-profit), some of the polarized opinions can be harmonized.

Discussions of IWS and CWS in India, nevertheless, remain entwined with privatization debates. For example, Björkman (2015, p.56) called the vision of CWS in Mumbai cast by World Bank consultants a technocratic "utopian fantasy." And Sangameswaran (2014, p.73) argues that "24x7 water supply [CWS] is both the result of as well as itself involves practices favouring commercialisation and privatisation." However, lest important critiques of privatization dismiss the merits of CWS, the following section summarizes 19th century perspectives on CWS. These early conclusions are contrasted with present perspectives and demonstrate that narratives about the merits of CWS are not simply an invention of a privatization-promoting agenda.

2.2.3 Nineteenth-century perspectives on IWS

IWS quality

While theories of miasma (i.e., that smells transmit illness), which were prominent in the 19th century, have been eclipsed by germ theory, early sources wisely argued that IWS deteriorates water quality "to such a degree as to render it wholly unfit for use" (Health of Towns Association, 1846, Sec.58). Dr. Carpenter (1875) identified IWS to be the cause of Typhoid Fever in Croydon, England. His explanation of the public health risks caused by intrusion in IWS holds much the same as today's explanations (e.g., Lee and Schwab (2005)). The degradation mechanisms suggested by early sources included domestic water storage and contaminant intrusion (Bolton, 1884; Secretary of State for India in Council, 1875; Carpenter, 1875).

Bolton (1884, p.8) described domestic water storage as the "domestic abomination" for which the "radical remedy ... would be the universal adoption of the system of 'constant supply.'" Recent studies continue to find that water quality degrades between the point-of-collection and point-of-use and that domestic storage affects the stored water quality (Wright et al., 2004; Kumpel and Nelson, 2013). Bolton (1884) recommended that if water was to be stored, it needed to be subsequently filtered, but he did not speak to this inherently favoring the affluent. Today, in Delhi, the affluent are more likely to filter their water than the poor (Ghosh et al., 2016; Zérah, 2000; Choe et al., 1996).

Coping costs and willingness to pay

Coping costs are the costs borne by customers in order to compensate for the inadequacy of the water supply system (e.g., the cost of buying a water filter). The Health of Towns Association (1846, Sec.59) was a committee investigating if London should adopt CWS. It argued that IWS "puts the consumers to great and constant inconvenience in obtaining water, which is felt peculiarly [sic] by the poorer classes." They also observed that "among the evils of an intermittent supply ... are the loss of time waiting" at public standpipes (Health of Towns Association, 1846, Sec.62). They also noted that CWS saves significant costs to households as there is no need to purchase expensive domestic storage tanks.

More recently, in Delhi, Zérah (2000) found that households spend 1.6 times more on expenses related to IWS than the water utility's total budget. Financial coping costs were similar for the rich and poor, but the cost of wasted time was 13 times higher for the poor (Zérah, 2000). Pattanayak et al. (2005) found a similar pattern in Kathmandu, where households spend twice as much money collecting, pumping, storing, treating, and purchasing alternate sources of water than they spend on their monthly water bill. Because richer households can spend more on coping costs, they can avoid many of the consequences of IWS (Pattanayak et al., 2005; Dutta and Tiwari, 2005). In addition to spatial inequity, therefore, IWS can induce inequity based on the socioeconomic status of households.

Capital costs and upgrading costs

Early perspectives on the costs of IWS as compared to CWS were divided. The Health of Towns Association (1846, Sec.67) argued that CWS would save capital costs because a new system built to run continuously "requires smaller mains and pipes" than an intentionally IWS. Conversely, Vernon-Harcourt (1890, p.410) argued that upgrading an existing IWS to a CWS would be expensive because it "necessitates the strengthening and very careful inspection of the pipes, joints, and fittings, to prevent fracture and avoid leakage under a continual and increased pressure." More recent experience sides with Vernon-Harcourt (1890). For example, The World Bank (2013) pilot project in Hubli-Dharwad replaced the entire water distribution network in order to achieve CWS and avoid the necessary careful inspections described by Vernon-Harcourt (1890). The pilot project's cost was $225/per person (not per connection!) (The World Bank, 2013, 2011).

Fire suppression

Early proponents of CWS systems in England and the U.S. were also influenced by concerns for fire suppression. The Health of Towns Association (1846, Sec.75) conceded that CWS "is equally advantageous with a view to the protection of property." Reynolds (1873, p.310) found that "many fires that, under the present [intermittent] system, become serious, would be checked at the outset under constant supply." Specifically Reynolds (1873, p.310) claimed that deficient water supply in London was to blame for 58 fires in 1872. The London Board of Health (1850) also noted that two-thirds of fires could be speedily extinguished if water was available within five minutes. Liverpool established their "water-works specially for sanitary purposes, and as a security against fires" (London Board of Health, 1850, p.260).

In North America, the creation of large city piped-water systems followed major fires and epidemics (Anderson, 1988). The insurance lobby and its control of fire insurance rates mobilized government support for reliable water supply in the U.S. and in England (Anderson, 1988; Jacobson, 2001; Reynolds, 1873).

The 1875 report on Calcutta's water supply suggests, however, that narratives connecting fire suppression with CWS were not universal (Secretary of State for India in Council, 1875). More recently in India, fire was found to be the 5th largest risk to all industries in 2013 (Nair, 2013). Yet fire-suppression continues to be absent from dialogue about CWS in India. This historical perspective begs the question: is the lack emphasis on fire suppression part of why CWS have not been adopted in India?

Wastage

Discussions of water wastage in the 19th century and today are confounded by poor and overlapping definitions. In agriculture, the lack of water meters for individual irrigators in 19th-century Punjab left waste defined as water that entered the irrigation system, but was not delivered to the customer (Gilmartin, 2003). By contrast, waste in urban water distribution in 19th-century sources seems to include customer leakage or overuse (e.g., Health of Towns Association (1846)).

This thesis will define water wastage that occurs during the supply stage as *leakage*. Water that is wasted because it slowly drains out of the pipes during the non-supply stage is a system's *dead-volume losses*. Water that flushes contaminants and rust out of the system at the start of the supply stage is defined as *flushing water*. *Customer wastage* is water that is discarded when some customers empty their storage containers at the start of a new supply stage. Finally, *on-premise leakage* is leakage that occurs on a customer's premise.

The Health of Towns Association (1846, Sec.69) argued that CWS would reduce on-premise leakage because "high pressure renders a running tap a great nuisance." In support of their theory, the town of Wolverhampton apparently saw a 22% decrease in household water use under CWS (London Board of Health, 1850, p.142). More generally, towns that converted to CWS reported an average decrease in total water requirements by 50% (London Board of Health, 1850, p.314). Much of this saved water was likely due to the decrease in dead-volume losses (Carpenter, 1875; London Board of Health, 1850). In systems with short supply stages, the dead-volume losses could easily have been equivalent to the total customer demand. This is especially true of networks constructed to run intermittently, which require larger diameter pipes and therefore have larger dead volumes.

Other 19th-century perspectives on wastage argue the opposite: "waste from carelessness and bad fittings is alleged as a reason for entertaining the question of supplying water on the intermittent system" (Secretary of State for India in Council, 1875, p.232). To convert an IWS to a CWS requires a major retrofit to "avoid leakage under a continual and increased pressure" (Vernon-Harcourt, 1890, p.410).

Today, discussions of leakage and IWS are also confused by the metrics. Most utilities, regulators, and academics continue to track leakage as a percentage of the total supply (e.g., MoUD (2010)), inspite of recommendations to the contrary (e.g., Frauendorfer and Liemberger (2013)). Even the World Bank-sponsored benchmarking program for Indian water utilities sets leakage targets as percentages (i.e., 'non-revenue water' $\leq$ 20%; MoUD (2010, p.28)). One major danger of this leakage metric is that many IWS in India report leakage levels between 20 and 50% (Eales, 2010), which are similar to leakage levels in sophisticated CWS, where 20-30% is common (Mutikanga, 2012). Utilities and regulators may believe mistakenly, therefore, that their leakage rates are close to international norms. However, since leakage is strongly correlated with duty cycle, metrics must reflect this (Kumar, 1997).

To the author's knowledge, no recent researchers have explicitly considered the dead-volume losses associated with IWS. The author calculated that dead-volume losses associated with IWS in two affluent neighborhoods of two cities in India were 4% (15 L/connection) and 9% (50 L/connection) of customer demand per supply cycle (details in Section A.1.2). Customers in IWS who live in low lying areas and/or have suction pumps, however, are able to extract some of this dead volume, which reduces the proportion of the dead volume that is true waste.

Discussion

Amidst entwined agendas of privatization and CWS, some argue that the benefits CWS are constructed in order to justify privatization. On the contrary, even 19th-century sources advocated for CWS because of its better water quality, improved equity, lower costs, and reduced fire risks.

Chapter 3

A parsimonious model of IWS

> Parsimony is desirable because . . . when important aspects of the truth are simple, simplicity illuminates, and complication obscures
>
> Box (1979, p.2)

Parsimony in modeling is an approach that is extremely reluctant to add complexity unless it is absolutely required. It is the principle advocated for in Ockham's Razor (Latin: *lex parsimoniae*, 'the law of parsimony') and predates Ockham himself. Box (1979) demonstrates that parsimonious models can be more robust to errors and, due to their simplicity, more useful.

Recent work to understand and improve the performance of IWS has focused on detailed simulations, and sometimes optimizations, of specific networks (e.g., Siew et al. (2016); Mohapatra et al. (2014); Solgi et al. (2016); Soltanjalili et al. (2013); Ameyaw et al. (2013)). Unfortunately, any simulation "is only as good as the field data used to set it up . . . [and] getting complete field data is difficult" (McIntosh, 2014, p.52). Emphasizing this, Sangameswaran (2014, p.71) argues that the information required to establish an accurate model of an IWS "is totally at odds with the chaotic arrangements that actually characterize Indian cities."

Instead of the traditional, simulation-based approaches that rely on detailed network-specific information (e.g., pipe diameters and configurations), this chapter proposes and validates a parsimonious model of IWS that does not use detailed network-topology information. Due to the proposed model's simplicity, causal relationships become perceptible and the optimality of operational strategies may be explored without simulation or experimentation. The model is constructed from the perspective of the system operator and focuses primarily on variables that the operator could observe.

3.1 Current methods of modeling IWS

In hydraulic simulations of CWS, customers are assumed to demand and receive a flow rate of water that varies over time. This demand is then used as a boundary condition for the hydraulic models (Tanyimboh and Templeman, 2010). In IWS, when pressure is low or absent (e.g., during the non-supply stage), customers cannot always receive the water they demand directly from the pipe network. Such customers adapt by storing water in their homes, further changing the behavior of the system (Abu-Madi and Trifunovic, 2013; De Marchis et al., 2010; McIntosh, 2003; Macke and Batterman, 2001; Kumpel et al., 2017). Despite such differences, when designing or upgrading an IWS, the industry standard is to model the IWS as a CWS, claiming that it will soon be operated continuously (Vairavamoorthy and Elango, 2002).

To model the effects of low or absent pressure, many advocate for the inclusion of *pressure-dependent demand* (PDD) in hydraulic simulations of IWS (e.g., Reddy and Elango (1989); Batish (2003); Tanyimboh et al. (2003); Cheung et al. (2005); Mohapatra et al. (2014)). In the simplest formulation of PDD, flow to each customer is modeled as flow out of an orifice, which increases with pressure. This PDD formulation captures the behavior of customers who leave their taps open and whose storage tanks do not fill before the supply stage concludes.

The effects of customer storage can be modeled by including customer tanks in the hydraulic simulation (Macke and Batterman, 2001). Such tanks fill at a pressure-dependent rate (i.e., behave like PDD) until they fill, after which flow into them ceases. In this modeling approach, customers have *volume-dependent demand* (VDD).

More advanced simulations of IWS include the process by which pipes fill at the start of supply (simpler models begin with full pipes). De Marchis et al. (2010) present a utility-scale implementation of a model in which the filling front is assumed to be perpendicular to the pipe's cross-section (i.e., a one-dimensional (1-D) filling process) and in which air in the pipe is assumed to have atmospheric pressure everywhere. Unfortunately, their model is not publicly available and their validation step considered only data from locations which had also been in their calibration step. Finally, some models attempt to capture the filling front's two-dimensional (2-D) behavior (e.g., Lieb et al. (2016)). To the author's knowledge, there are no published examples of two-dimensional filling models being calibrated and validated at the utility scale.

3.2 Model construction

The primary sources of complexity in models of IWS are i) the interactions between upstream and downstream customers, ii) the non-linearity of pipe friction and customer demand, and iii) missing or inaccurate information about how the network is connected. To avoid these complexities, this section constructs a model that considers the average behavior of an IWS by considering its leaks and customers. First, the behavior of a single leak is generalized to model leakage across a network. Second, flow to all customers in the network is modeled by the behavior of the network's average customer. Finally, the total water required by a network is considered to be the superposition of the water required by leaks and customers.

This strategy greatly simplifies the resultant model, but it has two major drawbacks. First, by focusing on the network's average behavior, variation in how well customers are served cannot be assessed. This is problematic as IWS increase inequity as compared to CWS, especially at the extremities of an intermittent network. Second in IWS, the average network pressure is strongly influenced by the duty cycle (the duty cycle affects average flow rates and thereby pressure losses and the average network pressure). This coupling is not captured because pressure is treated as an exogenous (i.e., constant and independent) variable. Assessing the parsimony of a model which includes endogenous pressure variations is left for future work.

3.2.1 Notational strategy

Most IWS managers discuss their water supply in terms of volumes per day (e.g., production capacity of 100 million liters per day), or in terms of a volume per capita (i.e., person) per day (e.g., 300 liters per capita per day (lpcd)). Both metrics are technically average flow rates (volumes divided by time), but practitioners' discuss them as if they were volumes. To make the model that follows accessible to such practitioners, its notation matches their vocabulary; V represents volume per day (i.e., an average flow rate), Q represents an instantaneous flow rate, and $\boldsymbol{V}$ represents a true volume.

In systems with a supply period of two days (i.e., water is supplied once every other day), customers will demand twice their daily water requirements. Representing a customer's demand as a daily volume (V_D; i.e., average flow rate) accounts for this accumulation of demand without needing to consider the supply period.

Without major source upgrades, most intermittently-operated water utilities are limited in the water they have available to input into their networks. From a distributional perspective, this total water availability is also a daily volume (i.e., average flow rate), V_T.

Water systems operate in contractual and/or regulatory environments that have performance targets. The model's construction assumes that each system has a target minimum average pressure (H_{target}) and that each system is supposed to be operated continuously $t = 1$.

To help generalize the derived models, non-dimensional variables are frequently used. All non-dimensional variables are lower case. Three key non-dimensional variables are:

1. Duty cycle, $t \in [0, 1]$, (e.g., a system supplying water for six hours every other day and a system supplying water for three hours daily, both have $t = 0.125$);

2. Pressure head, h, defined during an IWS' supply stage and normalized by the

targeted pressure head (H_{target});

3. Daily volume (v) of leaks (v_L), customer demand (v_D), water input into the system (v_P), and total available water ($v_T \equiv 1$); each normalized by the total daily volume of available water for a system or sub-system (V_T).

A comprehensive definition of variables can be found in the Nomenclature section in the front matter of this thesis.

3.2.2 Leakage

The standard model for the leakage rate (Q_L) out of a single leak in a pipe is the orifice equation (Colombo and Karney, 2002; American Water Works Association, 2009):

$$Q_L = C_d A[2g(H - H_C)]^{\alpha} \left(\frac{86400 \text{ seconds}}{1 \text{ day}}\right) \tag{3.1}$$

where α accounts for the pressure dependency of the flow rate, C_d is a constant that accounts for the shape of the orifice (and corrects units when $\alpha \neq 0.5$), A is the area of the orifice, g is gravitational acceleration, and H and H_C are system and external fluid pressures. A single, rigid, round orifice would have $\alpha = 0.5$, but cracks in pipe networks can open wider with higher pressures, a behavior that can be modeled by higher values of α (American Water Works Association, 2009).

This model of a single leak (Eq 3.1) can be extended to model many leaks aggregated together (Colombo and Karney, 2009). Aggregated leaks can be represented by an equivalent orifice area (EOA) (of size A), whose Q_L matches the sum of all leaks. When leaks are aggregated together, a higher value of α can account for elevation differences between the aggregated leaks (Gupta and Bhave, 1996); α is typically modeled as between 0.5 to 2.5, with 1.15 being a reasonable estimate for a network with a range of pipe materials (Lambert, 2002; Al-Ghamdi, 2011) and 1.0 being standard practice (American Water Works Association, 2009).

Even along a single pipe, the leakage location, end-point pressure, and end-point demand all affect the leakage rate (Colombo and Karney, 2002). Accurately accounting for leakage without detailed network information, therefore, is not possible. Nevertheless, the proposed model assumes that given an average system pressure H, the EOA and α can be adjusted to compensate for the spatial distribution of leaks.

During the supply stage, the majority of leaks occur in locations without external fluids in their vicinity. The effect of external fluids on the outward leakage rate is, therefore, neglected ($H_C \approx 0$). Averaging by the duty cycle, t, and combining constants into K_L, the daily volume of a network's leakage simplifies to:

$$V_L = tQ_L = K_L AtH^{\alpha} \tag{3.2}$$

While higher pressures are known to increase the rate of pipe bursts and therefore induce a permanent change in A (Thornton and Lambert, 2005), the orifice equation model for leakage does not account for such coupling. Accounting for this is highlighted as an opportunity for future work.

In order to non-dimensionalize Eq 3.2, for a given IWS, a corresponding 'ideal network' is theorized. The ideal network has the same topology and customers, but can be operated at the targeted/ideal duty cycle and pressure (i.e., $t = h = 1$). Furthermore at the ideal duty cycle and pressure ($t = h = 1$), this ideal network has the targeted (e.g., project, national, or international targets) level of leakage, V_{LC}. To achieve this level of leakage, the ideal network will probably require a much smaller EOA than the current network. The relative EOA, a, of any network is defined as that network's current EOA divided by the EOA of that network's ideal network. Therefore, by definition, in the ideal network $a \equiv 1$. For almost any IWS, $a >> 1$.

An arbitrary system may differ from its ideal system in three ways: duty cycle t, pressure head h, and EOA a. Therefore, the daily volume of leaks in an arbitrary system is:

$$V_L \equiv V_{LC} a t h^{\alpha} = Q_L t \tag{3.3}$$

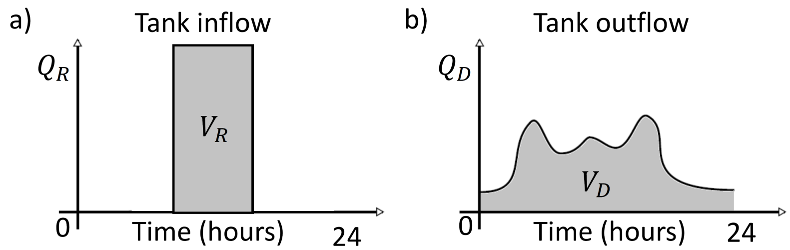

Figure 3-1: **Domestic storage and its capacitive effect on demand.** a) The instantaneous flow rate received by a customer's tank (Q_R) is driven by the availability and pressure of water in an IWS. b) If the IWS satisfies the customer (i.e., $V_R = V_D$), the customer's instantaneous domestic demand (Q_D) is served by their storage tank and is unaffected by IWS. Modified from Walter (2015).

3.2.3 Behavior of a single customer

Fan et al. (2014) suggest that the dependence of customer consumption on duty cycle decreases when $t \gtrsim 0.25$. Similarly, Hamilton and Charalambous (2015) report that the total customer consumption reduced by only 15% when the duty cycle was reduced from $t = 1 \rightarrow 0.25$ in Limassol, Cyprus. Therefore, in this simple model, customer demand will be considered independent of the system's characteristics (i.e., an exogenous variable).

Customers can either be satisfied or unsatisfied by an IWS. A satisfied customer receives the daily volume of water (V_R) they demand (V_D). An unsatisfied customer receives less than they demand (i.e., $V_R < V_D$). Between supply stages, customer storage tanks act as capacitors. They allow the domestic consumption patterns of satisfied customers to be unaffected by IWS (Abu-Madi and Trifunovic (2013); Klingel (2010); Walter (2015); Fig 3-1).

The daily volume received by unsatisfied customers increases with longer duty cycles and higher pressures. Specifically, unsatisfied customers are assumed to keep their taps open, and therefore, behave like the orifice equation (Eq 3.1).

Combining these two possibilities for a customer:

$$V_R = \begin{cases} V_D & : \text{ Satisfied} \\ K_D t h^{\phi} & : \text{ Unsatisfied} \end{cases} \tag{3.4}$$

where K_D is a combined constant that accounts for topography and pipe characteristics. Physically, K_D is the daily volume of water that a customer could receive with a fully open connection to an ideally-pressurized CWS (i.e., a system in which $h = t = 1$). ϕ is the pressure exponent of customer demand and is not necessarily the same as α.

3.2.4 Aggregate customer demand

Generalizing the model of a single, residential customer (i.e., Eq 3.4) to a network model, consider two extremes: a *Satisfied IWS* in which every customer receives as much water as they demand, and an *Unsatisfied IWS* in which no customer receives as much water as they demand. While a network may be fully satisfied or fully unsatisfied, most large IWS are a combination of the two; advantaged customers are easily satisfied while tail-end customers struggle to get enough water. As a first-order model, the transition between satisfied and unsatisfied is modeled as instantaneous. This modeling simplification obscures the inequity of supply in IWS that satisfy some of their customers, but not others.

Pipe pressure varies significantly throughout an IWS. Mapping pressure drops, however, requires network-specific information, which this model attempts to avoid. Instead, the model assumes that the average daily volume of water received by customers (V_R) in an IWS can be modeled exactly as in Eq. 3.4, where h and t are the pressure and duty cycle best representing the whole network.

Non-dimensionalizing each daily volume in Eq. 3.4 by the system's total available daily volume of water V_T, yields:

$$v_R = \begin{cases} v_D & : \text{Satisfied IWS} \\ k_D t h^{\phi} & : \text{Unsatisfied IWS} \end{cases} \tag{3.5}$$

where $k_D = K_D/V_T$ and is the percent of a system's total daily volume that customers could hydraulically receive if they left their taps fully open while the system was operated at $t = h = 1$.

According to Eq 3.5, the transition between satisfied and unsatisfied IWS occurs at $v_D = k_D t h^\phi$. To simplify notation, consider γ_S to be the minimum value of th^ϕ required to make this transition. Accordingly:

$$\begin{aligned} \gamma_S &= th^\phi && : v_D = k_D t h^\phi \\ \therefore \gamma_S &= \frac{v_D}{k_D} = \frac{V_D}{K_D} && \end{aligned} \tag{3.6}$$

Similarly, for a given pressure head (h), the minimum duty cycle required to provide satisfied IWS (t_S) is:

$$t_S = \frac{\gamma_S}{h^\phi} \tag{3.7}$$

Combining satisfied and unsatisfied demand and using γ_S (from Eqs 3.4, 3.5, and 3.6) yields:

$$V_R = \min(V_D, V_D \frac{th^\phi}{\gamma_S})$$

$$\therefore V_R = V_D \min(1, \frac{th^\phi}{\gamma_S}) \tag{3.8}$$

$$\therefore v_R = v_D \min(1, \frac{th^\phi}{\gamma_S}) \tag{3.9}$$

This model (Eqs 3.8 and 3.9) assumes that all demand behaves as if it were residential. From the available data, IWS receive more than two-thirds of their revenue from residential customers (data from Van den Berg and Danilenko (2011), author's calculation not shown). Accordingly, the model of residential demand is extended to model the total demand of an IWS.

3.2.5 Combining customers and leaks

Most utilities have an operational choice about how much of their available total supply (V_T) to input into the network (V_P). V_P is the superposition of the volume

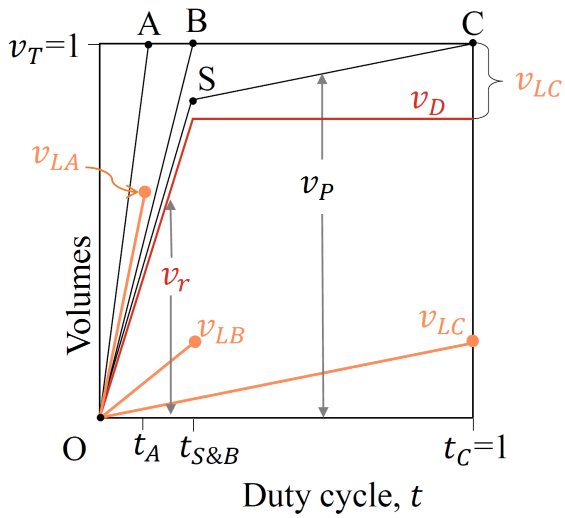

Figure 3-2: **The combined demand and leak model.** For three systems OA, OB, and OSC, the input daily volume (v_P; thin black lines) is the superposition of the daily volume received by customers (v_R; red line of medium weight) and the leaked volume (v_L; thick orange lines). The maximum duty cycle of each system is t_A, t_B, and t_C, respectively. The system is satisfied at $t_S = t_{S\&B}$ and has a total water availability of $v_T \equiv 1$.

received by customers V_R (Eq 3.8) and the volume leaked V_L (Eq 3.3):

$$\begin{aligned}
\therefore V_P &= V_R + V_L \\
&= V_D \min(1, \frac{th^\phi}{\gamma_S}) + V_{LC}ath^\alpha \\
\therefore v_P &= v_D \min(1, \frac{th^\phi}{\gamma_S}) + v_{LC}ath^\alpha \qquad (3.10)
\end{aligned}$$

Fig 3-2 plots v_P for a network described by the line segments OSC. Holding pressure constant, v_P is also plotted for that same network if its EOA were to increase by 5x (OB) or by 15x (OA). The daily volume received by customers v_R and the volume leaked v_L are shown separately. v_L can also be seen as the difference between v_P and v_R.

At the points A, B, and C in Fig 3-2, all available water has been supplied $v_P = v_T = 1$ and it is not possible to input any more water into the network (e.g., because the reservoir is empty). Accordingly, system OA has a maximum duty cycle of t_A. Point B in system OB sits at the transition between unsatisfied and satisfied; as such, its maximum duty cycle is $t_B = t_S$ (denoted $t_{S\&B}$ in Fig 3-2). Point C in system OSC is a CWS ($t_C \equiv 1$).

Most water system improvement projects target a final leakage v_L of 15-20%, implying that demand comprises the rest of the input volume. Therefore a reasonable guess for a system without economic or absolute scarcity would be $v_D = 0.8$. Fig 3-2 depicts a system with $v_D = 0.8$ and $t_S = 0.25$.

Before concluding this section, it must be reemphasized that t does not represent time. For example, a system operating at point C does not necessarily first satisfy all of its customers (in t_S) and then spend the remainder of its supply stage supplying only leaks. In a predictable IWS (Galaitsi et al., 2016), customers know when the supply will arrive and satisfied customers in such systems may spread out their demand (Batish, 2003; Abu-Madi and Trifunovic, 2013). Fig 3-2, therefore, does not depict the system's evolution with time, but instead shows the system's final state as a function of a given duty cycle that customers have had time to adjust to.

3.3 Model validation

The ideal validation of any network model would use field data. The proposed model was not validated in the field for two reasons. First, the complexity of IWS (e.g., Fig 2-3) thwarts such attempts. Second, since the duty cycle can affect customers and their satisfaction, intentionally changing the duty cycle substantially in an existing network was not possible. Instead, the proposed model was compared to hydraulic simulations of four publicly-available reference water distribution networks. The validation presented in this chapter considers the accuracy of the proposed model of $V_P(t, V_D, a)$. Other parameters (h, α, ϕ) were not explored.

3.3.1 Reference networks

The reference networks (originally CWS) were adapted to behave as IWS using the VDD methodology of Macke and Batterman (2001). To ensure the converted files were representative of actual IWS, before conversion the original demand at each node of

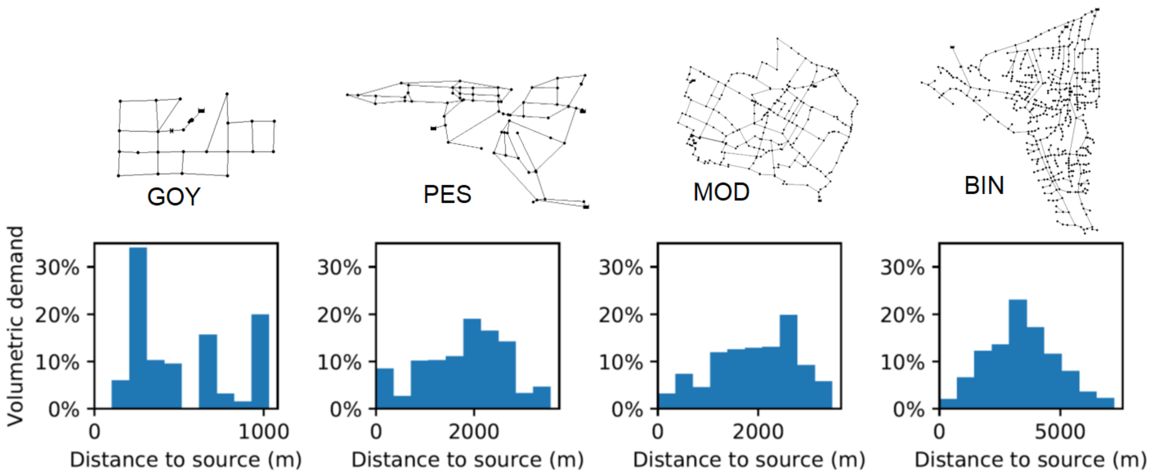

Figure 3-3: **The network layout of each of the four reference networks** (GOY, PES, MOD, and BIN). Below the network maps are histograms depicting how far water travels in each network from sources to customers.

each network was segmented into 15% pressure-dependent leakage and 85% volume-dependent demand. In addition, check-valves were added to sources in networks with more than one source (for full details of the CWS to IWS conversion, see Appendix B.1).

Characteristics of the four reference networks are summarized in Table 3.1 and their topology is shown in the top of Fig 3-3. Selected reference networks ranged in complexity from only 31 pipes to 454 pipes. Even larger reference networks were found to be unstable when converted to their equivalent IWS for some values of customer demand and/or leakage. The GoYang (GOY) network was originally presented by Kim et al. (1994), features 23 nodes and is supplied with a 4.5kW pump. The Pescara (PES) and Modena (MOD) networks were originally presented by Bragalli et al. (2012) and are skeletonized versions of two Italian cities; they are both gravity fed from several reservoirs. The Balerma Irrigation Network (BIN) was adapted by Reca and Martínez (2006) from an irrigation network in Spain. Its nodes range in elevation by over 100m and its average nodal pressure in CWS simulations was 81m.

Table 3.1: **Reference network characteristics and sources.**

Name	Pipes	Junctions	Elevation	Pumps	Reservoirs	Pressure[a]	Source
full (acronym)	n	n (% with demand)[b]	max-min	n	n	mean	
GoYang (GOY)	31	23 (91%)	9m	1	1	26m	Kim et al. (1994)
Pescara (PES)	99	71 (90%)	27m	0	3	30m	Bragalli et al. (2012)
Modena (MOD)	317	272 (90%)	11m	0	4	25m	Bragalli et al. (2012)
Balerma[c](BIN)	454	447 (99%)	103m	0	4	81m	Reca and Martínez (2006)

[a] Mean nodal pressure in the hydraulic simulation of each unmodified (continuous) network
[b] Percent of junctions in the initial network with strictly positive demand
[c] Balerma Irrigation Network

Access to the original network files is described in Wang et al. (2014); files are hosted by the University of Exeter. The modified IWS versions of each network are included as supplemental information in the companion journal article about this model (*in preparation*).

The distance from each node to its closest source was calculated for each network using Dijkstra's algorithm, implemented in the Water Network Tool for Resilience v.0.1.4 (WNTR; Murray et al. (2018)) package in Python 2.7.14. Fig 3-3 displays the distribution of distances between customers and their closest source, weighted by the volume demanded by the customer.

3.3.2 Reference simulation method

In IWS where customers with tanks are satisfied, VDD method of Macke and Batterman (2001) assumes that all customers fill their tanks as soon as possible. In reliable IWS, however, some customers may choose to withdraw water later in the supply stage (Batish, 2003; Abu-Madi and Trifunovic, 2013). This spreading of demand would decrease the peak flow rate predicted by VDD and reduce the system's pressure variations during the supply stage. As the proposed model does not capture any pressure variation during the supply stage, the typical VDD method is a more conservative test case than a simulation method where demand is spread throughout the supply stage.

Since customer demand does not spread out in response to duty cycle in VDD models, simulations of a VDD network in the time domain are equivalent to simulations with respect to duty cycle. For example, two hours into the supply stage, the simulated characteristics of a VDD network are the same whether its duty cycle is $t = 0.167$ (two hrs/day) or $t = 0.917$ (22 hrs/day).

In a VDD network with a constant source pressure (e.g., a reservoir), as customers are satisfied, the network's average pressure increases. The proposed model does not capture this endogenous pressure change. The model's pressure term captures only exogenous pressure changes (e.g., increasing the reservoir's level). The proposed model could have been validated against simulations of VDD networks where the simulated network's average pressure was held constant (e.g., by varying the reservoir level as a function of duty cycle), but such a scenario is less physically meaningful. Instead, the model is compared to VDD simulations where the source pressure was held constant (e.g., reservoir level held constant). Validating against a fixed input represents a more conservative (i.e., difficult) test-case.

Hydraulic simulations were done using the EPANET2 solver (Rossman, 2000) implemented in WNTR (Murray et al., 2018). The intermittent versions of each reference network were simulated using an extended-period simulation with 10-minute simulation and reporting timesteps and a simulation period of 24 hours. Simulation results were converted back to duty cycle by dividing the simulated time by the simulation period (i.e., dividing by 24 hours). In the proposed model and the hydraulic simulations, pressure exponents were assumed to be $\phi = 0.5$ and $\alpha = 1.0$.

3.3.3 Calibration method

Each reference network was simulated using the method described above. The simulation resulted in $V_L(t)$ and $V_R(t)$ for each network with $t \in [0, 1]$ in increments of approximately 0.007 (Fig 3-4a). The proposed model of $V_R(t)$ (Eq 3.8) depends on two parameters, the total customer demand (V_D) and the rate at which demand can be satisfied ($Q_R = K_D h^\phi$). $\hat{Q}_R$ was estimated using a least-squares fit of the simulation results, where $\hat{}$ indicates an estimated parameter (Fig 3-4a). Similarly, the proposed model for $V_L(t)$ depends only on $Q_L = V_{LC} a h^\alpha$; $\hat{Q}_L$ was also estimated using a least-squares fit (Fig 3-4a). To allow for testing against networks in which customers are never satisfied, V_D was not calibrated; the true value from the reference network was used in the proposed model (Fig 3-4a).

3.3.4 Validation method

After calibration, the proposed model of $V_P(t)$ was compared to simulation results across a range of V_D and a (i.e., $\Delta V_D/V_D^0 \in [-50\%, 400\%]$ in increments of 25% and $\Delta a/a^0 \in [-80\%, 700\%]$ in increments of 20%). The goodness-of-fit between the model

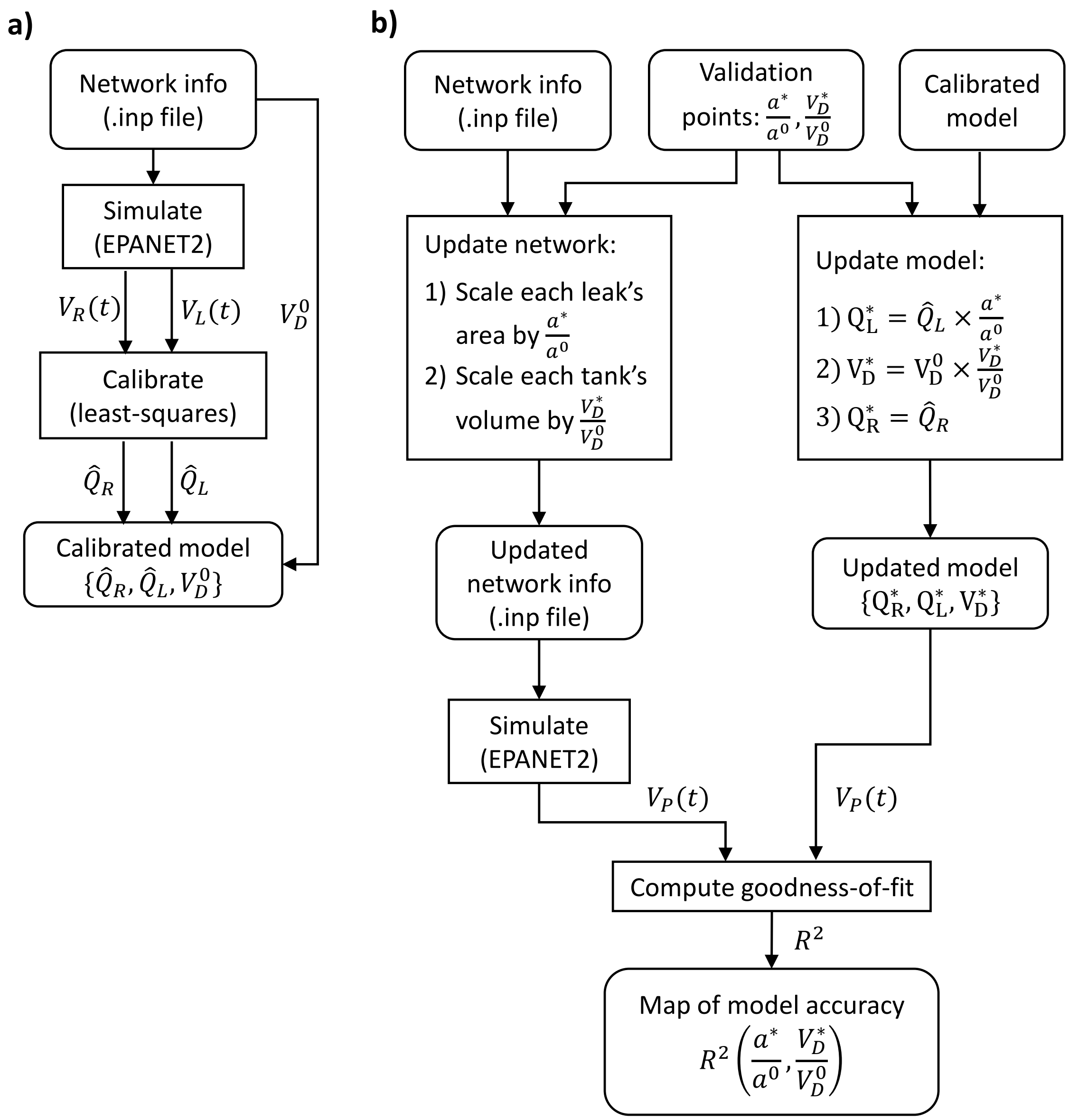

Figure 3-4: **Model calibration and validation method.** a) calibration method; model includes fitted parameters for leak flow rate, $\hat{Q}_L$, and customer flow rates, $\hat{Q}_R$, as well as the true value of initial customer demand V_D^0. b) validation method; for each given validation point, network information was updated and the network was re-simulated. These results ($V_P(t)$) were compared with with calibrated model once its parameters were also updated. The resultant goodness-of-fit (R^2) was recorded as a function of the validation point used to generate it.

and simulation was quantified by the R-squared value for each pair $\{V_D^*, a^*\}$.

To modify the IWS reference networks for each new $\{V_D^*, a^*\}$, the cross-sectional area of each customer tank was scaled by V_D^*/V_D^0 (Fig 3-4b). In a similar way, the area of each leak was scaled by a^*/a^0 (Fig 3-4b). All other parameters (i.e., network topology, source pressure, and pressure exponents) were held constant.

To modify the proposed model, the calibrated value of $\hat{Q}_L$, used in Eq 3.3, was scaled by a^*/a^0 (Fig 3-4b). The new value of V_D^* was used directly in Eq 3.8 to predict $V_R(t)$, holding $\hat{Q}_R$ at its calibrated value (Fig 3-4b).

For example, to test the model's prediction of $V_P(t)$ when customer demand and EOA have both doubled, the calibrated model's input parameters of V_D and $\hat{Q}_L$ were both doubled. The resultant model's prediction of $V_P(t)$ was then compared with the VDD simulation of each reference network, where the volume of each customer's tank and the area of each leak in the system were all doubled.

3.3.5 Validation results

The model matched the behavior of the four reference networks, of increasing complexity, at the calibration point (B in Figs 3-5 and 3-6a) with an R-squared value of 0.97, 0.94, 0.97, 0.87 for GOY, PES, MOD, and BIN networks, respectively. For variations of $\Delta V_D/V_D^0 \in [-50\%, +100\%]$ and $\Delta a/a^0 \in [-20\%, +100\%]$, the model's prediction of $V_P(t)$ matched with simulations such that $R^2 > 0.80$ (Fig 3-5). To demonstrate the limits of the proposed model, V_D and a were varied much more than would be expected in the normal aging and growth of a water distribution network (Fig 3-5).

When demand increases substantially, the proposed model under-predicts $V_R(t)$ (Fig 3-6b). When the EOA increases substantially, the model over-predicts $V_L(t)$ (Fig 3-6c; the opposite error). These errors are mitigated when both EOA and demand are high (Fig 3-5). Accordingly, scenarios A and C were selected such that only one parameter is increased to show the model's limitations in extreme cases. Fig 3-6 shows $V_P(t), V_R(t), V_L(t)$, and $H(t)$ for each reference network at the calibration point (B), with +400% (i.e., 5x) demand (A), and with +700% (i.e., 8x) EOA (C).

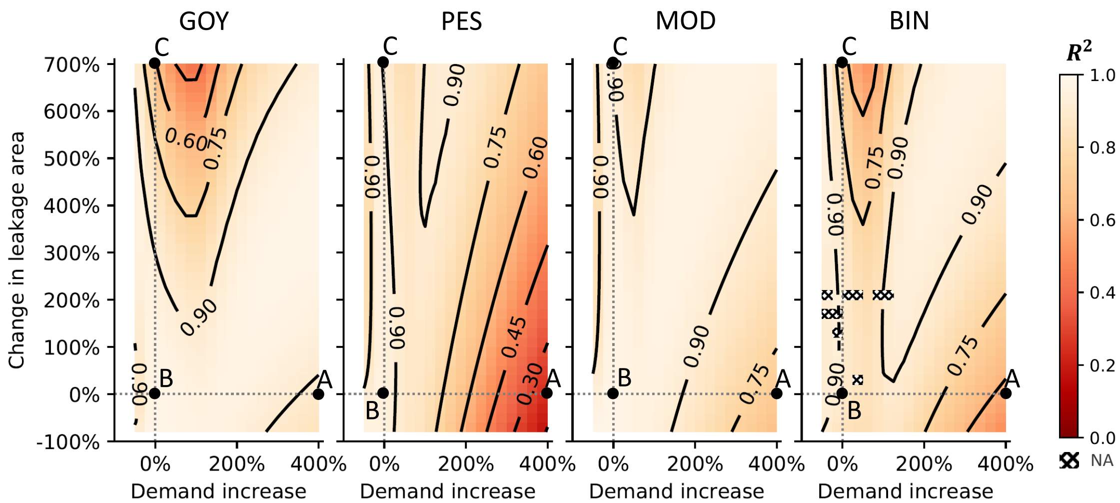

Figure 3-5: **Model's fit with VDD simulations.** For each reference network (i.e., GOY, PES, MOD, and BIN) shading and contour lines show the R-squared (R^2) fit between the model's prediction and VDD simulations of the total water required as demands and EOA vary in the range of [-50%,+400%] and [-80%,+700%] of their initial values, respectively. Points A, B, and C are explored in detail in Fig 3-6. The proposed model was calibrated at B. The R^2 value 'NA' (checkerboard shading) indicates the numerical simulation was unstable (only in BIN).

Increasing the EOA, even up to +700%, had little effect on the customer model's accuracy ($V_R(t)$; Fig 3-6b). In the worst case (BIN) the R-squared fit reduced by 0.05 (to R^2=0.77, Fig 3-6b). Large increases in the demand, however, did reduce the accuracy of the customer model. When demand increased by +400% (i.e., 5x), the accuracy of the customer model dropped substantially (R^2=0.12 in the worst case of PES; Fig 3-6b). The proposed customer model assumed that Q_R was unaffected by changes in V_D. In reality, as customers close to the network's source(s) demand more and more water, they consume a larger fraction of the total supply. Concentrating the demand close to the sources decreases the effective hydraulic resistance of the network and therefore increases Q_R. The effect was most prominent in PES which had more (2.7x more) of its demand in the closest tenth of its network than any of the other three reference networks (Fig 3-3).

The proposed leakage model ($V_L(t)$) is much less robust to changes in EOA and customer demand than the proposed customer model ($V_R(t)$; Figs B-1 and B-2). When demand increased by +75%, the R-squared fit of the leak model was negative

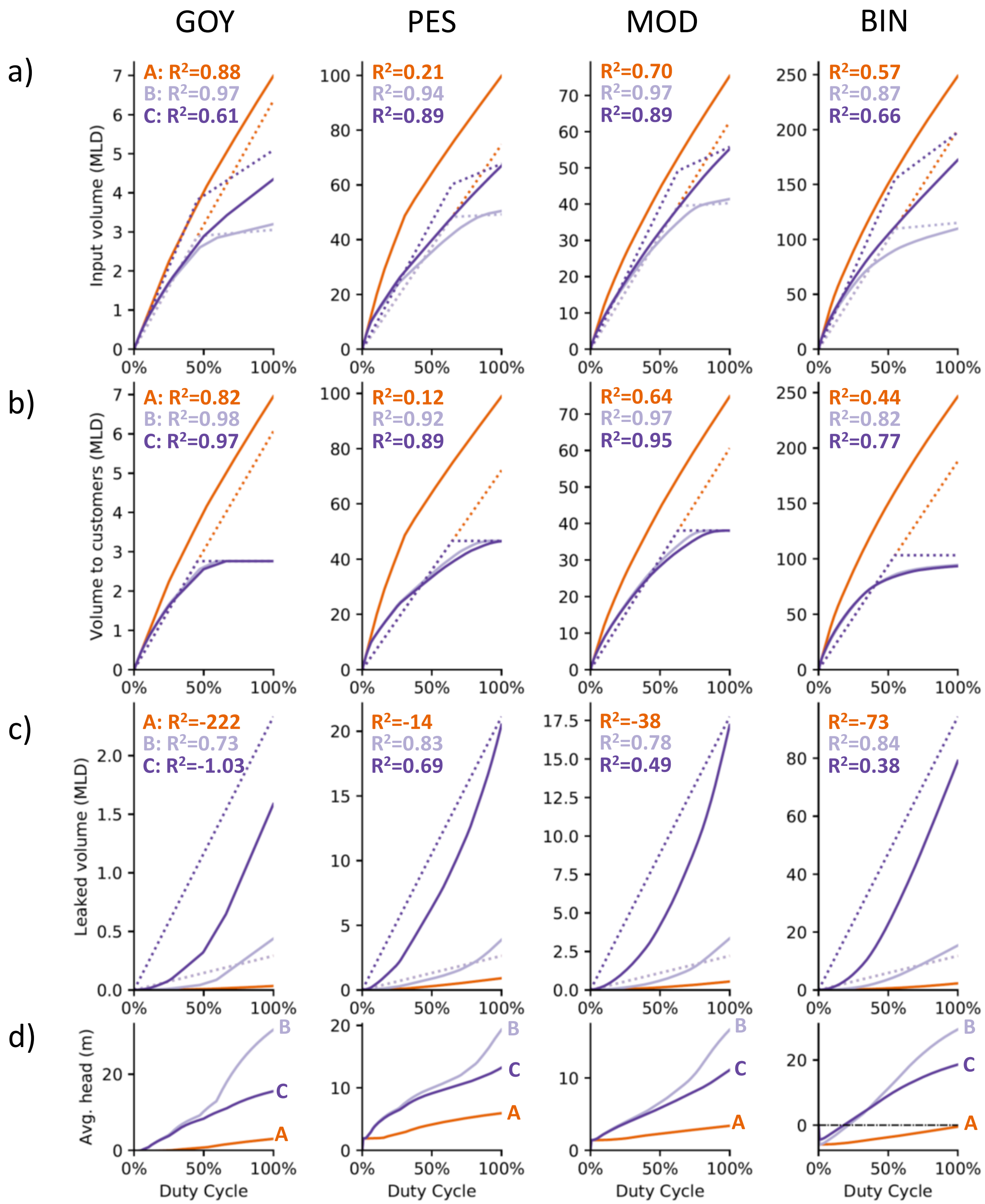

Figure 3-6: **The model's fit at calibration and extreme values.** For GOY, PES, MOD, and BIN, the model's predictions (dotted lines) for $V_P(t)$, $V_R(t)$, and $V_L(t)$ are compared to VDD simulations (solid lines) in the a), b), and c). d) VDD simulations of the network's average pressure with increasing duty cycle. Scenarios B (light purple, the model's calibration point), A (darker orange, +400% demand), and C (darkest purple, +700% EOA) match the labels in Fig 3-5.

for all four reference networks (Fig B-1). A negative R-squared indicates that the simulated results are better fit by their average value than by the proposed model. In the simulated networks, increases in demand prevent customers from being satisfied. Without satisfied customers, the simulated network pressure could not build like it did in the calibration scenario (e.g., between scenarios B and A in Fig 3-6d). This major pressure difference is not captured by the proposed model, which, therefore, over-predicts $V_L(t)$ (Fig 3-6d). For example, in BIN, the network-averaged pressure for most of scenario A was negative (Fig 3-6d). Including first-order, endogenous pressure variations would substantially improve the proposed model.

The proposed model of a network's input volume $V_P(t)$ is more robust than either of its components, whose errors frequently cancel (Figs 3-5 and 3-6a). As networks are likely to grow in demand and EOA, this cancellation of errors is fortuitous.

3.4 Discussion and future work

Trends in modeling IWS have been to increase the complexity and accuracy; this chapter attempted the opposite (Table 3.2). The relatively good agreement between the proposed model and more complex simulations suggests that important aspects of how IWS behave are indeed simple. Perhaps, therefore, IWS are a case where "simplicity illuminates, and complication obscures" (Box, 1979, p.2).

While Totsuka et al. (2004) outlined three causes of IWS (technical, economic, and absolute scarcity), the proposed model can help explain these causes and distinguish between them. Specifically, when $v_D > 1$ the network does not have enough total water and therefore suffers from economic or absolute scarcity. When $\gamma_S > 1$ the network's distributional capacity limits its ability to satisfy customers and it therefore suffers from economic scarcity. Finally, when an IWS has $v_D < 1$ and $\gamma_S < 1$, it suffers from technical scarcity. In addition to adding detail to the framework of Totsuka et al. (2004), the model distinguishes between satisfied and unsatisfied customers. Satisfied customers are customers whose water supply is "constant enough" and "available when needed." Therefore, this framework may prove useful in measuring and advancing

Table 3.2: **IWS modeling methods**, their features, and examples of their use.

Pipe info[a]	PDD[b]	VDD[c]	Filling 1-D[d]	2-D[e]	Examples
✓					Industry
✓	✓				Batish (2003)
✓	✓	✓			Macke and Batterman (2001)
✓	✓	✓	✓		De Marchis et al. (2010)
✓	✓			✓	Lieb et al. (2016)
	∼[f]	✓			*Proposed parsimonious model*

[a] Pipe characteristics and connectivity
[b] Pressure-dependent demand
[c] Volume-dependent demand
[d] Water-air front is parallel to pipe cross-section
[e] Partially-filled pipes are captured
[f] Models the effects of exogenous changes to the average pressure, but not of endogenous pressure variations

global water goals.

Three opportunities to further the validated the proposed model are suggested:

1. The proposed model's accuracy with respect to changes in exogenous (e.g., source) pressure could be tested with the methods described in this chapter.

2. A new simulation method could be implemented to study the implications of filling dynamics on the proposed model.

3. The model's predictive power could be validated by instrumenting a system that was undergoing a major shift in its characteristics. For example, a drought would change V_T (perhaps then the author would be included in Sainath's (1999) observation that 'everybody loves a good drought').

In addition to further model validation, three opportunities to improve the proposed model are suggested:

1. Including endogenous pressure effects would substantially improve the accuracy of the leakage model. Such an effort could begin by considering uniformly distributed leakage along a single pipe.

2. By considering the average customer, this model neglects spatial variations in how well customers are served by the network. This is especially important to note for customers at the network's fringes, who are notoriously under-served (Vairavamoorthy et al., 2007a), and for customers who share a connection and will therefore receive only a fraction of the 'average' (Kumpel et al., 2017). Accounting for this variation without network-specific information could perhaps be done with Cheng and Karney's (2017) scaling relationships.

3. Higher pressures are known to increase the burst rate in piped networks (Thornton and Lambert, 2005) and shorter duty cycles are thought to accelerate the rate at which piped networks degrade (Klingel, 2012; Charalambous and Laspidou, 2017). Including such longer term effects of the system pressure and duty cycle would create a more holistic model of IWS.

Parsimonious models are more robust to misinformation and easier to interpret than more complicated models. Box (1979, pp.2-3) argues, therefore, that "cunningly chosen parsimonious models often do provide remarkably useful approximations." The following three chapters apply and extend the proposed model to demonstrate its utility as an approximation of an IWS.

Chapter 4

Effects and causes of IWS

> More research is needed to demonstrate which interventions are most appropriate in the different intermittency conditions.
>
> Galaitsi et al. (2016, p.18)

Within the literature on IWS, theories abound as to the causes and effects of IWS (Galaitsi et al., 2016). The system model derived in Chapter 3 provides a theoretical framework to evaluate these claims. Specifically, this chapter uses the model to quantify three potential effects of IWS: lower leakage, lower customer consumption, and lower total water requirements. In a similar fashion, this chapter uses the model to quantify the relative magnitudes of three potential causes of IWS: less water available to the utility, increased customer demand, and degradation in pipe quality. Each of these will be first explored with a graphical example and then generalized with analytic expressions. Next, as a case study, this chapter explores how system changes will affect the MNWS project in Delhi. And finally, this chapter ends with a discussion of the implications of this model.

This chapter specifically considers IWS that are facing technical scarcity, not economic or absolute scarcity (Totsuka et al., 2004) (i.e., $v_D < 1$ and $\gamma_S \leq 1$). Implicitly, therefore, this chapter assumes that IWS could be avoided through leak repair and operational strategies. As the IWS considered in this chapter are sustained by utility choices, this chapter adopts the perspective of the utility managing the IWS. While this chapter attempts to add knowledge and technique to the operation of an IWS, at its outset it is acknowledged that knowledge and technique are only two components of what is necessary to improve a dysfunctional system (Morgan, 2002).

Recall that the IWS model of Chapter 3 is summarized by Eq 3.10:

$$v_P = \begin{cases} v_D + v_{LC} a t h^{\alpha} & : t h^{\phi} \geq \gamma_S \text{ (Satisfied)} \\ v_D \frac{t h^{\phi}}{\gamma_S} + v_{LC} a t h^{\alpha} & : t h^{\phi} < \gamma_S \text{ (Unsatisfied)} \end{cases} \tag{4.1}$$

4.1 Effects of a reduced duty cycle

4.1.1 Graphical example

Consider the effects of reducing the duty cycle in three systems: an unsatisfied IWS where $t = 0.25$, a satisfied IWS where $t = 0.25$, and a satisfied, initially-continuous water supply (i.e., $t = 1$ and $\gamma_S < 1$). In each system, customer demand is assumed to be 80% of the available water. The remaining 20% of available water is assumed to be leaked from each system in its initial state.

The effects of reducing the duty cycle by one third are shown in Fig 4-1. For the unsatisfied IWS shown as line OB, reducing the duty cycle by one third ($t_B \rightarrow t_{B1}$) reduced customer consumption ($v_D \rightarrow v_{RB1}$), leakage ($v_{LB} \rightarrow v_{LB1}$), and the total water required to be input ($B \rightarrow B1$), each by one third (Fig 4-1a).

However, in the cases of the initially-continuous system (OC in Fig 4-1a) and of the satisfied IWS (OE in Fig 4-1b), reducing the duty cycle did not affect customer consumption (by definition, consumption in a satisfied system is not affected by small changes in the duty cycle). The reduced duty cycle nevertheless did reduce leakage by one third in both systems ($v_{LE} \rightarrow v_{LE1}$ and $v_{LC} \rightarrow v_{LC2}$). Since leakage was assumed to be one fifth (20%) of the total input volume in both satisfied systems, the savings of one third applies only to one fifth of the total input water and, therefore, the total water requirements were reduced by one fifteenth (6.7%). In this example, therefore, reducing the duty cycle by a fixed percentage affected a satisfied IWS and a satisfied,

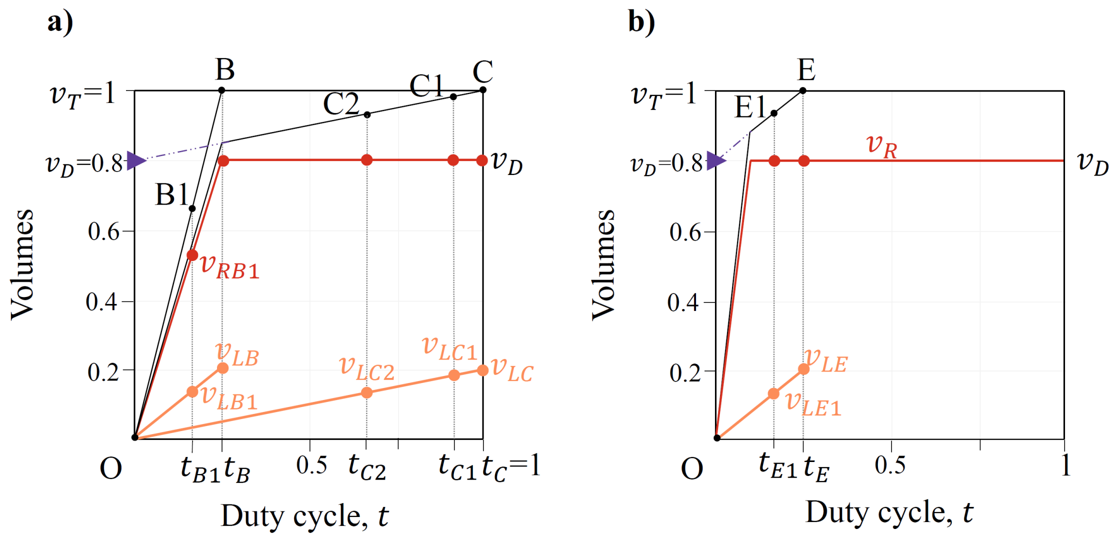

Figure 4-1: **The effects of shorter duty cycles.** The effects of a reduced duty cycle on the volume input into the system (v_P, thin black lines OB, OC, OE), the volume received by customers (v_R, red lines of medium weight), and the volume lost to physical leaks (v_L, thick orange lines). Where the slope/gradient (purple dashed and dotted line) of the line $v_P(t)$ intersects the y-axis at v_D (purple triangle), the system is satisfied.

initially-continuous system equally.

When the duty cycle is reduced by a constant amount, here taken to be one third of $t = 0.25$ (i.e., 0.083), leakage in the satisfied and initially-continuous system ($C \rightarrow C1$) is only reduced by one twelfth (8.3%, 4x less than in the case of the intermittent systems). This reduction in leakage corresponds to reducing the total water required for the CWS by only one sixtieth (1.7%). These results are summarized in Table 4.1.

In each of the considered examples, the distinction between satisfied and unsatisfied IWS determines the y-intercept of the slope of $V_P(t)$; where the y-intercept is equal to customer demand, the system is satisfied (Fig 4-1).

4.1.2 Analytic results

To generalize the previous examples, the effects of the duty cycle on the system can be captured by the partial derivatives of leakage, volume received by customers, and

Table 4.1: **The quantitative effects of shortened duty cycle** (t) on an unsatisfied IWS, a satisfied IWS, and an initially-continuous water supply. Each system is taken to initially deliver 80% of its water to customers, while 20% goes to physical leakage.

		Unsatisfied IWS	Satisfied IWS	Satisfied CWS[a]	
		(B→B1)	(E→E1)	(C→C2)	(C→ C1)
Duty cycle	Δt	-0.083	-0.083	-0.333	-0.083
	$\Delta t/t$	-33%	-33%	-33%	-8.3%
Leakage	$\Delta V_L/V_L$	-33%	-33%	-33%	-8.3%
Demand	$\Delta V_R/V_R$	-33%	0	0	0
Total	$\Delta V_P/V_P$	-33%	-6.7%	-6.7%	-1.7%

[a] Initially-continuous water supply

total water input into the system, each taken with respect to the duty cycle.

From Eq 3.3:

$$\begin{aligned} V_L &= V_{LC} a t h^{\alpha} \\ \therefore \frac{\partial V_L}{\partial t} &= V_{LC} a h^{\alpha} = \text{constant} = \frac{V_L^0}{t^0} \end{aligned} \tag{4.2}$$

where V_L^0 and t^0 are V_L and t evaluated in the initial state of the system. This calculation is equivalent to evaluating the constant slope using 'rise over run.'

Similarly, modeling demand suppression, from Eq 3.4 yields:

$$\begin{aligned} V_R &= \begin{cases} K_D t h^{\phi} & : t h^{\phi} < \gamma_S \text{ (Unsatisfied)} \\ V_D & : t h^{\phi} \geq \gamma_S \text{ (Satisfied)} \end{cases} \\ \therefore \frac{\partial V_R}{\partial t} &= \begin{cases} K_D h^{\phi} = \text{const.} = \frac{V_R^0}{t^0} & : t h^{\phi} < \gamma_S \text{ (Unsatisfied)} \\ 0 & : t h^{\phi} > \gamma_S \text{ (Satisfied)} \\ \text{undefined} & : t h^{\phi} = \gamma_S \end{cases} \end{aligned} \tag{4.3}$$

As expected from the structure of Eq 4.1, the effect of reducing the duty cycle on

Table 4.2: **The analytical effects of shorter duty cycles.** Superscript ^{0} indicates a variable evaluated at its initial value; all partial derivatives are constant.

Effect	Gradient	Unsatisfied IWS	Satisfied IWS
Reduced leakage	$-\frac{\partial V_L}{\partial t}$	$\frac{-V_L^0}{t^0}$	$\frac{-V_L^0}{t^0}$
Demand suppression	$-\frac{\partial V_R}{\partial t}$	$\frac{-V_R^0}{t^0}$	0
Reduced water required	$-\frac{\partial V_P}{\partial t}$	$\frac{-V_P^0}{t^0}$	$\frac{-V_L^0}{t^0}$

the total input water is the linear combination of the gradients in Eqs 4.2 and 4.3:

$$\frac{\partial V_P}{\partial t} = \begin{cases} V_D \frac{h^\phi}{\gamma_S} + V_{LC} a h^\alpha = \text{const.} = \frac{V_P^0}{t^0} & : t h^\phi < \gamma_S \text{ (Unsatisfied)} \\ V_{LC} a h^\alpha = \text{const.} = \frac{V_L^0}{t^0} & : t h^\phi > \gamma_S \text{ (Satisfied)} \\ \text{undefined} & : t h^\phi = \gamma_S \end{cases} \tag{4.4}$$

These effects of IWS are summarized in Table 4.2 and help understand the examples explored at the start of this section.

4.1.3 Discussion

In both unsatisfied and satisfied IWS, reducing the duty cycle by a given percent change ($\Delta t/t$) reduced leakage by that same fraction. However, in systems with already short duty cycles, a given absolute reduction in duty cycle (Δt) equates to a larger percent change and therefore has a magnified effect on leakage. More generally, all effects of IWS (except demand suppression in unsatisfied IWS) were found to scale linearly with $\Delta t/t$ and therefore have magnified impacts at low values t.

The duty cycle's reduction of the total water required by a system was larger in unsatisfied IWS than in satisfied IWS by the ratio V_P^0/V_L^0 (Table 4.2). For example, in a system with 20% leakage, reducing the duty cycle will be 5x more effective at reducing the input water required if customers are unsatisfied. This may explain the conflicting perspectives on IWS' effect on leakage. From the perspective of a satisfied IWS or CWS, reducing the duty cycle may not save very much water, while from the perspective of an unsatisfied IWS, the idea of increasing the duty cycle is untenable.

Finally, the graphical example suggested a possible method for determining if an IWS is satisfied, using only the gradient of $v_P(t)$. This method also applies to the more-easily-measured parameter $V_P(t)$:

$$V_{intercept} = V_P(t^0) - t^0(\frac{\partial V_P}{\partial t})$$
$$\therefore V_{intercept} = \begin{cases} V_P^0 - t^0 \frac{V_P^0}{t^0} = 0 & : th^\phi < \gamma_S \text{ (Unsatisfied)} \\ V_P^0 - t^0 \frac{V_L^0}{t^0} \equiv V_D & : th^\phi > \gamma_S \text{ (Satisfied)} \\ \text{undefined} & : th^\phi = \gamma_S \end{cases} \tag{4.5}$$

Therefore, where the y-intercept of $\partial V_P/\partial t$ is the customer demand, the system is satisfied.

4.1.4 Implications

In contrast to the ambiguity of the Sustainable Development Goal's target 6.1 and the UN's articulation of the human right to water (i.e., water supplies should be either "available when needed" or "continuous enough"), Eq 4.5 provides the first theoretical foundation for distinguishing between sufficient (i.e., satisfied) and insufficient (i.e., unsatisfied) IWS. Beyond just a theoretical distinction, this difference depends only on parameters that could be measured in the field. For a given system with known, or estimated demand, by observing the how the system's water requirements change as a function of small changes in duty cycle, the system could then be classified as satisfied or unsatisfied.

Real systems are not usually entirely satisfied or unsatisfied (e.g., there was not a sharp inflection point in Fig 3-6a); as such, this test would need to be modified to quantify the degree to which a system was satisfied. Nevertheless, the test would provide a quantitative method of evaluating progress towards current global goals.

Much of the recent literature on IWS has tried to reassure utilities that i) IWS is not an effective means of controlling customer demand, and that ii) converting to CWS does not require extra water (The World Bank, 2013; Charalambous and Laspidou, 2017). The gradients in Table 4.2 are helpful qualifiers for such claims. Where demand is satisfied and leakage is low, the water requirements for converting to CWS can be low. However, for utilities managing unsatisfied IWS, their trial-and-error operations have taught them that the water-demand gradient for their system (V_P^0/t^0) is steep and if that gradient were constant, converting to CWS would require $1/t^0$ more water. The water-demand gradient is not, however, constant; the gradient reduces when unsatisfied systems become satisfied. Nonetheless, without leak repair, converting to CWS will still increase leaked volumes by at least $1/t^0$ and for currently unsatisfied systems, demand will also increase. Having a unifying framework to account for the perspectives of CWS, satisfied IWS, and unsatisfied IWS will be important if the policy-level prosing about CWS is going to create change at the utility level.

4.2 Causes of a reduced duty cycle

4.2.1 Graphical example

Consider again the same three systems as before. This section models how much each system would have to reduce its duty cycle to compensate for three changes: a 10% reduction in the available total water, a 10% increase in the volume demanded by customers, and a 10% increase in the EOA of each system. In each system, initial customer demand is taken to be 80% of the initially available water, as before.

Reducing the available water by 10% causes the unsatisfied IWS (OB in Fig 4-2a) to move from point B to point B3, reducing its duty cycle by 10%. For both satisfied systems (i.e., OC and OE), customer demand was inelastic; therefore, the water supply deficit had to be compensated for with reduced leakage. Accordingly, the leakage rate (initially 20%) needed to reduce by half, which required reducing both duty cycles by 50% (C to C3 and E to E3 in Figs 4-2a and b).

Increases in customer demand have no effect on the unsatisfied IWS's duty cycle (Fig 4-2c). Increased demand does, however, decrease the fraction of demand that the

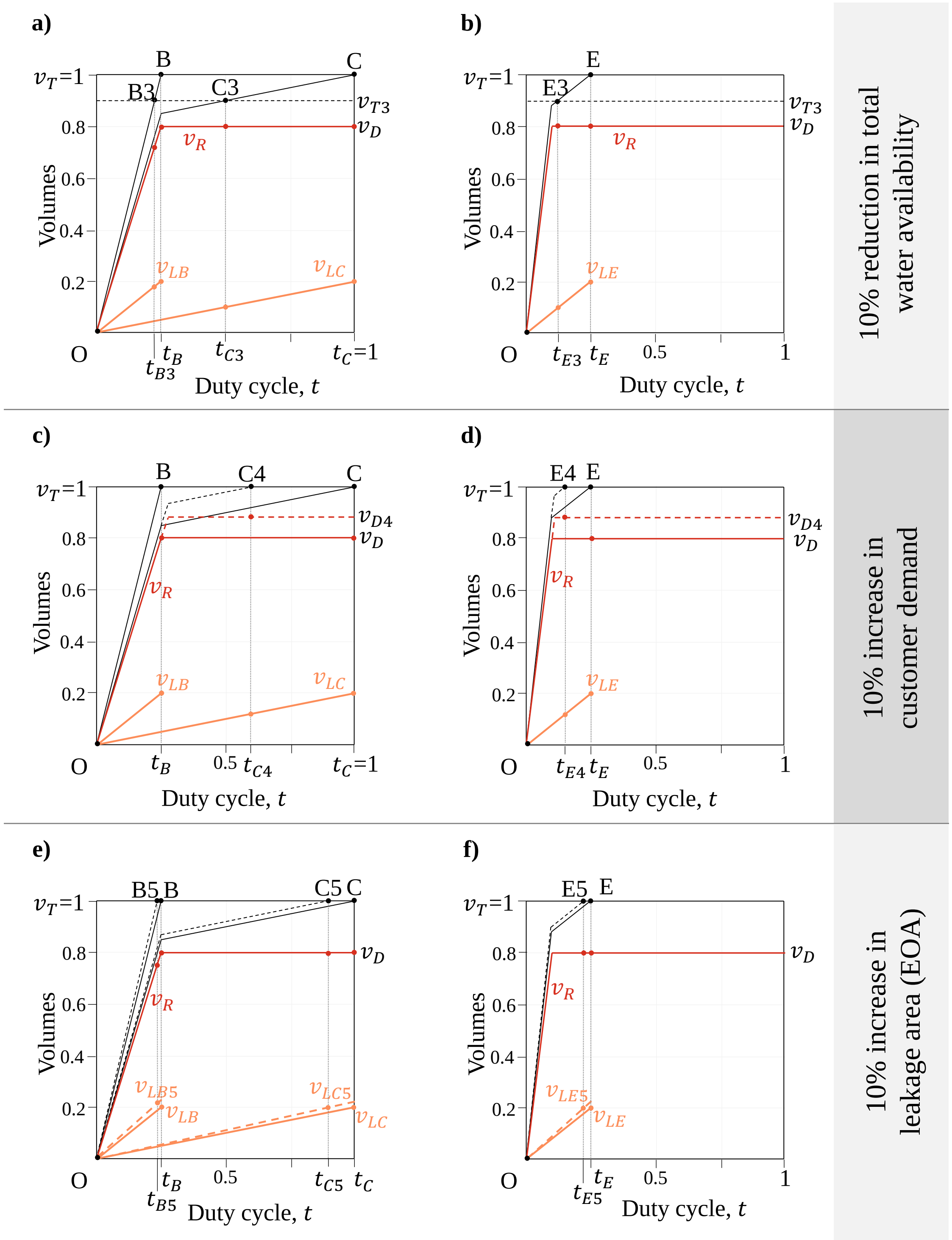

Figure 4-2: **The quantitative causes of IWS.** The reduction in duty cycle induced by system changes for three systems (OB, OC, and OE). The systems' new configurations are shown with dashed lines in each subfigure. Subfigures a) and b) show a reduction in the available water by 10%; c) and d) show an increase in demand by 10%, and e) and f) show an increase in EOA by 10%.

Table 4.3: **Quantitative causes of IWS.** The required reduction in duty cycle caused by reduced available water, increased customer demand, and increased EOA, for three systems: an unsatisfied IWS ($t^0 = 0.25$), a satisfied IWS ($t^0 = 0.25$), and an initially-continuous water supply ($t^0 = 1$). Before these changes, each system had a leakage rate equal to 20% of its initially-available water.

Change in t caused by:	Unsatisfied IWS (B)	Satisfied IWS (E)	CWS[a] (C)
10% water shortage	$\Delta t = -0.025$ ($\Delta t/t^0 = -10\%$)	$\Delta t = -0.125$ (-50%)	$\Delta t = -0.5$ (-50%)
10% demand increase	$\Delta t = 0$ (0%)	$\Delta t = -0.1$ (-40%)	$\Delta t = -0.4$ (-40%)
10% leakage (EOA) increase	$\Delta t = -0.0049$ (-1.96%)	$\Delta t = -0.023$ (-9%)	$\Delta t = -0.091$ (-9%)

[a] Satisfied, initially-continuous water supply (C).

unsatisfied IWS meets. For both the satisfied systems (OC and OE), a 10% increase in demand increased the total demand from 80% of the available water supply to 88%. Therefore leakage, which starts at 20%, must be reduced to 12%. To accomplish this, the duty cycle must decrease by 40% in both satisfied systems (Figs 4-2c and d).

Finally, if the EOA of each system increased by 10%, leakage would, unchecked, increase to 22% of the total supply, requiring a supply increase of 2%, which is not available. Accordingly, the unsatisfied IWS compensates for the increased EOA with a reduction in its duty cycle by 1.96% (2/102). The CWS and the satisfied IWS, again have to make up the difference with leakage alone, necessitating a 9% (2/22) reduction in duty cycle in each case. These results are summarized in Table 4.3.

4.2.2 Analytic results

Generalizing these examples, the effect of insufficient total available supply can be modeled by $\partial t/\partial V_T$, (recall t is duty cycle, not time!) which is simply the inverse of

Eq 4.4:

$$\therefore \frac{\partial t}{\partial V_T} = \begin{cases} \frac{1}{V_D \frac{h^\phi}{\gamma_S} + V_{LC} a h^\alpha} = \text{const.} = \frac{t^0}{V_P^0} & : th^\phi < \gamma_S \text{ (Unsatisfied)} \\ \frac{1}{V_{LC} a h^\alpha} = \text{const.} = \frac{t^0}{V_L^0} & : th^\phi > \gamma_S \text{ (Satisfied)} \\ \text{undefined} & : th^\phi = \gamma_S \end{cases} \tag{4.6}$$

Increased demand is modeled as an increase in the volume of demand (V_D), not the ease at which the demand is satisfied by the system (K_D). Rearranging Eq 4.1 and assuming that each utility inputs all of its (constant) available volume (i.e., $V_P = V_T$):

$$t = \begin{cases} \frac{V_T}{K_D h^\phi + V_{LC} a h^\alpha} & : th^\phi < \gamma_S \text{ (Unsatisfied)} \\ \frac{V_T - V_D}{V_{LC} a h^\alpha} & : th^\phi \geq \gamma_S \text{ (Satisfied)} \end{cases} \tag{4.7}$$

$$\therefore \left.\frac{\partial t}{\partial V_D}\right|_{K_D} = \begin{cases} 0 & : th^\phi < \gamma_S \text{ (Unsatisfied)} \\ \frac{-1}{V_{LC} a h^\alpha} = \text{const.} = -\frac{t^0}{V_L^0} & : th^\phi > \gamma_S \text{ (Satisfied)} \\ \text{undefined} & : th^\phi = \gamma_S \end{cases} \tag{4.8}$$

The effect of increased EOA on supply duration for an unsatisfied IWS is found by rearranging Eq 4.1, again assuming that all available water is input into the system ($V_P = V_T$):

$$\begin{aligned} V_T &= V_D \frac{th^\phi}{\gamma_S} + V_{LC} a t h^\alpha & : th^\phi < \gamma_S \text{ (Unsatisfied)} \\ \therefore t &= \frac{V_T}{V_D h^\phi / \gamma_S + V_{LC} a h^\alpha} & : th^\phi < \gamma_S \text{ (Unsatisfied)} \\ \therefore \frac{\partial t}{\partial a} &= V_T \left(\frac{-V_{LC} h^\alpha}{(V_D h^\phi/\gamma_S + V_{LC} a h^\alpha)^2} \right) \neq \text{constant} & : th^\phi < \gamma_S \text{ (Unsatisfied)} \\ &= V_T \left(\frac{-V_{LC} h^\alpha}{(V_T/t)^2} \right) \\ \therefore \frac{\partial t}{\partial a} &= \left(\frac{-V_{LC} h^\alpha}{V_T} \right) t^2 = (\text{const.}) t^2 = \frac{-t v_L}{a} & : th^\phi < \gamma_S \text{ (Unsatisfied)} \end{aligned} \tag{4.9}$$

Table 4.4: **The analytical causes of IWS.** The duty cycle reduction required by supply shortfall, demand increase, and EOA increase. Superscript ^{0} indicates a variable evaluated at its initial value.

Causes	Gradient	Unsatisfied IWS	Satisfied IWS
Supply shortfall	$-\frac{\partial t}{\partial V_T}$	$-\frac{t^0}{V_T^0}$	$-\frac{t^0}{V_L^0}$
Demand increase	$\frac{\partial t}{\partial V_D}$	0	$-\frac{t^0}{V_L^0}$
Leakage (EOA) increase	$\frac{\partial t}{\partial a}$	$-\frac{t}{a} v_L{}^{\ddagger}$	$-\frac{t}{a}{}^{\ddagger}$

‡ Unlike other derivatives shown, these are not constant

Similarly, in a satisfied IWS:

$$
\begin{aligned}
t &= \frac{V_T - V_D}{V_{LC} a h^{\alpha}} && : th^{\phi} > \gamma_S \text{ (Satisfied)} \\
\therefore \frac{\partial t}{\partial a} &= \left(\frac{V_T - V_D}{V_{LC} h^{\alpha}}\right)\left(\frac{-1}{a^2}\right) \neq \text{constant} = \frac{-t}{a} && : th^{\phi} > \gamma_S \text{ (Satisfied)}
\end{aligned} \tag{4.10}
$$

These findings are summarized in Table 4.4.

4.2.3 Discussion

In the narratives about IWS, 'greedy customers' are often blamed for the existence of IWS. The model demonstrates that high customer demand can necessitate IWS, however, ongoing increases in demand in already unsatisfied IWS are not the cause of further reductions in duty cycle (Table 4.4). To the knowledge of the author, this classification of when customer demand can and cannot affect an IWS's duty cycle has not been identified in the literature to date.

From the utility's perspective, unsatisfied IWS are more robust than satisfied IWS. Unsatisfied IWS are less influenced by changes in total water availability and by increases in EOA than satisfied IWS (by a factor of v_L in both cases; Table 4.4). Moreover, unsatisfied IWS are unaffected by customer demand. While demonstrating the robustness of unsatisfied IWS is an important outcome of this analysis, it must be noted that the robustness comes at the cost of customer satisfaction. From the perspective of the customer, unsatisfied IWS are the least robust. In satisfied IWS, changes in duty cycle do not affect the volume received by customers.

All derivatives were found to be either constant, zero, or increasing in magnitude with respect to duty cycle (Table 4.4). As the duty cycle decreases, therefore, equal percent changes in system characteristics will induce smaller and smaller absolute change in the duty cycle (Table 4.4). Regulators and benchmarking efforts should, therefore, be cautious if they rely on the duty cycle to assess or compare IWS with low duty cycles.

The duty cycle of systems, subject to increases in customer demand (total or per capita), increases in EOA, or reductions in available total water will degrade more quickly for satisfied IWS, and more slowly (or not at all) once systems are unsatisfied (Table 4.4). Engineers in charge of IWS are subject to significant and conflicting political pressures to ensure customers are content; they "often reallocate water from areas of low political pressure to areas of higher pressure, constantly making adjustments until people stop shouting" (Anand, 2011, p.553). An IWS system or sub-system with $t > t_S$ is therefore likely to have its duty cycle reduced, either passively (e.g., through increased EOA or growth in consumption), or actively (e.g., to divert water elsewhere). The tipping point between satisfied and unsatisfied IWS, therefore, is a local optimum for system operators.

4.3 Case study: MNWS

Chapter 2 summarized the context of water supply in Delhi and of private-sector participation in water projects in India. One important application of the derivations in this chapter is assessing project feasibility. The Malviya Nagar Water Services (MNWS) project in Delhi is one such example.

MNWS is a distribution project tasked not only with converting a fraction (about 1%) of Delhi's system from 3-8 hours/day to CWS, but also with reducing the total water input from 286 lpcd to 150 lpcd (Table 4.5). Performance penalties for intermittent supply and/or low pressure are only waived if MNWS does not receive a bulk

Table 4.5: **MNWS targets.** Targets from Delhi Jal Board (2012b,c); penalties from Delhi Jal Board (2012g).

Performance indicator	Baseline (2012)	Target	Deadline	Max penalty[c] (% of revenue)
Water supply coverage (% of population)	84%	100%	2014	20%
Water supply (lpcd input to system)	286	150	2021	20%[d]
Continuity (hours/day)	3-8	24	2014	20%
Metering (% of connections)	41%	100%	2014	20%
Non-revenue water (%)	68%	15%	2021[a]	100% [e]
Water quality (% samples within standard)	"not meeting"	100%	2014	10%
Complaint response (% redressed within 24 hours)	no data	80%	2014	20%[f]
Bill collection (% of billed total collected)	81%	95%	2021[b]	100% [e]

[a] <40% by 2014, <30% by 2016, and <20% by 2019
[b] >85% by 2019
[c] Penalty = Revenue x max penalty x (actual - target)/target. The maximum total penalty cannot exceed 10% of monthly revenues.
[d] 1% per day of non-compliance, excluding supply interruptions for planned maintenance <12 hours are allowed. Unclear if these can be scheduled daily.
[e] Total revenue scales with billed and collected revenue, therefore these do not have dedicated penalties, but are structural incentives. They are exempt from the 10% maximum penalty
[f] Applies if <95% under review or <80% resolved within 24 hours

water supply of 150 lpcd. More details about MNWS are included in Appendix A.1.1.

4.3.1 MNWS target robustness

At the outset of the project, the area had 68% NRW and so it was likely unclear how much of the total water input went to customers and how much went to leakage. In the ideal scenario set forth by the contract, total water input would be 150 lpcd and NRW 15%. Given that Indian standards suggest that at least 135 lpcd be provided to city residents, it is likely that the contract envisioned a physical leakage rate of 10% and the remaining third of NRW would therefore account for non-paying customers. Achieving an NRW level of 15% in a high-pressure CWS would put this project in the 81st percentile for global CWS (author's calculation not shown, but based on the IBNET data (Van den Berg and Danilenko, 2011)); a major feat for an IWS. Concerningly, however, this achieved feat would have no margin for error. With a physical leakage of only 10%, a change in population or per capita demand by only 5% would require cutting the system's duty cycle by 45% (from Eq 4.8; Fig 4-3a):

$$\begin{aligned}
\Delta t &= \int_{V_D^0}^{1.05V_D^0} \frac{\partial t}{\partial V_D} dV_D \\
\therefore \Delta t &= \int_{V_D^0}^{1.05V_D^0} \frac{-t^0}{V_L^0} dV_D \\
\therefore \Delta t &= 0.05 V_D^0 \frac{-t^0}{V_L^0} \\
\therefore \frac{\Delta t}{t^0} &= 0.05 \frac{-V_D^0}{V_L^0} \\
\therefore \frac{\Delta t}{t^0} &= -0.05 \frac{v_D^0}{v_L^0} = -0.05 \frac{0.9}{0.1} = -45\% \qquad (4.11)
\end{aligned}$$

Accurately predicting either population growth or customer demand within 5% is nearly impossible for a growing city like Delhi, but accurately predicting their product is even less possible. Even if the MNWS project achieves its goals, it will not be robust. Because of its contract design, a successful MNWS project would still be only a 6% error away from returning to less than 12 hours of supply per day.

4.3.2 MNWS target feasibility

Beyond having no margin for error in the targeted scenario, achieving the targeted scenario may also be difficult due to the required demand reduction. Assuming that half of the project area's NRW (68%) was due to physical leakage (a regional approximation suggested by McIntosh (2014)), then initial customer demand would be 189 lpcd.

If the project received 150 lpcd of supply volume without achieving any demand reduction or leak repair, its duty cycle would (conservatively assuming the system is

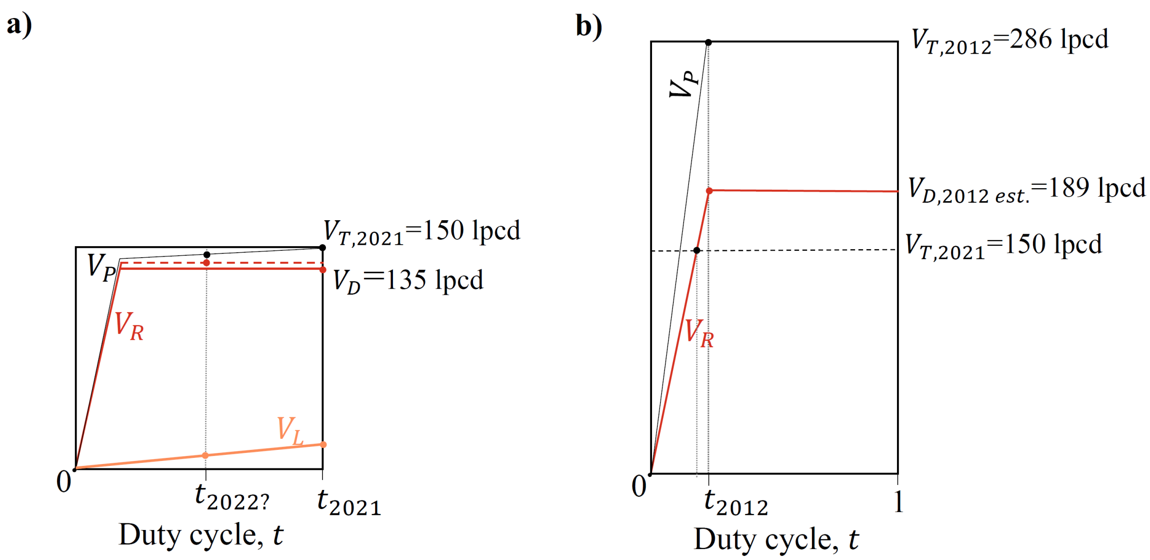

Figure 4-3: **MNWS target robustness and feasibility.** a) Project robustness. The contracted ideal is depicted (solid lines) with $t_{2021} = 1$. A customer demand increase of 5% (dashed red line) induces duty cycle reduction to $t_{2022?}$. b) Target feasibility. Without demand reduction, when the total water available reduces to 150 lpcd (dashed black line), the duty cycle will reduce (vertical dotted lines).

unsatisfied) reduce by -48% (Eq. 4.6; Fig 4-3b):

$$
\begin{aligned}
\Delta t &= \int_{V_{T,2012}}^{V_{T,2021}} \frac{\partial t}{\partial V_T} dV_T \\
\therefore \Delta t &= \int_{V_{T,2012}}^{V_{T,2021}} \frac{t_{2012}}{V_{T,2012}} dV_T && : th^{\phi} < \gamma_S \\
\therefore \Delta t &= (V_{T,2021} - V_{T,2012}) \frac{t_{2012}}{V_{T,2012}} && : th^{\phi} < \gamma_S \\
\therefore \frac{\Delta t}{t_{2012}} &= \frac{150 - 289}{289} = -48\%
\end{aligned}
\tag{4.12}
$$

This problem cannot be solved through leak repair alone. Without demand reduction, it must be suppressed by shortened duty cycles. With zero leaks, to suppress demand to only 150 lpcd the duty cycle will need to be reduced by 21% (189-150)/189). If demand must be reduced enough to allow for 10% physical leakage, then the duty cycle must be reduced by 29%.

To control demand without reducing the duty cycle, higher prices are often suggested (e.g., Seetharam and Bridges (2005); Van den Berg et al. (2008)). However, in order to avoid public criticism of privatization, the price seen by customers is not often under the private operator's control (e.g., Van den Berg et al. (2008)). Therefore without a price signal to control V_D and with V_T out of their control, the means by which the MNWS project could achieve its targets (high-pressure, continuous water supply) are unclear. Even if every single leak were found and fixed, without demand reduction, duty cycles in MNWS will need to shorten, not lengthen. In fact, in 2017, residents complained that MNWS's duty cycles had indeed shortened (ToI, 2017).

This example demonstrates that the relationships derived in this chapter and Chapter 3 can help utilities, regulators, and funding agencies structure and execute better projects (e.g., where success is physically feasible). The proposed model is uniquely useful because it can be used before the start of a project (i.e., *a priori*), as it does not require detailed network information.

4.4 Conclusions

The examples, graphs, and derivations in this chapter constitute a framework that can be used to evaluate and/or predict the causes and effects of changing a water system's duty cycle. With international and national attention being placed on issues of water availability, understanding what creates and sustains IWS will be critical to achieving policy goals (be they CWS or water that is 'available when needed'). Eq 4.4 provides the first theoretical foundation for distinguishing between the satisfied and unsatisfied IWS. Further work is needed to validate its ability to determine customers' satisfaction in real-world conditions with only readily-available utility data.

Distinguishing between satisfied and unsatisfied IWS proved crucial to understanding which causes and effects were most influential for which systems. The fragility of satisfied systems with low leakage levels and especially of CWS was demonstrated in stark contrast to the robustness of unsatisfied IWS. Unfortunately, the robustness of unsatisfied IWS, which benefits utilities, comes by reducing the water delivered to customers. To increase system robustness without reducing water delivered to customers, projects should plan on reserving extra available water so that if there are unexpected changes in the system, duty cycles do not need to shift dramatically. This would be most important for systems that target low leakage levels and long or continuous duty cycles (as most projects to improve IWS do).

Tools to understand the causes and effects of IWS will better equip utilities, policy makers, and regulators to operate, design, and monitor intermittent and continuous water supply projects. The tools demonstrated in this chapter showed how MNWS' limited total water availability and its limited ability to influence customer demand make the MNWS project unlikely to succeed.

Before concluding, it should be emphasized that the first-order relationships derived in this chapter do not capture the longer-term (potentially-negative) effects of IWS. Hamilton and Charalambous (2015) demonstrated that after two years of IWS in a city in Cyprus, when that system returned to CWS, the total leakage had increased by 15%. While some of this increase may have been because routine leak repair was postponed or thwarted by IWS, IWS may also have accelerated the system's baseline rate of leakage increase.

Based on the potentially-accelerated growth in EOA and the severe implications for water quality due to IWS, IWS should not be adopted without careful consideration. Nevertheless, the literature discussing IWS should avoid claiming that IWS does not reduce leakage. Utilities are the target audience of such literature and they are very aware of the short-term effects of changing their duty cycle, which include reduced leakage.

4.4.1 Full disclosure statement

The author has an unrelated, ongoing collaboration with the MNWS project. The outcome of the MNWS case study could be interpreted as decreasing MNWS' culpability should the project fail to meet its targets. The author declares that this potential conflict of interest has not motivated or influenced the results presented here. MNWS had no role in the analysis presented here or in the choice to publish it.

Chapter 5

Maximizing gross margin in IWS

> Optimising existing systems that deliver water to the household represents 'low-hanging fruit' for rapidly expanding safe water access.
>
> Shaheed et al. (2014, p.192)

The articulation of the second law of thermodynamics (systems tend towards disorder; entropy increases) in the mid-nineteenth century shifted how the technical community viewed its relationship to nature and induced an enduring focus on minimizing the 'natural' tendency towards waste (Wise and Smith, 1989; Gilmartin, 2003). The need to minimize waste appears in mid-nineteenth century engineering discussions of whether to use intermittent or continuous water supply in London and Calcutta (Health of Towns Association, 1846; London Board of Health, 1850; Secretary of State for India in Council, 1875). Since 1992, when the Dublin Statement declared water as an "economic good," conceptions of financial waste and water waste have become entangled (UN, 1992, Principle 4). This entanglement is manifest in the global prevalence of the metric 'non-revenue water' (NRW). While technically a financial metric (unsold water divided by produced water), NRW has become a proxy for leakage and is a key performance indicator for water utilities. Unsold water now defines a water system's waste and efficiency. Since the late 1990's, India's water sector reforms have mirrored global trends and focused on economics rather than engineering (Sangameswaran, 2014).

To compliment the important discourse about the benefits and limitations of using economic tools and/or private corporations to manage and improve the water sector (see Section 2.2), this chapter explores the expected behavior of Rational Water, a hypothetical water utility governed only by short-term financial incentives. As Rational Water is constructed to maximize its short-term financial gains, this chapter will focus primarily on Rational Water's gross margin. Gross margin (GM) is typically defined in percent as (Revenue − Costs)/Revenue. However, it is occasionally accounted for using gross margin dollars (Ψ; Revenue − Costs). In systems where costs grow faster than revenue, maximizing gross margin percent may lead to trivially small revenues; therefore, unless noted otherwise, this chapter will adopt the latter definition of gross margin (i.e., gross margin dollars). Similarly, Rational Water is assumed to act only in order to maximize its gross margin dollars, unless otherwise noted.

It may be desirable from a public health, political, or social standpoint to have a water utility behave in a certain way. Recent policy discourses in India have focused on high-pressure CWS being such a desired behavior. This chapter aims to identify where the desired behavior of water utilities aligns or diverges from economic rationality (i.e., the behavior of Rational Water). This chapter will show when (if ever) unregulated private sector involvement in water supply may result in the desired outcomes. This chapter will also quantify what performance incentives are required to ensure Rational Water adopts the desired behavior.

Chapter 2 gives context for private sector involvement in water supply in India. To provide examples of existing performance metrics for such projects, this chapter begins with a brief summary of four privatization contracts in India. Next, this chapter supplements the IWS model of Chapter 3 by including the financial gains and losses associated with input water, water delivered to customers, and leak repair.

Applying the supplemented model of Chapter 3, this chapter explores five components of Rational Water's expected behavior. The first two components consider how Rational Water would operate an IWS, if its pipe quality (EOA) were held constant. The first of these considers the supply pressure and duty cycle that maximize Rational Water's gross margin. The second component imposes a minimum supply pressure and then considers the incentives required to ensure Rational Water would provide all of its available water to the network.

The third component considers the circumstances in which Rational Water would repair its leaks (reduce its EOA) in order to provide high-pressure CWS. The fourth considers how Rational Water would allocate water between independent subnetworks in order to optimize its performance over a number of possible benchmarks, including gross margin and NRW. And finally, the fifth component explores Rational Water's ideal supply period (i.e., 1/frequency).

Performance incentives link a utility's technical performance to its financial returns. Components two and three explore scenarios where technical performance and financial returns conflict and therefore these sections derive the minimum incentives required for Rational Water to adopt the desired performance.

5.1 Examples of performance contracts in India

This section summarizes the key, publicly-available, contract details from three public-private-partnerships in Delhi (MNWS, MVV, and NWS) and one in Nagpur (Orange City Water (OCW)). Each of these contracts layout detailed performance metrics, dates by which they need to be met, and penalties that are incurred if the targets are not met. Some project documents describe targets that have no financial penalties associated with non-compliance. Only financially-penalized targets are summarized here.

Each contract included performance penalties (and sometimes bonuses) if targets were missed. Penalties are weighted by the maximum potential deduction from the contractor's payment. Most penalties scaled linearly (e.g., penalty=(total revenue)*(penalty weight)*(target-actual)/target). Penalties for missing targets relating to NRW ranged from 5-100% (Table 5.1). Penalties for intermittent supply (lack of continuity) ranged from 10% to 30% (Table 5.1).

Table 5.1: **PPP performance incentives.**

Project	MNWS	MVV: Meharauli	MVV: Vasant Vihar	OCW	NWS
City	Delhi	Delhi	Delhi	Nagpur	Delhi
	Maximum revenue penalty for missed target (%)				
NRW	100%[a*]	-	16%[e]	20%[h]	5%[j]
Metering	20%[a]	20%[c]	-	-	-
Quality	10%[a]	10%[c]	-	10%[h]	20%[j]
Coverage	20%[a]	20%[c]	-	-	10%[j]
Continuity	1%/fail[a]	1%/fail[c]	16%[e]	1%/fail[h]	10%[j]
Pressure	-	20%[c]	-	-	-
Collection efficiency	100%[a*]	-	2%[e]	-	-
Energy efficiency	100%[a*]	-	-	-	-
Complaint responsiveness	20%[a]	20%[c]	4%[e]	-	20%[j]
Maximum total penalty	10%/y[b]	10%/y[d]	10%/y[f]	-	-
	Effective penalties due to remuneration structure (%)				
NRW	100%[a]	-	16%[g]	100%[i]	100%[k]
Collection efficiency	100%[a]	-	2%[g]	100%[i]	-

[a] Delhi Jal Board (2012g, Sechedule 8)
[b] Delhi Jal Board (2012c, Article 27.2)
[c] Delhi Jal Board (2012h, Sechedule 8)
[d] Delhi Jal Board (2012d, Article 27.2)
[e] Delhi Jal Board (2012i, Sechedule 8)
[f] Delhi Jal Board (2012e, Article 27.2)
[g] Delhi Jal Board (2012e, Article 13.1.3)
[h] Dinesh Rathi & Associates (2008, pp. 40-43)
[i] Dinesh Rathi & Associates (2008, p. 123)
[j] Delhi Jal Board (2012a, pp.466-484)
[k] Delhi Jal Board (2012f, p. 62)
* Exempt from maximum total penalty

To limit the risk of the private operator, MNWS and MVV projects capped the total penalty that could be assessed against the operator at 10% per year (Table 5.1). Reviewed documents for OCW and NWS did not include a penalty cap (Dinesh Rathi & Associates, 2008; Delhi Jal Board, 2012a), but the cap's absence from the OCW documents may be because the only available document was a detailed project report and not the full request for proposal.

Anand (2011) warns that water supply improvement projects are more than technical and are embedded with value judgments about who is deserving of what quality of water supply. Perhaps the MVV project provides such an example. It has two separate sets of indicators for its two zones (Meharauli and Vasant Vihar), one of which (Meharauli) as of 2014 housed 94% of Delhi's unscheduled supply zones (75 of 80 in 2014; locations are not indicated in Fig 2-3).

While each contract differs in which metrics are penalized and by how much, one major difference between contracts is the structure by which the operator gets paid (remunerated; Table 5.1). MNWS and OCW contracts base their operator remuneration on collected billings (Dinesh Rathi & Associates, 2008; Delhi Jal Board, 2012c) and NWS bases it on billed volumes (Delhi Jal Board, 2012f, p. 62). In each of these three cases, therefore, the operators' revenue scales linearly with the volume of water it bills. Therefore, while the contract penalty percentages may appear balanced, the effective penalty for missing the non-revue water target is therefore 100% for each of these three projects (Table 5.1). Similarly, the penalty for collection efficiency is also 100% in MNWS and OCW projects (Dinesh Rathi & Associates, 2008; Delhi Jal Board, 2012c). These structural financial penalties may easily overshadow other hydraulic performance incentives.

In a more promising model, MVV assesses a monthly management fee independent of the billed volume (Delhi Jal Board, 2012e, Article 13.1.3). This reduces the relative influence of NRW as compared to other performance incentives.

Table 5.2: **Overlapping definitions of NRW and physical leaks.** Normalized by the total volume of water input into the system (V_T), the fraction of water that goes to physical leaks (np), unauthorized customers ($n(1-p)$), or paying customers ($1-n$) is shown by the italicized expressions.

<table>
<tr><td rowspan="3">Total input volume
1</td><td rowspan="2">NRW
n</td><td>Physical leaks
np</td></tr>
<tr><td>Unauthorized or non-paying customers
$n(1-p) = u(1-np)$</td></tr>
<tr><td>Revenue water
$1-n$</td><td>Paying customers
$1-n = (1-u)(1-np)$</td></tr>
</table>

5.2 Financial model of IWS

To supplement the model of Chapter 3, this section includes the variable revenues and costs associated with different operational modes for a piped-water system. A model for the costs associated with leak detection and repair is also proposed. These will be used to explore the financial consequences of Rational Water's operation and management strategies throughout the remainder of the chapter.

5.2.1 Variable revenues and costs

Of the total volume of water input into a water network, a (volumetric) fraction n does not derive revenue (i.e., is NRW; Table 5.2). Conversely, the fraction $1-n$ of input water is delivered to paying customers. The volumetric fraction of the input water that goes to physical leaks is np, where p is the percent of NRW that is due to physical leaks. As np is the fraction of the total supply that goes to physical leaks, the remainder (i.e., $1-np$) goes to customers (paying and non-paying). The fraction delivered to non-paying customers is $u(1-np)$, where u is the fraction of customer consumption that is not paid for. Equivalently, this fraction is also the NRW less physical leakage (i.e., $n-np$). These ratios and their relationships are summarized in Table 5.2.

The hydraulic behavior of paying and non-paying customers is assumed to be identical. Chapter 3's IWS model of V_R, accounts for the volume delivered to both paying and non-paying customers. This section adds the distinction of paying cus-

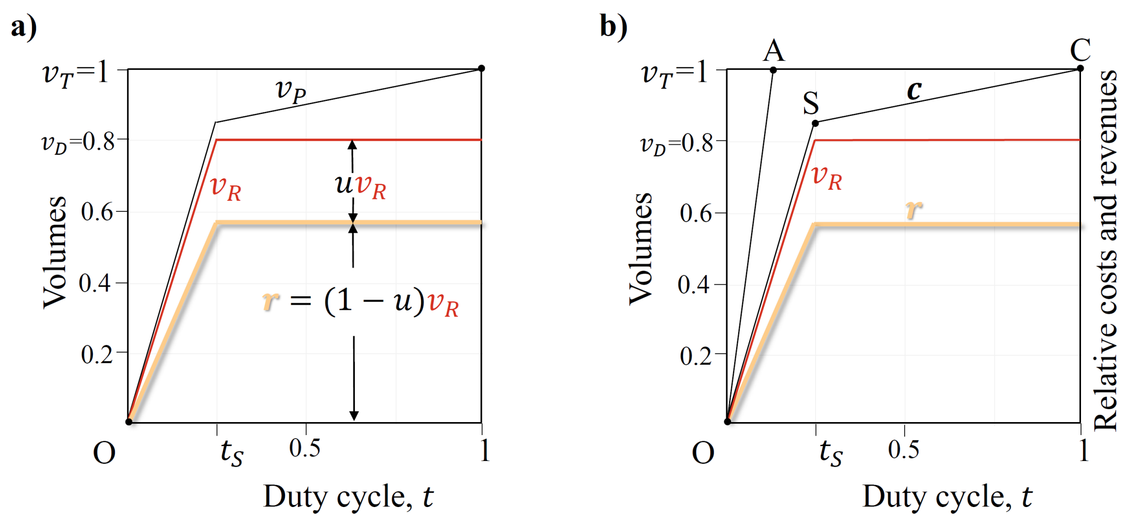

Figure 5-1: **Revenue from IWS.** The fraction $(1-u)$ of paying customers is superimposed on the model of input volume (thin black lines) and customer consumption (red lines of medium weight). The volume of water received by paying customers $(1-u)v_R$ is shown as thick, light-orange lines. If variable costs and revenues are normalized by CV_T and RV_T, then they follow exactly the lines of v_P and $(1-u)v_R$, shown as c (thin black lines) and r (thick light-orange lines), respectively, in panel b).

tomers, which is shown in Fig 5-1.

In order to explore a utility's economic incentives for supplying water or upgrading a system, the price at which a utility sells water is represented by R, whose units are dollars per cubic meter of water sold. Similarly, a utility's variable costs can be modeled by C, in dollars per cubic meter of water pumped. A utility's total variable costs will therefore be CV_P and its total revenues $RV_P(1-n)$. Both costs and revenues are non-dimensionalized by the maximum possible revenues and costs that a utility could incur, which would happen if the utility delivered and sold all of its available water. Revenues are, therefore, normalized by RV_T and costs by CV_T. Non-dimensional revenues and costs are denoted r and c, respectively (Fig 5-1b).

For algebraic convenience, a utility's *price margin* (m) is defined as its maximum possible gross margin percent (in a system with 0% NRW):

$$m \equiv \frac{R - C}{R} \tag{5.1}$$

$$\therefore \frac{C}{R} = 1 - m \tag{5.2}$$

Note that this definition of price margin differs from the gross margin because it does not account for the influence of NRW (leaks and non-paying customers) on margin. A utility's gross margin percent will be:

$$\begin{aligned} GM &= \frac{\text{Rev} - \text{Cost}}{\text{Rev}} \\ &= \frac{RV_P(1-n) - CV_P}{RV_P(1-n)} \end{aligned}$$

$$\therefore GM = \frac{R(1-n) - C}{R(1-n)} = 1 - \frac{C}{R(1-n)} \tag{5.3}$$

$$\therefore GM = 1 - \frac{1-m}{1-n} = \frac{m-n}{1-n} \tag{5.4}$$

To simplify the algebra that follows, R_a represents an equivalent price of water were the utility's total revenue spread all water it delivered to customers (i.e., paying and non-paying customers):

$$\text{Rev} = V_R(1-u)R = V_R R_a$$

$$\therefore R_a = (1-u)R = (\frac{1-n}{1-np})R \tag{5.5}$$

5.2.2 Costs of leak repair

Water networks develop new leaks over time; bursts and reported leaks are typically modeled as increasing linearly with time (Lambert and Fantozzi, 2005). The model proposed thus far holds system parameters constant and, therefore, does not capture temporal trends like increases in EOA.

The International Water Association (IWA) proposes that systems have a certain unavoidable rate of leakage that depends on the system's size, density, and pressure

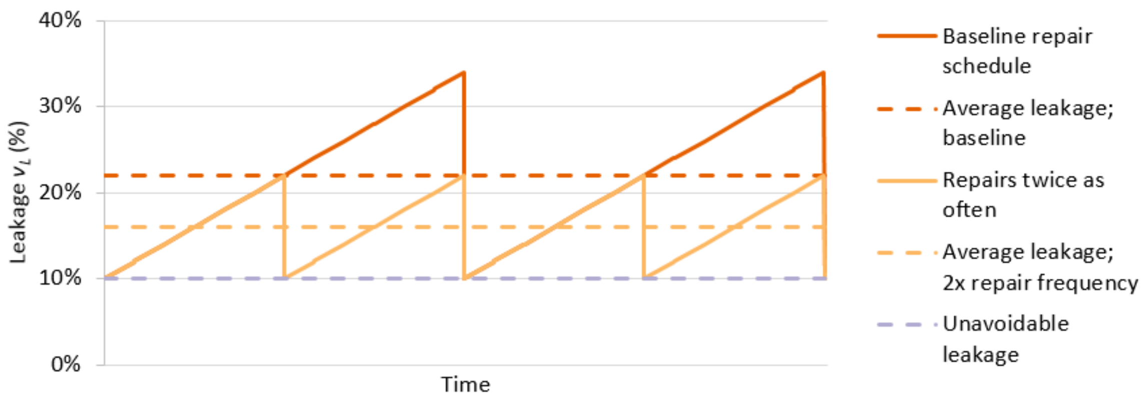

Figure 5-2: **IWA leak repair model.** Leaks grow linearly with time, until detected and repaired, after which the IWA assumes the system returns to its baseline leakage level (gray dashed line, here shown as 10%). Doubling the leak detection (from baseline dark orange to yellow) results in a new average leakage level (dashed yellow) that is halfway between the baseline average (dashed dark orange) and the unavoidable leakage level.

(Lambert and Fantozzi, 2005; Lambert and McKenzie, 2002). While this leakage is not technically 'unavoidable,' it is prohibitively expensive to find.

The IWA assumes that a single leak detection campaign (and its associated leak repairs) will return a system to its baseline level of leakage. Under this model, any system's average level of leakage depends only on its baseline leakage level, the rate of leakage increase, and the frequency of leak detection (and repair) (Lambert and Fantozzi, 2005). Doubling a utility's leak detection frequency, therefore, would reduce its leakage by half of the difference between its current average leakage level and its baseline level (Fig 5-2). Unfortunately, the IWA's assumption that all avoidable leaks can be identified in a single campaign does not apply well to IWS with large EOA (Kumar, 1997).

In the context of intermittent systems with high leakage rates, Kumar (1997) suggests that multiple rounds of leak detection and repair are required before most leaks can be fixed. Specifically, Kumar suggests that Tata Consulting Engineers in India typically are able to reduce a network's leakage by 50% after an initial round of leak detection and repair.

Therefore, both the IWA model for leak detection and the one proposed by Kumar (1997) imply that the costs of leak detection grow asymptotically as the leakage level approaches its minimum possible value. Following Kumar (1997), this model considers the costs of finding and repairing 50% of a system's leaks to be approximately constant for a given system, K_R. Accordingly, in a system with an arbitrary EOA (a_X), the cost to obtain a targeted EOA (a_C) is:

$$\mathrm{Cost}_{a_X \to a_C} = -K_R \log_2\left(\frac{a_C}{a_X}\right) \tag{5.6}$$

It will be convenient to non-dimensionalize K_R by the potential revenues that the water system could earn if it operated with its targeted level of NRW (n_C):

$$k_R = \frac{K_R}{RV_T(1-n_C)} \tag{5.7}$$

For systems with extremely high leakage rates, it may be more cost effective to replace the pipes as opposed to finding and fixing their leaks. This is not accounted for in the proposed model. The model, therefore, will overestimate the costs of reducing the EOA in systems where piping should be replaced instead of repaired.

5.3 Optimal operations without penalties

In the absence performance penalties, Rational Water's gross margin dollars (Ψ) can be described by superimposing its water price R and variable cost C onto Eq 3.10:

$$\begin{aligned}
\Psi &= \mathrm{Rev} - \mathrm{Cost} \\
\therefore \Psi &= R(1-u)V_R - CV_P \\
\therefore \Psi &= \begin{cases} (R(1-u)-C)V_D - CV_{LC}ath^{\alpha} & : th^{\phi} \geq \gamma_S \\ th^{\phi}\left((R(1-u)-C)\frac{V_D}{\gamma_S} - CV_{LC}ah^{\alpha-\phi}\right) & : th^{\phi} \leq \gamma_S \end{cases}
\end{aligned} \tag{5.8}$$

Where u is the volumetric fraction of customer consumption that does not generate revenue.

Structured as a maximization problem, Rational Water's choice of duty cycle and supply pressure is:

$$\underset{h,t}{\text{maximize}} \qquad \Psi = V_T \left[(R(1-u) - C)v_R - Cv_{LC}ath^{\alpha} \right] \tag{5.9}$$

$$\text{subject to} \qquad v_R + v_{LC}ath^{\alpha} \leq 1 \tag{5.10}$$

$$v_R = \begin{cases} v_D \frac{th^{\phi}}{\gamma_S} & : th^{\phi} \leq \gamma_S \\ v_D & : th^{\phi} \geq \gamma_S \end{cases} \tag{5.11}$$

$$t, h \in [0, 1] \tag{5.12}$$

Appendix C.1 explores this maximization problem in detail and demonstrates that provided $\alpha > \phi$, as expected, the optimal operating strategy is to lower pressure until the system becomes a CWS, which requires extremely low supply pressures. Specifically, at $t = 1$, the optimal pressure is always less than $\gamma_S^{1/\phi}$ (Eq C.13). For small values of γ_S and fractional values of ϕ, h_{optimal} can be extremely small. This strategy of low pressure supply is not an artifact of the average customer model used in this thesis; it also applies to simple, flat, tree-structured networks where non-linear friction is accounted for (Appendix C.2).

The derivations included in Appendices C.1 and C.2 suggest that in all cases Rational Water would provide extremely low-pressure CWS instead of IWS, yet globally almost one billion people are served by IWS. The difference between the derived optimal duty cycle, and the observed duty cycles in global utilities may be because in real systems, h cannot be arbitrarily reduced. Pressure is additionally constrained by equity and water quality requirements.

5.3.1 Equity constraints on pressure

In an unsatisfied IWS with elevation differences between customers, the pressure head experienced by a customer with elevation E is $H - E$. The daily volume received by that unsatisfied customer will therefore be proportional to $(H - E)^{\phi}$. Given a maximum elevation difference from the average elevation ($\Delta E_{\max}$), pressure is constrained by the minimum acceptable daily volume delivered to a customer. Normalizing by the average daily volume delivered to all customers $\overline{V_R}$:

$$
\begin{aligned}
\frac{V_{R,\min}}{\overline{V_R}} &\leq \left(\frac{H_{\text{equity}} - \Delta E_{\max}}{H_{\text{equity}}}\right)^{\phi} \\
\therefore \left(\frac{V_{R,\min}}{\overline{V_R}}\right)^{1/\phi} &\leq 1 - \frac{\Delta E_{\max}}{H_{\text{equity}}} \\
\therefore H_{\text{equity}} &\geq \frac{\Delta E_{\max}}{1 - \left(\frac{V_{R,\min}}{\overline{V_R}}\right)^{1/\phi}}
\end{aligned}
\tag{5.13}
$$

Consider, for example, a system in which customer elevation varies by 5m from the average and in which 25% is the maximum acceptable reduction in volume due to elevation changes. Therefore $\Delta E_{\max} = 5m$ and $V_{R,\min}/\overline{V_R} = 0.75$. Therefore, in this example, the equity-induced minimum pressure is $5/(1 - 0.75^2) = 11.8m$.

5.3.2 Quality constraints on pressure

Low-pressure supply presents a risk of contaminant intrusion (Besner et al., 2011; Kumpel and Nelson, 2014). Increasing the supply pressure will reduce this risk, but the pressure at which diminishing returns occurs is unknown. Kumpel and Nelson (2014) observed that a pressure of 7-12m limits contamination and above 12m, they observed no contamination in an IWS in India. Similarly, Besner et al. (2011) suggest that pressure in CWS should be maintained above 14m. However operating at higher pressures in an IWS often implies reducing the duty cycle. Chapter 6 specifically considers the water quality trade-offs between increasing the duty cycle and increasing pressure.

5.3.3 Discussion of optimal operations without penalties

The derived optimal supply pressure is very low, especially for systems that are currently IWS and have high EOA. Take, for example, India's pressure target of 17m (in cities with multi-story buildings (CPHEEO, 1999)). The optimal pressure of $h = 0.0225$ for the example used in Appendix C.1 (OA in Fig C-2c), would correspond to a supply pressure of 0.38m. Even Rational Water is not likely to lower its supply pressure as low as suggested by Eq C.13. Doing so would enrage customers and supply only those with the lowest pipe connections.

Most IWS already operate at low pressure and therefore this section's suggestion of increasing the duty cycle by decreasing pressure will not be immediately implementable. Nonetheless, some IWS do supply at high pressure, especially where elevation changes substantially throughout the network (e.g., Erickson et al. (2017)). In such networks, simply reducing the pressure may not be feasible; however, through carefully designed pressure zones, average pressures may be reduced. This section detailed why Rational Water might choose to invest in doing so.

Another limitation to the strategy of low pressure supply is customers who adapt by installing their own suction pumps. Because such pumps can provide 4m or more of suction pressure, the optimal supply pressure in a flat system with universally present suction pumps would be four meters lower than in the same system without pumps. Since the optimal pressure is often below 4m without pumps (Eq C.13), with pumps, the 'optimal' supply pressure could therefore be negative. This is problematic because low and negative pressures pose a substantial contaminant intrusion risk (Besner et al., 2011; Kumpel and Nelson, 2014). For example, in Delhi, where pumps are nearly ubiquitous, the public utility (DJB) has claimed "in 90 per cent of the cases of contaminated water supply, we found that the culprits were booster [suction] pumps" (Bagga, 2012). Taylor (2014) demonstrated a prototype valve capable of preventing suction pumps from inducing negative pressure in the network.

5.4 Incentives required for full supply

Given the practical concerns limiting the adoption of the optimally-low supply pressure (Eq C.13), this section assumes that a system has an externally imposed minimum pressure. For a given pressure head, this section derives the conditions necessary to ensure that Rational Water's gross margin dollars will increase if it supplies all of its available water (i.e., $v_P = 1$; e.g., operates at point A, B or C for systems OA, OB, or OSC in Fig 3-2). In this section NRW (n) and physical losses (p) are defined at the point where the reservoir is empty (i.e., at $v_P = 1$, or equivalently at A, B, or C).

5.4.1 Unsatisfied IWS

In the unsatisfied regime, inputing more water into the network accrues more revenue but also increases costs, therefore only under some conditions will Rational Water input all of its available water.

Along OA: At the point A in Fig 3-2, the reservoir is drained completely ($v_P = v_T = 1$), and $v_{LA} = n_A p_A$ and $v_{DA} = 1 - n_A p_A$. The gross margin dollars of the utility (Ψ) for any point along OA is, therefore:

$$\begin{aligned}
\Psi &= \text{Rev} - \text{Cost} \\
\therefore \Psi &= (R_a - C)V_R - CV_L \\
\therefore \Psi &= (R_a - C)V_D \frac{th^\phi}{t_A h_A^\phi} - CV_{LA}\frac{th^\alpha}{t_A h_A^\alpha} && : th^\phi < \gamma_S \\
&= \frac{th^\phi V_T}{t_A h_A^\phi}\left[(R_a - C)(1 - n_A p_A) - C n_A p_A \left(\frac{h}{h_A}\right)^{\alpha-\phi}\right] && : th^\phi < \gamma_S \qquad (5.14)
\end{aligned}$$

Within the unsatisfied region, Rational Water is justified in increasing its duty cycle until all available water is distributed as long as its gross margin increases with respect to duty cycle. This is equivalent to requiring:

$$\frac{\partial \Psi}{\partial t} > 0$$

which is true iff (from Eq 5.14):

$$\left(\frac{R(1-n_A)}{C(1-n_Ap_A)}-1\right)(1-n_Ap_A) > n_Ap_A\left(\frac{h}{h_A}\right)^{\alpha-\phi}$$

$$\therefore m > 1-\frac{1-n}{1-np\left(1-\left(\frac{h}{h_A}\right)^{\alpha-\phi}\right)} \qquad : n=n_A, p=p_A$$

$$\therefore m > n \qquad : h=h_A, n=n_A \tag{5.15}$$

$$\therefore \frac{R-C}{R} > n \qquad : h=h_A, n=n_A \tag{5.16}$$

Recall that m is defined as Rational Water's price margin ($m = (R-C)/R$). Therefore, if Rational Water operates an unsatisfied IWS, it has incentive to increase its duty cycle until the reservoir runs out, provided its price margin is larger than its NRW (i.e., $m > n$, Eq 5.15).

Similarly, gross margin increases with respect to pressure if:

$$\frac{\partial\Psi}{\partial h} > 0$$

which is true iff:

$$\left(\frac{R(1-n)}{C(1-np)}-1\right)(1-np)\phi\frac{th^{\phi-1}}{t_Ah_A^{\phi}} > np\alpha\frac{th^{\alpha-1}}{t_Ah_A^{\alpha}}$$

$$\therefore m > 1-\frac{1-n}{1-np\left(1-\frac{\alpha}{\phi}\left(\frac{h}{h_A}\right)^{\alpha-\phi}\right)} \tag{5.17}$$

Since $h \in [0, h_A]$, the condition required for full supply to be incentivized can be conservatively estimated as:

$$m > 1-\frac{1-n}{1+np(\frac{\alpha}{\phi}-1)}\ (>n) \qquad : \alpha > \phi \tag{5.18}$$

Along OB: These same equations hold along the line OB, provided NRW and physical loss percentages are defined at the point when $v_p = 1$ for the new system (i.e., $n = n_B$ and $p = p_B$). Just as above, a utility has incentive to increase duty cycle as long as $m > n$, and to increase supply pressure when Inequality 5.17 holds true.

Along OS: The case is slightly different at the point S, since there is still water left in the reservoir (i.e., $v_P < 1$). However, if NRW at point S (n_S) is defined as a fraction of the input water (not available water), Eq 5.15 holds. A utility is incentivized to increase its duty cycle until customers are satisfied as long as its price margin is larger than its observed NRW (i.e., $m > n_S$; for reference, $n_S < n_C$). Beyond the point S (i.e., along SC), the system becomes satisfied and is considered below.

5.4.2 Satisfied IWS

Consider the line SC in Fig 3-2, across which customers are all satisfied; moving along the line SC has no effect on Rational Water's billing or revenue. However, moving from S to C requires more water to be input into the system, which increases Rational Water's costs. A rational utility would, therefore, only supply water continuously (at point C) if the penalty it avoided by doing so was larger than the costs of treating and pumping the additionally-leaked water. Consider, therefore, a generalized penalty of size $P(t,h)$. Rational Water will only pump until CWS is achieved if:

$$\begin{aligned} &P(t,h) > CV_{LC} - CV_{LC}th^{\alpha} && : th^{\phi} \geq \gamma_S \\ \therefore\ &P(t,h) > CV_{LC}(1 - th^{\alpha}) && : th^{\phi} \geq \gamma_S \end{aligned} \tag{5.19}$$

None of the contracts reviewed in Section 5.1 utilized a combined penalty for both duty cycle and pressure; each instead had separate penalties (if any) for the duty cycle and supply pressure. Therefore, to facilitate comparison with existing contracts, this section considers duty cycle and pressure penalties separately. To match the typical penalty structure used in public-private partnerships in India, the penalty is assumed to scale with a given fraction (i.e., weight w) of the total project revenues $RV_T(1-n)$.

For a contract that penalizes $t < 1$ linearly and has a penalty structure $P(t) =$

$w_t R(V_T)(1-n)(1-t))$, then CWS will be incentivized as long as:

$$\begin{aligned}
\frac{\partial(\text{Costs} + P(t,h))}{\partial t} &< 0 \\
\therefore \frac{\partial(CV_{LC}th^{\alpha})}{\partial t} &< -\frac{\partial\left(w_t R(V_T)(1-n)(1-t)\right)}{\partial t} \\
\therefore CV_{LC}h^{\alpha} &< w_t RV_T(1-n) \\
\therefore w_t &> h^{\alpha}\frac{C}{R}\left(\frac{v_{LC}}{1-n}\right) \\
\therefore w_t &> h^{\alpha}(1-m)\left(\frac{np}{1-n}\right)
\end{aligned} \tag{5.20}$$

As the required weight does not depend on the duty cycle, a constant linear penalty with respect to $(1-t)$ is rational. Further, because $h \leq 1$, neglecting the effect of pressure head is conservative. Finally, since the required penalty does not depend on the available water supply (V_T), this incentive problem does not arise because supplies are constrained. Such penalties, therefore, should be considered in any IWS performance contract.

Since Section 5.3 highlighted that Rational Water would likely provide very low pressure supply continuously, it is curious that incentives for a utility to achieve the targeted pressure head $h = 1$ appear explicitly in only one of five reviewed contracts. This contract (MVV's Meharauli zone) penalized up to 20% of the operator's (fixed) fee (F) for low pressure supply (i.e., $P(h) = w_h F(1-h)$). To match the structure of other equations, this fixed fee is normalized by the total project revenues ($f = F/(RV_T(1-n))$). For such a pressure penalty to be rational, the following inequality must hold (comparing the partial derivatives):

$$\begin{aligned}
\frac{\partial}{\partial h}\left(CV_{LC}th^{\alpha}\right) &< -\frac{\partial}{\partial h}\left(w_h F)(1-h)\right) \\
w_h F &> \alpha CV_{LC}th^{\alpha-1} \\
\therefore w_h &> \alpha th^{\alpha-1}\frac{Cnp}{fR(1-n)} \\
\therefore w_h &> \alpha th^{\alpha-1}\frac{(1-m)np}{f(1-n)}
\end{aligned} \tag{5.21}$$

Unlike in the case of the linear duty cycle penalty, w_t is a function of h unless $\alpha = 1$. When $\alpha \neq 1$, this penalty is inefficient as it must assume the worst case value of h. If $\alpha < 1$, the required penalty decreases with h and increases rapidly when $h \approx 0$. Conversely, if $\alpha \geq 1$, it is conservative to assume $h = 1$. This inefficiency would have been eliminated if the penalty scaled with $(1 - h^\alpha)$.

In all cases of α, it is conservative to assume $t = 1$. And as long as $\alpha \geq 1$, then the penalty weight can be set as:

$$w_h > \alpha \frac{(1-m)np}{f(1-n)} \tag{5.22}$$

5.4.3 Discussion of incentives required for full supply

This section has demonstrated that if Rational Water is unsatisfied, it has incentives to increase its duty cycle provided its price margin is high enough. However, without a penalty (no matter what its price margin is), Rational Water has no financial incentives to increase its duty cycle or pressure past the point where customers are satisfied.

The required penalty to incentivize CWS is reduced if a utility operates at lower pressure, has a higher margin, has lower NRW, and/or has fewer physical losses (Eq 5.20). Similarly, the penalty required to incentivize high-pressure supply is reduced if a utility operates with a shorter duty cycle, has fewer physical losses, and/or has leaks that are less pressure dependent (i.e., smaller α) (Eq 5.21).

As the variable costs of increasing supply in a satisfied IWS scale with th^α, penalizing low duty cycles linearly was found to be efficient. Conversely, where $\alpha \neq 1$, penalizing low pressure linearly was less efficient. The most efficient penalty, however, would combine penalties for t and h; no reviewed contracts contained such a penalty. When penalizing t and h individually, each variable's penalty must fully compensate for the additional costs of leaks in high-pressure CWS (Eq 5.19). The two penalties together, therefore, will over-penalize an under-performing utility by up to 2x.

Concerningly, only one of five reviewed contracts penalized pressure deficits, leaving the other four contracts implicitly incentivizing low-pressure supply (Table 5.1).

Even where regulators may desire 'low-pressure' water supply (e.g., the minimum pressure of 2m in OCW contract (Dinesh Rathi & Associates, 2008)), Section 5.3 suggests that without penalties or regulation, Rational Water's supply pressure will be unreasonably low. Therefore, incentivized minimum pressures are likely necessary to ensure water safety and equitable distribution.

Finally, from a regulator's perspective, both pressure and duty cycle are likely to be measured by pressure loggers (i.e., data-recording pressure sensors). Therefore, including penalties for both duty cycle and pressure, individually or combined, will not increase the cost of monitoring. Furthermore, the distinction between duty cycle and supply pressure is blurred when either variable is very small (e.g., is a system with 0.1m of pressure for 24 hours per day, really a CWS?). Accordingly, coupling the definitions of duty cycle and pressure and monitoring them together may improve contracted outcomes. An example of this can be found in the OCW contract, where continuity is defined as time spent with pressure more than 2m (Dinesh Rathi & Associates, 2008, p.123). Curiously, however, in that specific contract (which claims to be a CWS project), the contractor is penalized only if the supply pressure drops below 2m for more than 24 hours, which would allow daily intermittent water supply to exist without penalty.

5.5 Incentives for leak repair

Thus far, each section has assumed that a network's pipe quality (EOA) would remain constant (e.g., each utility was constrained to its given operating curve OA, OB, OSC, or OD). This section considers Rational Water's incentives to repair its leaks, thereby moving between operating curves. The appropriate incentives are assumed to be in place to ensure that, given a system curve, Rational Water will input all of its available water ($v_P = 1$). A constant input volume makes Rational Water's variable costs constant for all systems considered in this section. Rational Water's incentives will be governed, therefore, by its revenue, penalties, and the costs associated with leak repair. This section considers the incentives needed for Rational Water to upgrade an arbitrary network, initially operated at point X (where $v_P = 1$), to the ideal network, operated at point C (where, by definition, $t = h = a = 1$ and with $v_P = 1$).

5.5.1 EOA reduction required from X to C

For any point X with known NRW, n_X, and physical loss percent, p_X:

$$\begin{aligned} v_{LX} &= n_X p_X = v_{LC} a_X t_X h_X^{\alpha} \\ \therefore a_X &= \frac{n_X p_X}{v_{LC} t_X h_X^{\alpha}} \end{aligned} \tag{5.23}$$

Therefore, the required fractional reduction in EOA to move from any point X to C (where $t = h = 1$) is given by Eq 5.23:

$$\begin{aligned} \frac{a_C}{a_X} &= \frac{n_C p_C t_X h_X^{\alpha}}{n_X p_X t_C h_C^{\alpha}} \\ \therefore \frac{a_C}{a_X} &= \frac{n_C p_C t_X h_X^{\alpha}}{n_X p_X} \qquad : t_C = h_C = 1 \end{aligned} \tag{5.24}$$

Since all water is distributed ($v_P = 1$), the volume received by customers (v_R in Eq 3.5) is given by:

$$\begin{aligned} v_{RX} &= v_P - v_{LX} = 1 - n_X p_X \\ \therefore n_X p_X &= 1 - v_{RX} \\ &= 1 - \begin{cases} v_D \frac{t_X h_X^{\phi}}{\gamma_S} & : t_X h_X^{\phi} < \gamma_S \\ v_D & : t_X h_X^{\phi} \geq \gamma_S \end{cases} \\ \therefore n_X p_X &= 1 - (1 - n_C p_C) \min(1, \frac{t_X h_X^{\phi}}{\gamma_S}) \end{aligned} \tag{5.25}$$

Substituting Eq 5.25 into 5.24 yields:

$$\therefore \frac{a_C}{a_X} = \frac{n_C p_C t_X h_X^\alpha}{1-(1-n_C p_C)\min(1, t_X h_X^\phi/\gamma_S)}$$
$$\therefore \frac{a_C}{a_X} = \begin{cases} t_X h_X^\alpha & : t_X h_X^\phi \geq \gamma_S \\ t_X h_X^\alpha \frac{n_C p_C}{1-(1-n_C p_C)\frac{t_X h_X^\phi}{\gamma_S}} & : t_X h_X^\phi < \gamma_S \end{cases} \tag{5.26}$$

Finally, Eq 5.6 translates this EOA ratio into a repair cost.

5.5.2 Increased revenue from X to C

Moving from point X to C will increase revenue by the following:

$$\begin{aligned} \Delta \mathrm{Rev}_{X \to C} &= RV_T\left((1-n_C)-(1-n_X)\right) \\ &= RV_T(n_X - n_C) \end{aligned} \tag{5.27}$$

However, it is not clear *a priori* if either n or p remains constant during system improvements. Rather, as a more reliable starting assumption, the volumetric ratio of unpaying demand to total (u) is assumed to remain constant. Another possible assumption would be that unpaying demand reduces proportionally to EOA as leaks are repaired. This second possibility is left as an opportunity for future work.

From Table 5.2:

$$\begin{aligned} 1-n_X &= (1-u_X)v_R \\ \therefore n_X &= 1-(1-u_X)v_D \min(1, \frac{t_X h_X^\phi}{\gamma_S}) \end{aligned} \tag{5.28}$$

Substituting Eq 5.28 into 5.27 and assuming that the percentage of customers who pay remains constant ($u_C = u_X = u$) yields:

$$\begin{aligned}
\Delta\text{Rev}_{X\to C} &= v_D RV_T \left((1-u_C) - (1-u_X)\min(1, \frac{t_X h_X^{\phi}}{\gamma_S}) \right) \\
&= RV_T v_D (1-u) \max\left(0, 1 - \frac{t_X h_X^{\phi}}{\gamma_S}\right) \\
\therefore \Delta\text{Rev}_{X\to C} &= RV_T (1-n_C) \max\left(0, 1 - \frac{t_X h_X^{\phi}}{\gamma_S}\right) \qquad (5.29)
\end{aligned}$$

As expected, this suggests that revenues will increase only if the starting system (at point X) is unsatisfied.

5.5.3 Linear penalties required to ensure leak repair

To ensure that Rational Water will upgrade its system, a penalty is sometimes required. As suggested by Section 5.4, this section assumes a combined penalty for both duty cycle and pressure. Moreover, to match typical contracts in India, the penalty is initially assumed to scale with the total project revenues. The penalty incurred for operating at point X would, therefore, depend on the duty cycle and pressure head of the system at point X ($P(t_X, h_X)$). As a first example of one such penalty, consider:

$$P(t_X, h_X) = RV_T(1-n_C)w(1-t_X h_X^{\phi}) \qquad (5.30)$$

where w is the penalty's weight (i.e., the maximum fraction of revenues that can be lost when the penalty is applied in its fullest).

To ensure Rational Water upgrades to high-pressure CWS, the penalty should be larger than the cost of any required leak repairs less any additional revenue:

$$P(t_X, h_X) > \text{Cost}_{a_X\to a_C} - \Delta\text{Rev}_{X\to C} \qquad (5.31)$$

Substituting Eqs 5.30, 5.6, and 5.29 into Eq 5.31:

$$RV_T(1-n_C)w(1-t_Xh_X^{\phi}) > -K_R\log_2(a_C/a_X) - RV_T(1-n_C)\max\left(0, 1-\frac{t_Xh_X^{\phi}}{\gamma_S}\right)$$

$$\therefore w > \frac{1}{1-t_Xh_X^{\phi}}\left(-k_R\log_2(a_C/a_X) - \max\left(0, 1-\frac{t_Xh_X^{\phi}}{\gamma_S}\right)\right)$$

$$\therefore w > \frac{1}{1-t_Xh_X^{\phi}}\begin{cases}-k_R\log_2(t_Xh_X^{\alpha}) & : t_Xh_X^{\phi} \geq \gamma_S \\ -k_R\log_2(\frac{t_Xh_X^{\alpha}n_Cp_C}{1-(1-n_Cp_C)t_Xh_X^{\phi}/\gamma_S}) - (1-\frac{t_Xh_X^{\phi}}{\gamma_S}) & : t_Xh_X^{\phi} < \gamma_S\end{cases} \tag{5.32}$$

Where k_R is the cost of reducing leaks by 50% (K_R) normalized by the ideal project's revenues ($RV_T(1-n_C)$). Said differently, k_R is the percent of a project's total potential revenue that is required to find and repair 50% of a network's leaks.

The required penalty is therefore a function of k_R, $t_Xh_X^{\phi}$, γ_S, n_Cp_C, and $h_X^{\alpha-\phi}$ (Eq 5.32). To simplify the discussion that follows, it is assumed that $h_X^{\alpha-\phi} = 1$, which could occur if either $\alpha = \phi$ or $h_X = 1$. Additionally, a project's ideal leakage level (n_Cp_C) is taken to be 15%.

To explore how the required penalty weight (w) changes as a function of the remaining three parameters, discrete values of γ_S were selected (i.e., $\gamma_S \in \{0.1, 0.25, 0.5\}$). For each value of γ_S, a separate subplot was created (e.g., Figs 5-3a, b, and c). In each subplot, for a given value of th^{ϕ} (varied along the x-axis) and value of k_R (varied along the y-axis), the required value of w is shown by the contour lines (Fig 5-3). Where the required penalty weight w is negative, it suggests that no penalty is required. Required weights between 0 and 30%, are typical of projects in India. Penalties ranging from 30% to 100%, are large, but potentially feasible. Penalties greater than 100% were deemed non-viable.

A project may be able to upgrade a network to CWS without reducing its gross margin (i.e., no penalty is required $\therefore w \leq 0$) if two conditions are met: i) if the network begins with suppressed demand ($th^{\phi} < \gamma_S$, i.e., is an unsatisfied IWS); and ii) if reducing leaks by 50% costs less than 11% of the project revenues (i.e., $k_R < 0.11$; Fig 5-3). Projects with lower initial values of th^{ϕ} are, however, more sensitive to the

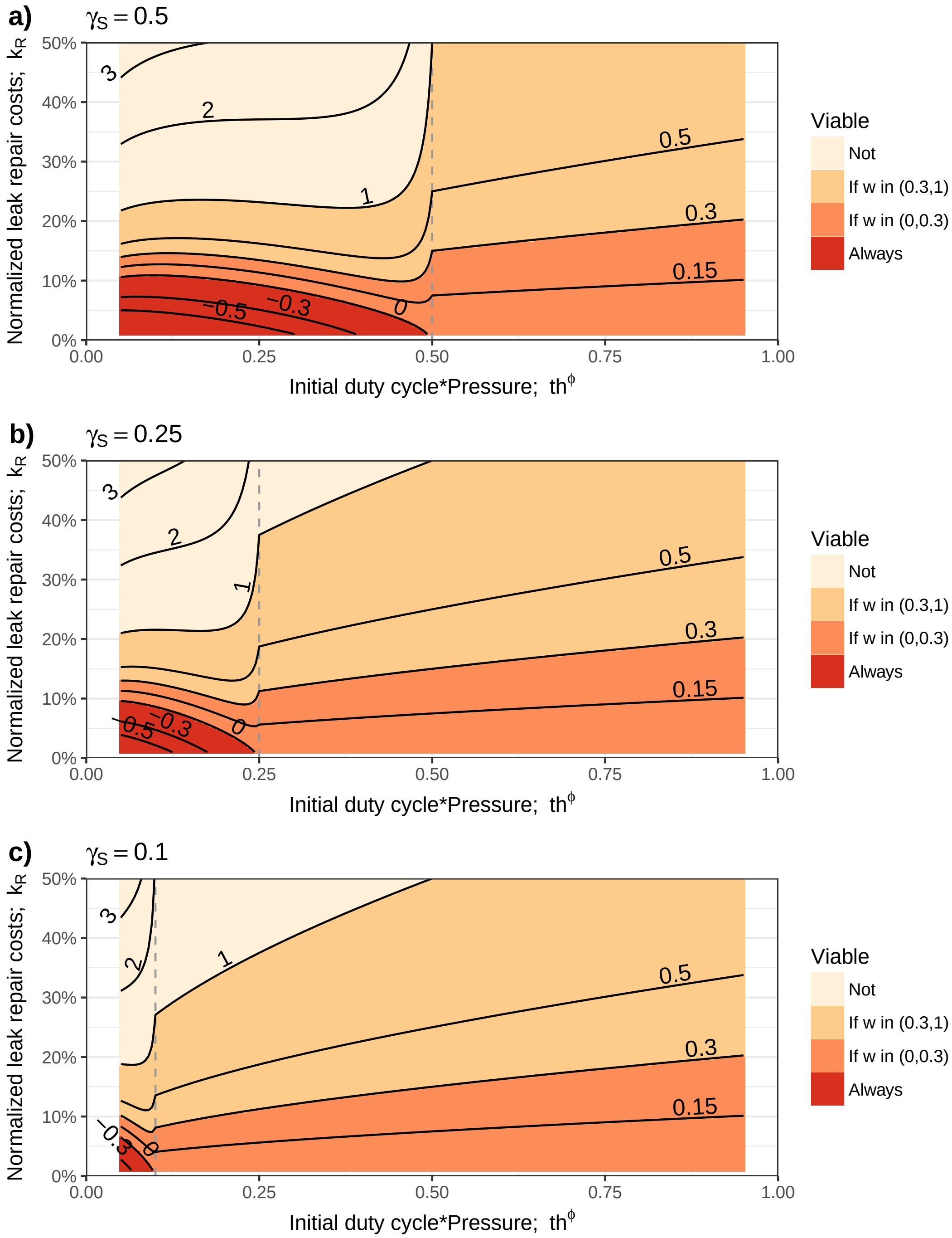

Figure 5-3: **Linear penalty weights required for Ψ-neutral CWS.** Contours show the minimum weight required, w, for the transition to high-pressure CWS ($t = h = 1$) to improve a utility's gross margin given a starting point th^{ϕ} (x-axis) and cost of repairing 50% of leaks (k_R, y-axis). Fill distinguishes how reasonable the penalty weight is: $w < 0$, none-needed (dark red); $w \in (0, 0.3)$, typical (orange); $w \in (0.3, 1)$, unusually large (light orange); and $w > 1$, not-reasonable (off-white). Plots a), b), and c) show $\gamma_S \in \{0.5, 0.25, 0.1\}$. The penalty structure is $P(t, h) = w(1 - th^{\phi})RV_T(1 - n_C)$. To the right of the vertical, gray dashed lines, the system is satisfied ($th^{\phi} \geq \gamma_S$).

costs of leak repairs. When $\gamma_S = 0.5$, for example, doubling the cost of leak repair from 10% to 20% of a project's revenues can change a project's gross margin by 100% of the project's revenues (Fig 5-3). Understanding the costs of leak repair will, therefore, be critical to assessing project viability.

For projects where no penalty is required for high-pressure CWS to increase the utility's gross margin, as leaks are repaired and as th^{ϕ} increases, the system will become satisfied. The utility (in the absence of a penalty) has no financial incentives to continue to improve its system beyond this point where customers are satisfied (i.e., $th^{\phi} = \gamma_S$). Therefore, while upgrading to high-pressure CWS could be gross-margin-neutral for some utilities, in the absence of penalties, it will not maximize their gross margin.

To ensure that high-pressure CWS maximizes a utility's gross margin, the penalty must be the maximum penalty required as a utility transitions along a horizontal line in Fig 5-3 from its starting position towards $th^{\phi} = 1$. Fig 5-4 depicts these gross-margin-maximizing penalty weights. In all cases a strictly positive weight was required and so without penalties, Rational Water is unlikely to adopt high-pressure CWS.

Figs 5-3 and 5-4 depend on the value assumed for $h_X^{\alpha-\phi}$. Holding $h_X^{\alpha-\phi}$ constant at a value less than one, causes $w \to \infty$ as $th^{\phi} \to 1$ (Eq 5.32; Fig C-4). Mapping the effects of duty cycle and pressure increases separately could provide additional insights into efficient system improvement strategies, but is left for future work.

5.5.4 Fixed (non-linear) penalties required to ensure leak repair

In three of five contracts reviewed (Section 5.1), a fixed penalty was incurred any time CWS was not supplied. In two of these contracts, the operator would lose 1% of monthly revenue per day of non-continuous supply. Missing the target every day in a month would reduce monthly revenues by 30%; therefore, this penalty has an equivalent weight of 30% ($w_F = 0.3$). If weighted correctly, this type of non-linear

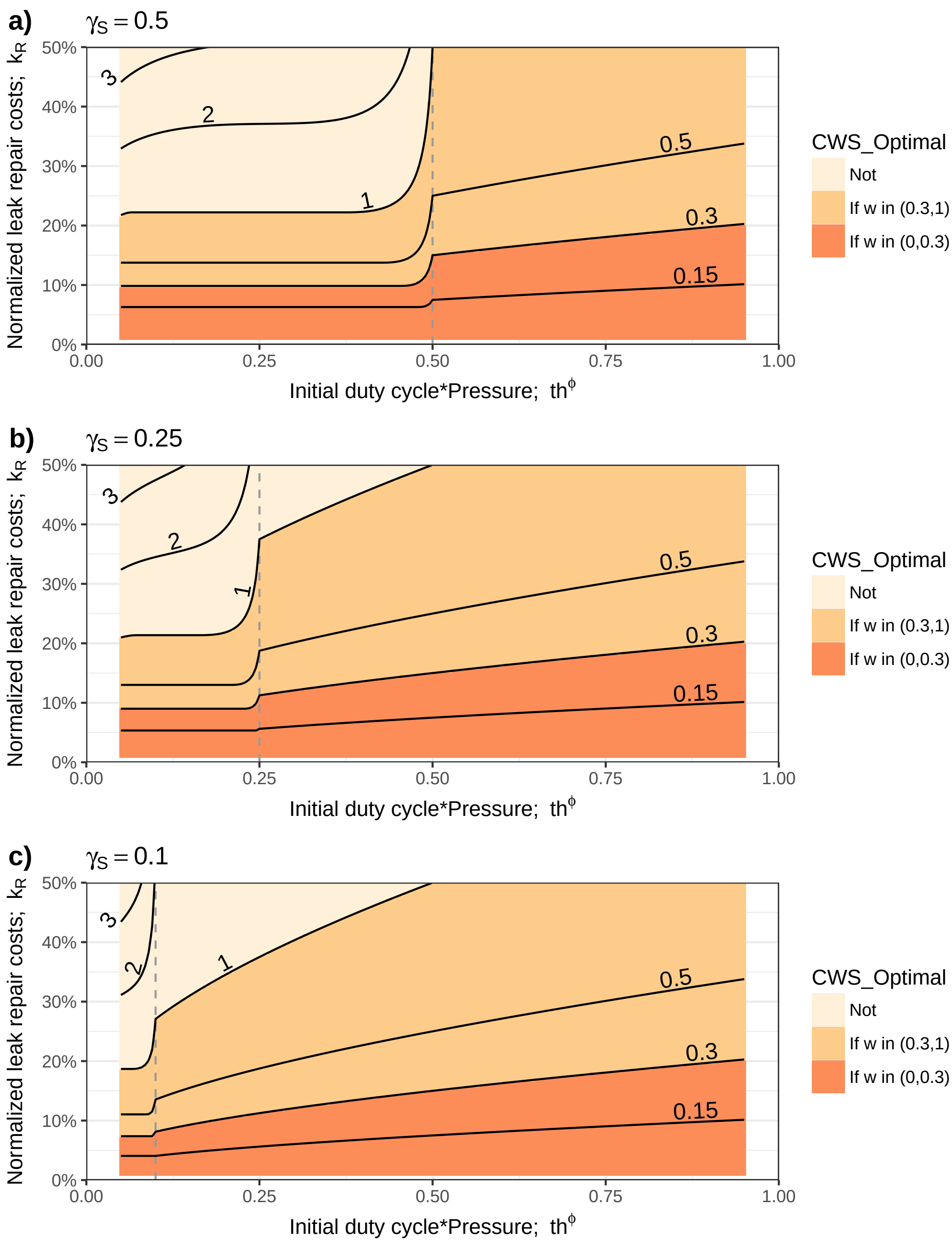

Figure 5-4: **Linear penalty weights required for Ψ-maximizing CWS.** Contours show the minimum weight required, w, for the transition to high-pressure CWS ($t = h = 1$) to maximize a utility's gross margin given a starting point th^{ϕ} (x-axis) and cost of repairing 50% of leaks (k_R, y-axis). Fill distinguishes how reasonable the penalty weight is: $w < 0$, none-needed (dark red); $w \in (0, 0.3)$, typical (orange); $w \in (0.3, 1)$, unusually large (light orange); and $w > 1$, not-reasonable (off-white). Plots a), b), and c) show $\gamma_S \in \{0.5, 0.25, 0.1\}$. The penalty structure is $P(t, h) = w(1 - th^{\phi})RV_T(1 - n_C)$. To the right of the vertical, gray dashed lines, the system is satisfied ($th^{\phi} \geq \gamma_S$).

penalty could also incentivize leak repair.

To explore potential fixed penalties, the model assumes a penalty structure $P = w_F RV_T(1-n)$, where the penalty is incurred anytime a water system operates below its target of $t = h = 1$ (i.e., the full penalty is applied anytime $th^\phi < 1$). Adapting Eq 5.32 for a fixed penalty, w_F, yields:

$$w_F > \begin{cases} -k_R \log_2(t_X h_X^\alpha) & : t_X h_X^\phi \geq \gamma_S \\ -k_R \log_2(\frac{t_X h_X^\alpha n_{CPC}}{1-(1-n_{CPC})t_X h_X^\phi/\gamma_S}) - (1 - \frac{t_X h_X^\phi}{\gamma_S}) & : t_X h_X^\phi < \gamma_S \end{cases} \tag{5.33}$$

The minimum required weights (w_F) are plotted in Fig 5-5. These penalty weights are independent of how regularly the utility's performance is assessed and can be interpreted as the revenue decrease incurred if a project never achieved its targets. The structure of dividing a fixed penalty up into daily or weekly performance seems ideal. As such, even if a utility had a temporary failure, it would still have incentives to improve its system.

As in the case of linear penalties, initially-unsatisfied IWS have the lowest (and potentially-negative) penalty weights required where leak repair costs are small (Fig 5-5). Conversely, where leak repair costs are high, initially-unsatisfied IWS may also require the highest penalties (e.g., $w_F > 1$ as $th^\phi \to 0$ if $k_R > 0.23$ in Fig 5-5). The profitability of projects attempting to upgrade unsatisfied IWS (or any system with a low value of th^ϕ) will, therefore, be sensitive to the cost of leak repair.

When leak repair costs are low enough in unsatisfied IWS, the transition to CWS can increase a utility's gross margin without any penalties (Fig 5-5). For example, a system with $\gamma_S = 0.5$, $k_R = 0.05$ and $th^\phi = 0.12$ requires a penalty of -0.39 (Fig 5-5a). This implies that by transitioning from $th^\phi = 0.12 \to 1$, the utility's gross margin dollars will increase by 39% of the total project revenue. However, during that transition, as the utility travels horizontally across the graph, it will need to cross the contour line $w_F = 0$, after which, there are no additional incentives to continue to increase th^ϕ.

To assist in setting contract penalties, Fig 5-6 plots the penalty weight required

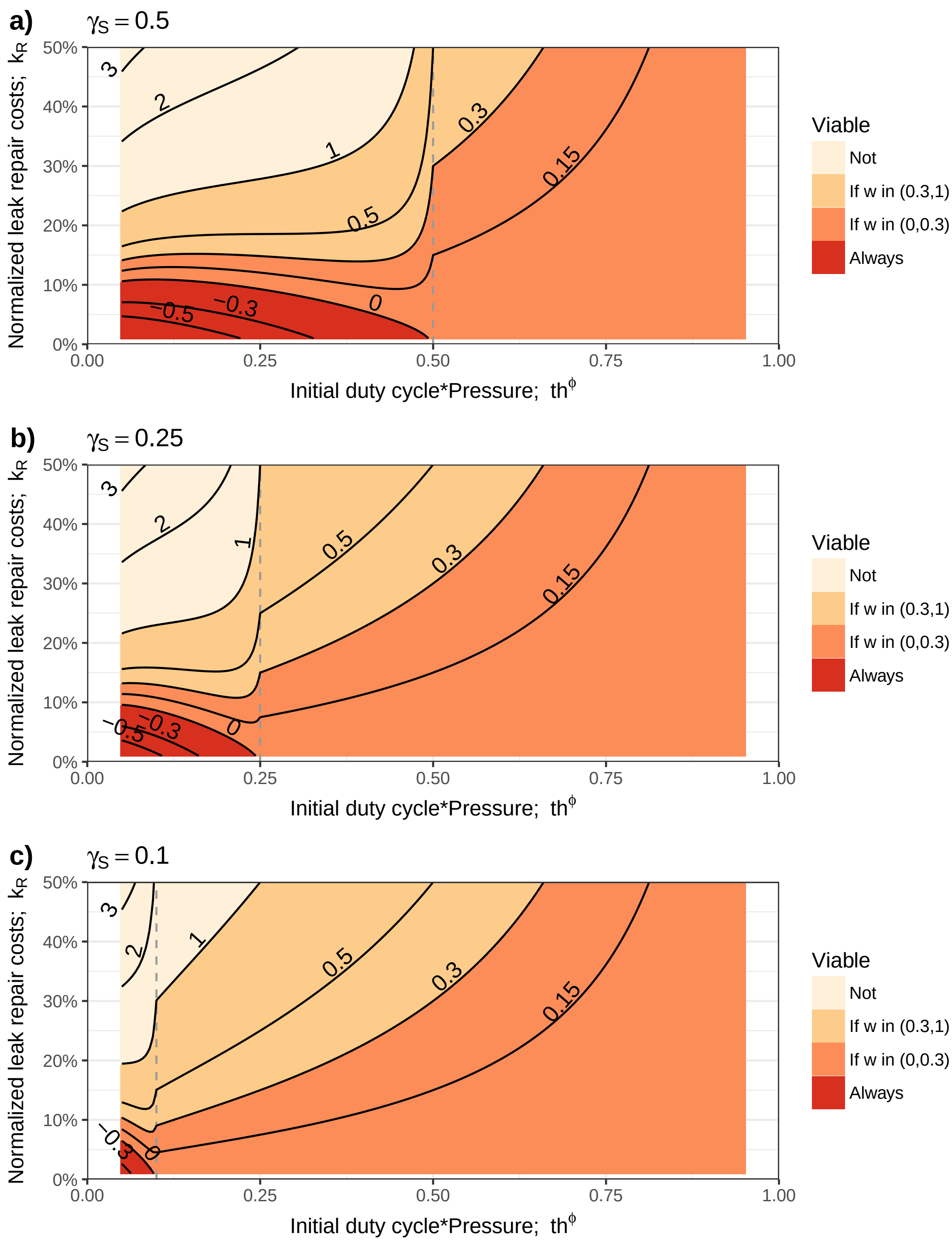

Figure 5-5: **Fixed penalty weights required for Ψ-neutral CWS.** Contours show the minimum weight required, w_F, for the transition to high-pressure CWS ($t = h = 1$) to improve a utility's gross margin given a starting point th^{ϕ} (x-axis) and cost of repairing 50% of leaks (k_R, y-axis). Fill distinguishes how reasonable the penalty weight is: $w_F < 0$ none-needed (dark red); $w_F \in (0, 0.3)$, typical (orange); $w_F \in (0.3, 1)$ unusually large (light orange); and $w_F > 1$ not-reasonable (off-white). Plots a), b), and c) show $\gamma_S \in \{0.5, 0.25, 0.1\}$. The penalty structure is $P(t, h) = w_F RV_T(1 - n_C)$. To the right of the vertical, gray dashed lines, the system is satisfied ($th^{\phi} \geq \gamma_S$).

to ensure that upgrading to high-pressure CWS maximizes a utility's gross margin. As in the case of linear penalties, a strictly positive penalty was always required (Fig 5-6). Therefore, unregulated, financially-motivated utilities are not likely to upgrade their systems to be high-pressure CWS.

5.5.5 Discussion of penalty weights

Key trends are shared between linear and non-linear penalty weights. All else being equal, unsatisfied systems with higher values of γ_S have more suppressed demand and therefore require smaller penalties to ensure that CWS is the global optimum (Figs 5-4 and 5-6). If 30% is an appropriately assumed maximum feasible penalty weight, it may not be possible to incentivize a utility to upgrade to CWS if $k_R > 0.12$. Worse still, if $\gamma_S = 0.1$, then CWS projects may not be feasible if $k_R > 0.07$.

For a given absolute cost of 50% leak reduction (K_R), the value of k_R is reduced as the total project revenues are increased. This matches with trends for longer contracts to give utilities more time to recoup initial investments.

Within the region of commonly-observed penalties weights ($w_F \leq 0.3$), specifying γ_S precisely is not required to set a conservative Ψ-maximizing penalty. In all cases the penalty can be conservatively estimated by using a higher value of γ_S and a lower value of th^{ϕ} than expected (Figs 5-4 and 5-6). Conversely, for higher penalty weights (e.g., $w_F \approx 1$), a larger change in the required penalty can be observed near the satisfaction point (Figs 5-4 and 5-6); accordingly knowing if an IWS is satisfied is important for projects with large penalties.

The effects of γ_S were smaller when the penalty was set to ensure CWS maximized gross margin (Figs 5-4 and 5-6) than when CWS needed only to improve a utility's gross margin (Figs 5-3 and 5-5). This implies that knowing γ_S is more important for the bidder on the contract (as it greatly affects the amount of money to be made during the upgrade), than for the contract designer.

Considering gross-margin-maximizing penalties, linear penalties were much less sensitive to the initial operating point of the system and to the system's satisfaction point. This may make linear penalties more robust in systems where little is know

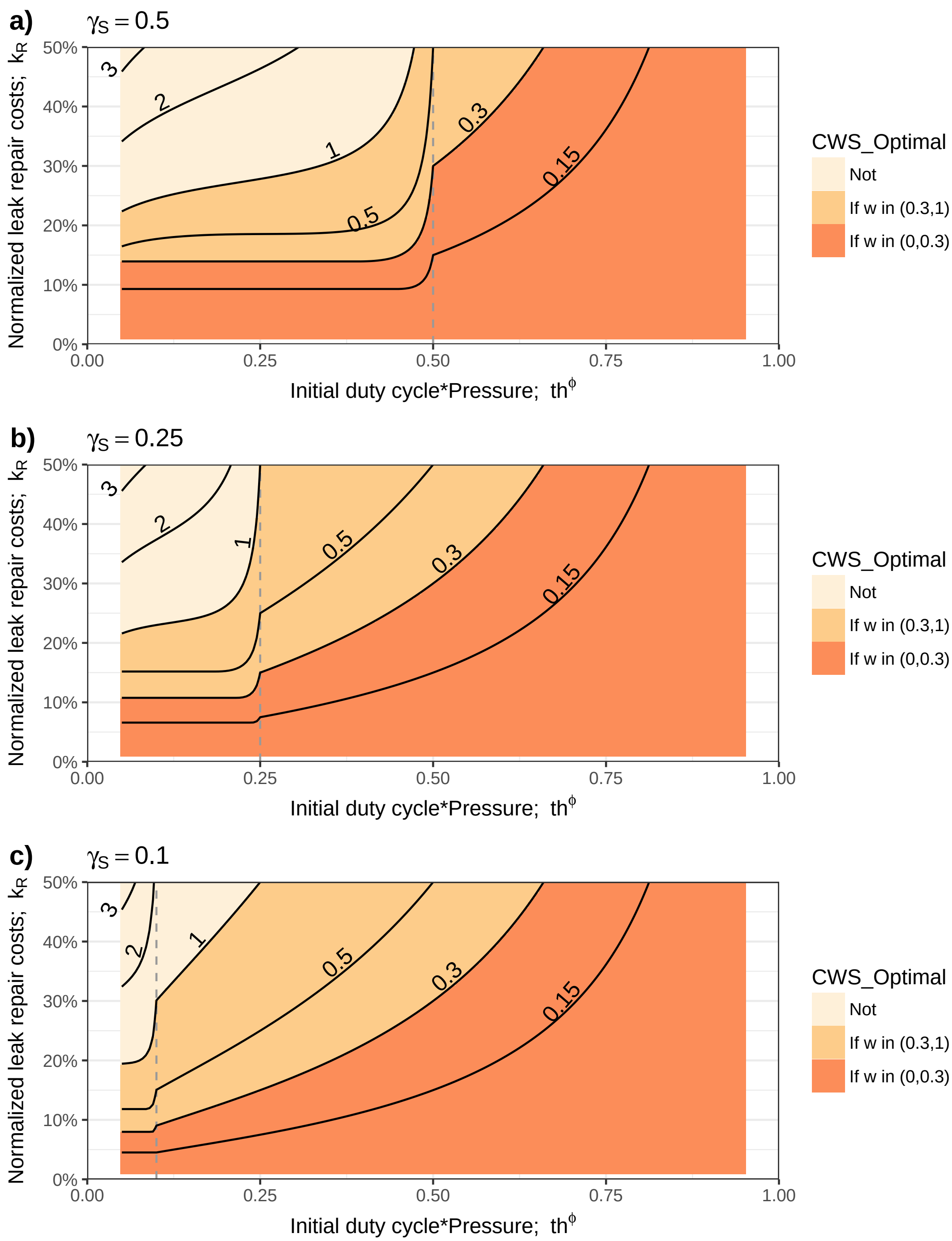

Figure 5-6: **Fixed penalty weights required for Ψ-maximizing CWS.** Contours show the minimum weight required, w_F, for the transition to high-pressure CWS ($t = h = 1$) to maximize a utility's gross margin given a starting point th^{ϕ} (x-axis) and cost of repairing 50% of leaks (k_R, y-axis). Fill distinguishes how reasonable the penalty weight is: $w_F < 0$ none-needed (dark red); $w_F \in (0, 0.3)$, typical (orange); $w_F \in (0.3, 1)$ unusually large (light orange); and $w_F > 1$ not-reasonable (off-white). Plots a), b), and c) show $\gamma_S \in \{0.5, 0.25, 0.1\}$. The penalty structure is $P(t, h) = w_F RV_T(1 - n_C)$. To the right of the vertical, gray dashed lines, the system is satisfied ($th^{\phi} \geq \gamma_S$).

about their operation. Conversely, fixed penalties were deemed viable across a much larger range of leak repair costs. Moreover, since completing the transition from IWS to CWS is expected to have substantial benefits for equity and water quality, some form of bonus or non-linear penalty is recommended, otherwise utilities may operate with $t \in (0.95, 0.99)$ but incur only insignificant linear penalties.

Since this section used variables that were normalized by total project revenues, no accounting for the time value of money was done. This underestimates the penalties (ongoing expenses) required to incentivize leak repair (an upfront expense). This omission is most problematic for projects spanning many years; accounting for this is left for future work.

5.6 Optimal distribution between zones in IWS

This chapter has, thus far, considered a system to be a monolithic entity with a single duty cycle and pressure. However, most utilities operate at least several partially- or fully-independent subnetworks (e.g., Delhi's 845 zones in Fig 2-3). This section considers how Rational Water could maximize its gross margin if it were managing independently-controllable subnetworks. After deriving Rational Water's expected behavior when managing unsatisfied sub-networks, this section considers how Rational Water's performance indicators would be affected by its supply strategy. Finally, Rational Water's expected behavior is considered if it manages only satisfied sub-networks. As the effects of pressure have been explored above, this section considers each subnetwork to have a fixed supply pressure. Additionally, the price and costs of water (R and C) are assumed to be the same for all subnetworks.

Consider first the case where Rational Water manages a single reservoir and controls how its available supply volume is divided between two independent and unsatisfied sub-networks: VIP Village and Commoner's Crescent. NRW is much higher in Commoner's Crescent than VIP village due to older pipes (higher EOA, a) and proportionally more non-paying connections (u).

5.6.1 Maximizing gross margin

Assuming that each subnetwork operates with a fixed (and potentially different) supply pressure, the gross margin (Ψ) of each subnetwork is given by Eq 5.8, and scales linearly with the duty cycle. Similarly, the volume input to each unsatisfied subnetwork scales linearly with the duty cycle (Eq 3.10). Normalizing the gross margin generated by each subnetwork (Eq 5.8) by the volume supplied to it (Eq 3.10), provides a normalized gross margin (Υ):

$$\therefore \Upsilon = \frac{\Psi}{V_P} = \frac{(R(1-u)-C)h^{\phi}\frac{V_D}{\gamma_S} - CV_{LC}ah^{\alpha}}{V_D\frac{h^{\phi}}{\gamma_S} + V_{LC}ah^{\alpha}} \tag{5.34}$$

When supply pressure is held constant, this normalized gross margin is, therefore, constant for a given subnetwork. Taking the normalized gross margin of VIP Village to be Υ_V and that of Commoners' Crescent to be Υ_C, Rational Water's total gross margin will be:

$$\Psi = V_T(\lambda_V\Upsilon_V + \lambda_C\Upsilon_C) \qquad : \lambda_C + \lambda_V = 1 \tag{5.35}$$

where λ_i is the fraction of Rational Water's total water delivered to subnetwork i. Eq 5.35 holds true provided both subnetworks remain unsatisfied.

Rational Water's total gross margin will, therefore, be maximized by preferentially supplying the subnetwork with the highest normalized gross margin. Due to lower leakage levels and higher rates of payment, it is expected that VIP Village's normalized gross margin will be higher than Commoners' Crescent's. Therefore, Rational Water's optimal strategy is to preferentially supply VIP Village.

Assume each subnetwork i demands a fraction Λ_i of the total supply to become satisfied at its fixed pressure. If VIP Village's demand is larger than the available supply ($\Lambda_V \geq 1$), then Rational Water's optimal strategy is to supply 100% of its available water to VIP Village. If $\Lambda_V < 1$, Rational Water should supply only its remaining supply to Commoners' Crescent (i.e., $\lambda_C = 1 - \Lambda_V$). Compounding this inequity, per capita consumption in VIP village may be higher than in Commoners'

Crescent, delaying the point at which Rational Water would supply Commoners' Crescent.

More generally, take Rational Water to have an arbitrary set of separably-controllable subnetworks I, where each unsatisfied subnetwork i has a fixed normalized gross margin Υ_i, demands a fraction Λ_i of Rational Water's total supply, and receives a fraction λ_i of Rational Water's total water supply. Rational Water's total gross margin, therefore is:

$$\Psi = V_T \sum_{i \in I} \lambda_i \Upsilon_i \tag{5.36}$$

$$\text{where: } \sum_{i \in I} \lambda_i = 1,$$

$$0 \leq \lambda_i \leq \Lambda_i \qquad \forall i \in I$$

Therefore, Rational Water's optimal strategy is to preferentially supply its subnetworks in order of their normalized gross margin. Specifically, a subnetwork i should only be supplied if:

$$\lambda_j = \Lambda_j \qquad \forall j \in \{I | \Upsilon_j > \Upsilon_i\} \tag{5.37}$$

5.6.2 Minimizing NRW

Thus far in this chapter, Rational Water has been assumed to maximize gross margin. However, the metric of non-revenue water (NRW) is a more frequently discussed performance metric for water utilities. NRW (in percentage) is already normalized by the volume supplied to a given (sub)network. Specifically, NRW for an unsatisfied

IWS is:

$$n = \frac{uv_R + v_L}{v_P} \qquad : th^\phi \leq \gamma_S \tag{5.38}$$

$$= \frac{uv_D \frac{th^\phi}{\gamma_S} + v_{LC}ath^\alpha}{v_D \frac{th^\phi}{\gamma_S} + v_{LC}ath^\alpha} \qquad : th^\phi \leq \gamma_S$$

$$\therefore n = \frac{uv_D \frac{h^\phi}{\gamma_S} + v_{LC}ah^\alpha}{v_D \frac{h^\phi}{\gamma_S} + v_{LC}ah^\alpha} \qquad : th^\phi \leq \gamma_S \tag{5.39}$$

Therefore, for a fixed supply pressure, the NRW (n_i) of an unsatisfied subnetwork i is independent of its duty cycle. Rational Water's aggregate NRW, n, will be:

$$n = \frac{\text{unsold}}{\text{total}} = \frac{\sum_{i \in I} \lambda_i v_P n_i}{v_P}$$

$$\therefore n = \sum_{i \in I} \lambda_i n_i \tag{5.40}$$

$$\text{where: } \sum_{i \in I} \lambda_i = 1$$

$$0 \leq \lambda_i \leq \Lambda_i \qquad \forall i \in I$$

NRW is therefore minimized when Rational Water supplies water to its subnetwork with the lowest NRW, and only supplies an additional subnetwork when all the subnetworks with lower NRW values have been satisfied. Clearly, this 'optimal' control strategy is far from equitable. Additional performance incentives and regulations are required to preserve distributional equity and the welfare of all consumers.

5.6.3 Distribution strategies for fully satisfied networks

Similarly inequitable distribution strategies may arise if all subnetworks are satisfied. Consider again the case of VIP Village and Commoners' Crescent. As both subnetworks are satisfied, revenues are fixed. If Rational Water needs to distribute all of its water, variable costs will also be fixed.

If Rational Water seeks to maximize other metrics, such as duty cycle, it should again preferentially supply the subnetwork with the highest normalized efficiency for that metric. Consider, for example, the maximization of duty cycle, which is a key performance indicator for system improvement projects that have promised to deliver CWS. While Section 5.3 suggested t can be maximized by reducing pressure, in this section pressure is considered fixed.

Eq 4.6 suggests that the normalized effect of additional water on the duty cycle in a given subnetwork will scale as $1/(V_{LC}ah^{\alpha})$. Again, assuming VIP Village has a lower EOA (and therefore lower a), Rational Water should supply all of its additional water to VIP Village in order to efficiently maximize its average duty cycle.

This duty-cycle maximization strategy can be observed in India. CWS projects often begin with demonstration zones that are selected for their hydraulic feasibility (e.g., in the World Bank sponsored project in Hubli (Walters, 2013)). Where feasibility metrics are correlated with socioeconomic status, this inequity has additional implications. Decisions about which subnetwork will receive additional supply or be used as a demonstration project are frequently presented in purely technocratic terms, but Anand (2011, p.554) argues compellingly that water "systems respond at least as much to considerations of class as they do to those of topography."

5.6.4 Implications of VIP Village for benchmarking

Through efforts to compare utilities, to learn from what works, and to incentivize better performance, benchmarking has become widespread (e.g., Van den Berg and Danilenko (2011); Asian Development Bank and Ministry of Urban Development Government of India (2007); Alegre et al. (2016)). However, where subnetworks of IWS are unsatisfied, traditional performance metrics break down and incentivize inequitable supply.

Consider the World Bank's IBNET database, which holds self-reported performance indicators for 3085 different utilities delivering water to more than 996 million people (Van den Berg and Danilenko, 2011). Of these utilities, 659 (21%) have duty cycles <99% (i.e., <23.75 hrs/day). These IWS serve a population of 303 million people (for more details on the intermittent subset of the IBNET database, see Section 6.2.7).

Gross margin percent is implicitly tracked in the IBNET database (indicator 24.1). Many other IBNET indicators are also correlated with gross margin, including revenue metrics, cost metrics, and cash flow metrics. Each of these financial metrics (including NRW) will be maximized by preferentially supplying VIP village.

More broadly, of the 79 IBNET indicators, 32 (41%) would improve by preferentially supplying VIP Village, 46 (58%) would not meaningfully change, and only one indicator (customer complaints) might catch this inequitable supply strategy. The key limitation of all of these indicators is that they reflect system averages and totals. In order to detect equity, a different statistic is required (e.g., min, max, percentile, standard deviation, etc.). Calculating these alternative statistics requires more detailed data than many utilities may have available. However, given the pervasiveness of IWS that seem to preferentially supply based on class (Anand, 2011), including equity-focused statistics in benchmarking efforts should be a priority.

The IWA's 2016 performance indicators address this possibility in one of their variable definitions. When measuring how long a system with subnetworks has been pressurized (i.e., assessing the duty cycle), Alegre et al. (2016, p.338) suggest that the average be weighted by the number of service (i.e., customer) connections in each subnetwork, not by the volume delivered to each subnetwork. This connection-weighted duty cycle is then used to adjust the system's physical losses and infrastructure leakage index in terms of an equivalent system that is pressurized continuously (Alegre et al., 2016, p.221). Both the population-weighted duty-cycle metric and its effect on reported leakage rates incentivize longer duty cycles to subnetworks with more customers and therefore incentivize a more equitable supply.

Unfortunately, this population-weighted metric still incentivizes Rational Water to fully supply one of its subnetworks at the cost of others (although the optimization now accounts for the population served). If Rational Water wishes to minimize its reported leakage according to the new IWA metrics, it should continue to supply water only to VIP Village if VIP Village's per capita flow rate of leaks (while the system is pressurized and supplied) is less than the per capita flow rate of leaks in Commoners' Crescent (while the system is pressurized and supplied); otherwise, water should be supplied only to Commoners' Crescent (see Eq C.28 in Section C.4).

5.6.5 Discussion of zonal equity

This section considered how Rational Water would distribute its water between sub-networks (zones). The supply strategy that prioritizes VIP Village is far from an academic curiosity. Customers in real IWS receive varying access to water based on their political influence and class, as well as hydraulic and topological factors (Anand, 2011). For example, Guragai et al. (2017) found that the duty cycle experienced by customers in the Kathmandu Valley, Nepal, varied between and within service areas. The inequality in duty cycle within eight of ten service areas was induced by a few households receiving long duty cycles, as opposed to lots of households receiving short duty cycles (Guragai et al., 2017). While hydraulic feasibility and political influence may explain some of this inequity, this section highlights that an economically-motivated water utility also has reason to preferentially service some neighborhoods over others.

Engaging the public at the design stage of water supply improvement projects may increase the accountability of projects that target different duty cycles and/or pressures for different neighborhoods. Unfortunately, because such 'technical' decisions are typically framed as purely hydraulic, public engagement is unlikely to change the project's outcomes. Perhaps instead, more accountability on the part of project funders and designers is required. Funders should carefully scrutinize any project where 'hydraulic feasibility' overlaps with affluent or politically-connected neighborhoods.

The current IWA performance indicators could benefit from three refinements. First, the duty cycle metric suggested by Alegre et al. (2016, p.338) provides no specification of what pressure must be maintained in order to count as the system being pressurized. Section 5.3 demonstrated that Rational Water is likely to use low pressure supply, and utilities and/or regulators using this metric should be careful to standardize the minimum pressure required to count as time when the system is pressurized. Second, additional metrics that use population-weighted averages are more likely to capture the equity of a system. For example, the duty cycle was used to adjust only four metrics: three of 43 operational indicators, and one of 34 quality of service indicators (Alegre et al., 2016). Apart from metrics that track complaints, only one additional IWA metric could capture Rational Water's inequitable strategy (the IWA recommends measuring service interruptions in people-hours). And third, as suggested earlier, using metrics that capture the distribution of system parameters would better reflect how a system's disadvantaged customers are served.

5.7 Optimal supply frequency

The duty cycle (t) of an IWS is independent of the supply period (T =1/frequency of supply). Given a duty cycle (e.g., t=1/6), should Rational Water provide supply for a long time occasionally (e.g., 24 hours every six days ($T = 6$ days)) or for a short time frequently (e.g., four supply cycles of one hour every day ($T = 0.25$ days))? This section considers the optimal frequency in terms of its effect on equity, leakage and quality.

To explore the optimal supply frequency, consider Fig 5-7. The vertical axis is the supply duration (τ; i.e., the duration of a supply stage) shown in hours, and the horizontal axis is the supply period (T=1/frequency; i.e., time elapsed between the start of sequential supply stages) in days. If $t = 1$, a system provides CWS; if $t < 1$, the system is intermittent. The minimum duty cycle t_S required to provide customers with V_D is shown as the angled bottom of the Satisfied IWS zone and depends on the system's pressure head h, the exponent ϕ, and on γ_S.

5.7.1 Equity considerations

Thus far, discussions about the duty cycle have not considered how much storage capacity ($\boldsymbol{V_S}$) customers must have in order to be satisfied by an IWS. Kumpel et al. (2017) found that customers' storage capacity significantly affected their access to water in an IWS with a supply period of six days (i.e., $T = 6$).

Customer consumption during the supply cycle can be substantial (Kumpel et al., 2017). However, as a conservative first approximation, this consumption is not con-

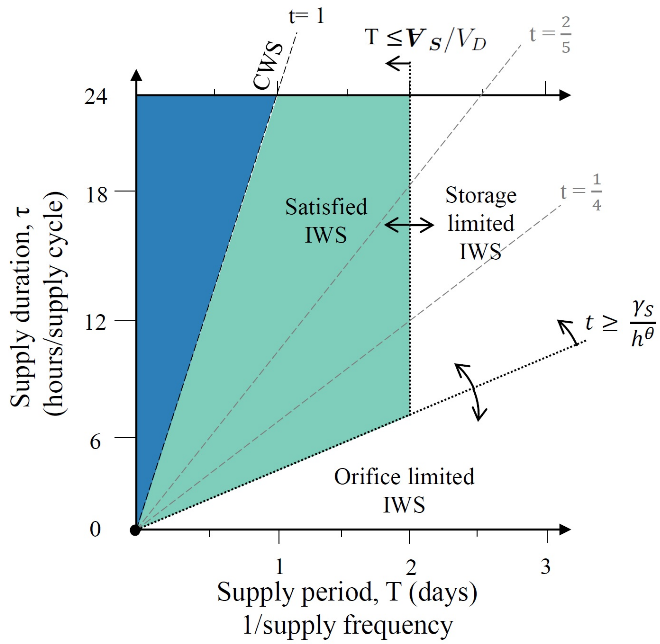

Figure 5-7: **Optimal supply frequency.** The implications of the supply period (T = 1/frequency), duty cycle (t), supply duration (τ), and customer storage capacity ($\boldsymbol{V_S}$) on customer satisfaction.

sidered. Therefore, in order to be satisfied by an IWS, customers must have enough storage capacity to hold their daily volume of demand for each day until the next supply cycle, $\boldsymbol{V_S} \geq TV_D$. Therefore, independent of t, in order to satisfy customers, a system must provide water with a period of $T \leq \boldsymbol{V_S}/V_D$. When $T > \boldsymbol{V_S}/V_D$, the IWS is *storage limited* and not all customers can be satisfied. The system satisfaction test, proposed in Eq 4.5, can only detect orifice limited unsatisfied IWS and cannot determine the extent to which customers are storage limited.

5.7.2 Leakage and water quality considerations

The volume of water contained in a network's pipes is the network's *dead volume* ($\boldsymbol{V_{DV}}$). After each supply cycle, the network depressurizes. The water left in the pipes is lost to leakage, is delivered to customers without a positive pressure barrier to prevent contamination, or stagnates until the start of the next supply cycle. None of these options are good for customers or the utility.

At the start of the supply stage, an IWS must refill any components of the dead volume lost to leakage or delivered to customers. This flushing phase is more contaminated than the steady state phase (Kumpel and Nelson, 2014). Chapter 6 will suggest, however, that the volume of contaminants in the flushing phase is roughly proportional to $(1-t)$, independent of T and of the flushing phase's duration. Nonetheless, as customers are delivered much of the dead volume without the protection of positive pressure, minimizing its relative magnitude will still improve water safety.

The ratio of the dead volume to the (absolute) volume of water a utility delivers to its customers is $\boldsymbol{V_{DV}}/(TV_R)$. This ratio is minimized by increasing the supply period (i.e., lowering the supply frequency).

5.7.3 Discussion of optimal supply frequency

The dead volume is a consequence of IWS that is under-discussed in the literature. In theory, concerns of leakage and water quality suggest that less frequent IWS are preferable. However, infrequent supplies require customers to have more storage capacity, which favors the rich, who can afford higher coping costs. Therefore, where utilities have a choice, the optimal supply period would appear to be $T \approx \boldsymbol{V_S}/V_D$, where $\boldsymbol{V_S}$ is taken to be the minimum storage capacity of the poorest customers in the network. In practice, the choice of the supply period is also limited by the service reservoir capacity.

5.8 Conclusion

This chapter explored the expected behavior of Rational Water and the conditions and/or penalties required to ensure that it would distribute all of its water, and would undergo the leak repairs necessary to achieve high-pressure CWS. This chapter showed strong, natural incentives for Rational Water to increase its supply duration and/or pressure (i.e., th^{ϕ}) and to repair its leaks up to the point were customers were satisfied. In the absence of penalties, Rational Water has no incentives to supply an IWS beyond the point where it becomes satisfied. This incentives problem cannot be solved by expanding supply capacity and must be addressed with regulations (financial or otherwise).

This conclusion is most concerning for the sufficiency of the water supply for those at an IWS' fringes. Assuming that in real networks, customer satisfaction is asymptotically reached, Rational Water is unlikely to provide universal access to water that is 'available when needed.' Instead it is likely to provide only the majority of customers with sufficient supply, strategically under-serving customers at its network's fringes.

In the absence of economic or absolute scarcity and without performance penalties, it is hypothesized that most IWS are operated as marginally satisfied IWS ($th^{\phi} \approx \gamma_S$). The existence of unsatisfied IWS is likely to signify major water shortage issues that require more than distributional solutions to remedy (i.e., IWS face more than just technical scarcity).

For a flat network, Rational Water's optimal supply pressure was found to be unrealistically low. This result, however, demonstrates that high-pressure and long duty-cycles conflict. Rational Water should consider supplying at the lowest pressure permitted by concerns of water quality and equitable access.

Some initial conditions allow utilities to upgrade to CWS and increase their gross margin without a penalty, but penalties are always required to ensure that high-pressure CWS is the global optimum for utilities like Rational Water. Smaller penalties are needed when utilities start closer to their targeted performance points. Contract designers should consider both linear and non-linear penalties.

The distinction between unsatisfied and satisfied IWS has proven yet again to be a key determinant of how a system will be run. This distinction also proved important when setting equitable targets and benchmarks. Absent from the literature to date, this distinction represents a significant contribution of this thesis.

Finally, this chapter also put forward the new concept of *orifice-limited* and *storage-limited* (unsatisfied) IWS. To ensure equity, a utility should provide water with a short enough supply period for its poorest customers to be able to store enough water until the subsequent supply stage. Provided customers are able to store enough water, it seems optimal to increase the supply period.

Combining results from the sections of this chapter, it appears that Rational Water's optimal supply strategy is to minimize its supply pressure (until constrained by quality or equity concerns). At this minimum pressure, its duty cycle should only be long enough that customers are marginally satisfied. And finally, its supply period should be as long as possible (until the poorest customers are about to be storage limited).

The confluence of financial and technical metrics is most problematic in IWS. For example, in India, visions of CWS have been used to motivate, if not justify, new water supply projects done in collaboration with the private sector (Anand, 2015; Sangameswaran, 2014; Walters, 2013; Björkman, 2015). Motivated by CWS, these projects are often designed and executed with an emphasis on minimizing financial waste. Unfortunately, this financial (over-)emphasis encourages utilities to behave like Rational Water. This chapter demonstrated how this can incentivize projects towards inequitable supply and towards very low pressures. By exploring Rational Water's expected behavior, this chapter has clearly demonstrated the need for careful regulation where utilities (public or private) are expected to act with financial motives while operating or upgrading IWS.

Chapter 6

Scaling relations to evaluate leakage and intrusion

> There is a need for ... applied research to understand how to optimize design and operating conditions and monitoring practice to reduce water quality risks in IWS.
>
> Kumpel and Nelson (2016, p.548)

6.1 Background

Section 1.1 defined the supply and non-supply stages of an IWS and the flushing and steady-state periods within the supply stage. While the concentration of fecal indicator bacteria can be 18-20 times higher during the flushing phase, the steady-state phase lasts an average of nine times longer (Kumpel and Nelson, 2014). Therefore, customers' total contaminant exposure can only be minimized when it is understood how operational strategies affect water quality during both phases of supply.

Previous investigations of operational strategies to improve the water quality of IWS have focused on improving the residual chlorine concentration during the steady-state phase (Solgi et al., 2016; Goyal and Patel, 2015; Mohapatra et al., 2014) and identifying likely locations of contaminant intrusion during the non-supply stage

(Vairavamoorthy et al., 2007c,b). None of these approaches explore how operational changes would affect water quality during both the flushing and steady-state phases of the system.

Elala et al. (2011) and Kumpel and Nelson (2014) suggest four modes by which IWS can degrade water quality: *contaminant intrusion*, where contaminants enter the system from the vicinity of the distribution pipes; *biofilm growth and/or sloughing*, where the hydraulic conditions of IWS encourage biofilm growth and/or detachment; *domestic storage*, where IWS force customers to use domestic storage containers which create opportunities for recontamination through poor hygiene; and *backflow*, where contaminants enter into the system from customer premises. Kumpel and Nelson (2013, 2014) have confirmed that intrusion is a likely contamination mechanism. Accordingly, this chapter considers the factors which affect the volume of contaminants that can intrude into IWS.

Contaminants can only intrude into a pipe network when: i) there are physical pathways (at leaky joints, or through fractures in the pipes), ii) there are contaminants in the same vicinity, and iii) there is an inward pressure gradient (Lindley and Buchberger, 2002). The risk of contaminant intrusion in CWS is typically calculated using: i) the outward leakage rate to assess the size of physical pathways; ii) the assumption of ubiquitous contaminants; and iii) the measured or modeled magnitude and duration of low pressure events (Ebacher et al., 2012; Kirmeyer and Martel, 2001; Besner et al., 2011). This approach conservatively estimates the maximum volume of fluid that could intrude into the water supply system without specifically considering the concentration (if any at all) of contaminants in the intruding fluid. This chapter extends this standard approach by explicitly considering the duty cycle and by distinguishing between the flushing and steady-state phases.

First-order models, despite their many simplifications, can provide important insights into complex systems (Box, 1979). Chapter 3 validated that an IWS could be approximated by its average customer and a single leak on that customer's supply pipe. The chapter extends that methodology to include a single intrusion source along that same customer's pipe. *First*, the model of Chapter 3 is used to determine the required extent of leak repair as the duty cycle and/or supply pressure is improved under water-scarce scenarios. *Second*, Chapter 3's model is extended to study how duty cycle, supply pressure, and leak repair can affect the volume of intruded, potentially-contaminated fluids present during the flushing and steady-state phases. And *third*, the implications of this extended model are quantified by applying it to self-reported performance indicators for IWS serving 108 million people. A modified version of this chapter, along with parts of Chapter 3, has been published as Taylor et al. (2018b).

6.2 Model construction

6.2.1 Leaks and intrusion

Wherever a pathway exists between the interior and exterior of a pipe, the potential for outward leakage and inward intrusion exist. For a given pathway, both inward and outward flows cannot occur simultaneously. However, across a variably-pressurized network surrounded by externally-pressurized fluids, inward and outward flows may occur simultaneously at different locations. To simplify the model that follows, these flows are accounted for independently, which ensures that the equations describing each are always greater than or equal to zero.

Eq 3.1 models a system's volume of leakage (V_L). This equation assumes that the effect of external fluids on the system's total leakage rate is negligible. Where external fluids are in the vicinity of a pathway into the pipe, it is common practice to model their rate of intrusion (Q_C) as flow through an orifice (Besner et al., 2011):

$$Q_C = C_d A_C [2g(H_C - H)]^{\beta} \tag{6.1}$$

where, β accounts for the pressure dependency of intrusion, C_d is an orifice coefficient accounting for the shape of the orifice (and correcting units when $\beta \neq 0.5$), A_C is the size of the orifice where intrusion is occurring, and g, H, and H_C are as in Equation 3.1.

Since external fluid pressure is not likely to be high enough to act to close an orifice, a single intrusion location likely has $\beta \approx 0.5$ (although Besner et al. (2011) caution that this common assumption has not been experimentally investigated). When multiple intrusion orifices are aggregated into an equivalent orifice, a different value of β can account for changes in H between sites.

External fluid pressure: In CWS, pipes laid below the water table are a common location for intrusion. The external fluid pressure is often modeled as the pipe depth below the water table (Besner et al., 2011). For simplicity however, commercial models for intrusion risk often combine the various pipe depths into a single, average external fluid pressure (H_C) (Besner et al., 2011).

In IWS, many sources of contamination have very low or no pressure associated with them (e.g., moist soils); some sources may have pressure up to the buried depth of the water pipe (e.g., groundwater pressure); and, occasionally cross-connections with sewers pose a severe intrusion hazard.

Averaging Eq 6.1 by the fraction of time a system in unpressurized (i.e., $1-t$), the volume of potentially-contaminated fluid that intrudes during the non-supply stage (i.e., when $H = 0$), V_{CF}, is:

$$V_{CF} = (1-t)Q_{CF} = (1-t)K_C f_C A H_C^{\beta} \tag{6.2}$$

Where Q_{CF} is the intrusion rate during the non-supply stage, f_C is the probability that external fluids are in the vicinity of a given leakage/intrusion pathway, K_C is a combined constant, and H_C is the average external pressure of fluids surrounding the pipe (e.g., groundwater pressure). β accounts for the pressure dependency of the rate of intrusion.

Accounting for the intrusion potential during the supply stage is more complex. In an IWS, pressure varies substantially throughout the network and so even when the average system pressure head (H) is higher than the average pressure of external fluids (H_C), some intrusion may still occur (at locations where the internal pipe pressure is less than the external fluid pressure). In order to account for this possibility, the network pressure at a given leakage/intrusion pathway ($H_{x,y}$) is modeled by an unknown probability distribution $f()$. The intrusion rate during the supply stage, Q_C, is therefore:

$$Q_C = K_C f_C A \int_{-\infty}^{\infty} f(H_{x,y}) \min(0, (H_C - H_{x,y})^{\beta}) dH_{x,y} \tag{6.3}$$

To simplify the algebra that follows, this probabilistic model is represented by the function $\Theta()$. The volume (of potentially-contaminated fluid) that intrudes during the supply stage (V_C) is, therefore:

$$V_C = tQ_C = tf_C A\Theta(H_C - H) \tag{6.4}$$

Leak repair strategy: When utilities reduce their EOA, they are assumed to do so without strategically considering the location or pressure of potential intrusion sources. This assumption allows the ratio of leak pathways with intrusion sources in their vicinity (f_C) to remain constant during system improvements. Unfortunately, this also prevents the model from capturing the importance of removing high-risk intrusion sources (e.g., eliminating cross-connections between water pipes and sewers) (Vairavamoorthy et al., 2007c).

6.2.2 Intruded volume and the fate of intruded contaminants

This chapter models factors that govern the total volume of fluids intruding into the system, but does not differentiate between the concentration or health risks of intrusion sources. Similarly, it does not account for the possibility that intrusion sources could be depleted through intrusion or diluted through leakage. This approach is consistent with risk assessments for CWS (Ebacher et al., 2012; Kirmeyer and Martel, 2001; Besner et al., 2011; Fox et al., 2016).

Since only the intruded volume is considered, any contaminants it contains are implicitly treated as conserved species, neglecting disinfection and biomass growth. Similarly, the potential for the storage of contaminants in the biofilm, which may store pathogens and release them at a later time, is also neglected (Flemming et al., 2002) (e.g., sloughing of biofilms during flushing and steady-state phases).

While intrusion is modeled during both supply and non-supply stages, all of the intruded volume (and all of its contaminants) is assumed to exit the system exclusively through customer premises (i.e., no intruded volume leaks out of the system). This implies that the intruded volume which accumulated during the non-supply stage (V_{CF}) is also the intruded volume present during the flushing phase.

Limitations: Neglecting biofilm growth, storage, and sloughing may underestimate the effect that fluids which intrude during non-supply have on steady-state water quality. Conversely, neglecting disinfection may overestimate the importance of reducing intruded fluids in systems with consistently-high concentrations of residual disinfectant. Finally, neglecting the quality and potential dilution of intrusion sources may overestimate the importance of minimizing the potential flux of intruded fluids.

Quantification: While some practitioners measure reduction in contaminants as a percentage, many chemical and physical disinfection processes are measured by log reduction (LR) (Benjamin and Lawler, 2013). LR accounts for the fact that it is harder to remove the last traces of contamination (Benjamin and Lawler, 2013). LR has the added advantages of making the superposition of multiple effects linear, and increasing the ease of displaying different reduction values. Accordingly, LR is used to account for the relative reduction in the volume of intruded (and potentially-contaminated) fluids from an original volume, V_C^0, to the final, V_C^* (Benjamin and Lawler, 2013):

$$\mathrm{LR} = \log_{10}(\frac{V_C^0}{V_C^*}) = -\log_{10}(\frac{V_C^*}{V_C^0}) \tag{6.5}$$

Implicitly, this metric assumes that V_C^0 is strictly positive (i.e., $V_C^0 > 0$).

LR = 1.0, 2.0, 3.0 correspond to 90%, 99%, and 99.9% reductions in intruded fluids, respectively. A negative value of LR suggests that the intruded volume has increased.

6.2.3 Flushing phase's instantaneous, unmixed flow

Intrusion can occur during the non-supply stage, the flushing phase, and the steady-state phase of an IWS. However, in light of the limited duration of the flushing phase (Kumpel and Nelson, 2014), this chapter assumes that the flushing phase is instantaneous (i.e., the steady-state phase lasts for t). In addition, despite the continuous transition between flushing and steady-state phases, these two phases are modeled as distinct and mixing of the flushing phase with the steady-state phase is not accounted for.

The first assumption (instantaneous flushing) overestimates the potential volume of intruded fluids in the steady-state phase and underestimates it in the flushing phase. The second assumption (no mixing) has the opposite effect.

6.2.4 Simplifying an IWS to an equivalent node

The model proposed thus far is equivalent to supplementing the model of Chapter 3 with a single intrusion source upstream of the network's average customer. An IWS, therefore, can be reduced to an equivalent node, with a single pressure, demand, area for leakage, prevalence of intrusion sources, and average external fluid pressure, as shown in Fig 6-1.

6.2.5 Allowable increases in leakage

The variable l accounts for a utility's ability to accommodate additional leakage in their system, from its initial value (V_L^0) to its final (V_L^*), as a percentage of the initial volume of water input into the system (V_T^0):

$$l \geq \frac{V_L^* - V_L^0}{V_T^0} = \frac{V_L^0}{V_T^0}\left(\frac{V_L^*}{V_L^0} - 1\right) \tag{6.6}$$

Most IWS are constrained by the volume of water they have available and cannot allow leakage to increase (i.e., $l = 0$). However, l can be positive if system improvements lead to an increase in finished water production capacity (V_T) or diversions

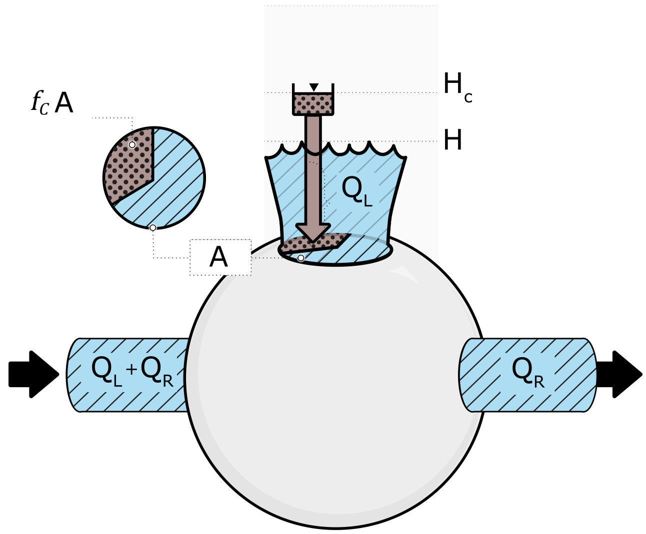

Figure 6-1: **Single node equivalent of an IWS.** The system or sub-system is modeled as an equivalent node, with pressure head H, average external fluid pressure H_C, flow to customers Q_R, and leakage flow Q_L; A is the equivalent area of pathways for leakage and $f_C A$ is the equivalent area for intrusion.

of water from other areas, or if the total water consumption (V_D) (paying plus non-paying customers) decreases. Conversely, if consumption increases, l can become negative.

6.2.6 Leakage metrics: NRW, UFW, and EOA

Non-revenue water (NRW) is the amount of water that is distributed, but does not generate revenue; it is often used as a proxy for leakage rates. Unaccounted for water (UFW) tracks how much water is missing from a utility's water balance of input minus output. In order to make use of the available data, the difference between UFW and NRW, which is usually small (Van den Berg and Danilenko, 2011), is neglected.

Despite the limitations of accounting for NRW (n) as a percentage of total input volume (Frauendorfer and Liemberger, 2013), this chapter continues to do so in order to use the reported NRW values from the available databases. To apply the proposed equations, an assumption is required about what fraction (p) of each utility's NRW is due to physical leakage. The fraction of the input volume that is lost to (physical) leakage is (Table 5.2):

$$V_L = pnV_T \qquad (0 \leq p \leq 1) \tag{6.7}$$

6.2.7 Data sources

The implications of the proposed model are quantified using self-reported water utility data from the World Bank's IBNET database (Van den Berg and Danilenko, 2011) and the 2007 Benchmarking and Data Book of Water Utilities in India (BDBWUI; Asian Development Bank and Ministry of Urban Development Government of India (2007); Table 6.1).

IBNET: The World Bank's IBNET database holds self-reported performance indicators for 3085 different utilities delivering water to more than 996 million people (Van den Berg and Danilenko, 2011). Of these utilities, 659 (21%) have duty cycles less than 99%. These IWS serve a population of 303 million people. Unfortunately, not all of these utilities report NRW, population, and duty cycle. Only the most recent data from the subset of IWS who report all three are included here.

Following Van den Berg's (2015) study of the IBNET database, outliers were excluded by considering only IWS reporting population and NRW between the 1st and 99th percentile values. Similarly, IWS reporting duty cycles less than the 1st percentile of IWS duty cycle were excluded. The resultant data set includes 325 utilities (Table 6.1). Almost half (46%) of the filtered database entries are from sub-Saharan Africa, and the dataset includes entries from only one South Asian country (Bangladesh). The mean duty cycle was 54%, and the mean NRW was 36%. Dataset entries occurred from 2001 to 2015 (Table 1). Unfortunately, the IBNET database does not report system or customer pressure.

BDBWUI: The BDBWUI details self-reported benchmarking data for 20 utilities in India serving 55 million people (Asian Development Bank and Ministry of Urban Development Government of India, 2007). Reported metrics include the average pressure head at customer connections, measured in meters of water column. The BDBWUI dataset reports leakage in terms of UFW instead of NRW, but as previously discussed, this difference is neglected and it is referred to as NRW.

To account for outliers the minimum and maximum values were omitted for NRW, pressure, and duty cycle. Utilities missing data were omitted. The resultant dataset included nine utilities serving a total of 13 million people (Table 2).

Combined: Together, these datasets represent 334 utilities, serving 108 million people with IWS. Four cities will be highlighted, each near the 25th or 75th percentile of their datasets (Table 6.2).

6.3 Scaling relations for pipe networks

6.3.1 Required reductions in EOA

Substituting Eqs 3.2 and 6.7 into Eq 6.6:

$$\begin{aligned} pn\left(\frac{t^*}{t^0}\left(\frac{H^*}{H^0}\right)^\alpha \frac{A^*}{A^0} - 1\right) &\leq l \\ \therefore \frac{A^*}{A^0} &\leq \left(\frac{t^0}{t^*}\right)\left(\frac{H^0}{H^*}\right)^\alpha \left(\frac{l}{pn} + 1\right) \end{aligned} \tag{6.8}$$

Each of the three terms in parentheses in Eq 6.8 refers to the scaling of EOA necessitated by a different aspect of system improvement: duty cycle, supply pressure, and additional leakage allowance. Increased supply pressure and/or duty cycle increases the necessitated repairs, while an additional leakage allowance (e.g., because of extra water available from a water treatment plant expansion) reduces them.

As proposed, the repair requirement suggests that utilities can allow their EOA to increase (e.g., by ceasing leak repair) if they also i) allow leakage to increase (e.g., by supplying extra water), ii) reduce duty cycle, and/or iii) reduce supply pressure (Eq 6.8). This may explain why low-pressure IWS are prevalent as they provide an easy alternative to the major infrastructure improvements needed to reduce EOA.

Table 6.1: **IWS in the filtered IBNET and BDBWUI databases.** Characteristics are subtotaled and combined.

Region	Countries	Utilities	Population served	Duty cycle	NRW	Pressure (m)	Year
	n	n	mean (range) total $\times 10^6$	mean (range)	mean (range)	mean (range)	range
EAP[a]	3	22	0.51 (0.031-7.1) 11.1	0.77 (0.08-0.96)	32% (19-62%)	N.R.[b]	2009-15
ECA[a]	8	76	0.06 (0.002-0.8) 4.4	0.57 (0.12-0.98)	47% (4-80%)	N.R.[b]	2001-14
LAC[a]	3	20	0.60 (0.022-7.5) 12.0	0.69 (0.17-0.96)	50% (34-69%)	N.R.[b]	2006-13
MENA[a]	3	11	0.42 (0.018-2.6) 4.6	0.43 (0.12-0.83)	29% (18-40%)	N.R.[b]	2010
SA[a]	1	46	0.12 (0.003-1.4) 5.4	0.33 (0.08-0.67)	19% (3-45%)	N.R.[b]	2014
SSA[a]	11	150	0.38 (0.004-4.8) 57.3	0.54 (0.06-0.98)	34% (4-79%)	N.R.[b]	2011-14
IBNET subtotal	29	325	0.29 (0.002-7.5) 94.9	0.54 (0.06-0.98)	36% (3-80%)	N.R.[b]	2001-15
BDBWUI	India	9	3.8 (0.6-13.0) 13.0	0.23 (0.04-0.46)	30% (13-57%)	4.3 (2.0-10)	2005-06
Total	30	334	0.38 (0.002-7.5) 107.9	0.53 (0.04-0.98)	36% (3-80%)	N.A.[c]	2001-15

[a] From IBNET database: East Asia and the Pacific (EAP), Europe and Central Asia (ECA), Latin America and the Caribbean (LAC), Middle East and North Africa (MENA), South Asia (SA), sub-Saharan Africa (SSA).
[b] Not reported
[c] Not applicable

Table 6.2: **Summary data for case study cities.**

Country	City	Population	Duty cycle	NRW	Pressure	Reporting Year	Dataset
		$\times 10^6$	(%)		(m)		
Tanzania	Dar es Salaam	1.93	0.33	56%	N.R.[a]	2013	IBNET
Yemen, Rep.	Hajjah	0.05	0.75	24%	N.R.[a]	2010	IBNET
India	Mumbai	13.00	0.17	13.6%	7	2005-06	BDBWUI
India	Varanasi	1.60	0.29	30%	3	2005-06	BDBWUI

[a] Not reported

This chapter focuses on the system improvement process and therefore assumes that the EOA does not increase (i.e., $\frac{A^*}{A^0} \leq 1$):

$$\therefore \frac{A^*}{A^0} \leq \min\left[1, \frac{t^0}{t^*}\left(\frac{H^0}{H^*}\right)^{\alpha}\left(\frac{l}{pn}+1\right)\right] \tag{6.9}$$

Assuming that utilities do as little work as possible (i.e., maximizing A^* subject to Eq 6.9):

$$\frac{A^*}{A^0} = \min\left[1, \frac{t^0}{t^*}\left(\frac{H^0}{H^*}\right)^{\alpha}\left(\frac{l}{pn}+1\right)\right] \tag{6.10}$$

In practice, Eq 6.10 is not universally applicable. For example, the CWS pilot project in Hubli-Dharwad replaced the entire pipe network ($A^* \approx 0$) (The World Bank, 2011). Nevertheless, Eq 6.10 provides a reasonable approximation as most capital improvement projects do not involve complete replacement of the pipe network.

6.3.2 Effect of reduced EOA

Since the EOA for leaks (A) is common to Eqs 3.2, 6.2, and 6.4, these equations suggest that reducing A by the fraction $\frac{A^*}{A^0}$ (in the case where $t^* = t^0$ and $H^* = H^0$) may also scale the volume of intruded fluids in the steady-state and flushing phases by the ratio $\frac{A^*}{A^0}$, provided the initial volume of each is non-zero:

$$\begin{aligned}
\left.\frac{V_L^*}{V_L^0}\right|_{t^*=t^0,H^*=H^0} &= \frac{t^0 A^* \left(H^0\right)^{\alpha}}{t^0 A^0 \left(H^0\right)^{\alpha}} && = \frac{A^*}{A^0} && : V_L^0 > 0 \\
\left.\frac{V_C^*}{V_C^0}\right|_{t^*=t^0,H^*=H^0} &= \frac{t^0 f_C A^* \Theta(H_C - H^0)}{t^0 f_C A^0 \Theta(H_C - H^0)} && = \frac{A^*}{A^0} && : V_C^0 > 0 \\
\left.\frac{V_{CF}^*}{V_{CF}^0}\right|_{t^*=t^0} &= \frac{(1-t^0) k_C f_C A^* H_C^{\beta}}{(1-t^0) k_C f_C A^0 H_C^{\beta}} && = \frac{A^*}{A^0} && : V_{CF}^0 > 0 \\
\therefore \left.\frac{V_L^*}{V_L^0}\right|_{t^*=t^0,H^*=H^0} &= \left.\frac{V_C^*}{V_C^0}\right|_{t^*=t^0,H^*=H^0} = \left.\frac{V_{CF}^*}{V_{CF}^0}\right|_{t^*=t^0} && = \frac{A^*}{A^0} && : V_C^0, V_{CF}^0, V_L^0 > 0
\end{aligned} \tag{6.11}$$

6.3.3 Effect of increased duty cycle

Steady-state: Eq 6.4 suggests that an increase in the duty cycle from $t^0 \rightarrow t^*$ (with other parameters held constant) may increase the volume of contaminants intruding into the system during steady-state by $\frac{t^*}{t^0}$, provided $V_C^0 > 0$:

$$\left.\frac{V_C^*}{V_C^0}\right|_{A^*=A^0, H^*=H^0} = \frac{t^* f_C A^0 \Theta(H_C - H^0)}{t^0 f_C A^0 \Theta(H_C - H^0)} = \frac{t^*}{t^0} > 1 \qquad : V_C^0 > 0 \tag{6.12}$$

To the author's knowledge, this relationship has not been noted in the literature on IWS, and contradicts the conventional belief that increasing the duty cycle is universally good for water quality. If all other factors are held constant, the intrusion rate into the system during the supply stage is independent of the duty cycle (t). The accumulated volume is, therefore, linearly dependent on the duty cycle (Eq 6.12), as highlighted in Fig 6-2. For systems where customer demand (V_D) does not significantly depend on the duty cycle (e.g., customer demand may vary by only 15-20% where $t \in [0.25, 1]$ (Fan et al., 2014; Hamilton and Charalambous, 2015)), Eq 6.12 additionally suggests that the concentration of intruded fluid in the steady-state phase may also increase with the duty cycle. Eq 6.12 does not suggest that water quality will degrade by converting a low-pressure IWS to a high-pressure CWS. Instead, it suggests that in two systems with equal pressure distributions, differing only in duty cycle, the one with the longer duration will allow more time for any steady-state intrusion to accumulate (Fig 6-2).

The model's simplifying assumptions obscure two mechanisms which could temper this finding: first, contaminant storage and growth, which were neglected, could allow intrusion during the non-supply stage to influence steady-state water quality. Second, pressure was fixed at the location of intrusion (i.e., was exogenous); otherwise, increased duty cycle (which reduces flow rates and therefore friction losses) would increase pressure and therefore reduce the intrusion rate during the steady-state phase. Adding these mechanisms could provide useful refinements of the current model.

Flushing: In keeping with conventional understanding, Eq 6.2 suggests that increasing the duty cycle may decrease the volume of fluids that intrudes during the

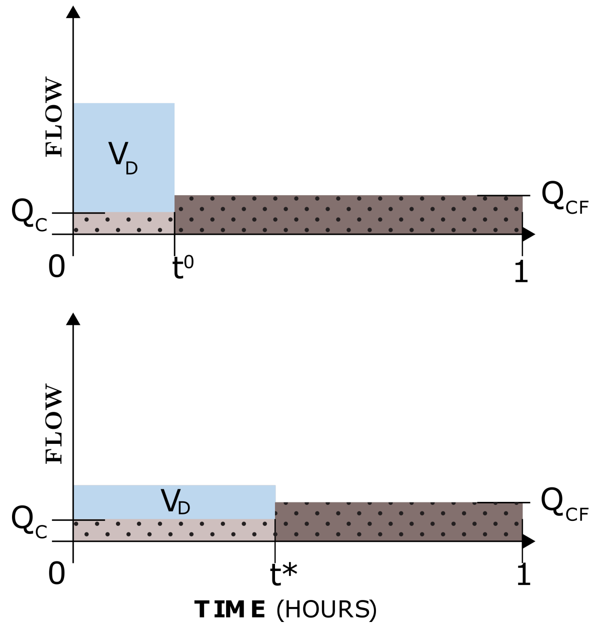

Figure 6-2: **Duty cycle's effect on intruded fluids.** Compare an initial system (top panel) with duty cycle t^0, customer demand volume V_D, and contaminant intrusion rates Q_C and Q_{CF} during the supply and non-supply stages, to the same system (bottom panel) if the duty cycle is lengthened (to t^*). If all else is held constant, Q_C and Q_{CF} are also constant.

non-supply stage and which is therefore present during the flushing phase by $\frac{1-t^*}{1-t^0} < 1$ (Eq 6.2; e.g., Fig 6-2).

Steady-state and flushing combined: Some customers are impacted by the total volume of intruded fluids in the system during steady-state and flushing phases. Assuming $t^* > t^0$ and $(V_C^0 + V_{CF}^0) > 0$, the combined intruded volume scales as:

$$\left.\frac{V_C^* + V_{CF}^*}{V_C^0 + V_{CF}^0}\right|_{A^*=A^0, H^*=H^0} = \frac{t^*\left(\frac{Q_C}{Q_{CF}} - 1\right) + 1}{t^0\left(\frac{Q_C}{Q_{CF}} - 1\right) + 1} \underset{(\text{if } Q_{CF} \geq Q_C)}{\leq 1} \quad : (V_C^0 + V_{CF}^0) > 0 \quad (6.13)$$

The condition $Q_{CF} \geq Q_C$ is met whenever:

$$
\begin{aligned}
& Q_{CF} \geq Q_C \\
& \iff k_C H_C^\beta \geq \Theta(H_C - H^0) \\
& \iff k_C H_C^\beta \geq \Theta(H_C - H^0) \\
& \iff \int_{-\infty}^{H_C} f(H_{x,y}^0) \left(1 - \frac{H_{x,y}^0}{H_C}\right)^\beta dH_{x,y}^0 \leq 1
\end{aligned} \tag{6.14}
$$

Deriving a simpler sufficient, but not necessary condition, if $H^0 \geq 0$ everywhere, then:

$$
\begin{aligned}
& \int_{-\infty}^{0} f(H_{x,y}^0) g() dH_{x,y}^0 \equiv 0 \qquad : \text{any function } g() \\
& \therefore \int_{-\infty}^{H_C} f(H_{x,y}^0) \left(1 - \frac{H_{x,y}^0}{H_C}\right)^\beta dH_{x,y}^0 = \int_{0}^{H_C} f(H_{x,y}^0) \left(1 - \frac{H_{x,y}^0}{H_C}\right)^\beta dH_{x,y}^0 \leq 1 \quad : \beta > 0
\end{aligned} \tag{6.15}
$$

Therefore, if $H^0 \geq 0$ everywhere in the system (i.e., $\int_{-\infty}^{0} f(H_{x,y}^0) dH_{x,y}^0 = 0$), the condition $Q_{CF} \geq Q_C$ is always met and larger duty cycles reduce the total intruded volume in both phases of supply. This qualification ($H^0 \geq 0$) is important as some neighborhoods have sub-atmospheric supply pressures due to customers using suction pumps (Kumpel and Nelson, 2016; Taylor, 2014).

Impact: Volumes of flushed water (and any associated contaminants) are not evenly distributed between customers. If duty cycles are increased, customers that do not currently consume any flushing water will have a higher risk of contaminant exposure. Conversely, customers that currently consume substantial volumes of flushing water will have a reduced risk of contaminant exposure.

Distinguishing between these effects has not been discussed in the literature and may help understand the health impacts of CWS. Ercumen et al. (2015) found that CWS only had significant health benefits for lower-income families, which they hypothesized might be due to the more frequent usage of water filters in higher-income families. This chapter suggests another plausible mechanism: if lower-income families were exposed to flushing water more than higher-income families, the water quality improvements due to CWS would be concentrated in lower-income families.

Similarly, while Adane et al. (2017) found a strong association (adjusted odds ratio of 4.8) between IWS and acute diarrrhea in children under five in slums in Addis Ababa, they found 94% of the water quality samples (across IWS and CWS) to be of low risk for *E. coli* contamination. While household storage is known to reduce water quality (Kumpel and Nelson, 2016), the IWS-induced risk of diarrhea could also have been caused by lower quality flushing water, missed by their sampling strategy, which did not distinguish between flushing and steady-state phases.

More generally, for utilities that only sample water quality in steady-state conditions (a common practice), this chapter suggests that the measured water quality would worsen after converting to CWS (assuming no increase in pressure or reduction in EOA). Regulators, utilities, and researchers studying IWS should specify more carefully which phase of supply is to be, or has been, measured (e.g., this has been reported by Kumpel and Nelson (2013); Erickson et al. (2017), but not Andey and Kelkar (2007); Shaheed et al. (2014); Adane et al. (2017)).

6.3.4 Combined effects of leak repair and duty cycle

Steady-state: When increased duty cycle is considered in combination with necessary reductions in EOA (to prevent an increase in V_L), the net effect on the intruded volume during the steady-state phase depends on the allowable increase in leakage (l). Combining Eqs 6.4 and 6.10, and assuming $V_C^0 > 0$:

$$\begin{aligned} \left.\frac{V_C^*}{V_C^0}\right|_{H^*=H^0} &= \frac{t^* f_C \Theta(H_C - H^0)}{t^0 f_C \Theta(H_C - H^0)} \min\left[1, \frac{t^0}{t^*}\left(\frac{H^0}{H^0}\right)^\alpha \left(\frac{l}{pn}+1\right)\right] && : V_C^0 > 0 \\ \therefore \left.\frac{V_C^*}{V_C^0}\right|_{H^*=H^0} &= \frac{t^*}{t^0} \min\left[1, \left(\frac{t^0}{t^*}\right)\left(\frac{l}{pn}+1\right)\right] && : V_C^0 > 0 \quad (6.16) \end{aligned}$$

In the limit where a utility cannot allow leakage to increase (i.e., $l = 0$), and must therefore conduct all of the necessary EOA reductions, Eq 6.16 suggests that increased duty cycle will have no net effect on the intruded volume in the steady-state phase

($\frac{t^*}{t^0}\frac{t^0}{t^*} = 1$). However, if a utility does less EOA reduction (perhaps by expanding its water supply capacity), Eq 6.16 suggests that increased duty cycle will increase the intruded volume in the steady-state phase.

Consider, for example, a utility with enough extra water to allow its leakage to increase by 50% ($\frac{l}{pn} = 0.5$). While such an increase may seem unreasonable, it can occur if the utility had 40% NRW, of which 50% was due to physical losses. In this case, a reasonable increase in production capacity of 10% would allow for a 50% leakage increase (i.e., $\frac{0.1}{0.5*0.4} = 0.5$). Assuming that some intrusion occurs during both supply and non-supply stages, Eqs 6.5 and 6.12 suggest that if the duty cycle is increased from $t^0 = 0.25$ to $t^* = 0.88$ hrs/day, the utility would have a log reduction (LR) $= -log_{10}(\frac{t^*}{t^0}) = -0.54$ due to increased duty cycle alone. However, Eq 6.16 also suggests that the LR from the combined effects of duty cycle and EOA reduction would be $-log_{10}(\frac{w}{pn}+1) = -0.17$. In both cases, the proposed equations suggest that the intruded volume in the steady-state phase will increase. Fig 6-3 plots a range of other scenarios.

Flushing: The net effect of increasing the duty cycle and its associated EOA reduction on the intruded volume in the flushing phase is modeled by Eqs 6.2 and 6.10:

$$\left.\frac{V^*_{CF}}{V^0_{CF}}\right|_{H^*=H^0} = \frac{(1-t^*)k_C f_C H_C^\beta}{(1-t^0)k_C f_C H_C^\beta}\min\left[1, \frac{t^0}{t^*}\left(\frac{H^0}{H^0}\right)^\alpha\left(\frac{l}{pn}+1\right)\right] \quad : V^0_{CF} > 0$$

$$\therefore \left.\frac{V^*_{CF}}{V^0_{CF}}\right|_{H^*=H^0} = \frac{(1-t^*)}{(1-t^0)}\min\left[1, \frac{t^0}{t^*}\left(\frac{l}{pn}+1\right)\right] \quad : V^0_{CF} > 0 \quad (6.17)$$

The predicted effect from increased duty cycle is $\frac{1-t^*}{1-t^0}$, while EOA reduction's effect is $\frac{t^0}{t^*}\left(\frac{l}{pn}+1\right)$. Both effects act to reduce intrusion-induced risk in the flushing phase, therefore their relative magnitudes are compared. For the example utility, Eqs 6.2 and 6.10 suggest a LR in the intruded volume in the flushing phase due to increased duty cycle of $-log_{10}\left(\frac{1-t^*}{1-t^0}\right) = 0.78$, and a LR from EOA reduction of $-log_{10}\left(\frac{t^0}{t^*}(\frac{l}{pn}+1)\right) = 0.37$. For this example, therefore, the increased duty cycle is expected to be substantially more important than EOA reduction for improving the safety of the flushing phase. Fig 6-4 shows these two predicted effects separately for

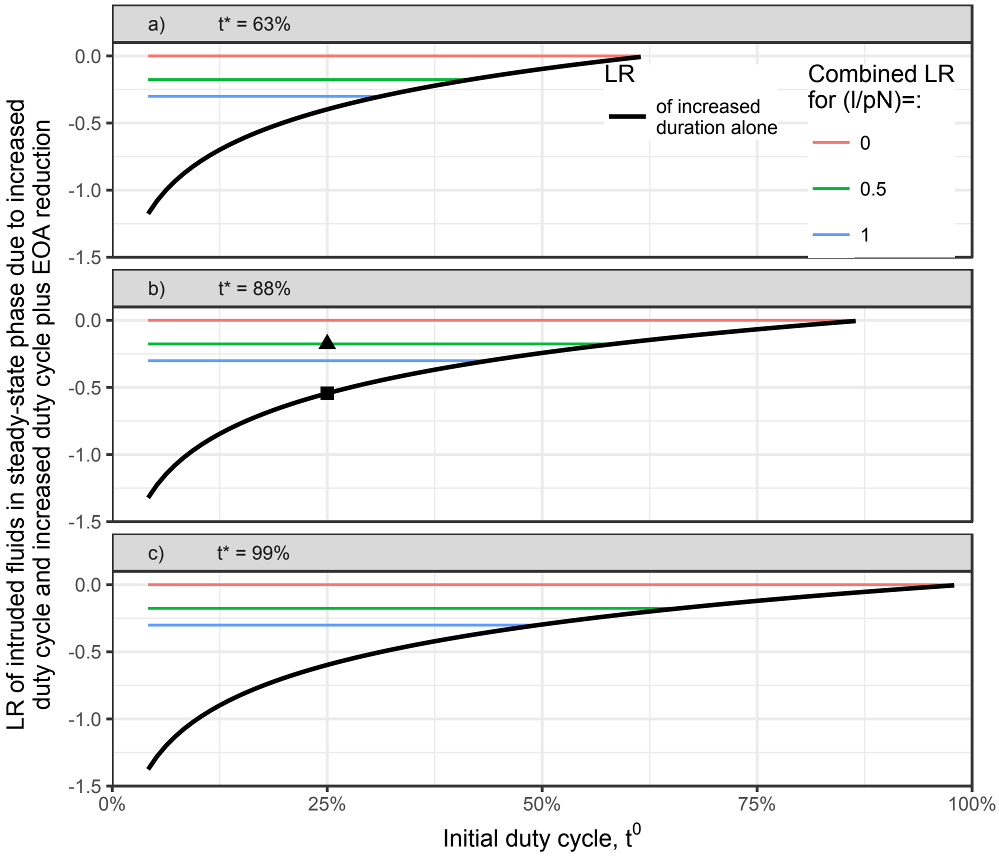

Figure 6-3: **Predicted log-reduction (LR) during steady-state from increased duty cycle and reduced EOA, combined.** The increase (negative LR) in the intruded volume in steady-state due to increased duty cycle (thick black line and square) and combined with the reductions in EOA required by increased duty cycle (colored thin lines). Simulated utilities with three levels of allowed leakage are shown: no allowed leakage (pink/upper lines), additional leakage equal to 50% of physical losses (i.e., $\frac{l}{pn} = 0.5$) (green/middle lines, and triangle), and additional leakage equal to 100% of physical losses (blue/lower lines). Final duty cycles of 63%, 88%, and 99% are shown in the top (a), middle(b), and bottom (c) panels, respectively. The text's example utility is also shown (triangle and square).

a range of simulated utilities.

As the increased duty cycle $t^* \to 1$, its effect on the safety of the flushing phase is expected to dominate over the effect of reduced EOA (Eq 6.17). Indeed, Eq 6.17 suggests that if $t^* = 88\%$, duty cycle dominates over the importance of reducing EOA for all cases with initial duty cycles $t^0 \geq 13\%$ (Fig 6-4b). Conversely, if the final duty cycle is brief, the necessary reductions in EOA may also substantially contribute to improved flushing safety. For example, if the final duty cycle $t^* = 63\%$ (Fig 6-4a), reducing EOA becomes more important in systems where leakage cannot increase substantially (i.e., $\frac{l}{pn} \leq 0.5$) and with initial duty cycles $t^0 \leq 38\%$ (Fig 6-4a).

Impact: Eqs 6.2 and 6.10 suggest that utilities wanting to improve the safety of their flushing water while operating with $t^* \leq 63\%$, should develop campaigns to reduce EOA and then reassess if additional contaminant reduction is required. More generally, the model suggests that projects which increase their duty cycle, should reduce their EOA by at least $\frac{t^0}{t^*}$ to preserve steady-state quality. Carefully monitoring EOA reductions should therefore be a priority for regulators and project managers.

Neither of the two recent cross-sectional studies of water quality in IWS are able to assess the steady-state predictions of this model. Kumpel and Nelson (2013) examined the water quality of a project that replaced 100% of the pipe network (The World Bank, 2011), rendering $A^* \approx 0$ (vs. Eq 6.10). Such a massive reduction in the EOA would offset the predicted harmful effects of increased duty cycle on steady-state water safety. Erickson et al. (2017) studied IWS in Arraiján, Panama, and did not find significant differences in steady-state water quality between zones with different duty cycles (likely due to high water quality). However Erickson et al. (2017) did find deterioration in the water quality of the flushing phase when the duty cycle decreased, as predicted by the proposed model (although the variance in this trend was high).

6.3.5 Effect of increased pressure

Since contaminant storage and growth was neglected, supply pressure has no effect on the volume of fluids that accumulate during the non-supply stage (Eq 6.2). Therefore, system pressure has no direct effect on the intruded volume in the flushing phase

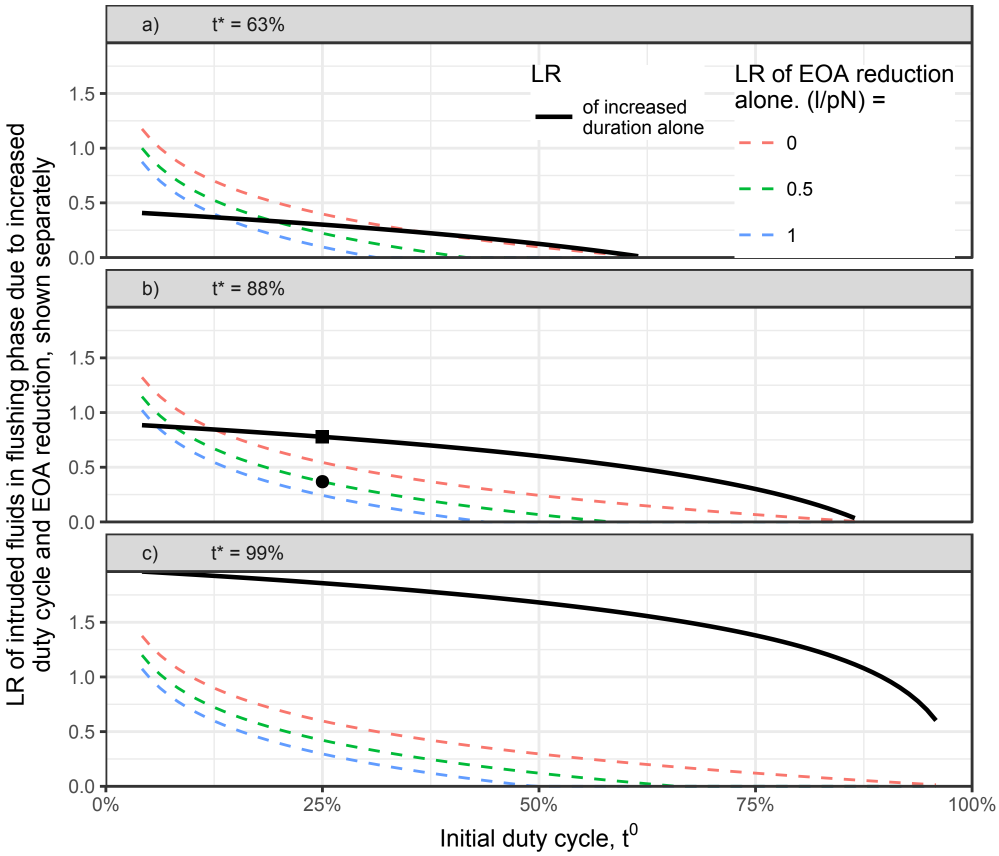

Figure 6-4: **Log-reduction (LR) during the flushing phase from increased duty cycle and reduced EOA, separately.** The LR during flushing attributable to increased duty cycle (thick black line and square dot), and due to the necessitated reductions in EOA (colored dashed curves), each plotted separately. Three levels of allowable leakage increase water are shown: no increase (pink/upper curves), a 50% increase in physical losses (i.e., $\frac{l}{pn} = 0.5$) (green/middle curves, and circle), and a 100% increase in physical losses (blue/lower curve). Final duty cycles of 63%, 88%, and 99% are shown in the top (a), middle (b), and bottom (c) panels, respectively. The text's example utility is also shown (square and circle).

Table 6.3: **Summary of the scaling equations effecting the risk of intrusion.** The intruded volume is predicted to scale by the ratio listed in the table when the system's duty cycle (t), pressure head (H), or EOA (A) is changed from a baseline (^{0}) to an improved state (*). Each column assumes that some intruded volume is present in the baseline scenario (i.e., $V_C^0, V_{CF}^0 > 0$).

Due to:	Steady-State $\frac{V_C^*}{V_C^0} =$	Flushing Phase $\frac{V_{CF}^*}{V_{CF}^0} =$	Combined Effect $\frac{V_C^* + V_{CF}^*}{V_C^0 + V_{CF}^0} =$
Reduced EOA	$\frac{A^*}{A^0} \leq \min\left[1, \frac{t^0}{t^*}\left(\frac{H^0}{H^*}\right)^\alpha\left(\frac{l}{pn}+1\right)\right]$		
Increased t $\lvert A^* = A^0, H^* = H^0$	$\frac{t^*}{t^0} > 1$	$\frac{1-t^*}{1-t^0} < 1$	$\frac{t^*\left(\frac{Q_C}{Q_{CF}}-1\right)+1}{t^0\left(\frac{Q_C}{Q_{CF}}-1\right)+1} \leq 1$ (if $Q_{CF} \geq Q_C$)
Increased H $\lvert A^* = A^0, t^* = t^0$	$\frac{\Theta(H_C - H^*)}{\Theta(H_C - H^0)} \leq 1$	None (i.e., 1)	Not considered

(V_{CF}). Conversely, due to the structure of $\Theta()$, a uniform increase in pipe pressure cannot increase the steady-state intrusion-induced risk. Assuming $V_C^0 > 0$:

$$\left.\frac{V_C^*}{V_C^0}\right|_{A^*=A^0, t^*=t^0} = \frac{t^0 f_C A^0 \Theta(H_C - H^*)}{t^0 f_C A^0 \Theta(H_C - H^0)} = \frac{\Theta(H_C - H^*)}{\Theta(H_C - H^0)} \leq 1 \qquad : V_C^0 > 0 \qquad (6.18)$$

In practice, this relationship has been observed to have a threshold after which the system pressure exceeds any plausible external fluid pressure and there are no further improvements in water quality (Kumpel and Nelson, 2014; Lindley and Buchberger, 2002).

6.3.6 Summary of the scaling equations

The proposed effects of EOA reduction, increased duty cycle, and increased supply pressure are summarized in Table 6.3 and graphically summarized in Fig 6-5.

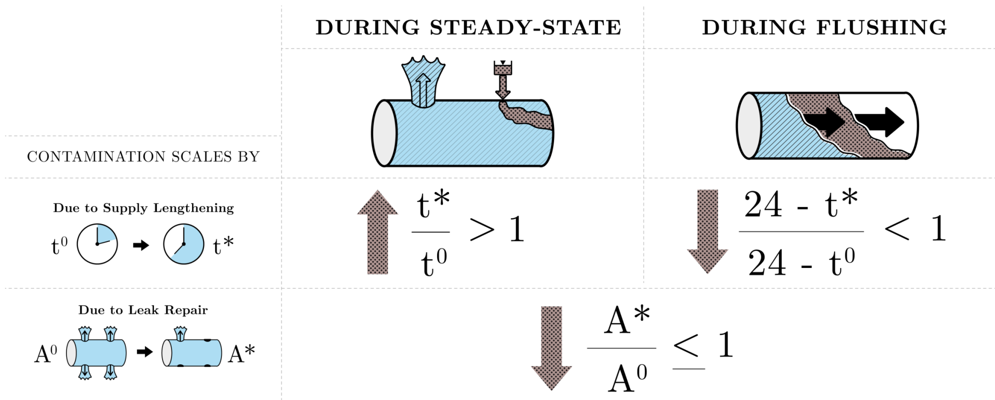

Figure 6-5: **Key scaling relationships governing the risk of intrusion.**

6.4 Quantitative implications for global IWS

Having defined a set of equations that relate duty cycle and supply pressure, EOA, and intruded volumes, this chapter now considers their implications using benchmarking data from IBNET and BDBWUI and project targets typical of India.

Official Indian targets for city water pipe networks are 17m of pressure and a duty cycle of 24 hrs/day (CPHEEO, 1999). The duty cycle target is relaxed to 23.75 hrs/day (i.e., $t^* = 0.99$) to: i) distinguish flushing vs. steady-state phases; and ii) enable definition of LR (if 100% of the intruded volume is removed from the flushing phase, $LR = \infty$). Attaining a 99% duty cycle would still be a major accomplishment for most IWS.

Neither dataset reports the fraction of NRW that is due to physical leakage (i.e., p), nor the allowable increases in leakage (i.e., l). Since the proposed equations depend on the ratio of $\frac{l}{p}$, utilities are simulated under two scenarios: i) where physical losses are a small percentage of NRW ($p = 1/3$) such that leakage can be allowed to increase substantially ($l = 0.1$; $\frac{l}{p} = 0.3$); and ii) where physical losses are 50% of NRW ($p = 0.5$) and the increase in leakage is constrained ($l = 0.01$; $\frac{l}{p} = 0.02$). Scenario ii) is more typical of conditions in South Asia (McIntosh, 2014).

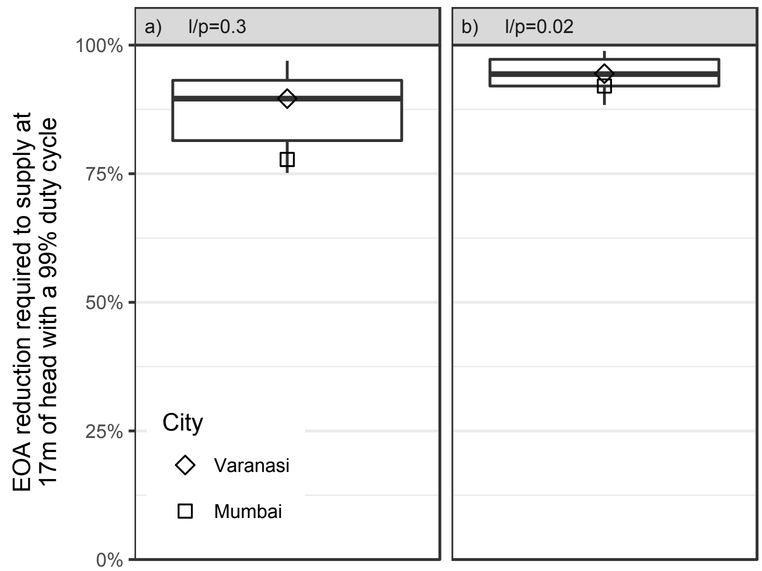

Figure 6-6: **Required EOA reductions in BDBWUI.** The model suggests that increasing the duty cycle to 99% and the pressure to 17m will require utilities to reduce their EOA by a fraction (y-axis) that depends on how much of their current NRW is physical loss (p) and their allowed leakage increases (l). Box plots summarize these required EOA reductions under scenarios i) and ii) $\frac{l}{p} = 0.3$ and b) $\frac{l}{p} = 0.02$).

6.4.1 Required EOA reductions

As duty cycle and supply pressure increase, the nine Indian utilities in the filtered BDBWUI database (Table 6.1) will have to reduce their EOA by varying amounts (Eq 6.10; Fig 6-6). The model predicts that in scenario i), the majority of Indian utilities will require more than 90% reduction in EOA in order to achieve their pressure and duty cycle targets (Fig 6-6). With the more reasonable assumptions in scenario ii), the required reduction in EOA predicted by the model increases to a median of 94%. Varanasi was the median city for these calculations (shown as a sample calculation in Appendix D). Mumbai reported a lower initial NRW and a higher initial pressure than Varanasi. This tempered its required reduction in EOA from 90% to 78% in scenario i) and from 94% to 92% in scenario ii) (shown in Fig 6-6).

The IBNET database does not include data on supply pressures so Fig 6-7 plots only the EOA reductions necessitated by increasing the duty cycle. To assist the reader in aggregating the many data points, a moving average of the 5th, 50th, and 95th percentile of utilities with initial duty cycles in a 0.04 (one-hour/day) window

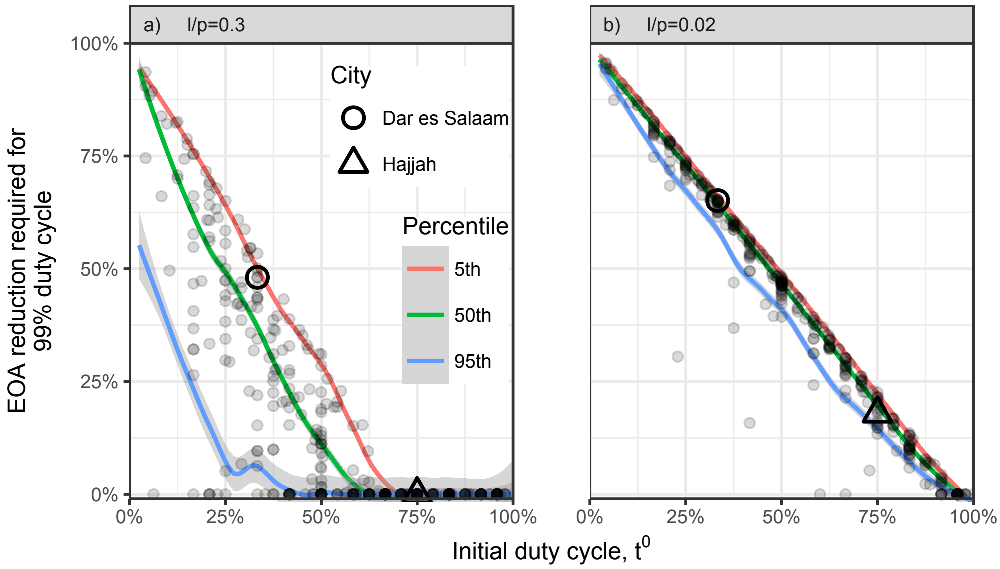

Figure 6-7: **Required EOA reductions in IBNET.** The model predicts that increasing the duty cycle to 99% will require utilities (grey dots) to reduce their EOA by a percentage (y-axis) that depends on their initial duty cycle (x-axis) and the ratio of allowed leakage increases (l) to the percent of their current NRW that is leakage (p). Each utility is plotted under scenarios i) and ii) (i.e., a) $\frac{l}{p} = 0.3$ and b) $\frac{l}{p} = 0.02$). For initial duty cycles within a 4% span (e.g., 23-27%), the 5th (red/upper line), 50th (i.e., median, green/middle line), and 95th (blue/lower line) percentiles are smoothed into the displayed curves.

is displayed. For example, in Fig 6-7a, utilities with initial duty cycles between 0.10 and 0.14 are predicted to require a median EOA reduction of 70%, with the 5th and 95th percentile being 82% and 32%, respectively.

Under scenario i) there is significant spread in the data. The required reduction in EOA for utilities with initial duty cycles $t^0 \in [0.21, 0.25]$ ranged from 11-67% for the 5th and 95th percentile of utilities (Fig 6-7). However, under the more reasonable assumptions of scenario ii), the required EOA reduction ranged only from 69-77% for the same range of t^0 (Fig 6-7).

Where additional leakage can be allowed (e.g., because of a recent expansion in production capacity), utilities with relatively high initial duty cycles (e.g., Hajjah) will not need to reduce their EOA. Conversely, utilities such as Dar es Salaam, with lower initial duty cycles and higher NRW are predicted to require almost 50% reductions in their EOA due to increased duty cycles, even under scenario i).

To cut capital costs, government agencies frequently advocate for repairing instead of replacing existing pipes. This chapter suggests that under initially-short duty cycles and low pressures, repairing existing pipes can create benefits. However, when networks transition to high-pressure CWS, extensive reductions in EOA will be required. Therefore, replacing most (if not all) pipes will likely be the economical solution if high-pressure CWS are to be achieved. In India, where the EOA must be reduced by a median of at least 90%, full pipe replacement should be the rule, not the exception.

6.4.2 Effects of increased duty cycle and EOA reduction

Fig 6-8a depicts the effects predicted by Eq 6.16 for each utility in the combined IB-NET and BSBWUI database. For utilities that allow leakage to increase substantially (scenario i), Eq 6.16 suggests that increasing the duty cycle increases the intrusion risk (i.e., the intruded volume) in the steady-state phase. For example, upgrading the system in Dar es Salaam would cause an increase in the intrusion-induced risk during the steady-state phase. Specifically, it predicts LR=-0.47 from increased supply, LR=$+0.28$ from required EOA reduction, and a net of LR=-0.19 (see Appendix D for a worked example of this calculation). No required-reduction in EOA is predicted in Hajjah, and its LR=-0.12 is the same as that due to increased duty cycle alone. Mumbai had the lowest (i.e., most negative) predicted LR during steady state among the four case study cities. Due to its low initial NRW, it requires less EOA reduction.

When leakage cannot increase substantially (scenario ii), the predicted benefits from EOA reduction eliminate most of the predicted harm of increased duty cycle. Fig 6-8b shows the combined values of LR= -0.01 and -0.03 for Dar es Salaam and Hajjah, respectively, during steady-state operations.

The difference between the two scenarios is evident in utilities with, for example, $t^0 \in [48\%, 52\%]$. Under scenario i), converting to CWS is predicted to increase the intruded volume present during steady-state by a median LR=-0.24 (90% confidence interval: $(-0.15, -0.30)$; Fig 6-8a). However, under scenario ii), the predicted LR could be held to a median of -0.02 $(-0.01, -0.07)$ (Fig 6-8b).

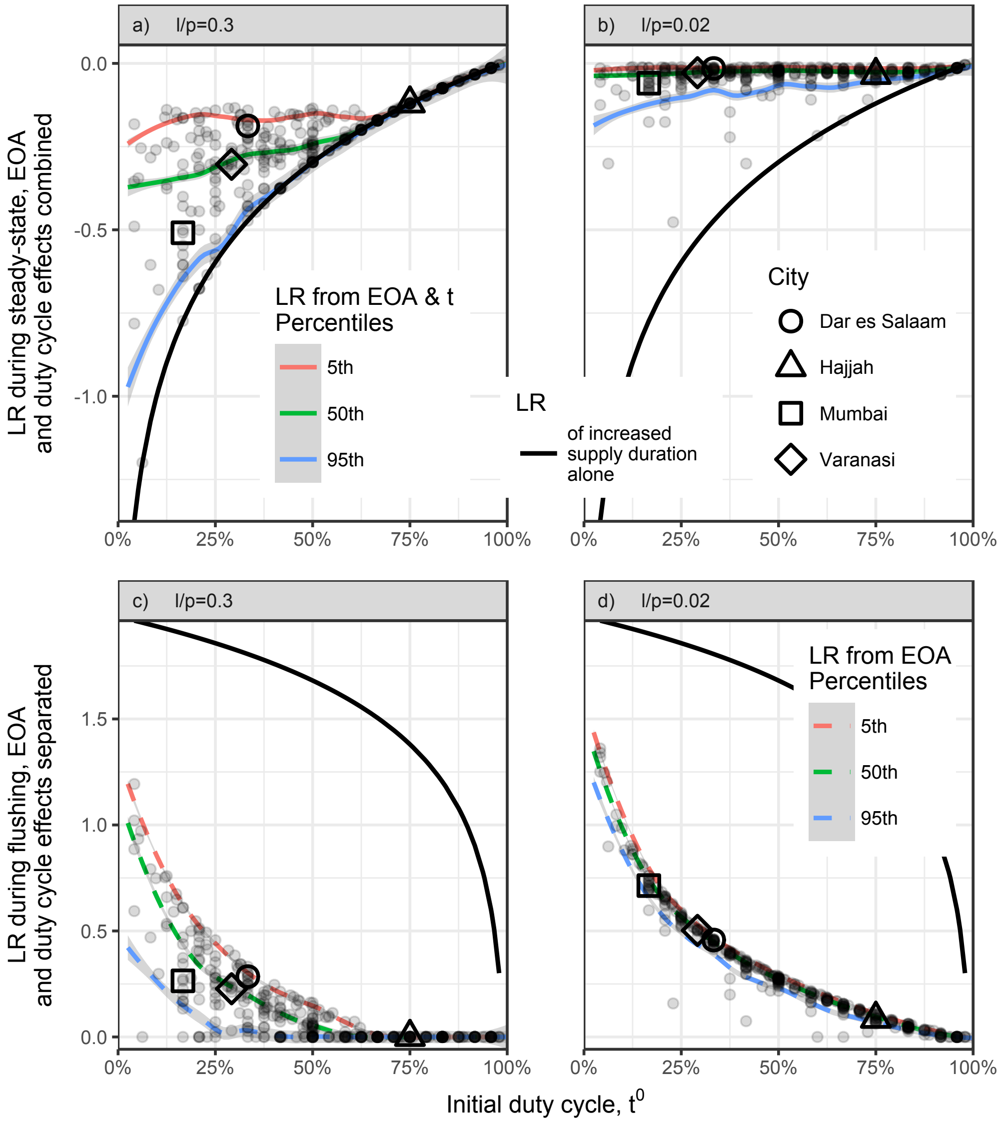

Figure 6-8: **Which improvements reduce the risk of intrusion?** For each utility (grey dot) in the filtered IBNET and BWBWUI database, the predicted log reduction (LR) of intruded volume in steady-state (a & b) and flushing (c & d) phases, attributable to increasing the duty cycle to 99% (thick black line) and attributable to the necessitated EOA reductions is plotted. For steady-state (a & b), the effects are considered together (solid thin lines), but for the flushing phase (c & d), the effect of EOA reduction is shown separately (dashed thin lines). Each utility is plotted under scenarios i) and ii) (i.e., $\frac{l}{p} = 0.3$ (a & c) and $\frac{l}{p} = 0.02$ (b & d)). For initial duty cycles within a 4% span (e.g., 23-27%), the 5th (red/upper line), 50th (i.e., median, green/middle line), and 95th (blue/lower line) percentiles are smoothed into the displayed curves.

Increased duty cycle is predicted to reduce the intruded volume present in the flushing phase by LR=1-2 for all utilities with $t^0 \leq 88\%$ (Fig 6-8c). When utilities cannot allow leakage to substantially increase (scenario ii), increased duty cycle is predicted to reduce the intruded volume present in the flushing by more than one order of magnitude more than the reduction in EOA it necessitated (i.e., $\Delta LR \geq 1$) for utilities with $t^0 \geq 8\%$ (Fig 6-8d).

This numerical application of the proposed model reinforces its key prediction: extensive EOA reduction is required to preserve steady-state water safety. It also shows that increased duty cycles are an appropriate focus for projects that wish to focus specifically on improving the safety of the flushing water, perhaps to benefit disadvantaged customers in the network. In order to measure the efficacy of such projects, however, utilities should sample during the flushing phase.

6.4.3 Effects of increased pressure

Due to the unknown form of $\Theta()$ (which stems from the unknown form of $f()$ in Eq 6.3), this section's analysis is limited to the LR induced by the pressure-necessitated reductions in EOA. These are predicted to be equal in the steady-state and flushing phases (Eq 6.11). For the two scenarios, Fig 6-9 plots the predicted LR for utilities in the BDBWUI due to the decrease in EOA required for $H^* = 17m$ as a function of initial supply pressure H^0.

Under scenario i), Mumbai does not require any EOA reduction to transition from its current supply pressure H^0 = 7m to H^* = 17m, which implies LR=0. This prediction is due primarily to Mumbai's low self-reported NRW. Conversely, Varanasi will require substantial reductions in EOA (LR = 0.45). More generally, under scenario i), cities with $H^0 \leq 3m$ are predicted to have LR $\geq$ 0.45 due to the EOA reductions necessitated by increasing the pressure (Fig 6-9a). For scenario ii), this effect is predicted to increase to a LR $\geq$ 0.72 (Fig 6-9b).

More generally, utilities that plan to increase their supply pressure to meet targets will need to undergo leak repair campaigns, unless they have very low current NRW levels and can allow leakage to increase. Where increased pressure is proposed to

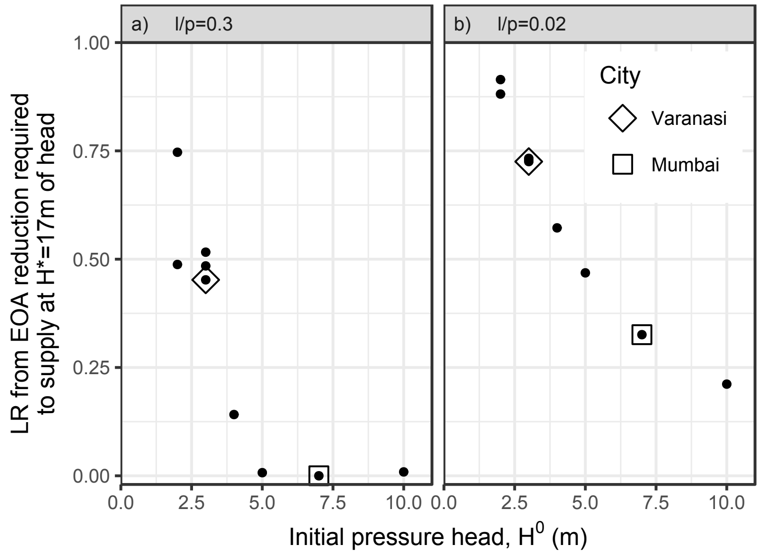

Figure 6-9: **Log reduction (LR) from pressure-necessitated EOA reductions.** As utilities (dots) in the filtered BDBWUI database increase supply pressures from their initial pressures (x-axis) to 17m, the proposed model suggests that EOA must be reduced. Different EOA reductions are required under scenarios i) and ii) (i.e., $\frac{l}{p} = 0.3$, left panel; and $\frac{l}{p} = 0.02$, right panel). These reductions in EOA are predicted to translate to LR in the intruded volume (y-axis).

reduce intrusion, leak repair should be undertaken first and then if necessary supplemented with pressure increases.

6.5 Conclusions and recommendations

The proposed and applied scaling equations, summarized in Table 6.3 and Fig 6-5, provide insights about how utilities may be able to improve their system performance and reduce their intrusion risk. This chapter proposes previously-unexplored couplings between system variables. It suggests that utilities, regulators, and academics alike should take care in distinguishing between water quality during steady-state and flushing phases, and in specifying performance metrics that do not conflict with one another. Hence six key implications and five opportunities for future work are highlighted:

6.5.1 Key implications

1. Distinguishing between IWS' predicted effects on flushing and steady-state quality is not something reported in the literature to date and may help understand the health benefits of CWS.

2. Sampling requirements should specify which phase of supply is to be tested. By default, utilities sample steady-state water quality, which typically is of higher quality. However, flushing phase water is often used by disadvantaged customers; its quality cannot be neglected.

3. For utilities in India that are currently planning to convert to high-pressure CWS, the model suggests that full pipe replacement should be the rule, not the exception.

4. Increasing duty cycle is likely important for projects focused on improving flushing water quality. However, to preserve water quality during the steady-state phase, such projects should also undergo substantial reductions in EOA.

5. Where increased pressure is proposed to reduce intrusion, EOA reduction should be done first and then, if necessary, supplemented by pressure increases.

6. Targets of increased duty cycle, increased pressure, and decreased NRW conflict. The EOA metric eliminates this conflict and better indicates pipe quality.

6.5.2 Future work

1. Testing the model and its predictions in field experiments could validate it and significantly influence IWS improvement policies and practices.

2. Quantifying the relative contributions of contaminant intrusion, contaminant regrowth, and biofilm sloughing to steady-state water contamination would help identify the key priorities for achieving safer IWS.

3. Investigating which customers consume flushing water (and why) could lead to innovative methods of reducing IWS' health burden.

4. Determining the relationship between intruded volume and average system pressure would allow this model to be substantially extended.

5. Water quality degradation is only one way in which IWS negatively affects households (Subbaraman et al., 2015). Supplementing this model with additional impacts of IWS would give a more holistic picture of the effects of IWS.

Chapter 7

Design of a water-only meter

> If water supply is intermittent, consumption cannot be accurately measured with conventional metering. Air . . . will cause the [conventional] water meter to spin
>
> McIntosh (2014, p.48)

7.1 Introduction

Available data suggest that 62% of IWS customers have water meters (global data from Van den Berg and Danilenko (2011)). These meters are typically either single- or multi-jet (Van Zyl, 2011) and their accuracy in IWS has been question by many (Arregui et al., 2006b; Cobacho et al., 2008; Criminisi et al., 2009; McIntosh, 2014; Fontanazza et al., 2015; Walter et al., 2017, 2018).

Customer metering is useful for measuring and controlling customer consumption. For example, meters can provide information about when customers become satisfied, which is critical to effectively managing IWS (Chapters 4 and 5). In addition, domestic water meters allow water pricing to influence customer consumption (McIntosh, 2003), which can influence the viability of IWS-improvement projects (e.g., Section 4.3). This second use of meters is more controversial. To avoid such debates, this chapter focuses on increasing the accuracy of water meters where they are already used.

IWS have three frequently-discussed effects on water meters. First, where duty cycles are long and customers are satisfied, customer tanks smooth out peak flow rates. The slowed flow rates cause domestic meters to under-register (Arregui et al., 2006b; Cobacho et al., 2008; Criminisi et al., 2009; Fontanazza et al., 2015). Second, at the start of an IWS' supply stage, water displaces the air that has filled many of the system's pipes. While some of this air may exit through air-release valves on larger water mains, air in the distribution piping of the network is forced out through customer meters, which register some of the air as if it were water (Walter et al., 2017, 2018). Third, exiting air, may also cause meters to spin too quickly, degrading their ability to measure low water flow rates.

Billing customers for air causes public outrage (e.g., Delhi's Chief Minister campaigned against the water utility, claiming that billing for air was evidence of corruption (Delhi BJP, 2016; Khandekar, 2014)). In two affluent neighborhoods in two major cities in India, the average volume of air passing through customer water meters was estimated to be 15 and 50 L/connection per supply stage (or 4% and 9% of billed volumes, respectively; Appendix A.1.2). On average these volumes may appear small, but customers do not each receive an equal amount of air. Elevation differences across a network cause air volumes to concentrate at a few households, further increasing the inequity of IWS.

In addition to improving equity, reducing customer outrage over meters will make installing meters at unmetered-connections easier. Globally, there are almost 380 million people who use IWS without meters (Van den Berg and Danilenko, 2011; Bivins et al., 2017). Avoiding metering air, therefore, represents a substantial opportunity for water utilities and water meter manufacturers.

Finally, inaccurate metering thwarts attempts to quantify leakage in a water supply system (which is most simply measured as input - output). Therefore, to enable utilities to better manage their systems and to address the understandable concerns of customers being billed for air, this chapter proposes a new design for a multi-jet meter that does not register air. In order to efficiently discuss the detailed design of this meter, this chapter breaks from the notational conventions used throughout the rest of the thesis. Most notably, V will represent the fluid's velocity, and t time.

7.2 Background

Van Zyl (2011) and Arregui et al. (2006a) provide comprehensive and complimentary summaries of the types of water meters and how they are used to manage water distribution systems. This section provides only a brief overview of the necessary information.

7.2.1 Types of water meters

Some flow meters measure the volumetric flow rate of water directly (positive displacement). Most measure the velocity of the water and infer its volumetric flow rate (inferential) (Van Zyl, 2011). Positive displacement meters are typically more accurate, especially at low flow rates (Van Zyl, 2011; Barfuss et al., 2011). However, they may also be more sensitive to particles in the fluid (Van Zyl, 2011), although Barfuss et al. (2011) did not find this to be the case for all positive displacement meters. Both single- and multi-jet water meters, common in IWS, are tolerant of particulate matter in the water.

Both single- and multi-jet meters are inferential. In each type, one or more jets of fluid enter the meter tangentially and interact with an impeller (Fig 7-1). The housing for the impeller is (supposed to be) filled with fluid that rotates with it. As such, the rotation of the impeller measures the fluid's velocity (not momentum as a Pelton wheel would).

Rotation of the impeller is transmitted to an indicator via a direct or magnetic coupling in wet- and dry-dial types (Fig 7-2; Van Zyl (2011); Arregui et al. (2006a)). Some meters also use a hybrid configuration where some gears are in contact with the metered fluid (to reduce friction) while the final gears are dry. In IWS, dry dials are essential to the longevity of the meter (Arregui et al., 2006a). Unfortunately, however, the magnetic coupling adds weight to the impeller and the registration gear to which it couples. This added weight increases the friction in both, making the

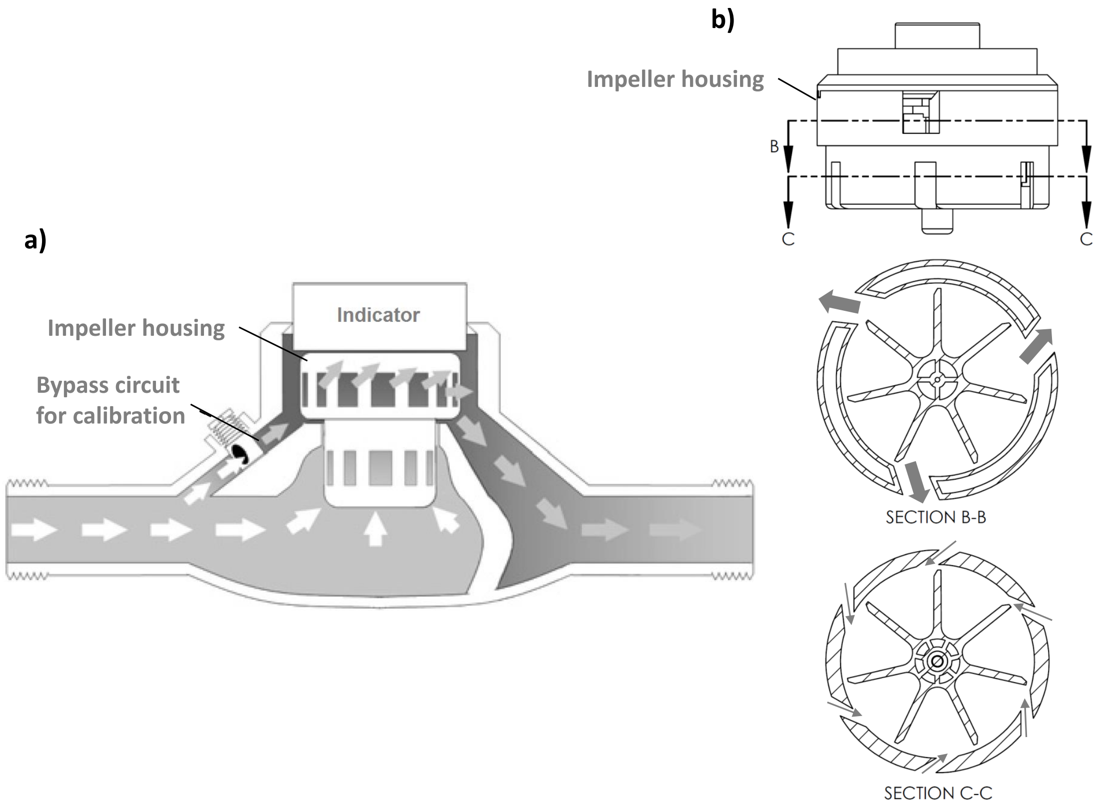

Figure 7-1: **Multi-jet meter's cross-sections.** a) flow enters on the left and either travels through the bypass circuit or through the impeller's housing (adapted from Arregui et al. (2006a)). b) the impeller's housing with section views; section B-B shows the outlet jets and section C-C shows the inlet jets.

registration of very low flows more difficult (Arregui et al., 2006a).

In multi-jet (and some single-jet) meters, to compensate for friction at low flow rates, the impeller is calibrated to over-register flow (Arregui et al., 2006a). This over-registration is then counteracted by a bypass circuit which allows some flow to avoid the impeller all together (Fig 7-1a). Blocking of the bypass circuit can cause substantial metering errors (Arregui et al., 2006a).

To maximize their accuracy at low flow rates, single- and multi-jet meters must minimize frictional torques imposed on the impeller. This is done by having the impeller constrained primarily by a pin-cup bearing (e.g., Fig 7-3a), in which the cup is either a synthetic ruby or sapphire (Arregui et al., 2006a). This cup provides both an axial constraint and a (low-stiffness) radial constraint.

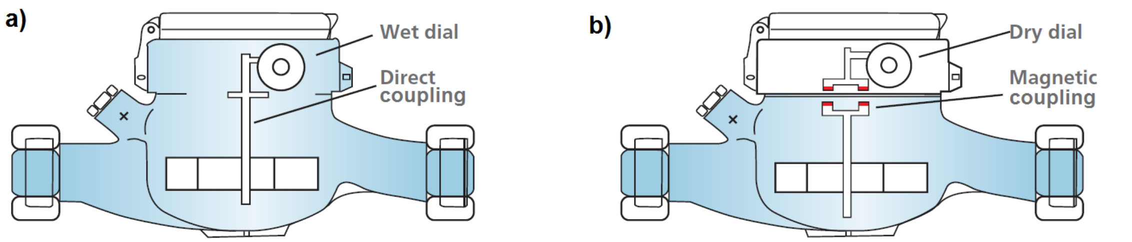

Figure 7-2: **Water meter indicator types.** a) a wet-dial indicator; b) a dry-dial indicator. Graphic adapted from Van Zyl (2011).

Single-jet meters are smaller and cheaper than multi-jet meters (Van Zyl, 2011). Multi-jet meters have better low-flow performance and life expectancy because the forces on their impeller and its bearings are more balanced (Van Zyl, 2011).

7.2.2 Accuracy of water meters

While international standards for water meters have been updated recently (ISO 4064, 2014; Van Zyl, 2011), many countries have yet to update their domestic standards (Van Zyl, 2011). This section summarizes parts of the older standard as it still applies in India (Bureau of Indian Standards, 1994). Van Zyl (2011) provide a summary of the difference between old and new standards. Henceforth, 'standard' will refer to the older standard.

Water meters are classified A through D, with D being the most accurate and A being not accurate enough to be used for billing (Van Zyl, 2011). The Indian standard, details classes A and B and does not prohibit the use of class A meters for domestic metering (Bureau of Indian Standards, 1994). A meter's accuracy is specified using its minimum, transitional, permanent (or nominal), and maximum flow rates ($Q_{\min}$, Q_t, Q_n, and $Q_{\max}$, respectively).

Both A and B classes have a maximum permitted error of $\pm 5\%$ between the minimum and 'transitional' flow rate ($Q \in [Q_{\min}, Q_t)$). Between the transitional and maximum flow rate ($Q \in [Q_t, Q_{\max}]$), errors of $\pm 2\%$ are permitted. The permanent flow rate is the largest flow rate to which a meter can be subjected to permanently without damage (typically $Q_n = 0.5 Q_{\max}$). The values of these critical flow rates

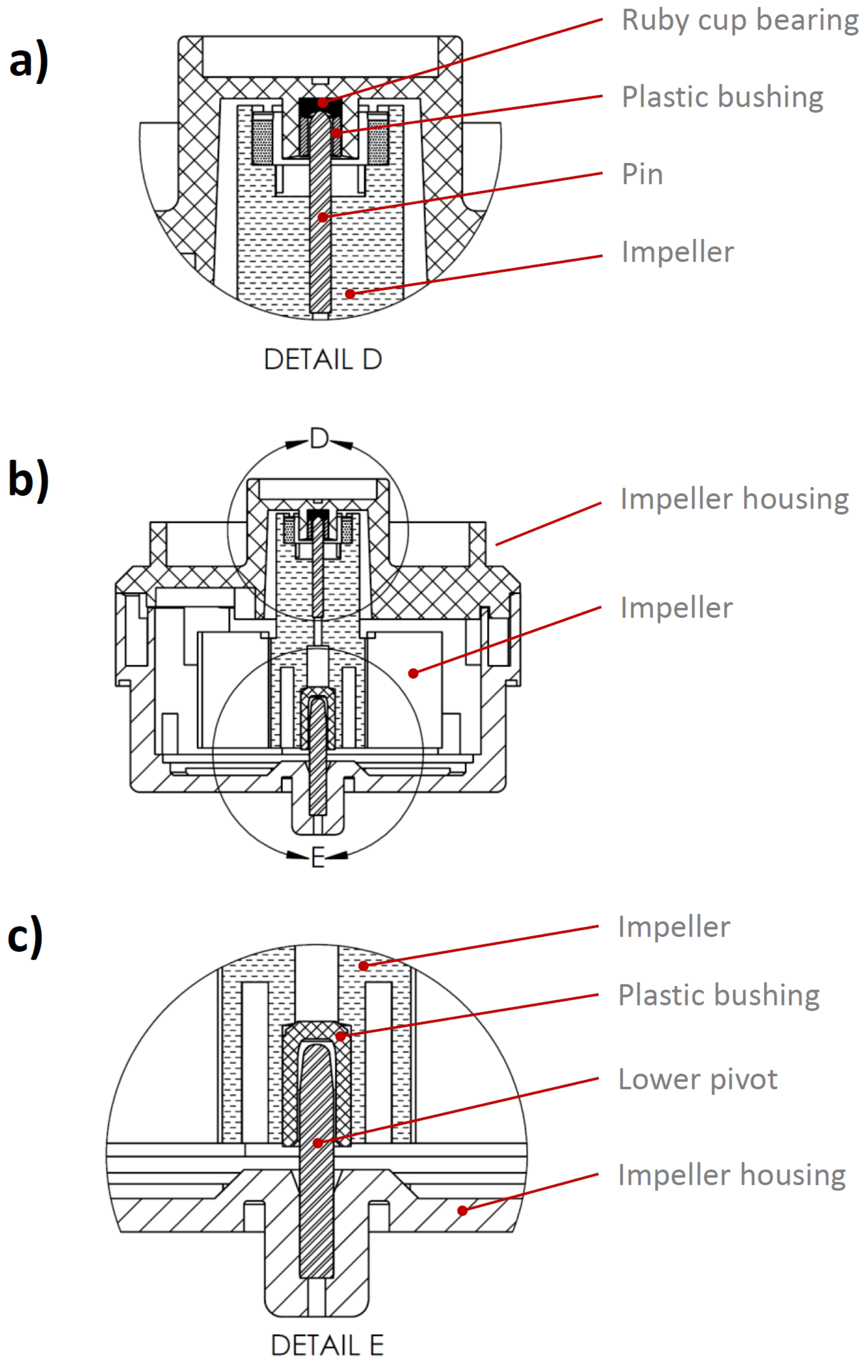

Figure 7-3: **Multi-jet meter's pin-cup bearing configuration.** b) cross-section of a typical (Elster) class B multi-jet meter. a) the low-friction, pin-cup bearing arrangement. c) the lower radial bushing. The lowest friction arrangement is with an upward preload as depicted. Without water in the meter to provide floatation, the lower pivot, shown in c), provides axial and radial constraint.

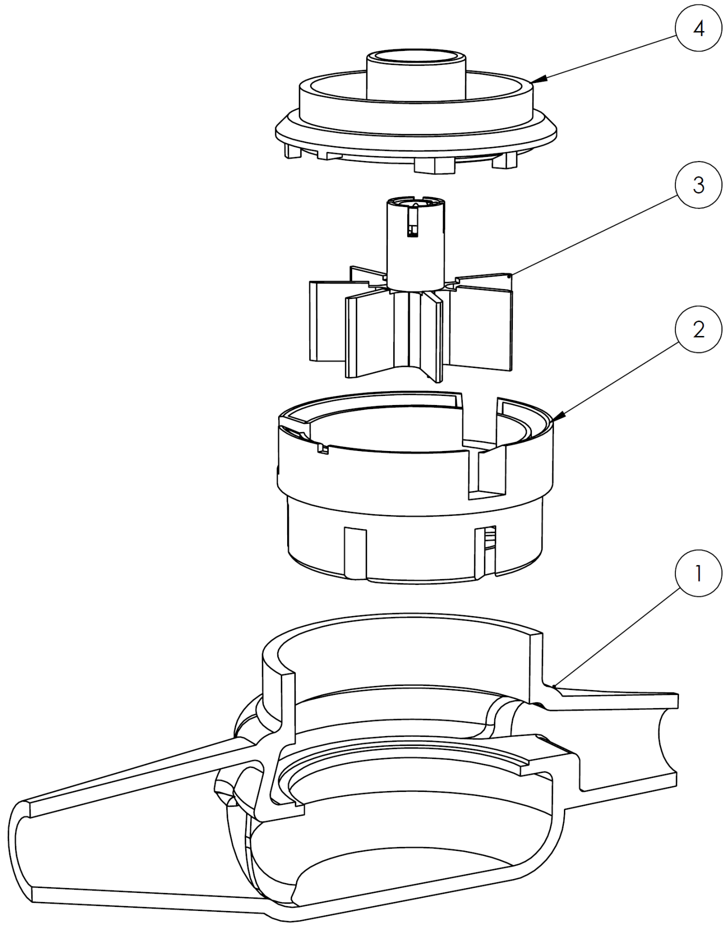

Figure 7-4: **Key components of a typical multi-jet meter.** 1) external brass housing shown in cross-section (bypass not shown). 2) the lower half of the impeller's housing. 3) the impeller assembly. 4) the top of the impeller's housing. The meter's indicator is not shown.

Table 7.1: **Water meter accuracy specifications** for 15mm meters in India. Meters must register within $\pm 5\%$ for $Q \in [Q_{\min}, Q_t)$ and $\pm 2\%$ for $Q \in [Q_t, Q_{\max}]$. From Bureau of Indian Standards (1994); units of liters per hour (LPH).

Class	$Q_{\min}$ LPH	Q_t LPH	Q_n LPH	$Q_{\max}$ LPH
A	60	150	1500	3000
B	30	120	1500	3000

vary by class of water meter and by the meter's size. For 15mm domestic meters, the accuracy requirements are repeated in Table 7.1 and Fig 7-5 (Bureau of Indian Standards, 1994).

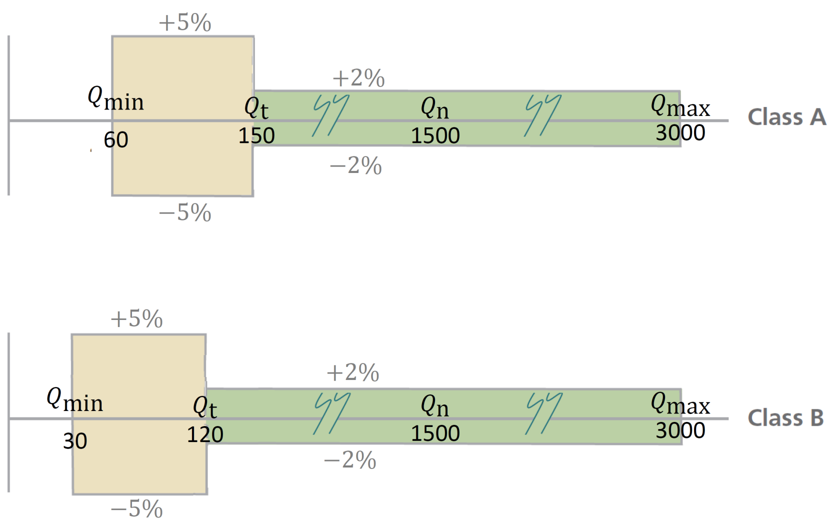

Figure 7-5: **Water meter accuracy specifications** for 15mm meters in India. Meters must register within $\pm 5\%$ for $Q \in [Q_{\min}, Q_t)$ and $\pm 2\%$ for $Q \in [Q_t, Q_{\max}]$. Units in liters per hour. Data from Bureau of Indian Standards (1994); graphic adapted from Van Zyl (2011).

A water meter's total accuracy depends on its accuracy at different flow rates and the distribution of flow rates it will measure. Arregui et al. (2006b); Cobacho et al. (2008); Criminisi et al. (2009); Fontanazza et al. (2015) have extensively studied how customer tanks and float valves act as capacitors to reduce the instantaneous flow rates associated with customer demand. Lower flow rates shift the flow patterns of customers into the regime where water multi-jet meters are least accurate.

US consumption patterns suggest that less than 9% of the volume delivered to

Table 7.2: **Customer consumption patterns.** Where tanks are present the (volumetric) percent of customer consumption below $Q_{\min}$ and in the range $[Q_{\min}, Q_t)$, and $\geq Q_t$ for a Class B, 15mm domestic water meter is shown.

Tank?	Country	Consumption distribution <30 LPH	30-120 LPH	>120 LPH	Error[a] Class B	Source
No	U.S.[b]	8.9%	3%	88%	-11%	(Bowen et al., 1993); in García et al. (2004)
Yes	Spain	28%	30%	41%	-31%	(Cobacho et al., 2008)
No	Spain[b]	10%	5%	85%	-12%	(Cobacho et al., 2008)
Yes	Spain	17%	11%	72%	-19%	(Arregui et al., 2006a)
No	Spain[b]	12%	9%	79%	-14%	(Arregui et al., 2006a)
Yes	Uganda	20%	23%	57%	-23%	(Mutikanga, 2012)

[a] Maximum total under-registration allowed using Class-B meters
[b] Arregui et al. (2006b) provide a more comprehensive summary of consumption studies in CWS

customers occurs at flow rates less than 30 liters per hour (LPH; Table 7.2). In three studies of consumption through tanks, this flow range accounted for 17-28% of total customer demand (Table 7.2). This range is below $Q_{\min}$ for Class B meters and may not be metered at all. Including the maximum permitted under-registration for each of the flow ranges shown in Table 7.2, 15mm class B meters at households without tanks could under-register by 11-14%. At households with tanks, this under-register can almost double (to 19-31%; Table 7.2). Accurately measuring low flow rates, therefore, is a critical function of domestic water meters.

The flow-reducing effect of tanks only occurs when customer tanks are full during the supply stage (e.g., in IWS with long duty cycles and satisfied customers). Tanks acting as capacitors are not a problem in systems in which customer tanks are not full for much of the supply stage (e.g., unsatisfied IWS).

Walter et al. (2017, 2018) quantified the accuracy implications of air flowing through domestic water meters. For dry, multi-jet meters, depending on the velocity of the air, 58-150% of its volume can be registered as if it were water (Walter et al., 2018). However, if the water meter's housing is partially full of water while air passes through it, over-registration is limited to 15% of the air's volume (Walter et al., 2018).

7.2.3 Prior art

Five existing solutions have been proposed to address the issue of air in water meters: avoid using water meters; install air release valves; use flow control valves; use electromagnetic flow meters; and keep meters partially wet. Each solution is explained briefly below.

Avoid water meters. Kumpel et al. (2017); Mastaller and Klingel (2017) have proposed alternative methods for measuring customer consumption in IWS. In both methods, a subset of customers have their consumption measured with surveys, water meters, or both. These alternative approaches hold promise for utilities without meters and could be integrated with the models developed earlier in this thesis. For the 62% of IWS customers with meters, however, accurate metering is still required.

Air release valves. Air-release valves (ARVs) are frequently used in water distribution networks to release trapped pockets of high-pressure air. ARVs allow air to flow through them, but close as water tries to flow through them. Preventing air from flowing through water meters, however, is different than releasing pockets of high-pressure air because in the former case, the air's pressure is lower and the air has an alternate escape path (though the meter).

At the start of the supply stage in an IWS, many customer taps are open. These open taps fix the pressure at the customers' end at atmospheric. Pressure upstream of an open tap can only build due to frictional losses. Frictional losses caused by air flowing through empty water pipes are much less than those incurred by water (in the ratio of $\rho_{\text{air}}/\rho_{\text{water}} \approx 0.1\%$ for fully turbulent flow). As such, the air being pushed out of a filling IWS is of such low pressure, it is often approximated as atmospherically pressurized (Liou and Hunt, 1996; De Marchis et al., 2010; Walter et al., 2017). This low-pressure air is unlikely to open ARVs that default to being closed.

Even where ARVs are open during pipe filling, exiting air can flow through both the ARV and the customer's meter and open tap. To prevent all air from passing through the meter, the metered path must have infinitely more resistance than the path through the ARV. For this reason, Arregui (2016, p.35) warns that ARVs "will not prevent large pockets of air passing through the meter under normal operating conditions ... [in IWS], this is not possible."

ARVs immediately upstream of customer meters also invite tampering. Temporarily-removed or jammed-open ARVs provide customers with unmetered water. Utilities in some IWS are, therefore, hesitant to install ARVs as a partial solution to metered air.

Flow control valves. Fontanazza et al. (2015) proposed and tested a pulsating flow device to reduce the tank-induced low and hard-to-measure flow rates in some IWS. Their device solves a fundamentally different problem and is not suited to low-pressure IWS (it requires 5m of pressure before customers get any water). In medium- and high-pressure IWS, however, such a device could function in combination with an ARV. As the pulsating device blocks all fluid flow through the meter until the pressure is at least 5m (0.5 atm), it would force air with pressure less than 5m out through the ARV. This potential solution combination is still prone to tampering.

A second type of flow control valve designed specifically to reduce the metering of air in water meters is the "Smart Valve" (Flow Dynamics, 2018). The Smart Valve is a pressure-reducing valve, which gets installed after a customer's water meter in high-pressure CWS. By reducing the pressure in the customer's home, the valve acts to increase the pressure upstream of the valve, including in the meter. With higher pressures in the water meter, any air bubbles are further compressed and so their volumetric influence on the billed volume is reduced. The Smart Valve, however, is not designed to prevent meters from measuring the flow of air alone. In addition, customers in low-pressure IWS would not accept a device that further reduced their pressure.

Electromagnetic meters. Electromagnetic meters do not meter air. Historically, they have been used to meter larger pipes. Recently, residential-sized units have become available (e.g., Elster (2013)). Unfortunately their cost is substantially more than mechanical meters and their performance as flow transitions between air and water has not been published.

Keep meter wet. Standards in India have long recommended that water meters be

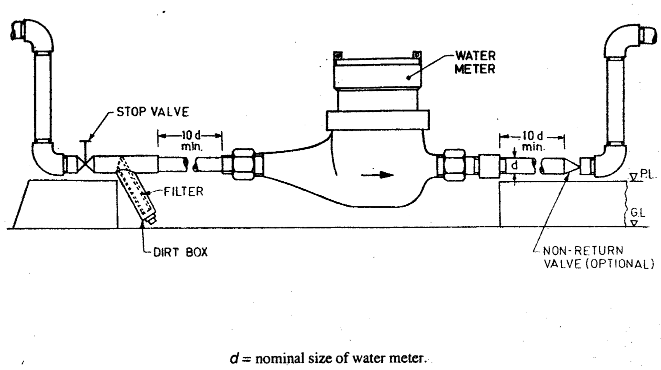

Figure 7-6: **Recommended water meter installation.** Top of the meter is below the nominal level of the pipe. Reproduced from Bureau of Indian Standards (1994).

installed below the level of the pipe so that they remain full of water during the non-supply stage of an IWS (Fig 7-6; Bureau of Indian Standards (1994)). Walter et al. (2018) quantified that the measured volume of air passing through a multi-jet meter is reduced by 85% when the meter has some residual water in its case. Despite the apparent efficacy of this simple solution, the author has never seen the recommended configuration used; it should be more widely adopted.

Customers dislike seeing their water meter spin while air exits their taps. Reducing the speed of this spinning, even by 85%, may not be sufficient to appease enraged customers. This chapter, therefore, proceeds to present the design of a mechanical, low-cost method of preventing customers from being billed for air.

7.3 Design

7.3.1 Functional requirements

To guide the design process, the functional requirements in Table 7.3 were specified. A water-only meter's primary functional requirement must still be to measure the flow of water accurately (FR1). Its ability to avoid the measurement of air (FR2) is only useful when FR1 is met. In an IWS, air is forced through the water meter by a column of water that follows the air (e.g., Fig 7-7). Therefore, while the meter is avoiding metering air, water will enter the meter and the meter must resume registering the

Table 7.3: **Water-only meter's functional requirements.**

	Functional requirement	Specification
FR1	Meter water accurately	Meet Class B accuracy specifications
FR2	Do not meter air	Up to air flow rates 1500 LPH
FR3	Meter water that follows air	Meter within 1L of fully-water flow
FR4	Tolerant of low pressure	Functions whenever $H_{\text{air}}, H_{\text{water}} > -4m$
FR5	Low loss coefficient	$<$ 10% increase in hydraulic resistance
FR6	Tolerant of particles	Functions with 2mm diameter particles
FR7	Tamper resistant	As much so as a conventional meter
FR8	Low cost	Marginal cost increase of $<$15%
FR9	Fail open	Water flows, despite failure or jamming
FR10	Safe for water systems	Meets NSF61 or equivalent
FR11	Tolerant of friction changes	Works while static friction $\mu \in [0, 0.8]$
FR12	Do not meter air following water	Stop metering within 1L of air

flow (FR3). FR1-3 define the key functional requirements for the water-only meter.

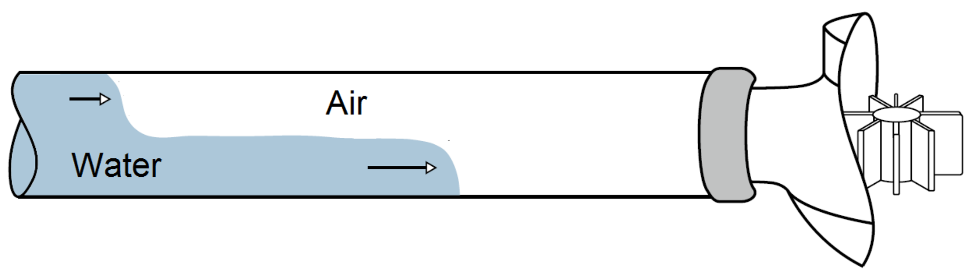

Figure 7-7: **Air and then water impacting a multi-jet meter.** Adapted from Walter et al. (2017).

FR4-11 restrict the acceptable solutions for FR1-3. As discussed in Section 7.2.3, any solution must work with low pressure air and/or water (FR4). Chapter 5 demonstrated that in low-pressure IWS, even small differences in pressure can lead to large changes in the volumes of water received by unsatisfied customers. Therefore, customers will only accept a new water meter design if it does not substantially change their water pressure. As a first-approximation, FR5 requires that the increase in hydraulic resistance of the water-only meter should be $<$ 10%. Pressure losses in domestic water meters in India are limited to 2.5m at Q_n and 10m at $Q_{\max}$ (Bureau of Indian Standards, 1994, clause 10.2).

Due to the meter's intended use in an IWS, it must be tolerant of particles in the fluid (FR6) and be at least as tamper resistant as a traditional water meter (FR7). Domestic water meters available in India range in price from \$20-40 USD. The additional costs associated with the water-only functionality should be less than 15% of the meters initial costs (incremental cost of $< \$3 - 6$ USD; FR8). As many customers rely on piped water supply for their daily water requirements, the water-only meter should fail such that customers still receive their water (FR9).

As the meter is in prolonged contact with domestic drinking water, it should meet the appropriate standards (FR10), which in the U.S. would be NSF61. Bureau of Indian Standards (1994, clause 10.1) requires that meters withstand a pressure of 160m for 15 minutes and 200m for 1 minute. Additionally, plastics "should not affect the potability of the water," should absorb less than 0.6% of their weight in water after submersion for 24 hours, and operate in 55°C without deformation or performance issues (Bureau of Indian Standards, 1994, clause 6.1.1).

After prolonged use in an IWS, the coefficient of friction will be highly uncertain. The meter, therefore, should work for any coefficient of static friction $\mu \in [0, 0.8]$ (FR11).

Finally, due elevation changes in the pipes leading into a customer's home, the water meter may initially be full of water while the pipes upstream of it are filled with air. When this air pushes through the water meter, it should not measure this air (FR12).

7.3.2 Strategies

In order to achieve FR8 (low cost), only mechanical strategies were considered. To achieve FR1-3 four strategies were initially considered:

S1 Release the air before the meter

S2 Measure the flow of air and subtract it from the conventional water meter's total

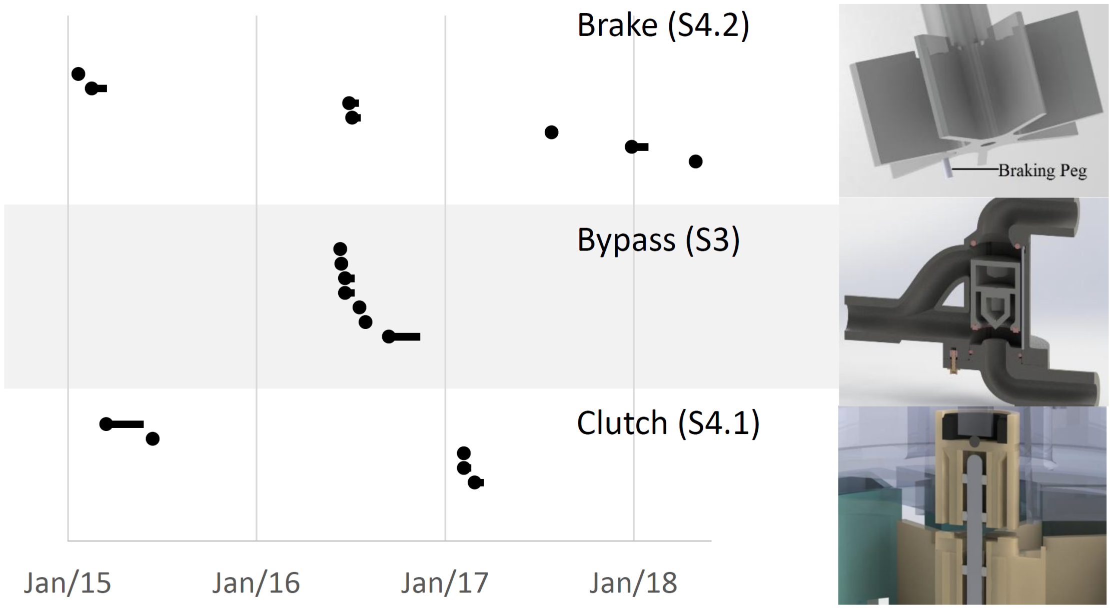

Figure 7-8: **Water-only meter's evolution and timeline.** Nineteen different designs were tested as part of three solution strategies: brake the impeller (S4.2); bypass the meter (S3); and clutch the meter (S4.1). Dots and lines indicate the start and duration of each design's testing. Representative CAD drawings for each strategy are shown to the right of the timeline.

S3 Force air to bypass the meter

S4 Prevent the meter from registering air's flow

Strategy S1 was eliminated based on feedback from utilities in India who suggested it was too prone to tampering, violating FR7. S2 was eliminated as measuring the flow of air would substantially complicate the meter and increase its costs, violating FR8. S3 and S4 were considered in more depth; specifically, nineteen versions of the water-only meter were attempted (Fig 7-8).

Bypassing the meter (S3), involves parallel flow paths. As discussed in Section 7.2.3, forcing a fluid (and especially air) through only one of two parallel paths requires blocking the one path. Several concepts for blocked pathways were explored, but their dynamic stability was difficult to predict and this strategy was ultimately abandoned.

Metering air could be avoided (S4) either by decoupling the impeller's motion from its indicator or by arresting the meter's motion. Specifically, the sub-strategies considered were:

S4.1 Decouple the system with a clutch

S4.1.1 Introduce a clutch within the indicator

S4.1.2 Introduce a clutch within the impeller

S4.1.3 Introduce a clutch between the impeller and the indicator

S4.2 Brake the system

S4.2.1 Brake the indicator

S4.2.2 Brake the impeller

Neither clutching not braking the indicator (S4.1.1 and S4.2.1) was pursued because dry-dial indicators are becoming more and more common for their longer life expectancy and higher tolerance to entrained particles (Fig 7-2).

Several concepts for introducing a clutch within the impeller successfully met FR1-3. However, once the impeller is segmented into two independent part, it requires additional bearings to support each segment. The additional bearings increase the meter's cost and reduce its performance at low flows.

Strategy S4.1.3 was tested by magnetically decoupling the impeller and indicator. However, when water follows air into the meter, the magnetic torque transmission could not be reliably reestablished while the impeller was spinning (violating FR3).

The final strategy: brake the impeller (S4.2.2), proved successful and is the focus of the remainder of this chapter.

7.3.3 Constraints

In order to develop different concepts for mechanisms and actuation, the mechanical properties, forces, and pressure losses associated with flows of air and water were estimated.

Water and air vary in, among other things, their surface tension, density, viscosity, coefficient of thermal expansion, thermal conductivity, and specific heat capacities

Table 7.4: **Relative mechanical properties of water and air** at 20°C and atmospheric pressure.

Property	Ratio of water:air
Surface tension	1:NA
Density	830:1
Viscosity	55:1
Coefficient of thermal expansion	1:50
Thermal conductivity	23:1
Specific heat capacity	4.2:1

(Table 7.4). Density differences can induce differences in weight (including flotation) and momentum.

The force required to arrest the forward momentum of each fluid was considered. The Elster, Class B, $Q_n = 1.5m^3/hr$, 15mm, multi-jet water meter was used as an example. It's impeller housing has 6 inlet jets each of area $14mm^2$ (Fig 7-1b). The force required to arrest all of the fluid's forward momentum was considered in two scenarios: arresting the all inlet jets, and arresting flow at the meter's inlet (15mm diameter).

The force, F_{jet}, imparted by a jet of water (of area A_{jet}) onto a surface that is removing the jet's forward momentum is given by:

$$\begin{aligned} F_{\text{jet}} &= \frac{d(mV)}{dt} \\ &= V\frac{dm}{dt} = V\rho Q \\ \therefore F_{\text{jet}} &= \frac{\rho Q^2}{A_{\text{jet}}} \end{aligned} \tag{7.1}$$

The forces associated with the two scenarios are considered at the minimum and maximum flow rates for water and air (Table 7.5). The forces associated with a jet of water, as compared to a jet of air, are larger by the ratio of $\rho_{\text{water}}/\rho_{\text{air}} \approx 830$ (Eq 7.1). The water meter operates over a range of 100x in flow rates. As Q is squared in Eq 7.1, this means that the forces vary by 10^4 for each fluid. Since the fluids only differ in density by 10^3,the maximum forces with air flowing through the device are larger than the minimum forces when water is flowing through the device (Table 7.5). This

Table 7.5: **Momentum forces in the water and air flows.** To make the small forces easier to intuit, they are also tabulated in grams of force.

Flow	Fluid	At inlet		6-jets	
(LPH)	-	(N)	(grams)	(N)	(grams)
30	Water	4E-4	0.04	0.03	3
3000	Water	4	400	300	3E+4
30	Air	5E-7	5E-5	4E-5	4E-3
1500	Air	1E-3	0.1	0.09	9

is a major constraint in the design space.

Pressure losses over small distances with turns and sharp corners are governed by minor losses, which scale with the fluid's density times its velocity squared ($\Delta P \propto \rho V^2/2$). At the highest air velocities and lowest water velocities, the minor losses in air are greater those in water (independent of the geometry). Major losses dominate if the fluid's path is much longer than the path's diameter. Given the small space envelope and requirement that the system be tolerant of particles (FR6), long narrow channels were avoided. Frictional losses alone, therefore, cannot differentiate between the two fluids.

The volume of the impeller's housing provides an upper limit on the possible flotation forces obtainable within the housing. In the reference (Elster) meter, the impeller's housing volume was about $50cm^3$. Because the vast majority of the volume is taken up by the impeller as it spins, for designs that can be implemented as a retrofit to existing meters, the maximum buoyancy force was limited to 1-2 grams.

7.3.4 Concept

FR3 (meter water following air) severely constrains the permitted brake designs. When water enters the meter following air, any braking mechanism will still be engaged. The engaged brake must, therefore, disengage while water is flowing through the meter. This requirement eliminates all brake designs that use the principle of 'self-help' (where the brake's strength increases as the force applied against it increases).

Based on the analysis of forces in the system, the maximum magnitude of F_{jet} is

$10^4\times$ larger than any flotation forces that would fit within the traditional envelope of a water meter (Table 7.5). Therefore, for designs that can fit within existing meters' housing, buoyancy forces alone are insufficient to actuate the brake in all circumstances.

Again, based on the force analysis, the brake's actuation cannot be based solely on the fluid's momentum (Table 7.5). This section, therefore, considers hybrid designs, in which at high (water) forces, the braking mechanism will self-open. To resist the tendency to self-open against air forces, buoyancy (or lack thereof) will be used.

To implement the hybrid actuation concept, two mechanism concepts were considered:

C1 Move the impeller into the brake

C2 Move the brake into the impeller

- C2.1 Axially from above
- C2.2 Axially from below
- C2.3 Radially from the outside
- C2.4 Radially from the inside
- C2.5 Off-axis motion

Actuation mechanisms using wicking and/or swelling were not considered as their response times (especially the time to dry in a wet environment) were assumed to be too slow.

Moving the impeller into a braking surface (C1) requires that the impeller have an extra degree of freedom. This additional freedom prevents the use of a pin-cup bearing, which is critical to the single- and multi-jet meter's low flow performance. Therefore, like S4.1.2, a moving impeller strategy could measure water and not air, but would fail to measure low flow rates accurately (FR1).

Radial motion was eliminated due to its complexity. The inside of the impeller houses the bearings and shaft, so no feasible concepts were discovered to brake the impeller radially from the inside (C2.4). Actuating from the outside inwards was possible (C2.3), but the radial motion might interfere with the action of the inlet or outlet jets. In either case, radial motion was found to be more complicated than axial motion.

Tilting one of the shafts, upon which the impeller rides, would provide off-axis motion (C2.5). This tilt could cause the impeller's bearings to seize and the impeller to stop. This concept was not pursued because the extra degree of freedom in the shaft would reduce its stiffness and could therefore compromise its steady-state performance under the high loads of the maximum water flow rates. In addition, jammed bearings would not self-open when high-momentum water entered the impeller's housing.

Actuating from above or below was found to be feasible. As particulate matter builds up at the base of pipes and meters, actuating from above avoids this build up and was pursued (C2.1). As the design was required to work under a wide range of friction values ($\mu \in [0, 0.8]$; FR11), actuating the brake from a rotary pivot (as opposed to a linear slide) minimized its sensitivity to friction. To begin with a simple design, the brake engages only one of the impeller's vanes. A selectively engaged brake, actuated about a rotary pivot, is typically known as a trigger mechanism. Its analysis is detailed in the subsection that follows.

A float was use do provide the buoyancy force. Given the turbulent flows associated with high water flow rates, the float needed to be constrained to prevent undesired motion. A rotary pivot provided this constraint and was not sensitive to the coefficient of friction.

The two critical modules for this design were the trigger and the float (Fig 7-9). The analysis and design of each is detailed in the section that follows.

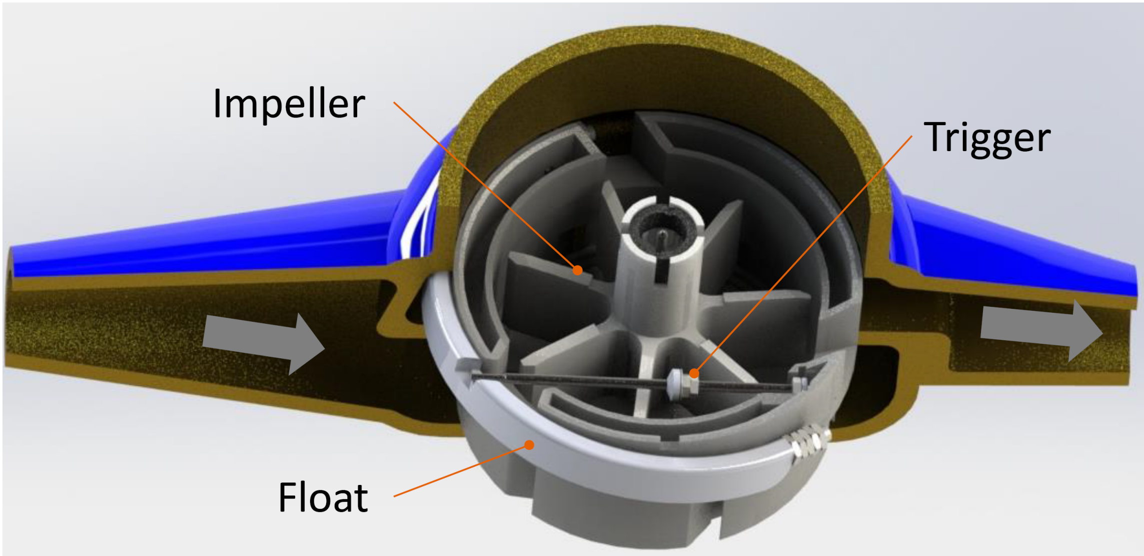

Figure 7-9: **CAD render of the water-only meter without its lid.** External brass housing is shown in cross-section.

7.4 Analysis

7.4.1 Trigger

The requirements for the trigger were simplified into two conditions. The trigger must hold when air imparts F_{jet}, and must self-open when water imparts F_{jet}. The tangential motion of the impeller was approximated as linear. Applying a coarse-to-fine method, friction at pivots is initially neglected. Key variables and external forces are shown in Fig 7-10. Internal forces acting on the trigger arm are equal and opposite to those acting on the impeller and float (7-10b and c).

The impeller in typical multi-jet meters is not completely constrained in the axial-direction. If its upward (flotation-enabled) preload is not present, it rests on its lower constraint (Fig 7-3c). This uncertainty in the impeller's position translates into uncertainty about where the impeller will contact the brake and is shown as Δy_{jet}.

Typical triggers employ a rolling element at brake interface to minimize friction. Due to the space constraints within the impeller's housing, a rolling element was not included. The trigger's brake meets the impeller at an angle α (Figs 7-10a and b).

Hold air. In the hold-air condition, $F_B = 0$ and the analysis simplifies. Taking

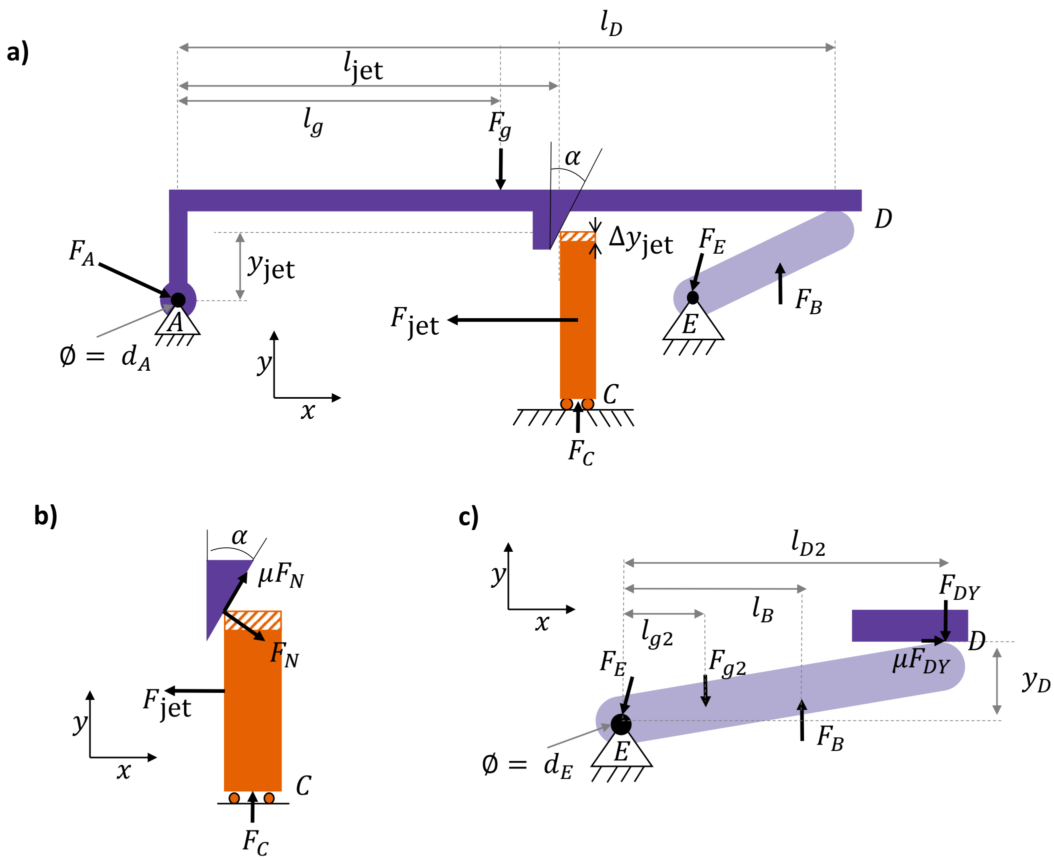

Figure 7-10: **Trigger free body diagrams.** a) trigger mechanism with only external forces. b) forces acting on the impeller blade (orange). c) forces acting on the float (light purple).

the sum of the moments about the trigger's pivot (point A in Fig 7-10a):

$$\sum_{\circlearrowright=+} M_A = F_g l_g - F_{\text{jet}} y_{\text{jet}} - F_C l_{\text{jet}} \tag{7.2}$$

Solving for the magnitude of the normal force F_N between the impeller and trigger (Fig 7-10b):

$$\begin{aligned} \sum F_x = 0 &= -F_{\text{jet}} + F_N \cos(\alpha) + \mu F_N \sin(\alpha) \\ \therefore F_N &= F_{\text{jet}} \frac{1}{\cos(\alpha) + \mu \sin(\alpha)} \end{aligned} \tag{7.3}$$

Using Eq 7.3 to solve for the impeller's y-direction reaction force (F_C; Fig 7-10b):

$$\begin{aligned} \sum F_y = 0 &= F_C - F_N \sin(\alpha) + \mu F_N \cos(\alpha) \\ \therefore F_C &= F_{\text{jet}} \frac{\sin(\alpha) - \mu \cos(\alpha)}{\cos(\alpha) + \mu \sin(\alpha)} \\ \therefore F_C &= F_{\text{jet}} \frac{\tan(\alpha) - \mu}{1 + \mu \tan(\alpha)} \end{aligned} \tag{7.4}$$

Substituting Eq 7.4 into Eq 7.2 and solving for the minimum size of F_g required to ensure the trigger holds:

$$\begin{aligned} &\sum_{\circlearrowright=+} M_A \geq 0 \\ &\therefore 0 \leq F_g l_g - F_{\text{jet}} y_{\text{jet}} - F_{\text{jet}} \frac{\tan(\alpha) - \mu}{1 + \mu \tan(\alpha)} l_{\text{jet}} \\ &\therefore \frac{F_g}{F_{\text{jet}}} \geq \frac{y_{\text{jet}}}{l_g} + \left(\frac{l_{\text{jet}}}{l_g}\right) \frac{\tan(\alpha) - \mu}{1 + \mu \tan(\alpha)} \end{aligned} \tag{7.5}$$

Conservatively assuming that $\mu \approx 0$ and rearranging to inform geometric choices:

$$\begin{aligned} \frac{F_g}{F_{\text{jet}}} &\geq \frac{y_{\text{jet}}}{l_g} + \left(\frac{l_{\text{jet}}}{l_g}\right) \tan(\alpha) \\ \therefore \frac{y_{\text{jet}}}{l_{\text{jet}}} + \tan(\alpha) &\leq \frac{F_g}{F_{\text{jet}}} \left(\frac{l_g}{l_{\text{jet}}}\right) \end{aligned} \tag{7.6}$$

Δy_{jet} was conservatively not included as it is easier to open the trigger when the impeller is high.

Self-open with water. Assuming F_B offsets F_g and no more, the trigger will self-open if:

$$
\begin{aligned}
\sum_{\circlearrowright=+} M_A &\leq 0 \\
\therefore 0 &\geq -F_{\text{jet}}(y_{\text{jet}} - \Delta y_{\text{jet}}) - F_{\text{jet}}\frac{\tan(\alpha) - \mu}{1 + \mu\tan(\alpha)} l_{\text{jet}} \\
\therefore \frac{y_{\text{jet}} - \Delta y_{\text{jet}}}{l_{\text{jet}}} &\geq \frac{\mu - \tan(\alpha)}{1 + \mu\tan(\alpha)}
\end{aligned} \tag{7.7}
$$

To account for friction at the trigger's pivot (point A), the reaction force at point A must be known. It can be conservatively approximated, however, as the sum of F_C, F_g and F_D. Friction from each of these components acts at the pivots radius ($d_A/2$), which is 50-150x less than the distance at which F_C and F_D act (i.e., $l_{\text{jet}} >> \mu d_A/2$ and $l_D >> \mu d_A/2$), therefore these contributors to F_A can be reasonably ignored. However, F_{jet} must be accounted for because y_{jet} is only one order of magnitude larger than $\mu d_a/2$. Eq 7.7 therefore becomes:

$$
\begin{aligned}
0 &\geq -F_{\text{jet}}(y_{\text{jet}} - \Delta y_{\text{jet}}) - F_{\text{jet}}\frac{\tan(\alpha) - \mu}{1 + \mu\tan(\alpha)} l_{\text{jet}} + \mu F_{\text{jet}} d_A/2 \\
\therefore \frac{y_{\text{jet}}}{l_{\text{jet}}} &\geq \frac{\mu - \tan(\alpha)}{1 + \mu\tan(\alpha)} + \frac{\Delta y_{\text{jet}} + \mu d_A/2}{l_{\text{jet}}}
\end{aligned} \tag{7.8}
$$

Combining Eqs 7.6 and 7.8 defines the feasible geometries:

$$
\begin{aligned}
\frac{\mu - \tan(\alpha)}{1 + \mu\tan(\alpha)} + \frac{\Delta y_{\text{jet}} + \mu d_A/2}{l_{\text{jet}}} \leq \frac{y_{\text{jet}}}{l_{\text{jet}}} &\leq \frac{F_g}{F_{\text{jet}}}\left(\frac{l_g}{l_{\text{jet}}}\right) - \tan(\alpha) \\
\therefore \mu\frac{1 + \tan^2(\alpha)}{1 + \mu\tan(\alpha)} + \frac{2\Delta y_{\text{jet}} + \mu d_A}{2 l_{\text{jet}}} \leq \frac{y_{\text{jet}}}{l_{\text{jet}}} + \tan(\alpha) &\leq \frac{F_g}{F_{\text{jet}}}\left(\frac{l_g}{l_{\text{jet}}}\right)
\end{aligned} \tag{7.9}
$$

The term in the center of the inequality can be thought of as the trigger's instability term. If $\Delta y_{\text{jet}} \to 0$ and $\mu \to 0$, then Eq 7.9 simply states that the gravity force to jet force ratio must be high enough to resist the trigger's instability. For a stable trigger,

$y_{\text{jet}} + \tan(\alpha) < 0$ and no gravity force is required for the mechanism to function. Given friction in the system and uncertainty in the impeller's y-position, a certain amount of instability is required to allow the system to self-open. With increasing instability in the trigger, however, the required gravity force F_g to hold the system closed also increases.

Space constraints limit the design's maximum buoyancy, which then limits the maximum weight of the trigger (F_g). Given a maximum trigger weight, the braking capacity of the trigger is maximized when F_g/F_{jet} is minimized. For reasonable values of $y_{\text{jet}}/l_{\text{jet}} \in [-0.4, 0.4]$ and $\alpha \in [0, 70°]$, Fig 7-11 plots the maximum required value of F_g/F_{jet} for any value of $\mu \in [0, 0.8]$. Representative values of $l_g/l_{\text{jet}} = 1$, $\Delta y_{\text{jet}}/l_{\text{jet}} = 0.03$, and $d_A/l_{\text{jet}} = 0.05$ were used to generate Fig 7-11; infeasible arrangements were not plotted.

Within the region considered, the optimal trigger design maximizes $y_{\text{jet}}/l_{\text{jet}}$ within the available geometry, and then minimizes α until the design becomes marginally feasible (i.e., in the lower right corner of the shaded half of Fig 7-11). Below the diagonal boundary in Fig 7-11, designs are infeasible.

As Fig 7-11 plots the upper bound of Eq 7.9, the feasibility line in the figure represents the lower bound (i.e., the condition where friction prevents the trigger from self-opening). Typically, where an optimal solution lies along a feasibility boundary, a certain safety factor would be implemented. Here, however, the maximum value of $\mu = 0.8$ has already accounted for a large margin of safety.

7.4.2 Float

The minimum buoyancy required to offset F_g (with variables defined as in Fig 7-10c) is:

$$\sum_{\circlearrowright=+} M_E < 0$$

$$\therefore l_B F_B \geq \mu F_E d_E/2 + F_{g2} l_{g2} + F_{DY} l_{D2} + \mu F_{DY} y_D \tag{7.10}$$

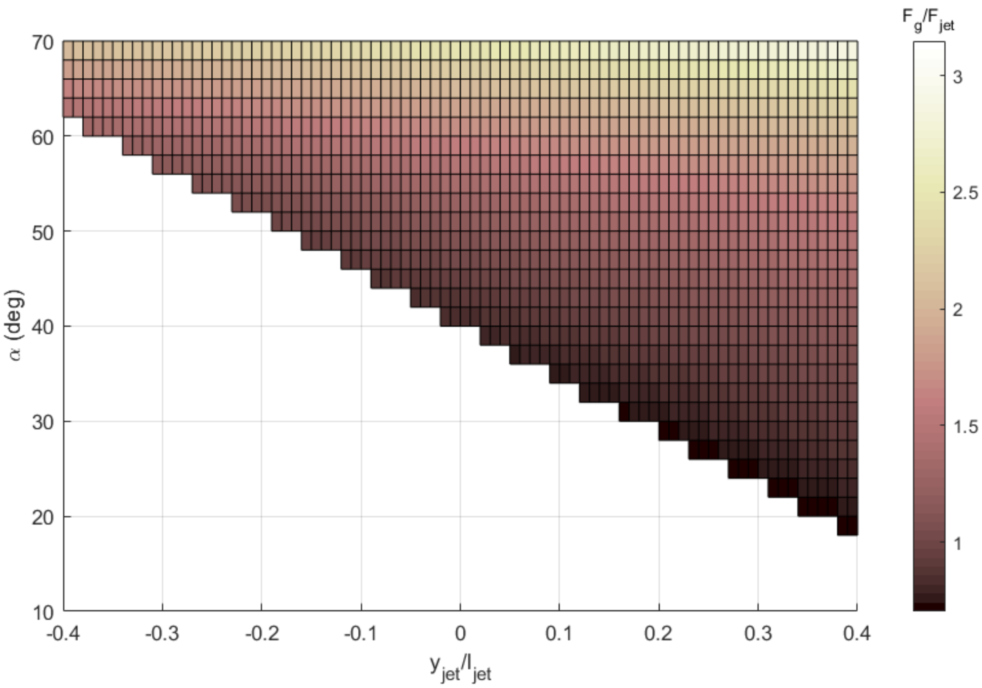

Figure 7-11: **Optimal trigger geometry.** For $y_{\text{jet}}/l_{\text{jet}} \in [-0.4, 0.4]$ (x-axis) and $\alpha \in [0, 70°]$ (y-axis), the minimum F_g/F_{jet} is shaded (color legend on right) for the worst-case friction $\mu \in [0, 0.8]$. Infeasible geometries are omitted (e.g., the plot's jagged lower edge).

Using superposition, for the float to offset F_g, $F_{DY} l_D > F_g l_g$. Substituting this in:

$$\therefore l_B F_B \geq \mu F_E d_E/2 + F_{g2} l_{g2} + F_g \left(\frac{l_g}{l_D}\right)(l_{D2} + \mu y_D) \tag{7.11}$$

By geometry $F_E < F_B$ and therefore it is conservative to substitute $F_E = F_B$ in the pivot-friction term:

$$\therefore l_B F_B \geq \mu F_B d_E/2 + F_{g2} l_{g2} + F_g \left(\frac{l_g}{l_D}\right)(l_{D2} + \mu y_D)$$

$$\therefore F_B(l_B - \mu d_E/2) \geq F_{g2} l_{g2} + F_g \left(\frac{l_g}{l_D}\right)(l_{D2} + \mu y_D) \tag{7.12}$$

Eq 7.12 bounds the upper limit of Eq 7.9 by the feasible flotation forces. It is, therefore, desirable to maximize F_B. Since, the buoyancy of a submerged object cannot exceed its volume, the volume of the float was maximized. The float was placed outside the impeller's housing in the void that collects flow from the outlet jets (i.e., the accumulator; Fig 7-9).

7.5 Detailed design

In order to keep the water-only meter's costs low (FR8), it was designed as a modification of an existing meter. Specifically, the Elster, Class B, 15mm, multi-jet meter was modified. By beginning with an existing meter, only the incremental production costs must be considered to evaluate FR8. The Elster team in Brazil sold the author many of their meters and provided additional bearing elements free of charge.

This section details the design of the trigger, the float, their interface, and the required modifications of Elster's impeller and its upper and lower housing (Fig 7-12). No modifications to the meter's case were made.

7.5.1 Trigger

To engage with the float on the outside of the housing, the trigger's beam exited the housing through an exit jet, which constrained the location of the trigger's pivot (Fig

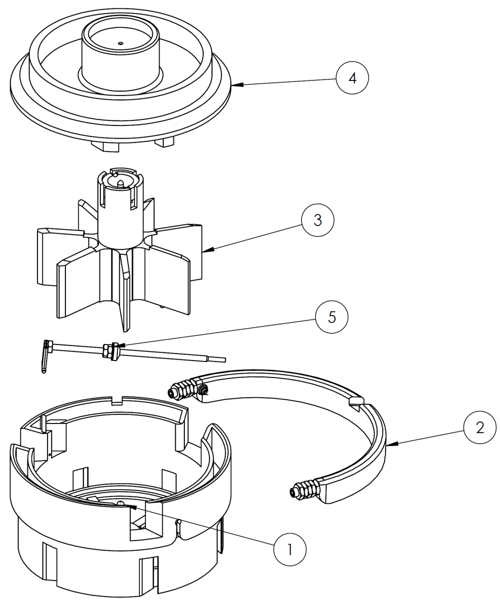

Figure 7-12: **Water-only meter component overview.** Trigger (5) and float assemblies (2) supplement lower and upper housing (1 and 4), and impeller assemblies (3).

7-13). The value of l_{jet} was thereby fixed. Keeping the trigger's pivot in the upper half of the housing similarly constrained the maximum value of y_{jet} (Figs 7-14 Detail D). Together these two distances set the optimal value of $\alpha = 30°$. While the trigger was analyzed as if its beam were parallel to the motion of the impeller's vane. In reality the beam was sloped down to improve the trigger's dynamic performance (Fig 7-1 Detail C). This initial angle was about 5°, therefore α was set to 26° (Fig 7-15).

Implemented as a proof-of-concept prototype, the trigger's design minimized custom parts and maximized reconfigurability (Fig 7-15). The trigger's beam is an 0-80 threaded rod and standard hex nuts add weight and mechanical support to the assembly. The angle α is achieved through a custom plastic threaded nut. The depicted spring washer did not achieve a sufficient preload and thread locker was used to maintain the position of the angled nut.

The analysis of the trigger's stability assumed that it was rigidly connected to its pivot (Eq 7.8). Initial tests showed that the angular stiffness of the threaded joint between the plastic pivot and the threaded rod was insufficient. An additional nut was used to supplement the prototype joint's stiffness (Fig 7-14 Detail D). The

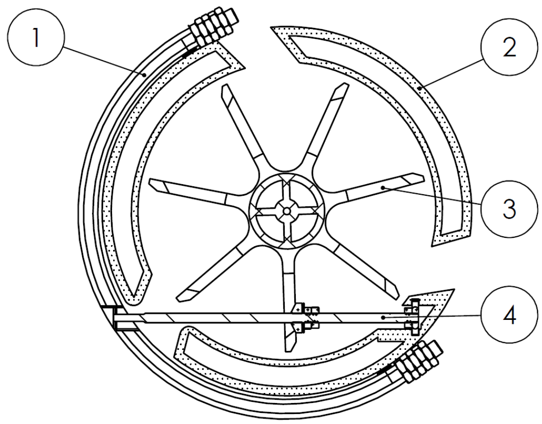

Figure 7-13: **Trigger alignment within impeller housing:** 1) float in accumulator; 2) lower impeller housing; 3) impeller; 4) trigger assembly. Partial cross-section; bottom not shown for clarity.

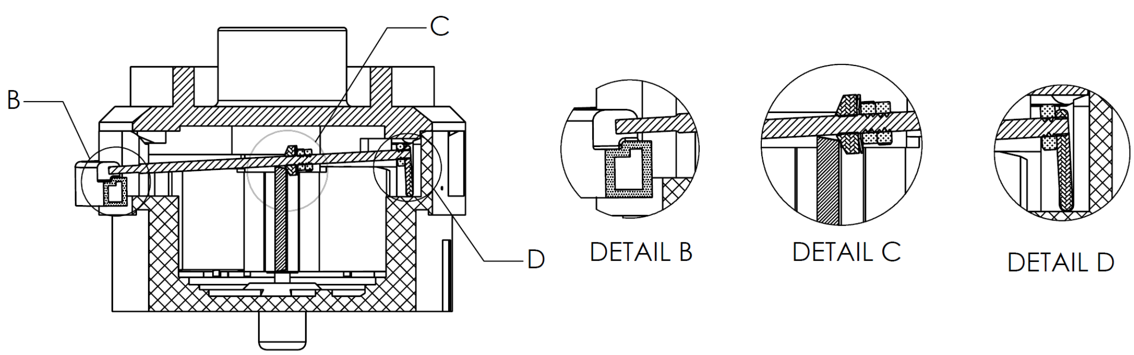

Figure 7-14: **Trigger cross-section in context.** Trigger mechanism implemented in an Elster, 15mm, Class B water meter. Detail B: threads on the 0-80 trigger shaft were removed to reduce friction with the floating pivot. Detail C: An angled nut along with a spring washer, and two support nuts engage the impeller blade. Detail D: trigger shaft's joint to a pivot arm is supported by an additional nut.

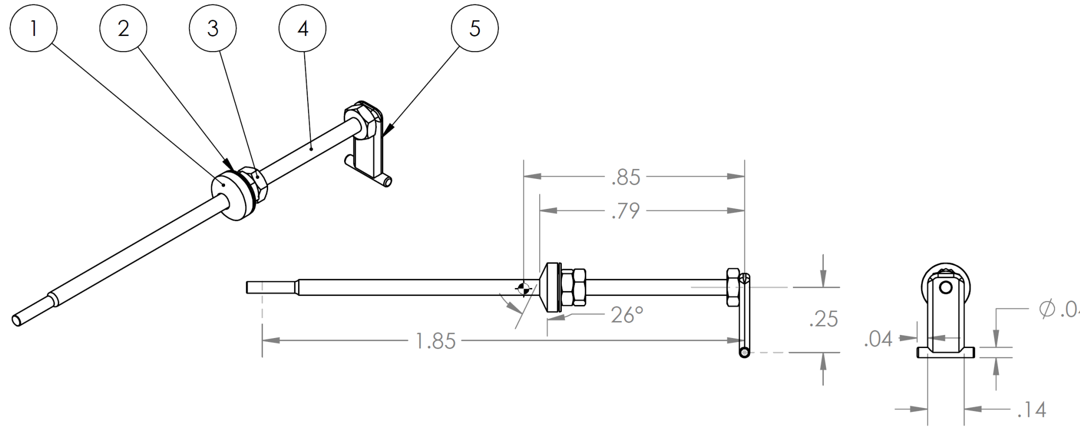

Figure 7-15: **Trigger assembly.** 1) custom plastic tapered nut; 2) spring washer; 3) 3x hex nuts; 4) 0-80 threaded rod with turned down tip; and 5) custom plastic pivot. Key dimensions are shown for illustrative purposes in inches.

threaded rod's end is turned down to minimize friction at the float interface (Fig 7-14 Detail B). In production, a straight metal rod could be press fit into a single, injection-molded part that would act as the pivot and the angled nut.

7.5.2 Float

The float is inserted into the meter's casing before the impeller's lower housing. For ease of assembly, the float is preloaded inwards so that it will snap into place. To achieve this preload, the float is a partial oval that deviates from circularity by 0.01 inches in radius along the axis of the hinge (Fig 7-16 Detail A). The float is hollow throughout, except for the region near the hinges (Fig 7-16 section views C-C and D-D). Counter weights serve to reduce $l_{g2}F_{g2}$ without substantially changing $F_B l_B$. The float's wall thickness is 0.025 inches, which was constrained by the manufacturing process, not the applied load.

In production, the flotation could be achieved through foam molding or by ultrasonically welding two halves of the float together. Counterweights could comprise a metal rod, of standard dimensions, press fit into the plastic float.

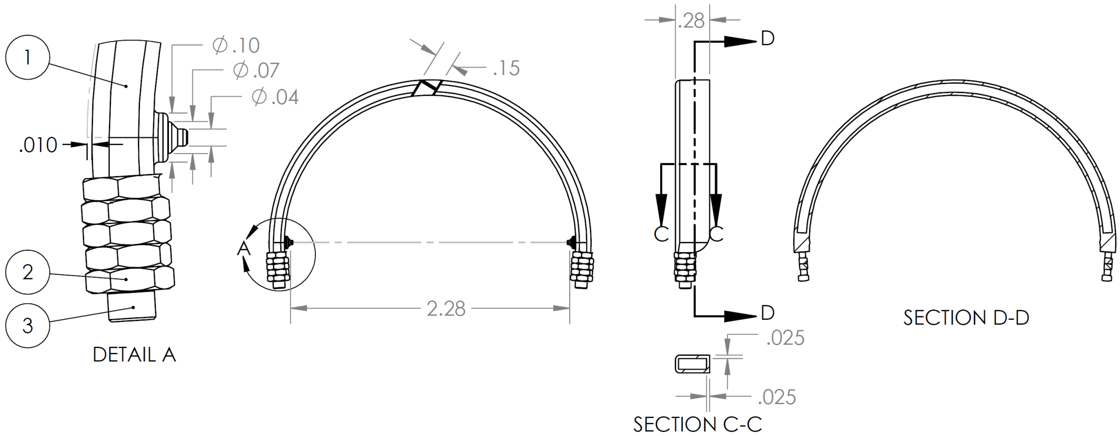

Figure 7-16: **Detail of float.** 1) Hollow, plastic float; 2) 5 nuts for counterweight; 3) 0-80 bolt. Detail A: hinge geometry and offset from circular by 0.01in in radius. Section C-C: the hollow float's 0.025in wall thickness. Section D-D: hollow region extends throughout the float except near the hinges.

7.5.3 Trigger-float interface

A major risk associated with using flotation to actuate the water-only meter, is that it could be tampered with by installing the meter up-side-down. As a counter measure, the trigger's beam rests on the float, but is not rigidly connected (Fig 7-14 Detail B). As such, if the water-only meter were installed up-side-down, the float and trigger would separate and both water and air would be metered.

7.5.4 Modifications to existing meter components

To accommodate the trigger and float, the existing impeller and its housing needed to be modified.

Impeller. Earlier versions of the water-only meter (not described herein) ensured that the impeller could only contact the trigger at the angled nut. If the impeller's vane was not initially in contact with the angled nut, the vane would accelerate into its collision with the nut. The resultant impact force was much larger than the anticipated static forces and would open the trigger, allowing the next vane to similarly accelerate into the nut. In these earlier designs, once the impeller was spinning, the trigger could not stop it (thus failing FR12).

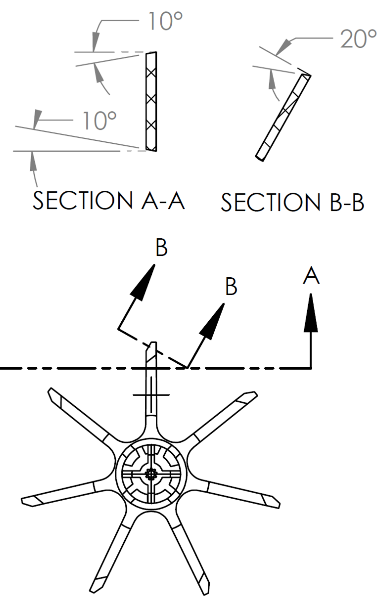

Figure 7-17: **Impeller modification.** The impeller rotates counter-clockwise from this top-view. Sections show its modification. Section A-A: a 10° chamfer was added to the top and bottom leading edge of the impeller's vanes. Section B-B: an additional 20° chamfer was added to the outer, angled section of the top leading edge.

In order to stop metering air while the impeller is already spinning (FR12), the final trigger design allows the impeller can make contact with the trigger's beam before the impeller engages the angled nut. While the trigger's beam does not stop the impeller, it prevents the it from accelerating. This allows the water-only meter to brake a moving impeller at low speeds. Beyond speeds where the brake can arrest the motion, the contact with the beam still slows the impeller's velocity.

To ensure the the impeller did not jam during contact with the beam, each vane's leading top edge was chamfered by 10°. To avoid changing the impeller's dynamic lift (or lack there of), a matching chamfer was added to each vane's leading bottom edge (Fig 7-17). Finally, at the tip of each vane, the angled front was chamfered by 20° (Fig 7-17).

Current impeller designs are injection molded without requiring any side pulls. The proposed modifications would not change this.

Housings. Material was removed from two sections of the impeller's top housing to allow clearance for the trigger to actuate (Fig 7-18). Similarly, the lower housing

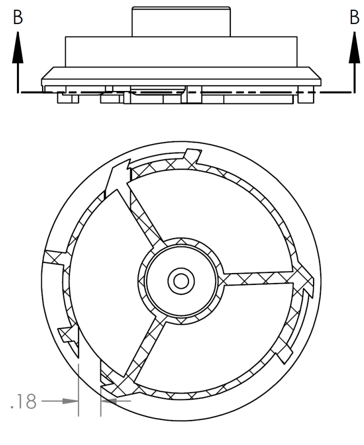

Figure 7-18: **Top housing modification.** Where Section B-B is asymmetrically-missing material, material was removed to allow the trigger to actuate.

had material removed to allow for the trigger's pivot and the float's hinge (Fig 7-19). As built, the hinge for the float (Fig 7-19 Detail D) would require a side pull. This side pull could be avoided if the material above the hinge were attached to the top housing instead of the bottom. The required changes in the existing housing are minimal and would not substantially increase tooling costs compared to the standard meter.

7.6 Performance

7.6.1 Analytic performance

As built, the water-only meter's properties are summarized in Table 7.6. Applying these dimensions in Eq 7.9, the minimum ratio of $F_g/F_{\text{jet}} = 0.75$. At this ratio, the braked meter would open for any air flows with $F_{\text{jet}} \leq 1$ gram of force. The analysis, however, assumed that the brake needed to hold in a frictionless environment. If $\mu \geq 0.2$, then the brake's holding force increases to 1.5 grams of jet force. In either case, the predicted holding capacity is substantially less than was thought to be required (i.e., 9 grams of force; Table 7.5).

The float, with its counterweights, provided 56% more buoyancy than required

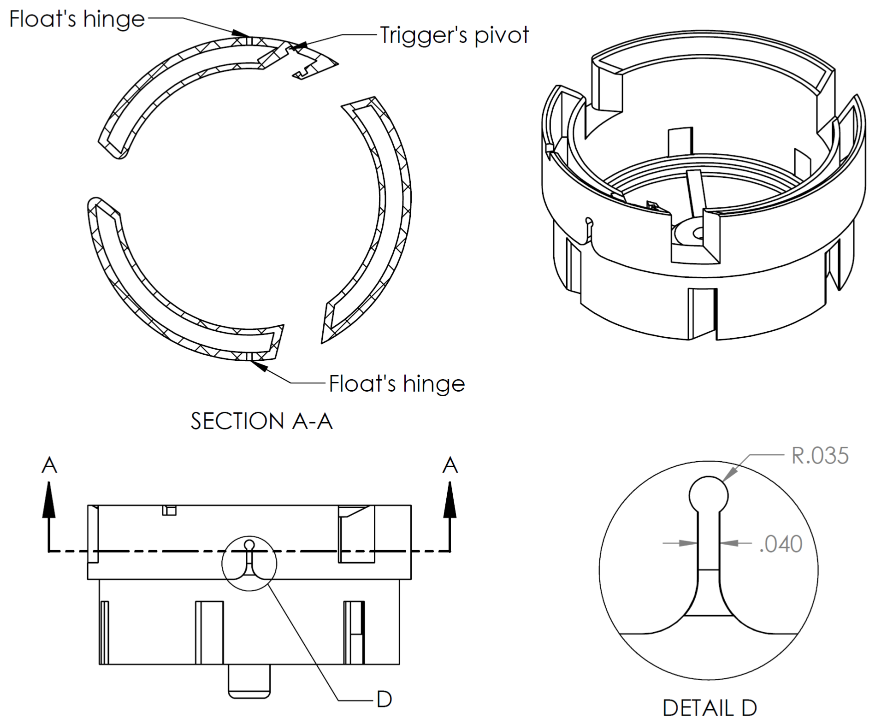

Figure 7-19: **Lower housing modification.** Section A-A: shows both places where the original housing design was modified. Detail D: shows the alignment feature used to snap the float in place.

Table 7.6: **Final trigger specifications.** Grouped by trigger geometry, float geometry, and forces. Variables as defined by Fig 7-10.

	Variable	Value	Units
Trigger	y_{jet}	0.18	in
	Δy_{jet}	0.02	in
	l_{jet}	0.79	in
	l_g	0.85	in
	l_D	1.85	in
	d_A	0.04	in
	α	30	$^\circ$
Float	l_B	0.68	in
	l_{g2}	0.36	in
	l_{D2}	1.68	in
	d_E	0.04	in
	y_D	0	in
Forces	$F_{g,\mathrm{dry}}$	0.78	grams
	$F_{g,\mathrm{wet}}$	0.67	grams
	F_B	2.51	grams
	F_{g2}	2.42	grams

(i.e., buoyancy had a factor of safety of 1.56; Eq 7.12 and Table 7.6).

7.6.2 Experimental methods

Four attributes of the water-only meter's performance were validated experimentally: first, the maximum flow rate of air it could brake; second, the maximum flow rate of air it could brake when air follows water; third, its accuracy when metering water only; and fourth, its accuracy when metering water that follows air.

The experimental setup consisted of three water meters connected in series with clear piping a minimum of 10 diameters long in between each. The middle meter was the water-only meter (WOM), a modified Elster, Class B, 15mm, multi-jet meter. Upstream and downstream meters were unmodified Elster meters of the same specification. The experimental setup allowed air, of regulated pressure, to flow through the meters. Pumped water, regulated through a manual needle valve, could flow through the meters. Reed switches provided pulse-flow data, which was read by a National-Instruments USB-6009 data acquisition unit and recorded in Labview 2017. The experimental setup is depicted in Fig 7-20.

To measure the dry holding capacity of the WOM, air pressure was slowly increased until the brake slipped. Air flow rates were measured in the conventional upstream and downstream meters (Fig 7-20). Pulse-flow data recorded the maximum flow rate before slippage.

To assess the WOM's ability to stop metering air that follows water, the system was filled with water, purged of air, and turned off. Air was then allowed to enter the system at a constant pressure. The WOM's ability to brake the air flow was measured as pass/fail.

To measure the steady-state accuracy of the WOM, the system was purged of air, and tuned to run at a specific flow rate. Each meter was read manually (to the fiftieths of a liter) before the system was turned on. After a variable time interval, the system was shut-off using the downstream valve and the time interval was recoded. Meters were re-read and flow rates inferred. Manual meter reading was preferred for low flow rates because the Elster meters provided only one pulse per liter.

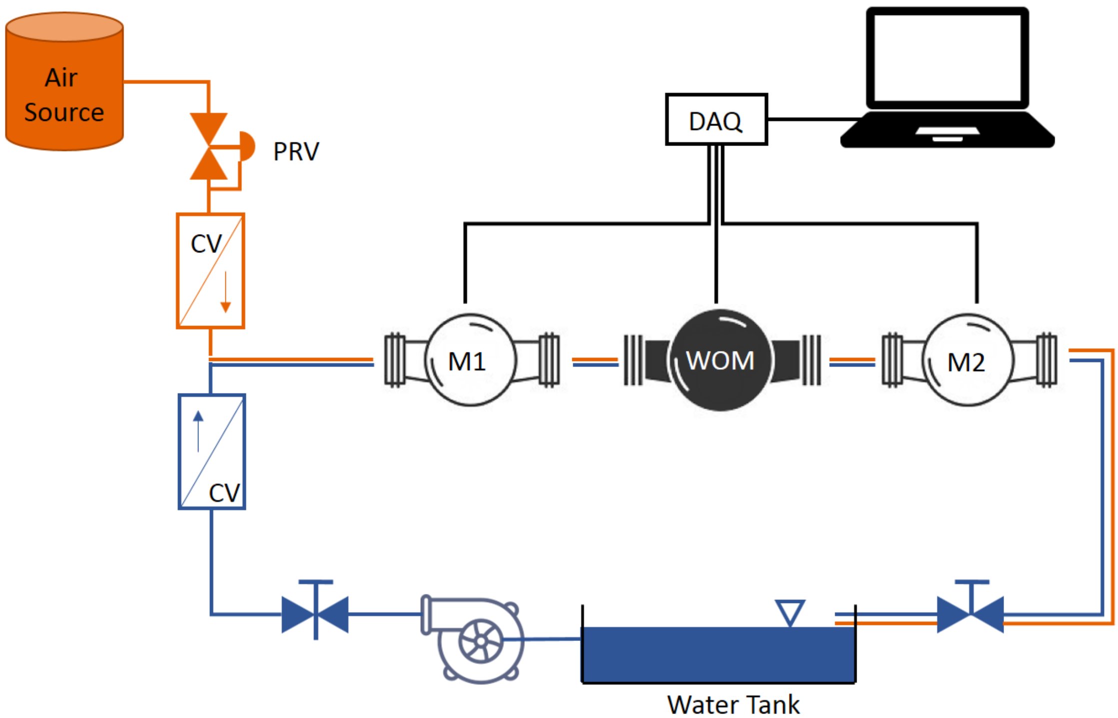

Figure 7-20: **Water-only meter's test setup.** Air flow is shown as orange lines, while water flows are in dark blue. Air flowing out of its pressure source was regulated through a pressure-reducing valve (PRV) and a check valve (CV). Water flowing out of the pump was regulated with a manually controlled needle valve. Pulse-flow data (black lines) were recorded through a data acquisition (DAQ) unit. Two reference meters (M1 and M2) were connected in series with the water-only meter (WOM). Not to scale.

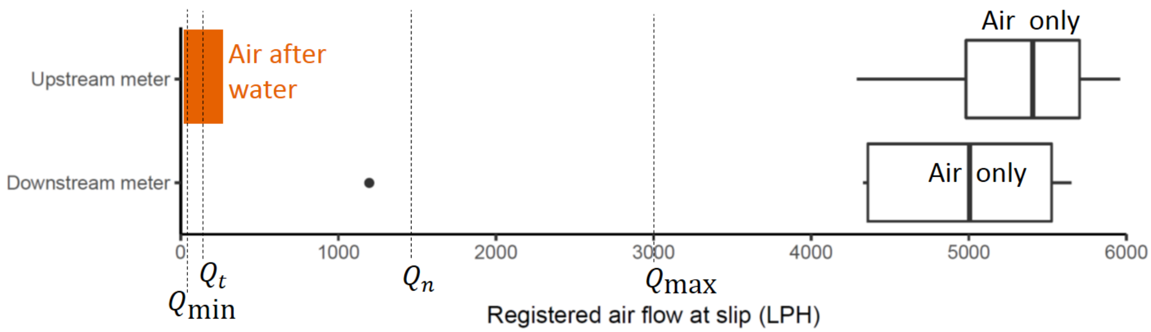

Figure 7-21: **Water-only meter's braking capacity.** For experiments that began with a dry system, box plots show the range of air flow rates measured by the upstream and downstream reference meters just before the water-only meter's brake released (N=8 for each meter). When air followed water, the WOM could only brake air flow rates in the solid orange box.

To assess the WOM's ability to meter water following air, the system was first filled with air. Subsequently, water was allowed to enter the system at approximately $Q_{\min}$. After the system reached steady state, the flow rate was slowly increased until the WOM's brake disengaged. The flow rate was measured immediately after the brake disengaged.

7.6.3 Experimental results

The WOM's brake successfully held until an average 4900 LPH of air was flowing through the system (N=8; Fig 7-21). Apart from the outlier in the downstream meter's data, the WOM consistently avoided metering air until the air's flow rate was at least 4000 LPH (Fig 7-21). This was more than required by FR2, and much more than predicted.

Since dry multi-jet meters can over or under-register the flow of air, Fig 7-21 may not represent the true air flow rate. Even conservatively accounting for worst extreme of over-registration (+50%; Walter et al. (2018)), the WOM still substantially out performed its required holding capacity.

During the experimental run which produced the outlier, it is suspected that water entered the downstream meter as its performance diverged from the upstream meter mid-run (Fig 7-22). In support of this theory, Walter et al. (2018) found that multi-jet

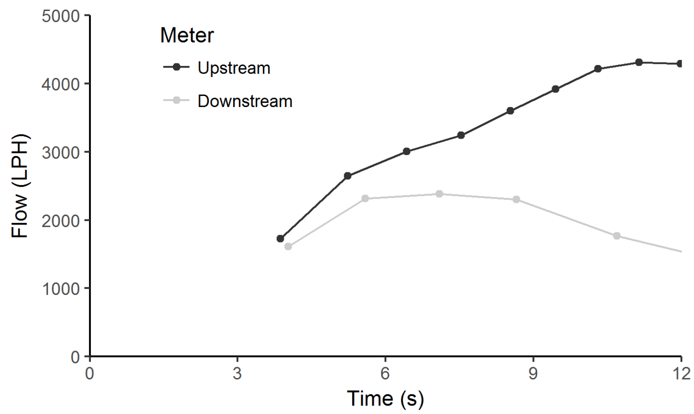

Figure 7-22: **Under-registration of air in downstream meter.** Flow rates are only displayed after the second pulse from the upstream (dark dots and lines) and downstream (lighter dots and lines) reference meters.

meters register only 15% of the air volume when there is residual water in them.

The WOM's braking capacity was substantially reduced if the WOM was initially full of water whem air entered the system. Since the experiment to test this capacity was pass/fail, the exact slipping point could not be studied. Instead, it was observed that the WOM stopped metering air that followed water in 78% (N=14) of tests where the air flow rate was less than 240 LPH. In every case above 240 LPH (N=7), the brake slowed the WOM's impeller, but could not completely avoid metering air. The range in which the WOM could brake air that follows water is superimposed on Fig 7-21.

In 22% of cases, the WOM measured air that followed water, even though the air's flow rate was <240 LPH. In these cases, the WOM's float dropped, but the trigger stayed in its elevated position. Surface tension was observed to adhere the trigger's beam to one of several of the surfaces which constrain its motion. The surface-tension-induced failure was more common at lower air flow rates than at flow rates close to 240 LPH. At higher flow rates, splashing and turbulence in the meter were more likely to jostle the trigger back into motion. A hydrophobic coating might minimize this effect.

The threshold air flow rate (240 LPH) was measured with reference meters that also began wet. As such, Walter et al. (2018) suggests that they would register 15% of the air's volume. Applying this correction factor, the threshold would have actually been 1600 LPH. The true threshold likely lies between 240 and 1600 LPH.

When measuring the flow of water, the WOM under-registered by an average of 10% (Fig 7-23a). While outside of the accuracy specifications for a Class B meter, much of this inaccuracy was induced by the use of prototyping methods and materials. By design, the WOM measures flow after it fills with water. At slow flow rates, however, the system's pipes and meters remained partially filled with air. As such, the WOM did not meter air until an average flow rate of 110 LPH (N=3; Fig 7-23b). The WOM, therefore, did not meet FR3 at low flow rates.

7.7 Discussion and future work

The designed and tested water-only meter successfully met its two most basic goals: to not meter air, and to meter water. However, it did not reliably meter water that followed air at low flow rates, or brake air that followed water at high flow rates. Addressing these limitations will be key to the meter's commercialization and implementation.

The meter's ability to brake air that follows water could be improved by coating the trigger's beam (from $l_{\text{jet}} \rightarrow l_D$) with a low-coefficient-of-restitution material. In addition, this ability could be improved by increasing the size of the float, the weight of the trigger, and adding a hydrophobic coating to the trigger. Increasing the float would require changes in the meter's outer casing. Before making major design decisions, however, more accurate air flow measurements are required to assess the true air flow rate at which the meter can no longer brake the impeller.

Geometric changes may improve the minimum flow rate at which water that follows air can be measured (e.g., Fig 7-6). However, solutions where the meter starts fully submerged may also make braking air that follows water a bigger challenge. A vertically-oriented water meter might address the competing needs of ensuring the meter starts empty but ends full. However, such a dramatic design change would make getting the new design adopted much harder.

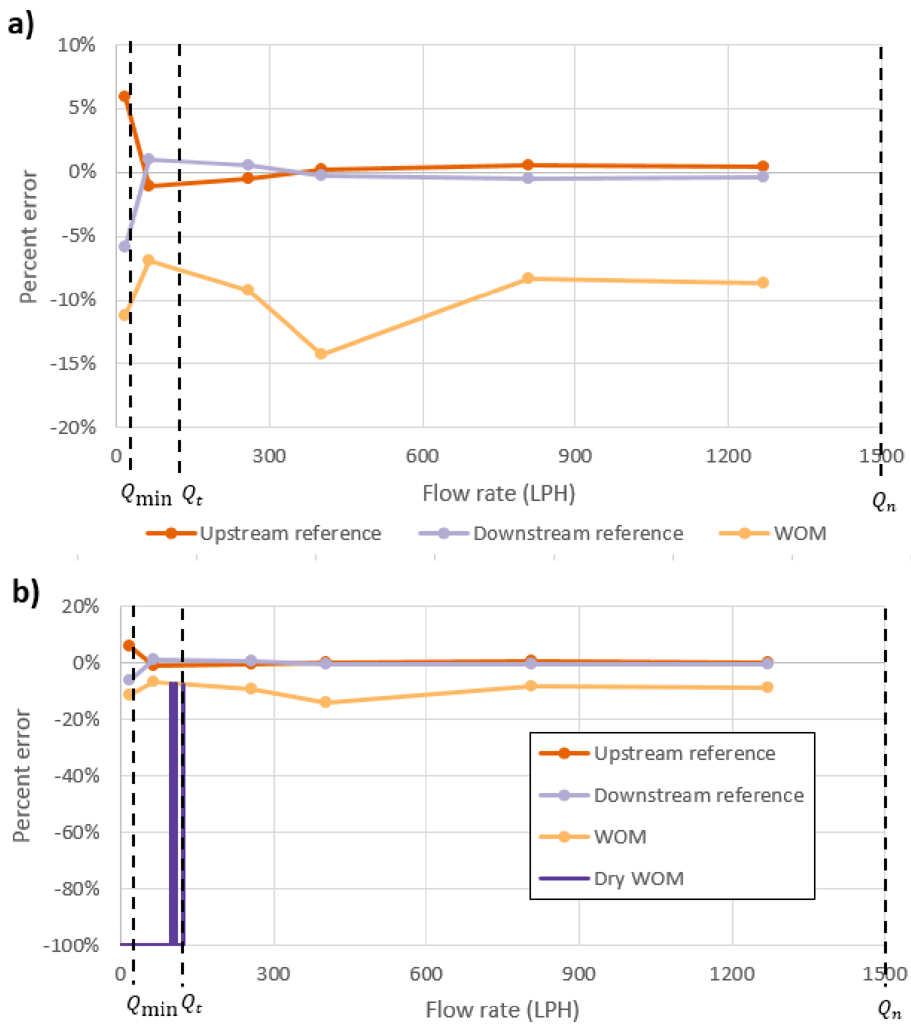

Figure 7-23: **Water-only meter's accuracy.** Taking the mean of upstream and downstream water meters as the reference, each meter's percent error is shown. a) With no air in the system, the accuracy of each meter was assessed at the points shown (upstream reference: orange; downstream reference: light purple; and water-only meter (WOM): light orange). b) Starting from a dry condition, the flow rate at which the WOM begins to register was tested three times (dark purple, vertical lines).

Additional work is also needed to identify and reduce the sources of friction in the current water-only meter. These improvements, however, are not as critical; those discussed above should be addressed first.

The proof-of-concept water-only meter, inspite of its limitations, has validated that a floating trigger can enable a mechanical multi-jet meter to differentiate between air and water flows. Partnering with an existing meter manufacturer to pursue the next iteration of the meter's design is recommended.

Chapter 8

Conclusions, implications, and future work

> [Water supply] needs to be continuous enough to . . . satisfy all needs, without compromising the quality of water.
>
> de Albuquerque (2010, para.19)

This thesis presented a suite of new models and a water meter as tools to better manage intermittent water supplies.

To provide context for the developed tools, a brief history of Delhi's water supply and its partial privatization was given. The complexity of Delhi's 845 distinct supply schedules exemplified why management tools for IWS are needed. Such tools must either be complex enough to capture the systems' details (no small feat in an IWS) or be general enough to capture the average performance of such systems.

Previous models of IWS have attempted to improve their accuracy by adding complexity. Such models are precise, but require more network information than is typically available in IWS. Even where the required information is thought to exist, its accuracy is questionable due to the complex arrangements and rearrangements that define how IWS operate and evolve.

Instead, this thesis developed simple models that are less dependent on network information. As such, they are more easily generalized and help to understand why IWS exist, persist, and how they can be optimally managed.

The hydraulic model superimposed the water required by an average leak onto the water received by an average customer demanding a fixed volume of water per day. Despite being piecewise linear, this model captured the majority of the variation observed in detailed simulations of complex, intermittently-operated reference networks. Important aspects of how IWS behave are simple.

The model's inflection point, at which customers become satisfied, is a critical parameter. It determines which causes and effects are most influential for which IWS. Satisfied systems with low leakage levels were shown to be extremely sensitive to changes in total water availability and customer demand. In contrast, unsatisfied IWS were found to be robust to changes in water availability, customer demand, and leakage. As such, utilities may prefer to operate as unsatisfied IWS. Robustness from the utility's perspective, however, disadvantages customers and increases inequity. Policy makers and global goals, therefore, encourage satisfied IWS. Characterizing the distinction between satisfied and unsatisfied IWS, and proposing how it could be measured, represents a substantial contribution of this thesis.

The financial model considered the behavior of Rational Water, a hypothetical utility governed only by short-term financial incentives. The model demonstrated the need for performance incentives and careful regulation when utilities (public or private) are governed by financial motives. Specifically, financial penalties are always required for high-pressure continuous water supply to maximize a utility's (short-term) gross margin. Both linear and non-linear penalty weights can be conservatively set knowing only the costs of leak repairs in a network (and nothing else about its topology). Unregulated utilities are likely to adopt low-pressure supply, which can compromise water quality and equity. The dangers of low pressure supply are magnified by customers using their own suction pumps. Where low-pressure IWS exist or are proposed, customer pumps must be addressed (e.g., with a hardware solution (Taylor, 2014)).

The water quality model showed that operational parameters could have opposite effects on the quality of the flushing and steady-state phases of supply. The proposed model is the first to predict how water quality changes in both supply phases.

Finally, to assist utilities in distinguishing when their customers are satisfied, the design and testing of a water meter, which does not register air flow, was presented. This water-only meter successfully metered water and did not meter air. It did not, however, reliably meter water that followed air at low flow rates, and, unfortunately, metered air that followed water at high flow rates. Addressing these limitations in partnership with a meter manufacturer will prove key to the water-only meter's improvement and commercialization.

For utilities running IWS, regulators overseeing IWS, academics studying IWS, and projects improving IWS, the complexity of IWS can be daunting. In addition to the hydraulic complexities of IWS, IWS are technopolitical systems, influenced by power, politics, and corruption. Amidst this complexity and apparent chaos, the validity and utility of the proposed models demonstrate that much of the behavior of IWS is simple. The proposed simple models enable operating, regulating, researching, and/or upgrading IWS to be done more efficiently.

8.1 Implications

1. The benefits of CWS have been recognized since the mid-nineteenth century. Critiques of the private sector's involvement in water supply are important, but should not extend to endorsing the status quo of unsafe, inequitable, and frequently-insufficient IWS.

2. Satisfied customers are customers whose water supply is "constant enough" and "available when needed." The models presented in this thesis, therefore, may facilitate measuring and achieving global water goals.

3. Much of how an IWS will respond to operational changes can be determined before a system-improvement project begins. As such, the feasibility of these projects should be more rigorously evaluated before they begin.

4. Amidst the conflicting and diverse perspectives on the causes and effects of IWS, the proposed and validated hydraulic model provides a framework to unify such perspectives by stating the conditions under which each cause and effect dominates.

5. Since marginally-satisfied IWS maximize a utility's short-term gross margin, performance incentives to ensure sufficient pressure and duty cycle are strongly suggested.

6. Water systems with long duty cycles and low leakage rates were found to be very sensitive to changes in water availability. Reserving extra water to account for unexpected fluctuations in demand and/or source availability can substantially improve system robustness.

7. To ensure financially-oriented utilities will fix their leaks and adopt high-pressure continuous water supply, financial penalties are required. To facilitate contract design, the size of such penalties was tabulated as a function of the cost of leak repair and a system's initial conditions.

8. Knowing the current level of demand satisfaction is not required to design a rational leak repair contract for an IWS, but it is required to estimate the project's costs and revenues.

9. Linear performance penalties needed to be larger than non-linear penalties, but were less sensitive to unknown system parameters; both penalty types should be considered during a project's design phase.

10. Penalties focused on either duty cycle (intermittency) or system pressure are inefficient, difficult to measure, and may lead to undesired outcomes. Both parameters can be measured simultaneously with pressure loggers. Both should be included in performance-based contracts for improving and/or operating IWS.

11. Given the natural incentives for a utility to satisfy its (paying) customers, the existence of unsatisfied IWS likely signifies water shortage issues requiring more

than distributional solutions.

12. Increasing the supply period (i.e., reducing the supply frequency) may improve water quality and reduce leakage. The maximum period, however, should be limited by the storage capacity of a system's most disadvantaged customer.

13. Distinguishing between IWS' predicted effects on flushing and steady-state water quality may help understand which customers will derive health benefits from CWS.

14. Operational parameters affect flushing and steady-state phases differently. Flushing phase water is often used by disadvantaged customers; its quality cannot be neglected. Regulators and researchers, therefore, should distinguish between each supply phase when mandating and/or reporting water quality sampling.

15. In each presented model, the distinction of satisfied vs. unsatisfied customers proved important. Even in complex networks where aggregated satisfaction is a spectrum rather than a classification, this distinction was useful. It should be added to the taxonomy of IWS.

16. The proof-of-concept water-only meter demonstrated that a purely mechanical meter can avoid metering air. The presented design may provide water meter manufacturers with new inspiration and analysis to pursue additional design iterations.

8.2 Future work

1. Much of the modeling work presented in this thesis is theoretical. Three additional validations of the hydraulic model are suggested. First, the hydraulic model's predictive power with respect to pressure changes should be explored using the VDD simulations presented in this thesis. Second, the hydraulic model should be tested against simulations that capture network-filling dynamics. Third, the hydraulic model should be validated with a field experiment.

2. Average performance indicators mask inequalities. Each of the derived models relies on such averages and could not, therefore, capture the equity implications of operational decisions; this is a major limitation of the proposed models. Including estimates of spatial variation, without using network-specific information, could allow the models to approximate the equity implications of IWS. Modeling network variation generally could perhaps be done using scaling laws that govern how water networks typically grow and spread (e.g., Cheng and Karney (2017)).

3. The hydraulic model treated the average system pressure as exogenous (i.e., constant and independent of other model variables). In reality, changes in duty cycle affect average flow velocities and therefore pressure losses and the average pressure in the network. As such, including endogenous pressure changes would substantially improve the hydraulic model's pressure and leakage predictions. This could be done by modeling uniformly-distributed leaks along a single pipe, or perhaps by incorporating the work of Cheng and Karney (2017).

4. Capturing endogenous pressure changes and/or the spatial variations proposed above would also substantially improve the model of contaminant intrusion.

5. The presented financial model is simplistic. Distinguishing between capital and operational expenses and accounting for the time-value of money will be important model refinements, especially when longer-term projects are considered.

6. Better indicators of intrusion would make assessing water safety in IWS more efficient. Such indicators would also make validating the proposed model of contaminant intrusion more feasible.

7. The proof-of-concept water-only meter demonstrated that a trigger-and-float architecture could measure water and not air, as desired. However additional development is required to increase the water-only meter's steady-state accuracy and to reduce the minimum flow rate required for air bubbles to exit the meter's housing.

8. IWS subject water meters to operating conditions that are still poorly understood. Recent research has begun to study these effects but more work is required to determine how and when air and water pass through domestic water meters in IWS.

In order to ensure that everyone has access to drinking water that is 'safe' and available 'when needed' by 2030, new operational strategies and management tools are required. This thesis developed a suite of new models that relate a utility's operational decisions to its water safety and availability. In each model, customer demand satisfaction was a critical parameter. To facilitate measuring demand satisfaction, this thesis described a new water-only meter. Where traditional domestic water meters measure air, this water-only meter would benefit both utilities and customers.

Appendix A

Supporting data

A.1 Context of Delhi

In order to understand per capita water production in Delhi over time, data were pooled from sources summarized in Tables A.1 and A.2.

A.1.1 MNWS characteristics

The MNWS project area is about 14 square kilometers and covers a population of 382 thousand people with 32 thousand customer connections (Koonan and Sampat, 2012). It spans 26 colonies in the South I and South III regions of South Delhi (Koonan and Sampat, 2012). The system has 56km of feeder main piping with 137km of distribution piping. Pipe materials are a mix of cast iron, pre-stressed concrete and mild steel for pipes larger than 100mm and predominantly galvanized iron for pipes smaller than 100mm (Delhi Jal Board, 2012g).

Koonan and Sampat (2012) question what services will be provided to residents not served by formal DJB connections at the start of the project; these areas house 91,500 people (23.9% of total project population). Sangameswaran (2014) explains that such exclusions are often framed in purely technical terms, but elucidate specific visions of what development should look like and who will have access to it (e.g., the implications of different rules for per capita water availability by rural vs. urban and

Table A.1: **Delhi's historic water production capacity.**

Year	Production ($\times 10^6$L/d)	Source
1892	8	(Jain, 1997)
1926	46	(Jain, 1997)
1946	136	(Jain, 1997)
1956	273	(Jain, 1997)
1966	651	(Jain, 1997)
1974	869	(Jain, 1997)
1978	924	(Jain, 1997)
1979	1151	(Jain, 1997)
1981	1379	(Jain, 1997)
1984	1565	(Jain, 1997)
1985	1715	(Jain, 1997)
1986	1806	(Jain, 1997)
1987	1861	(Jain, 1997)
1990	2093	(Jain, 1997)
1994	2389	(Jain, 1997)
1995	2616	(Jain, 1997)
1999	2475	(Government of NCT of Delhi, 2002)
2004	2955	(Government of NCT of Delhi, 2004)
2008	3273	(Government of NCT of Delhi, 2009)
2014	3796	(Government of NCT of Delhi, 2015)
2016	4069	(Government of NCT of Delhi, 2017)

Table A.2: **Delhi's historical population.**

Year	Population ($\times 10^6$)	Source
1911	0.410	(Asthana, 2009)
1941	0.918	(Jain, 1997)
1951	1.744	(Jain, 1997)
1961	2.658	(Jain, 1997)
1971	4.066	(Jain, 1997)
1981	6.222	(Jain, 1997)
1991	9.37	(Jain, 1997)
2001	13.851	(Census of India, 2001)
2011	16.79	(Census of India, 2011)
2017	19	Projected by the (Census of India, 2011)

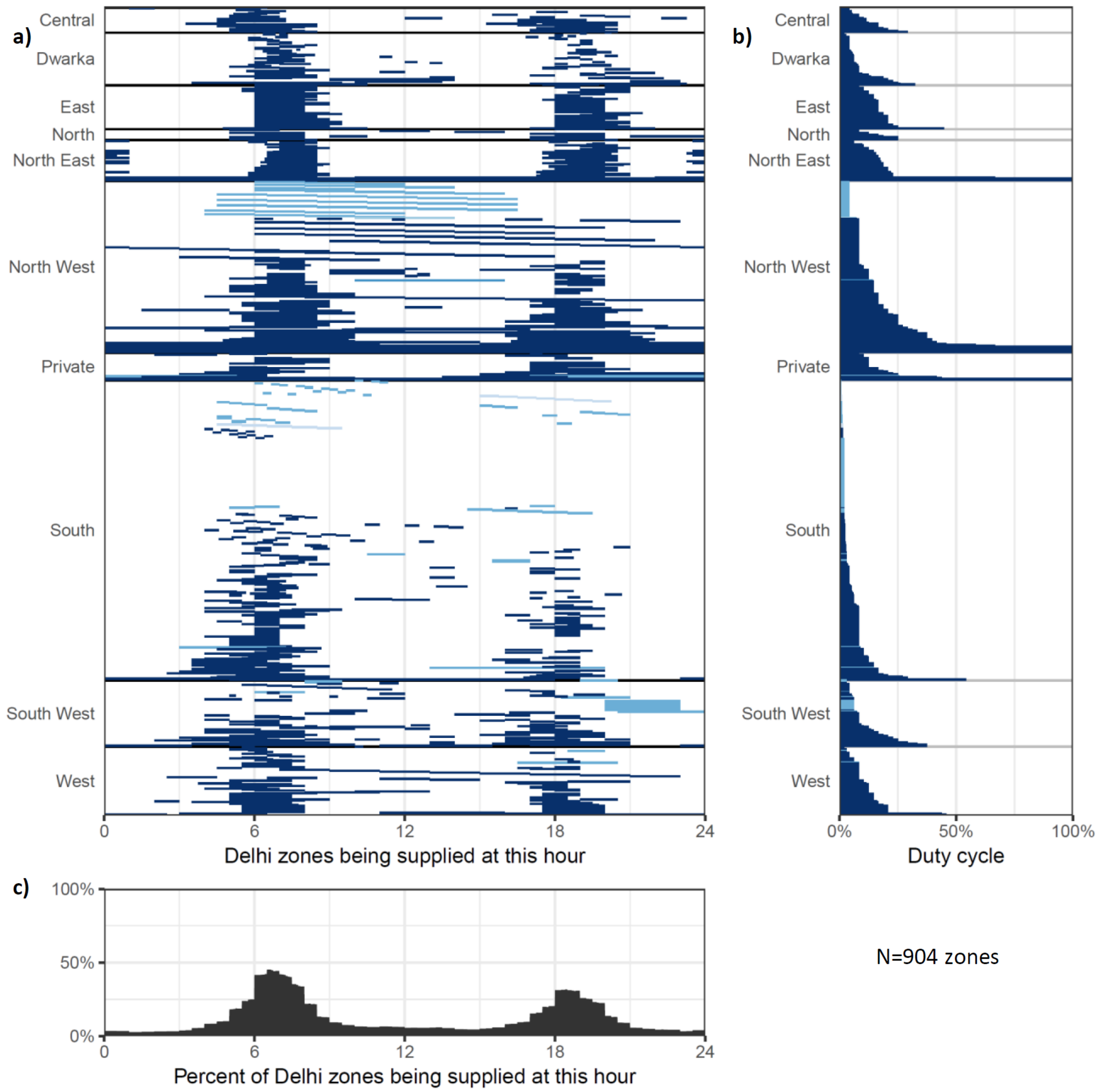

Figure A-1: **DJB's supply timing by city area.** The DJB describes schedules for 1196 different areas in Delhi; here they are segmented by administrative area. The d) shows the fraction of zones scheduled to be supplied daily (darkest blue), 4/7, 1/2, 3/7, and 1/3 days (lightest blue). From least frequently supplied to most (top to bottom in a & b), the supply schedule is shaded by time of the day in a). b) aggregates these to display the percent of DJB zones that are scheduled to be supplied at least a certain fraction (i.e., duty cycle; x-axis) of the time. Finally, c) shows the percent of zones that are being supplied throughout an average day. Data were aggregated from DJB (2014) and not weighted by population or supply volume.

its quality of life implications).

MNWS is responsible to pay 30% of the capital costs, excluding road restoration, and 100% of capital cost overruns (Delhi Jal Board, 2012g). Initial project budgets allocated 876.8 million INR (13.6$ USD) for the total costs, excluding road restoration (839.4 million INR) (Delhi Jal Board, 2012c, p.8). The total private capital contribution to the project was therefore 15.3%. This relatively small fraction of the total budget seems to support Sangameswaran's (2014) argument that private sector involvement does not substantially reduce the capital cost requirements of water supply improvement projects.

A.1.2 Dead volume

To assess the relative importance of dead volume losses in modern IWS, the dead volume losses were calculated for wealthy neighborhoods in two large Indian cities using their confidential hydraulic models. Larger pipes are often buried deeper and may not drain as quickly. Realistic estimates of dead volume losses should consider only a network's smaller pipes (perhaps $\leq 300mm$). The dead volume associated with IWS in these two example zones for pipes $\leq 300mm$ was 4% (15 l/connection) and 9% (50 l/connection) of customer demand per supply cycle (Fig A-2).

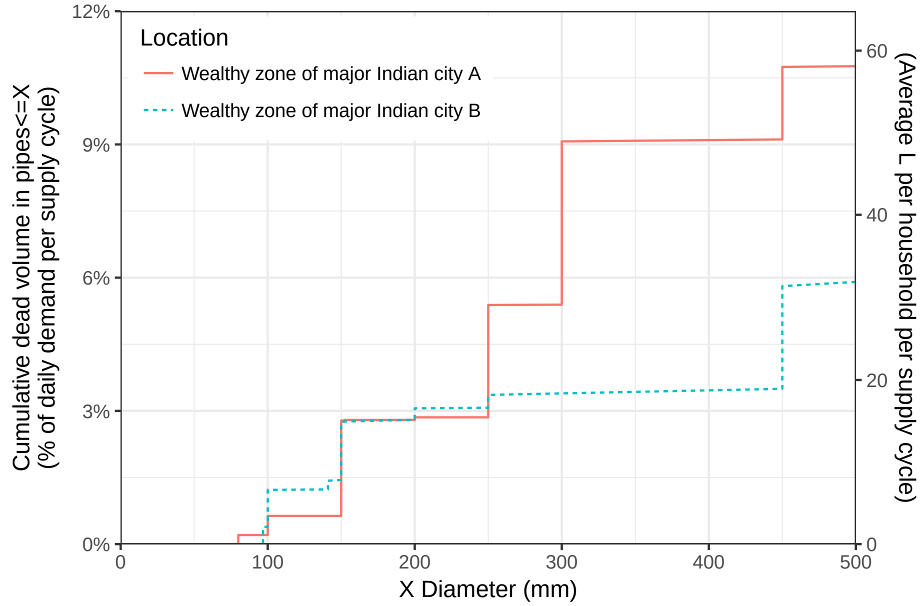

Figure A-2: **Dead volume in two zones of two large Indian cities.** The dead volume in pipes up to a certain diameter (x-axis) is shown as a percent of total customer demand (main y-axis), and converted to approximate liters per household per supply cycle (secondary y-axis)

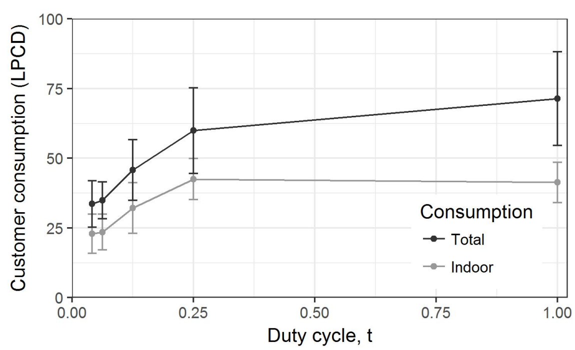

Figure A-3: Fan et al. (2014) surveyed 225 families in five rural villages in China, each with a different duty cycle. The supply period was one day in each village ($T = 1$day). Error bars represent one standard deviation in the metered consumption data from each village.

Appendix B

Supporting documentation for model validation

B.1 CWS to IWS conversion details

To include leakage, each reference network was run without modification (as a CWS) to determine its mean pressure head at all junctions ($\overline{H}$). Next, to prepare for the conversions below, in networks with multiple sources, reservoirs were connected to the network through check valves.

Then, at each node i, the demand was divided into leakage (assumed to be 15% of the initial nodal demand, $Q_{T,i}$) and customer demand (85% of the initial nodal demand). Finally, the mean pressure was used to determine the emitter coefficient at each demand node using Equation B.1:

$$
\begin{aligned}
Q_{L,i} &= C_i H_i^{\alpha} \\
\therefore C_i &\approx \frac{0.15 Q_{T,i}}{H_i^{\alpha}} \\
\therefore C_i &\approx \frac{0.15 Q_{T,i}}{\overline{H}^{\alpha}}
\end{aligned}
\tag{B.1}
$$

To match the proposed model, we took $\alpha = 1$.

The reference networks with added leakage were converted to an equivalent IWS

Table B.1: **IWS customer connection assumptions** used to convert CWS model to a volume-dependent IWS model.

Parameter	Value
Customer tank volume	1000 L
Customer tank height	1 m
Customer connection pipe length, L	10 m
Customer connection pipe diameter, D_i	15 mm
Customer connection pipe minor loss coefficient, $k_{m,i}$	8
Customer connection pipe roughness, C_{HW} [a] (Hazen-Williams C-factor)	110

[a] The BIN used Darcy-Weisbach friction equation with a constant roughness of 0.0025mm. Accordingly in BIN, the customer connection pipe was taken to have a roughness of 0.0025mm.

using the methodology of Macke and Batterman (2001). Households were assumed to consume 1000L/day, use cylindrical tanks 1m in height for water storage (connected through a check-valve), and connect to the network junction through a pipe with length $L = 10m$, diameter $D_i = 15mm$, C-factor roughness of $C_{HW} = 110$, and minor loss coefficient of $k_{m,i} = 8$ (Table B.1). Most CWS models aggregate multiple customers into a single node. In order to model VDD without adding one tank for every customer, we instead add one tank for every node. The tank must be connected through a pipe whose behavior mimics the aggregate effect of the customer pipes in parallel.

For a given node with daily demand V_i, where the average customer demand is V_D, then the number of equivalent customer connections, N, is:

$$N = \frac{V_i}{V_D} \tag{B.2}$$

Assuming the Hazen-Williams pressure loss formula applies to customer connections in parallel, then the pressure loss across the equivalent pipe, ΔH_N, should be equal to the pressure loss at each customer's connection, ΔH_i:

$$\begin{aligned}
\Delta H_N &= \Delta H_i \\
\therefore \frac{10.67(NQ_i)^{1.852}L_i}{C_{HW}^{1.852}D_N^{4.8704}} &= \frac{10.67Q_i^{1.852}L_i}{C_{HW}^{1.852}D_i^{4.8704}} \\
\therefore \frac{D_N}{D_i} &= N^{0.380}
\end{aligned} \tag{B.3}$$

Using this equivalent diameter (D_N), the equivalent minor loss coefficient, $k_{m,N}$, should be chosen so that the minor losses at an average customer connection, $\Delta H_{m,i}$, is equivalent to the minor losses across the equivalent pipe, $\Delta H_{m,N}$:

$$\begin{aligned}
\Delta H_{m,N} &= \Delta H_{m,i} \\
\therefore k_{m,N}\frac{V_N^2}{2g} &= k_{m,i}\frac{V_i^2}{2g} \\
\therefore k_{m,N}\frac{8N^2Q_i^2}{g\pi^2D_N^4} &= k_{m,i}\frac{8Q_i^2}{g\pi^2D_i^4} \\
\therefore \frac{k_{m,N}}{k_{m,i}} &= \left(\frac{D_N}{D_i}\right)^4\frac{1}{N^2}
\end{aligned} \tag{B.4}$$

Substituting Eq B.3 in B.4:

$$\therefore \frac{k_{m,N}}{k_{m,i}} = \left(N^{0.380}\right)^4\frac{1}{N^2} = N^{-0.479} \tag{B.5}$$

Finally, in networks with multiple sources, reservoirs were connected to the network through check valves.

B.2 Additional figures

Figs B-1 and B-2 further detail the accuracy of the leak and customer modules of the hydraulic model.

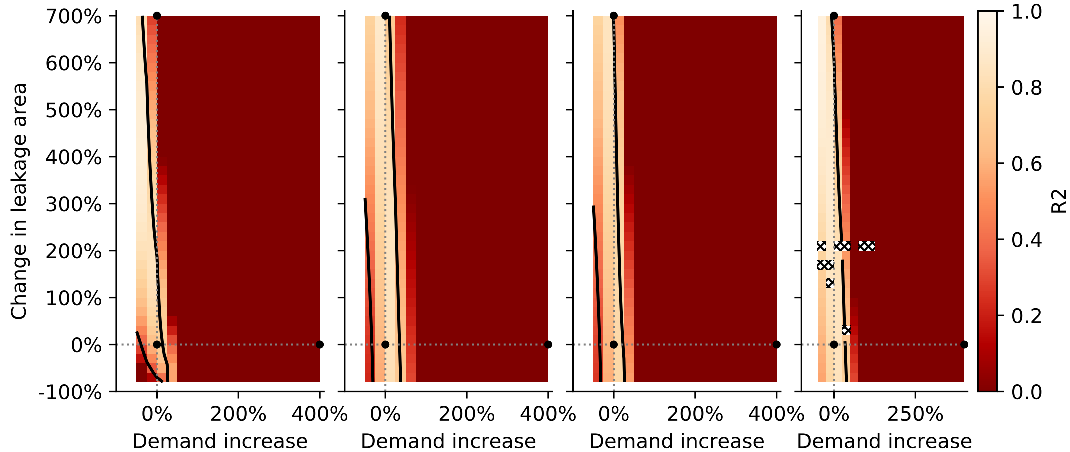

Figure B-1: **The leakage model's fit with VDD simulations.** For each reference network shading shows the R-squared ('R2') fit between the model's prediction of the daily volume received by customers and VDD simulations as demands and EOA vary in the range of [-50%,+400%] and [-80%,+700%] of their initial values, respectively. All negative values of R-squared are shown as the same shade of dark red. The proposed model was calibrated at 0%,0%. The R^2 value 'NA' (checkerboard shading) indicates the numerical simulation was unstable (only in BIN).

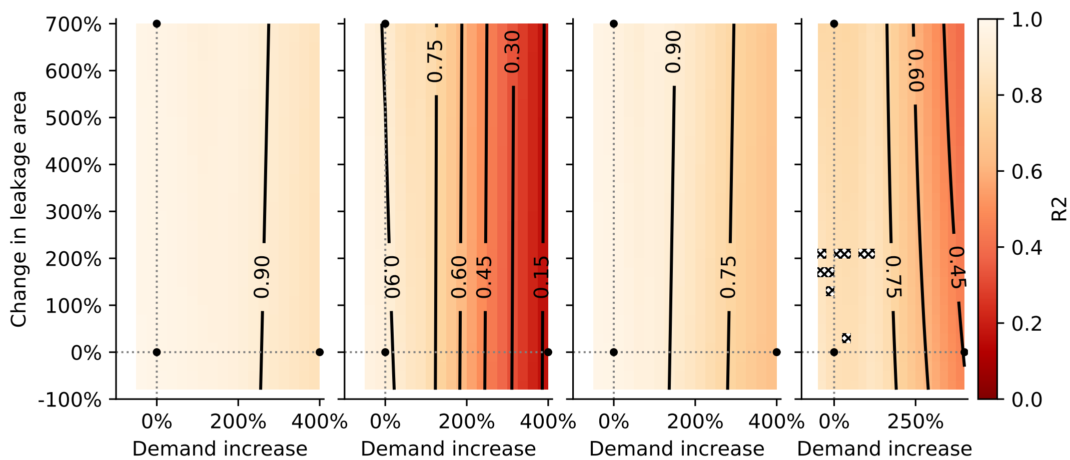

Figure B-2: **The customer model's fit with VDD simulations.** For each reference network shading and contour lines show the R-squared ('R2') fit between the model's prediction of the daily volume received by customers and VDD simulations as demands and EOA vary in the range of [-50%,+400%] and [-80%,+700%] of their initial values, respectively. The proposed model was calibrated at 0%,0%. The R^2 value 'NA' (checkerboard shading) indicates the numerical simulation was unstable (only in BIN).

Appendix C

Additional optimization of IWS

C.1 Optimal pressure analysis

To explore the maximization of gross margin dollars in an IWS (Eq 5.9), consider first the case of satisfied IWS (i.e., $th^{\phi} \geq \gamma_S$).

C.1.1 Satisfied IWS

In the satisfied case of Eq 5.8:

$$\Psi = R(1-u)V_D - CV_D - CV_{LC}ath^{\alpha} \qquad : th^{\phi} \geq \gamma_S \tag{C.1}$$

While revenue is independent of duty cycle and supply pressure, costs increase with respect to both (Eq C.1). Accordingly, the gross margin will be maximized when th^{α} is minimized (so long as the system continues to be satisfied). Therefore, the gross-margin-maximizing strategy for a satisfied IWS is to reduce the duty cycle and/or supply pressure until the system becomes marginally satisfied (i.e., $th^{\phi} = \gamma_S$).

The line SC in Fig 5-1b highlights this phenomenon with respect to duty cycle. Along SC, all customers are all satisfied; so moving along the line SC has no effect on Rational Water's revenue. However, moving from S to C requires more water to be input into the system, which increases Rational Water's costs. Accordingly, in the absence of performance penalties, Rational Water has no direct financial incentives to supply water beyond what is required to satisfy customers.

Technically a marginally-satisfied IWS ($th^{\phi} = \gamma_S$) is both satisfied and unsatisfied. Therefore, since the optimal strategy for a satisfied IWS is to be marginally satisfied, the optimal strategy for an unsatisfied IWS will also be the globally-optimal strategy.

C.1.2 Unsatisfied IWS

In an unsatisfied IWS, providing more water to the system increases the total costs, but also increases the total revenues. To understand the trade offs, consider the unsatisfied case of Eq 5.8:

$$\Psi = t\left((R(1-u)-C)h^{\phi}\frac{V_D}{\gamma_S} - CV_{LC}ah^{\alpha}\right) \qquad : th^{\phi} \leq \gamma_S \tag{C.2}$$

$$= th^{\phi}\left((R(1-u)-C)\frac{V_D}{\gamma_S} - CV_{LC}ah^{\alpha-\phi}\right) \qquad : th^{\phi} \leq \gamma_S \tag{C.3}$$

Rational Water's gross margin dollars (Ψ) will increase linearly with increased duty cycle (t) if the bracketed term following t is positive (Eq C.2). Conversely, if that bracketed term is negative, Rational Water's gross margin will be also, and is therefore maximized when $t = 0$ (i.e., no water is input into the system). Rational Water's objective function is, therefore, separable (Eq C.2); for any given value of h, Rational Water's gross margin is linearly scaled by t. Since gross margin is linear with the duty cycle, its maximum will occur at one or more constraints on the duty cycle. For an unsatisfied IWS, there are four constraints on the duty cycle: the duty cycle cannot be negative; the duty cycle cannot exceed one (CWS); the system must remain at most marginally satisfied; and t cannot be increased past the point when the utility has distributed all of its water. Algebraically, these are equivalent to:

$$t \geq 0 \tag{C.4}$$

$$t \leq 1 \tag{C.5}$$

$$th^{\phi} \leq \gamma_S \tag{C.6}$$

$$v_P \leq 1 \tag{C.7}$$

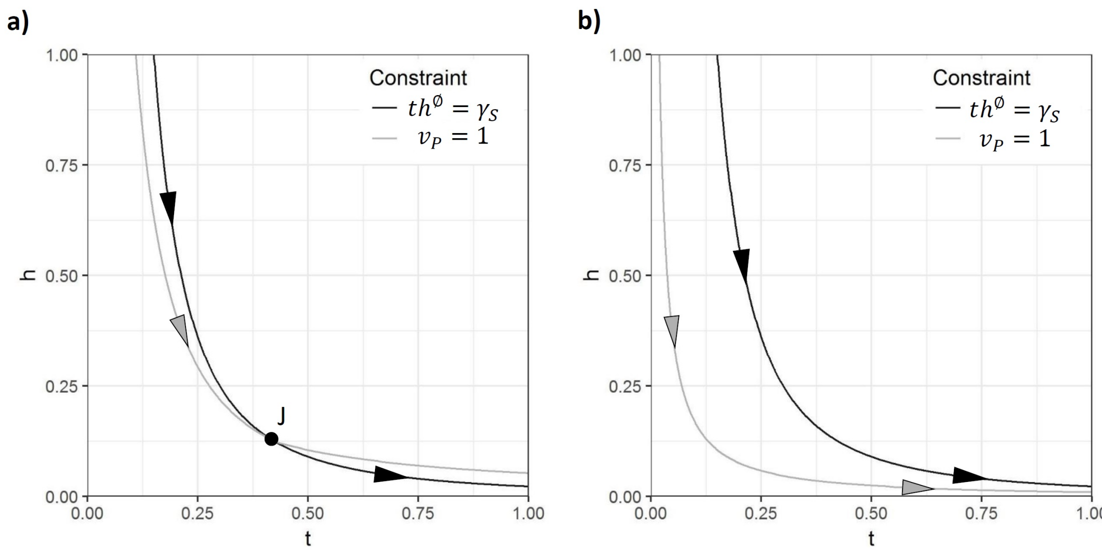

Figure C-1: **The solution space for maximizing gross margin** in two systems with $\phi = 0.5$, $\alpha = 1$, $\gamma_S = 0.15$, and $v_D = 0.8$. The operating point that maximizes gross margin dollars must lie to the lower left of both constraint curves. The left subfigure plots a network OA with $a = 19$, while the right plots OD with $a = 233$. To Scale.

To determine the globally-optimal value of (t, h), this section will explore along each constraint individually and then in combination. As an example, consider two systems (OA and OD), both with $\phi = 0.5$, $\alpha = 1$, $\gamma_S = 0.15$, $v_D = 0.8$. Systems OA and OD (Figs C-1a and b, respectively) have $a = 19$ and $a = 233$, respectively. Their constraints bound the feasible region in the lower left portion of each figure.

Individual constraints: When Constraint C.4 is tight (i.e., along the line $t = 0$), $\Psi = 0$ so this potential solution is neglected. When Constraint C.5 is tight (i.e., along $t = 1$), the Eq C.2 is non-linear with respect to h and has an optimum value; specifically:

$$\Psi = t\left((R(1-u) - C)\frac{V_D}{\gamma_S}h^{\phi} - CV_{LC}ah^{\alpha}\right) \qquad : th^{\phi} \leq \gamma_S$$

$$\therefore \frac{\partial \Psi}{\partial h} = t\left(\phi h^{\phi-1}\left[(R(1-u) - C)\frac{V_D}{\gamma_S}\right] - \alpha h^{\alpha-1}CV_{LC}a\right) \qquad : th^{\phi} \leq \gamma_S \qquad \text{(C.8)}$$

Setting the partial derivative in Eq C.8 to zero to find the value of h which maximizes gross margin dollars yields:

$$\begin{aligned}
\frac{\partial \Psi}{\partial h} &= 0 \\
\therefore \phi \left[(R(1-u) - C) \frac{V_D}{\gamma_S} \right] &= \alpha h_{\text{optimal}}^{\alpha-\phi} C V_{LC} a & &: th^{\phi} \leq \gamma_S \\
\therefore h_{\text{optimal}}^{\alpha-\phi} &= \left(\frac{R}{C} - \frac{1-np}{1-n} \right) \frac{\phi}{\alpha a \gamma_S} & &: th^{\phi} \leq \gamma_S \qquad \text{(C.9)}
\end{aligned}$$

Therefore, in the absence of additional constraints, the optimal pressure head is independent of the duty cycle and given by Eq C.9. When $\alpha = \phi$, the optimal solution is simply $th^{\phi} = \gamma_S$ and there are no relative advantages between pressure and duty cycle (Eq 5.8).

When Constraint C.6 is tight (i.e., $th^{\phi} = \gamma_S$), assuming $\alpha > \phi$ (as expected), Rational Water's gross margin will increase as h decreases (Eq C.3). Since the value of th^{ϕ} is fixed, reducing h implies increasing t. This strategy will continue to increase the gross margin until another constraint becomes tight (probably $t \leq 1$). Therefore, for any marginally satisfied system, when $\alpha > \phi$, as expected, revenue is maximized by decreasing the supply pressure and increasing the duty cycle until another constraint is met (e.g., $t = 1$). Increasing the gross margin by decreasing pressure in a marginally satisfied IWS is depicted as moving down and to the right along the black constraint curves in Figs C-1a and b.

When Constraint C.7 is tight (i.e., $v_P = 1$ or equivalently $V_P = V_T$), variable costs are fixed. Accordingly, gross margin is maximized when the ratio of leaks to water received by customers is minimized (from Eq 3.4):

$$\begin{aligned}
\frac{v_R}{v_L} &= \frac{v_D th^{\phi}}{\gamma_S v_{LC} a t h^{\alpha}} & &: th^{\phi} \leq \gamma_S \\
&= \frac{v_D}{v_{LC}} \left(a h^{\alpha-\phi} \right) & &: th^{\phi} \leq \gamma_S \\
\therefore \frac{v_R}{v_L} &\propto h^{\alpha-\phi} & &: th^{\phi} \leq \gamma_S \qquad \text{(C.10)}
\end{aligned}$$

Provided $\alpha > \phi$ (as expected), the proportion of water received by customers instead of leaks will increase with decreasing pressure in an unsatisfied IWS (Eq C.10). While decreasing h to reduce leakage, the water that is no longer leaked can be delivered to customers by increasing t (Eq 3.4), which increases Rational Water's gross margin. This strategy applies until one of the other constraints is met. Specifically, Rational Water should reduce its pressure and increase its duty cycle until either $th^\phi = \gamma_S$ or $t = 1$. Increasing the gross margin by decreasing pressure for a system that inputs all of its available water is depicted as moving down and to the right along the gray constraint curves in Figs C-1a and b. This strategy of low pressure supply is not an artifact of the simplified model used in this section; it more generally applies to any flat, tree-structured network under the expected range of exponent values (see Section C.2).

Combined constraints: Along both Constraints C.6 and C.7 the gross margin is maximized by decreasing h and increasing t. Independent of which constraint is tight, therefore, the optimal gross margin will occur at $t = 1$ (i.e., when Constraint C.5 is tight). Visually, this is equivalent to following the constraint lines in Figs C-1a and b until one arrives at $t = 1$.

Eq C.9 derived the optimal value of h along the line $t = 1$. When that value of h is less than both Constraints C.6 and C.7 at $t = 1$, it will be the globally-optimal value of h. Otherwise, the optimal value of h will lie at the lower of the two Constraints C.6 and C.7 at $t = 1$. These two intersection points are derived below.

At $t = 1$, Constraint C.6 simplifies to:

$$\begin{aligned} & th^\phi \le \gamma_S && : t = 1 \\ & \therefore h \le \gamma_S^{1/\phi} && \text{(C.11)} \end{aligned}$$

Similarly, at $t = 1$, Constraint C.7 simplifies, but remains implicit with respect to h:

$$\begin{aligned} & \frac{v_D}{\gamma_S} th^\phi + v_{LC} ath^\alpha \le 1 && : t = 1 \\ \therefore\ & \frac{1 - np}{\gamma_S} h^\phi + npah^\alpha \le 1 && \text{(C.12)} \end{aligned}$$

The gross-margin-maximizing operating point lies along $t = 1$ and combines these constraints and the unconstrained optimal h_{optimal} from Eq C.9:

$$h_{\text{optimal}} = \min \left[\left(\left(\frac{R}{C} - \frac{1-np}{1-n} \right) \frac{\phi}{\alpha a \gamma_S} \right)^{1/(\alpha-\phi)}, \gamma_S^{1/\phi}, h_P \right] \tag{C.13}$$

$$\text{where: } (1-np)\frac{h_P^{\phi}}{\gamma_S} + npah_P^{\alpha} = 1 \tag{C.14}$$

Where h_P is implicitly defined by Eq C.14.

For low leakage systems, the unsatisfied constraint (C.11) will constrain the system (e.g., Fig C-1a). However, at a critically large value of EOA, a_{crit}, the water availability constraint (C.12) is instead limiting (e.g., Fig C-1b). Substituting $h^{\phi} = \gamma_S$ from Constraint C.11, into Constraint C.12 at equality, yields:

$$\frac{1-np}{\gamma_S}\gamma_S + npa_{\text{crit}}\gamma_S^{\alpha/\phi} = 1$$

$$\therefore a_{\text{crit}}\gamma_S^{\alpha/\phi} = 1$$

$$\therefore a_{\text{crit}} = \gamma_S^{-\alpha/\phi} \tag{C.15}$$

Therefore, for $a > a_{\text{crit}}$, the water availability constraint is more stringent than the unsatisfied constraint, and so the system cannot be satisfied, even at $t = 1$.

To further understand these constraints and their implications for practical systems, a graphical example is presented below.

C.1.3 Graphical example of GM maximization

For any system, the optimal duty cycle is $t = 1$ and the optimal supply pressure is given by Eq C.13. Where the optimal pressure is given by the first term in Eq C.13, it will depend on R and C and is therefore difficult to explore graphically. Instead, this subsection will assume that R is set arbitrarily high enough so that one of the other two terms in Eq C.13 sets the optimal pressure.

Consider again the two networks OA and OD (initially depicted in Fig C-1a and b), where $\gamma_S = 0.15$, $\phi = 0.5$, $\alpha = 1$, $v_D = 0.8$, and $u = 0.3$ (depicted to scale in Fig C-2). Networks OA and OD have values of a equal to 19 and 233, respectively.

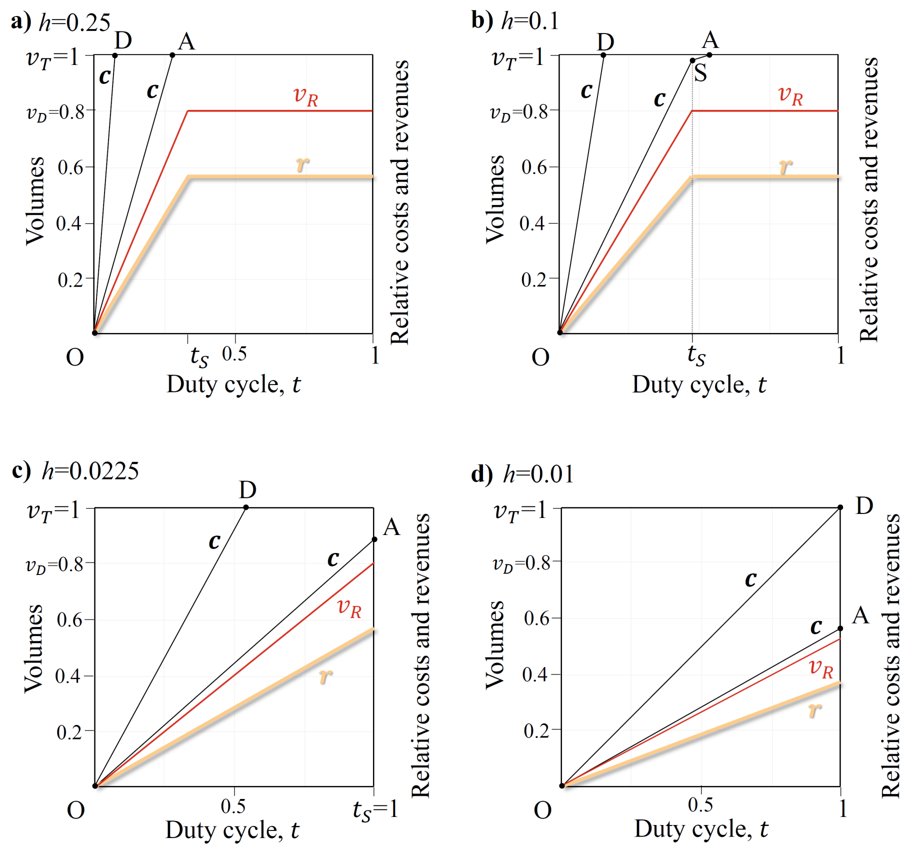

Figure C-2: **GM-optimal supply pressure.** a), b), c), and d), depict networks OD and OA under decreasing pressures $h \in \{0.25, 0.1, 0.0225, 0.01\}$, respectively. For network OD, operating at point D, revenue increases with decreasing h until $h = 0.01$. For network OA, operating at A, revenue is maximized in b) and c) and gross margin is maximized in c). Input volumes and normalized costs (thin black lines), revenues (thick light orange lines), and volumes delivered to customers (medium weight red lines) are shown at each pressure. To scale.

Whenever both networks are unsatisfied IWS, the revenue of each will be maximized by distributing all of the available water (e.g., operating at points D and A in Fig C-2a, where $h = 0.25$). To avoid the trivial scenario of no water input into the networks, assume that the price of water is set high enough to incentivize full supply. In this case, points A and D also maximize the gross margin for an unsatisfied IWS at a fixed pressure.

Network OA: As pressure is decreased, again assuming $\alpha > \phi$ as expected, the bracketed term in Eq C.2 will increase. For a given volume of distributed water, therefore, the gross margin dollars will increase with decreasing pressure. As pressure decreases (compensated for by longer duty cycles), the system OA becomes satisfied (at $h = 0.125$, not shown). Revenues then remain constant as h continues to decrease until $t_S = 1$ (Figs C-2b and c). While revenue is constant between $h = 0.125$ and $h = 0.0225$ (when t_S becomes 1), along the line segment SA, the gross margin is maximized by operating at point S instead of A.

As pressure (h) continues to decrease, t_S increases and at the point where $t_S = 1$ (Fig C-2c), the points S and A join and point A is a marginally satisfied IWS (i.e., $th^{\phi} = \gamma_S$). At pressures lower than $h = 0.0225$, the duty cycle cannot be increased any further to compensate for the lower pressures. Thus, for $h < 0.0225$, customers in system OA become unsatisfied, and the system's revenues and gross margin dollars decrease (Fig C-2d). Therefore, for system OA, gross margin is maximized at $h = 0.0225$ and $t = 1$ (point A in Fig C-2c).

Network OD: Due to the higher EOA in the network OD, it can never be satisfied (Fig C-1b). The gross margin is maximized when the pressure is reduced until the system can be operated as a (very) low pressure, unsatisfied, CWS (Fig C-2d). Using the starting assumption that R is set arbitrarily high, $h = 0.01$ is the globally optimal pressure for maximizing the gross margin of system OD.

C.2 Non-linear extension of optimal pressure analysis

This section supplements the first-order analysis of the previous section by considering the role of pipe friction in a flat, simple, tree-structured network. The network is assumed to be an unsatisfied IWS and therefore demand is modeled as pressure dependent demand (PDD, Equation C.16). Leaks continue to be modeled as pressure-dependent leaks (PDL, Equation 3.2).

If the pressure head (H) drops below a required minimum (H_{min}), the instantaneous flow rate demanded by customers (Q_D) cannot be fully supplied. Wagner et al. (1988) proposed that when pressure dropped below a known minimum pressure, flow to customers could be modeled as flow out of an orifice. The flow rate received by customers (Q_R), would therefore be:

$$Q_R = \begin{cases} Q_D & H \geq H_{min} \\ Q_D(\frac{H}{H_{min}})^{\phi} & 0 < H < H_{min} \\ 0 & H \leq 0 \end{cases} \tag{C.16}$$

where Wagner et al. (1988) took $\phi = 0.5$ as in the orifice equation. What this model attempts to capture is that if pressure is low enough, customers behave like an orifice emitter whose flow rate is dependent on pressure, not on their desires.

Making this orifice model explicit, consider a customer to have an equivalent demand orifice area (A_D) which is a constant for a given network:

$$Q_R = \begin{cases} Q_D & : H^{\phi} > \frac{Q_D}{A_D} \\ A_D H^{\phi} & : 0 \leq H^{\phi} \leq \frac{Q_D}{A_D} \\ 0 & : H < 0 \end{cases} \tag{C.17}$$

Non-linear pressure losses along pipes are modeled with the Hazen-Williams equation:

$$\Delta H = R_k Q_k^{\xi} \tag{C.18}$$

where ΔH is pressure head loss (m) along pipe k, R_k is the Hazen-Williams "C-factor", Q_k the pipe's flow rate (m^3/s), and ξ the flow exponent: 1.852 in the Hazen-Williams equation. Other friction equations have $\xi \in [1.85, 2.0]$.

Because the model includes pipe friction, the volume of leakage depends on the relative locations of leaks and demand within the network. Three tree configurations are considered analytically and are depicted in Fig. C-3.

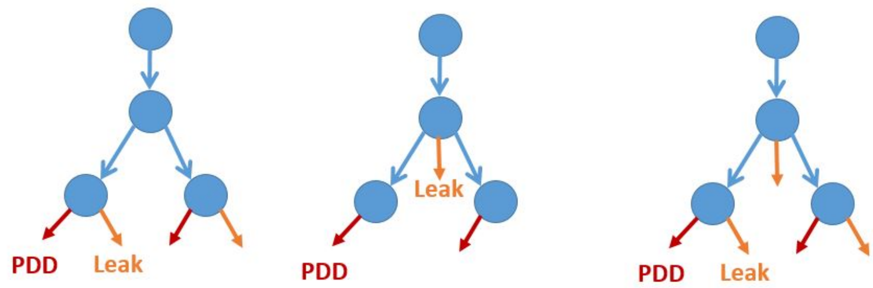

Figure C-3: **Relative locations of leaks and demand in a tree-structured IWS.** Pipe flows are shown with blue arrows and three topologies are considered:one where PDD [red arrow] and leaks (PDL) [orange arrow] are co-located at leaf nodes [left], one where PDL are upstream of PDD [center], and one where PDL are located at all nodes [right].

Rearranging Equations 3.2:

$$
\begin{aligned}
Q_L &= C_d A[2gH]^\alpha && : H_C = 0 \\
\therefore Q_L &= A_L H^\alpha && : A_L = C_d A(2g)^\alpha
\end{aligned}
\tag{C.19}
$$

where A_L is a fixed constant associated with the network's EOA. Similarly, assuming unsatisfied IWS simplifies Equation C.17 to:

$$
Q_r = A_D H^\phi \qquad : th^\phi \leq \gamma_S \tag{C.20}
$$

C.2.1 Demand and leakage at leaf nodes only

Because the system is assumed to be unsatisfied, the ratio of volumes is a linear multiple of the ratio of flow rates. The latter is algebraically simpler and considered herein. In the case where PDL and PDD occur only at leaf nodes, their ratio is given by the ratio of Equations C.19 and C.20):

$$
\begin{aligned}
\frac{Q_L}{Q_r} &= \frac{A_L H^\alpha}{A_D H^\phi} \\
\therefore \frac{Q_L}{Q_r} &\propto H^{\alpha-\phi}
\end{aligned}
\tag{C.21}
$$

Accordingly, so long as $\alpha > \phi$, as expected, NRW is reduced by supplying water at lower pressure (Equation C.21).

C.2.2 Leaf demand and upstream leakage:

When PDL is moved upstream, the PDL:PDD ratio is given by accounting for the higher upstream pressure caused by pipe friction. Taking H to be the pressure at the leaf, and pressure upstream to be H_u, then combining Equations C.18 and C.20:

$$
\begin{aligned}
H_u &= H + \Delta H \\
&= H + R_k Q_k^{\xi} \\
&= H + R_k (A_D H^{\phi})^{\xi} \\
\therefore \frac{Q_L}{Q_D} &= \frac{A_L (H + R_k A_D^{\xi} H^{\xi\phi})^{\alpha}}{2 A_D H^{\phi}} \\
&= \frac{A_L}{2A_D} (H^{1-\phi/\alpha} + R_k A_D^{\xi} H^{\xi\phi - \phi/\alpha})^{\alpha} \\
\therefore \frac{\partial Q_L / Q_D}{\partial H} &> 0 \\
&\iff (1 - \phi/\alpha) H^{-\phi/\alpha} + (\xi\phi - \phi/\alpha) R_k A_D^{\xi} H^{\xi\phi - \phi/\alpha - 1} > 0 \\
\therefore \alpha > \max(\phi, 1/\xi) &\rightarrow \frac{\partial Q_L / Q_D}{\partial H} > 0
\end{aligned}
\tag{C.22}
$$

So for this network topology, low pressure supply also minimizes NRW provided $\alpha > \max(\phi, 1/\xi)$.

C.2.3 Leaf demand and distributed leakage:

For the complicated case where leaks are at upstream nodes and at leaf nodes, the pipe pressure loss depends on the downstream demand and leakage. Taking upstream leakage to have a coefficient of A_{Lu} and downstream to have a coefficient of A_{Ld}:

$$\begin{aligned} H_u &= H + R_k(A_D H^{\phi} + A_{Ld} H^{\alpha})^{\xi} \\ \therefore \frac{Q_L}{Q_D} &= \frac{2A_{Ld}H^{\alpha} + A_{Lu}\left(H + R_k(A_D H^{\phi} + A_{Ld}H^{\alpha})^{\xi}\right)^{\alpha}}{2A_D H^{\phi}} \\ &= \frac{A_{Ld}}{A_D} H^{\alpha-\phi} + \frac{A_{Lu}}{2A_D}\left(H^{1-\phi/\alpha} + R_k(A_D H^{\phi-\phi/\alpha/\xi} + A_{Ld}H^{\alpha-\phi/\alpha/\xi})^{\xi}\right)^{\alpha} \end{aligned} \tag{C.23}$$

The first term is precisely the same as Equation C.21 and suggests NRW increases with increased pressure, provided $\alpha > \phi$. Similarly, the second term grows with increasing H provided:

$$\begin{aligned} &(1-\phi/\alpha)H^{-\phi/\alpha} + R_k\xi(A_D H^{\phi-\phi/\alpha/\xi} + A_{Ld}H^{\alpha-\phi/\alpha/\xi})^{\xi-1} \\ &\qquad \times \left[(\phi - \phi/\alpha/\xi)A_D H^{\phi-\phi/\alpha/\xi-1} + (\alpha - \frac{\phi}{\alpha\xi})A_{Ld}H^{\alpha-\phi/\alpha/\xi-1}\right] > 0 \end{aligned} \tag{C.24}$$

which is true when $\alpha > \max(\phi, 1/\xi)$ and $\xi > 1$. These conditions are sufficient to ensure that NRW is minimized by low pressure supply in this case and in the previous simpler cases. While the first condition ($\alpha > \max(\phi, 1/\xi)$) is not strictly guaranteed to be met, for reasonable parameter estimates, it is expected that these conditions will be met and that low pressure supply will minimize the ratio of leaks to customer demand.

C.3 An alternative assumption for penalty weights

The effect of assuming $h_X^{\alpha-\phi} = 0.707$ is shown in Fig C-4.

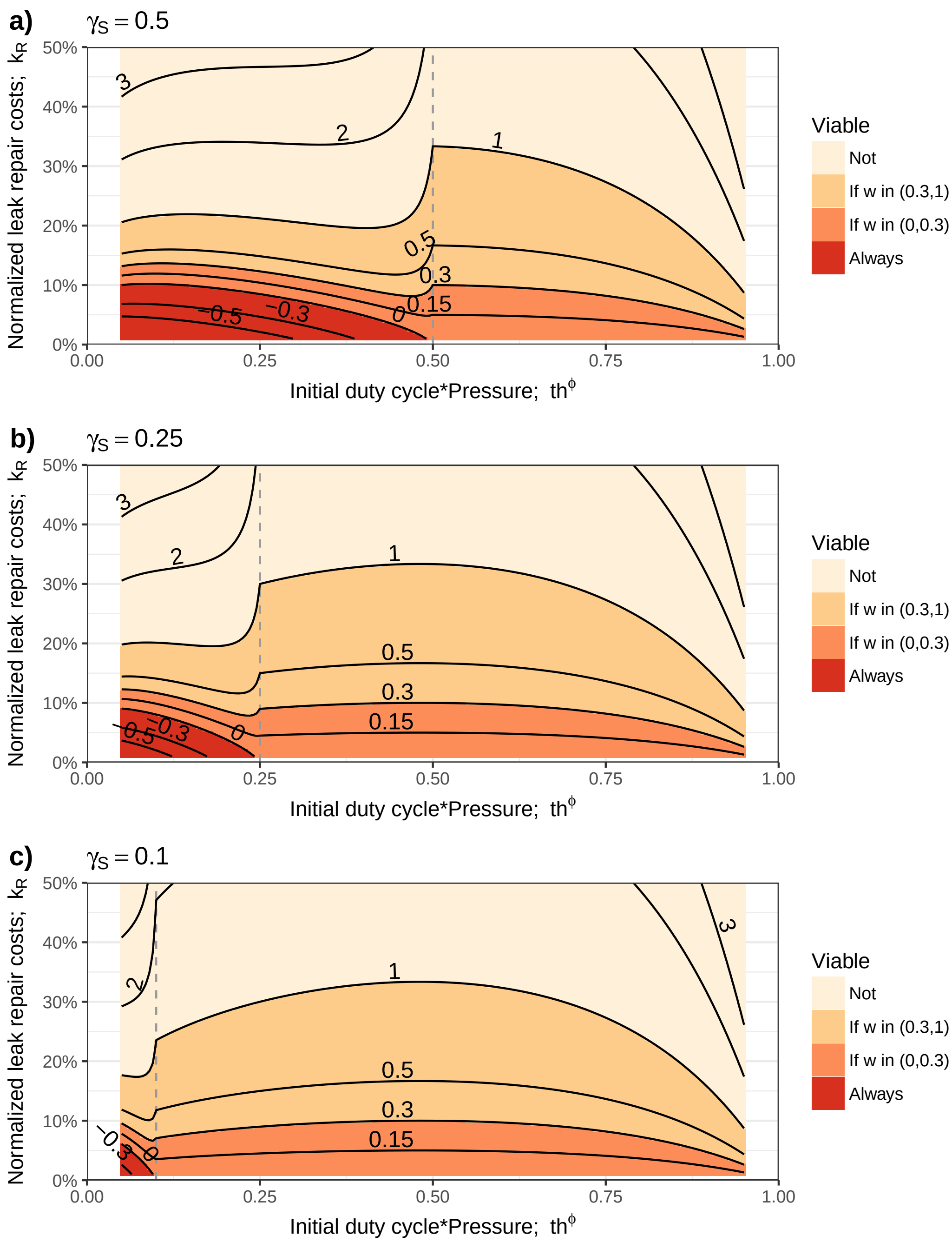

Figure C-4: **Low-pressure, linear penalty weights required for Ψ-neutral CWS.** Contours show the minimum weight required, w, for the transition to high-pressure CWS ($t = h = 1$) to improve a utility's gross margin given a starting point th^ϕ (x-axis) and cost of repairing 50% of leaks (k_R, y-axis). This plot assumes $h_X^{\alpha-\phi} = 0.707$, which induces the instability as $th^\phi \to 1$. Fill distinguishes how reasonable the penalty weight is: $w < 0$ none-needed (dark red); $w \in (0, 0.3)$, typical (orange); $w \in (0.3, 1)$ unusually larger (light orange); and $w > 1$ not-reasonable (off-white). Plots a), b), and c) show $\gamma_S \in \{0.5, 0.25, 0.1\}$. The penalty structure is $P(t, h) = w(1 - th^\phi)RV_T(1 - n_C)$. To the right of the vertical, gray dashed lines, the system is satisfied ($th^\phi \geq \gamma_S$).

C.4 Minimization of the IWA's leakage metric

For a fixed supply pressure, any unsatisfied subnetwork will leak a constant fraction of its input volume (Equation 4.1). The IWA's new leakage metric accounts for the population-adjusted duration of time that the system is pressurized. Therefore, for two subnetworks with leakage rates of Q_{L1} and Q_{L2}, pressurized for a duration of t_1 and t_2, and with populations P_1 and P_2, the total leakage rate is calculated as (Alegre et al., 2016, p.221):

$$Q_{\text{IWA}} = (t_1 Q_{L1} + t_2 Q_{L2}) \frac{P_1 + P_2}{t_1 P_1 + t_2 P_2} \tag{C.25}$$

For each unsatisfied IWS, its total input volume scales with its duty cycle, and so for a fixed available volume,

$$\begin{aligned} V_T &= t_1 Q_{T1} + t_2 Q_{T2} \\ \therefore t_2 &= \frac{V_T - Q_1 t_1}{Q_2} \end{aligned} \tag{C.26}$$

Substituting Equation C.25 into C.26, and taking the partial derivative:

$$\begin{aligned} \therefore Q_{\text{IWA}} = (P_1 + P_2) \quad & \frac{t_1 Q_{L1} + (V_T/Q_2 - tQ_1/Q_2) Q_{L2}}{t_1 P_1 + (V_T/Q_2 - tQ_1/Q_2) P_2} \\ \therefore Q_{\text{IWA}} = (P_1 + P_2) \quad & \frac{t_1 (Q_{L1} - Q_{L2} Q_1/Q_2) + Q_{L2} V_T/Q_2}{t_1 (P_1 - P_2 Q_1/Q_2) + P_2 V_T/Q_2} \\ \therefore \frac{\partial Q_{\text{IWA}}}{\partial t_1} = (P_1 + P_2) \quad & \frac{(Q_{L1} - Q_{L2} Q_1/Q_2)\,(t_1 (P_1 - P_2 Q_1/Q_2) + P_2 V_T/Q_2)}{(t_1 (P_1 - P_2 Q_1/Q_2) + P_2 V_T/Q_2)^2} \\ & - (P_1 + P_2) \frac{(P_1 - P_2 Q_1/Q_2)\,(t_1 (Q_{L1} - Q_{L2} Q_1/Q_2) + Q_{L2} V_T/Q_2)}{(t_1 (P_1 - P_2 Q_1/Q_2) + P_2 V_T/Q_2)^2} \end{aligned} \tag{C.27}$$

Setting the partial derivative greater than zero implies:

$$
\begin{aligned}
&\therefore \frac{\partial Q_{\text{IWA}}}{\partial t_1} > 0 \\
&\rightarrow (Q_{L1} - Q_{L2}Q_1/Q_2) \quad && (t_1(P_1 - P_2Q_1/Q_2) + P_2V_T/Q_2) \\
& && > (P_1 - P_2Q_1/Q_2)\,(t_1(Q_{L1} - Q_{L2}Q_1/Q_2) + Q_{L2}V_T/Q_2) \\
&\therefore \frac{P_2V_T/Q_2}{(P_1 - P_2Q_1/Q_2)} && > \frac{Q_{L2}V_T/Q_2}{(Q_{L1} - Q_{L2}Q_1/Q_2)} \\
&\therefore \frac{1}{P_1/P_2 - Q_1/Q_2} && > \frac{1}{Q_{L1}/Q_{L2} - Q_1/Q_2} \\
&\therefore P_1/P_2 < Q_{L1}/Q_{L2} \\
&\therefore \frac{Q_{L1}}{P_1} > \frac{Q_{L2}}{P_2} && \qquad\qquad\qquad\qquad\qquad\qquad\qquad\qquad \text{(C.28)}
\end{aligned}
$$

Therefore, the IWA leakage metric increases with respect to t_1 when the per capita leakage in subnetwork 1 is larger than in subnetwork 2. In such cases, therefore, Rational Water would maximize t_2, and provide no water to subnetwork 1. Conversely, when the per capita leakage rate is lower in subnetwork 1, Rational Water should supply only it (i.e., maximize t_1).

While the new IWS leakage metric does account for population which will, all else being equal, improve the degree to which the metric reflects equity, it still measures the system's average behavior and does not actually measure equity. Moreover, the metric itself encourages utilities like Rational Water to provide water exclusively to some zones at the expense of others.

Appendix D

Example calculations for Chapter 6

D.1 Varanasi

Required reduction in EOA is given by Eq 11. Varanasi reported $n = 0.3$, $H^0 = 3m$, & $t^0 = 7$. The target system goals are $t^* = 23.75$ and $H^* = 17m$. Therefore, Varanasi's required reduction in EOA is:

$$\begin{aligned} \frac{A^*}{A^0} &= \min\left[1, \frac{t^0}{t^*}\left(\frac{H^0}{H^*}\right)^{\alpha}\left(\frac{l}{pn}+1\right)\right] \\ &= \min\left[1, \frac{7}{23.75}\left(\frac{3}{17}\right)^{1}\left(\frac{l}{p0.3}+1\right)\right] \end{aligned}$$

for Scenario i), $\frac{l}{p} = 0.3$:

$$\begin{aligned} \therefore \frac{A^*}{A^0} &= \min\left[1, \frac{7}{23.75}\left(\frac{3}{17}\right)^{1}\left(\frac{0.3}{0.3}+1\right)\right] \\ &= 0.104 = 90\%\text{decrease} \end{aligned} \tag{D.1}$$

for Scenario ii), $\frac{l}{p} = 0.02$:

$$\begin{aligned} \therefore \frac{A^*}{A^0} &= \min\left[1, \frac{7}{23.75}\left(\frac{3}{17}\right)^{1}\left(\frac{0.02}{0.3}+1\right)\right] \\ &= 0.055 = 94\%\text{decrease} \end{aligned} \tag{D.2}$$

D.2 Dar es Salaam

LR in the intruded volume in the steady-state phase due to increased supply duration and EOA reduction is given by Eq 15. Dar es Salaam reported $n = 0.56$ and $t^0 = 8$. The target system goal is $t^* = 23.75$. Therefore, Dar es Salaam's LR during steady state is:

$$\begin{aligned} LR &= -log_{10}\left(\left.\frac{V_C^*}{V_C^0}\right|_{H^*=H^0}\right) = -log_{10}\left[\frac{t^*}{t^0}\min\left[1, \left(\frac{t^0}{t^*}\right)\left(\frac{l}{pn}+1\right)\right]\right] \\ &= -log_{10}\left(\frac{t^*}{t^0}\right) + \min\left[0, -log10\left[\left(\frac{t^0}{t^*}\right)\left(\frac{l}{pn}+1\right)\right]\right] \end{aligned}$$

for Scenario i), $\frac{l}{p} = 0.3$:

$$\begin{aligned} \therefore LR &= -log_{10}\left(\frac{23.75}{8}\right) + \min\left[0, -log10\left[\left(\frac{8}{23.75}\right)\left(\frac{0.3}{0.56}+1\right)\right]\right] \\ &= -0.47 + 0.29 = -0.18 \end{aligned} \tag{D.3}$$

for Scenario ii), $\frac{l}{p} = 0.02$:

$$\begin{aligned} \therefore LR &= -log_{10}\left(\frac{23.75}{8}\right) + \min\left[0, -log10\left[\left(\frac{8}{23.75}\right)\left(\frac{0.02}{0.56}+1\right)\right]\right] \\ &= -0.47 + 0.46 = -0.01 \end{aligned} \tag{D.4}$$

Bibliography

Abu-Madi, M., Trifunovic, N., 2013. Impacts of supply duration on the design and performance of intermittent water distribution systems in the West Bank. Water International 38, 263–282. doi:10.1080/02508060.2013.794404.

Adane, M., Mengistie, B., Medhin, G., Kloos, H., Mulat, W., 2017. Piped water supply interruptions and acute diarrhea among under-five children in Addis Ababa slums, Ethiopia: a matched case-control study. PLOS ONE 12, e0181516. doi:10.1371/journal.pone.0181516.

Al-Ghamdi, A.S., 2011. Leakage-pressure relationship and leakage detection in intermittent water distribution systems. Journal of Water Supply: Research & Technology-AQUA 60, 178–183. doi:10.2166/aqua.2011.003.

de Albuquerque, C., 2010. Progress report on the compilation of good practices. Addendum A/HRC/15/31/Add.1. United Nations Human Rights Council.

Alegre, H., Baptista, J.M., Jr, E.C., Cubillo, F., Duarte, P., Hirner, W., Merkel, W., Parena, R., 2016. Performance indicators for water supply services. IWA Publishing.

American Water Works Association, 2009. Water audits and loss control programs. Number M36 in AWWA manual. 3rd ed., American Water Works Association, Denver, Colorado.

Ameyaw, E.E., Memon, F.A., Bicik, J., 2013. Improving equity in intermittent water supply systems. Journal of Water Supply: Research and Technology—AQUA 62, 552. doi:10.2166/aqua.2013.065.

Anand, N., 2011. Pressure: the politechnics of water supply in Mumbai. Cultural Anthropology 26, 542–564. doi:10.1111/j.1548-1360.2011.01111.x.

Anand, N., 2012. Municipal disconnect: On abject water and its urban infrastructures. Ethnography 13, 487–509. doi:10.1177/1466138111435743.

Anand, N., 2015. Leaky states: Water audits, ignorance, and the politics of infrastructure. Public Culture 27, 305–330. URL: http://publicculture.dukejournals.org/content/27/2_76/305.short.

Anderson, L., 1988. Fire and disease: the development of water supply systems in New England, 1870-1900. Technology and the Rise of the Networked City in Europe and America , 141–142.

Andey, S.P., Kelkar, P.S., 2007. Performance of water distribution systems during intermittent versus continuous water supply. American Water Works Association. Journal 99, 99–106,12. URL: search.proquest.com/docview/221583003.

Arregui, F., 2016. Customer metering inaccuracies. Technical Report Appendix 3. UK. URL: http://www.leakssuite.com/wp-content/uploads/2016/09/New-Appendix-3.-Customers-metering-inaccuracies-Final-24th-Aug.pdf.

Arregui, F., Cabrera, E., Cobacho, R., 2006a. Integrated water meter management. IWA Publ, London. OCLC: 255430448.

Arregui, F.J., Cabrera, E., Cobacho, R., Garcia-Serra, J., 2006b. Reducing apparent losses caused by meters inaccuracies. Water Practice and Technology 1, wpt2006093. URL: http://wpt.iwaponline.com/content/1/4/wpt2006093.abstract.

Asian Development Bank, Ministry of Urban Development Government of India, 2007. Benchmarking and data book of water utilities in India. Asian Development Bank, Manila. URL: http://hdl.handle.net/11540/222.

Asthana, V., 2009. Water policy processes in India: discourses of power and resistance. Number 18 in Routledge contemporary South Asia series, Routledge, London ; New York. OCLC: ocn299281557.

Bagga, B., 2012. Water crisis grips Delhi, DJB blames residents. India Today URL: http://indiatoday.intoday.in/story/water-crisis-grips-delhi-djb-blames-residents/1/200100.html.

Barfuss, S.L., Johnson, M.C., Neilsen, M.A., 2011. Accuracy of in-service water meters at low and high flow rates. Water Research Foundation; U.S. Environmental Protection Agency, Denver, CO. URL: http://www.allianceforwaterefficiency.org/uploadedFiles/Resource_Center/Library/water_loss/WRF-Meter-Accuracy-2011.pdf.

Batish, R., 2003. A new approach to the design of intermittent water supply networks, pp. 23–26. doi:10.1061/40685(2003)123.

Benjamin, M.M., Lawler, D.F., 2013. Water quality engineering: physical/chemical treatment processes. John Wiley & Sons, Hoboken, N.J.

Van den Berg, C., 2015. Drivers of non-revenue water: a cross-national analysis. Utilities Policy 36, 71–78. doi:10.1016/j.jup.2015.07.005.

Van den Berg, C., Danilenko, A., 2011. The IBNET water supply and sanitation performance blue book. Technical Report. World Bank. URL: dx.doi.org/10.1596/978-0-8213-8582-1.

Van den Berg, C., Pattanayak, S., Yang, J.C., Gunatilake, H., 2008. Understanding demand when reforming water supply and sanitation: a case study from Sri Lanka. Technical Report 44723. The World Bank. URL: https://openknowledge.worldbank.org/handle/10986/11754.

Besner, M.C., Prévost, M., Regli, S., 2011. Assessing the public health risk of microbial intrusion events in distribution systems: conceptual model, available data, and challenges. Water Research 45, 961–979. doi:10.1016/j.watres.2010.10.035.

Bivins, A.W., Sumner, T., Kumpel, E., Howard, G., Cumming, O., Ross, I., Nelson, K., Brown, J., 2017. Estimating infection risks and the global burden of diarrheal disease attributable to intermittent water supply using QMRA. Environmental Science & Technology 51, 7542–7551. doi:10.1021/acs.est.7b01014.

Björkman, L., 2015. Pipe politics, contested waters: embedded infrastructures of millennial Mumbai. Duke University Press Books, Durham.

Bolton, S.F., 1884. London water supply. Published for the Executive Council of the International Health Exhibition, and the Council of the Society of Arts, by William Clowes and Sons, Limited. Google-Books-ID: ZFFKAAAAYAAJ.

Bowen, P., Harp, J., Baxter, J., Shull, R., 1993. Residential water use patterns. American Water Works Association Research Foundation, Denver, CO.

Box, G.E., 1979. Robustness in the strategy of scientific model building. Robustness in Statistics 1, 201–236. doi:10.1016/B978-0-12-438150-6.50018-2.

Bragalli, C., D'Ambrosio, C., Lee, J., Lodi, A., Toth, P., 2012. On the optimal design of water distribution networks: a practical MINLP approach. Optimization and Engineering 13, 219–246. doi:10.1007/s11081-011-9141-7.

Bureau of Indian Standards, 1994. Indian standard: water meters (domestic type) specification 6th revision.

BWSC, CDM, 2011. Water distribution system study final report. Technical Report FZ001118sec1 (2). Boston Water and Sewer Comission (BWSC). Boston, MA.

Carpenter, A., 1875. The fever at Croydon: and intermittent water-supply as a cause of typhoid. British Medical Journal 2, 632. URL: http://www.ncbi.nlm.nih.gov/pmc/articles/PMC2297736/.

Census of India, 2001. Population. URL: http://www.censusindia.gov.in/Census_Data_2001/India_at_glance/popu1.aspx.

Census of India, 2011. Primary census abstract 2011: NCT of Delhi. Census. Census of India.

Charalambous, B., Laspidou, C., 2017. Dealing with the complex interrelation of intermittent supply and water losses. IWA Publishing.

Cheng, L., Karney, B.W., 2017. Organization and scaling in water supply networks. Physical Review E 96. doi:10.1103/PhysRevE.96.062317.

Cheung, P.B., Van Zyl, J.E., Reis, L.F.R., 2005. Extension of EPANET for pressure driven demand modeling in water distribution system. Computing and Control for the Water Industry 1, 311–316. URL: http://env999.kangwon.ac.kr/leakage/2009/management/research/knowledge/08/na/artc_1147708476_40.pdf.

Choe, K., Varley, R.C., Bijlani, H.U., 1996. Coping with intermittent water supply: problems and prospects: Dehra Dun, Uttar Pradesh, India. Activity Report 26. Environmental Health Project, USAID. New Delhi, India.

Cobacho, R., Arregui, F., Cabrera, E., 2008. Private water storage tanks: evaluating their inefficiencies. Water Practice and Technology 3, wpt2008025. URL: http://wpt.iwaponline.com/content/3/1/wpt2008025.abstract.

Colombo, A.F., Karney, B.W., 2002. Energy and costs of leaky pipes: toward comprehensive picture. Journal of Water Resources Planning and Management 128, 441–450. doi:10.1061/(ASCE)0733-9496(2002)128:6(441).

Colombo, A.F., Karney, B.W., 2009. Leaks and water use representation in water distribution system models: finding a working equivalence. Journal of Hydraulic Engineering 135, 234–239. doi:10.1061/(ASCE)0733-9429(2009)135:3(234).

CPHEEO, 1999. Manual on water supply and treatment. 3rd ed., Central Public Health and Environmental Engineering Organisation, Ministry of Urban Development, New Delhi, India.

Criminisi, A., Fontanazza, C.M., Freni, G., La Loggia, G., 2009. Evaluation of the apparent losses caused by water meter under-registration in intermittent water supply. Water Science and Technology 60, 2373. URL: https://iris.unikore.it/retrieve/handle/11387/9682/102/Criminisi_Evaluation_of_the_apparent_losses_ca.pdf.

De Marchis, M., Fontanazza, C.M., Freni, G., La Loggia, G., Napoli, E., Notaro, V., 2010. A model of the filling process of an intermittent distribution network. Urban Water Journal 7, 321–333. doi:10.1080/1573062X.2010.519776.

Delhi BJP, 2016. Kejriwal govt. now promoting airflow meters which it protested earlier. URL: http://bjpdelhi.org/articles/press-release/1611/press-release-16-05-2016-delhi-state.

Delhi Jal Board, 2004. Delhi water supply and sewerage sector reform project. URL: delhijalboard.nic.in/djbdocs/reform_project/docs/docs/doc_project_prep_docs/introduction/DJB-ReformProject%2520-%2520Final.doc.

Delhi Jal Board, 2012a. Concession agreement. Draft Volume-II. Delhi Jal Board. Command area of Nangloi water treatment plant, Delhi. URL: http://web.archive.org/web/20130411014307/http://delhi.gov.in/DoIT/DJB/projectdetail/Nangloi_DPR.zip.

Delhi Jal Board, 2012b. Contract agreement. Technical Report Volume 1. URL: http://delhi.gov.in/DoIT/DJB/Contract_Agreement/CA_Malviya_Nagar.zip.

Delhi Jal Board, 2012c. O&M agreement. Draft request for proposal Volume-II. Delhi Jal Board. URL: http://web.archive.org/web/20130315124145/http://delhi.gov.in/DoIT/DJB/projectdetail/Malviya_Nagar.zip.

Delhi Jal Board, 2012d. O&M agreement. Draft request for proposal Volume-II Appendix-I. Delhi Jal Board. Mehrauli project area. URL: http://web.archive.org/web/20130315124706/http://delhi.gov.in/DoIT/DJB/projectdetail/Mehrauli.zip.

Delhi Jal Board, 2012e. O&M agreement. Draft request for proposal Volume-II Appendix-II. Delhi Jal Board. Vasant Vihar project area. URL: http://web.archive.org/web/20130315124706/http://delhi.gov.in/DoIT/DJB/projectdetail/Mehrauli.zip.

Delhi Jal Board, 2012f. Request for proposal. Draft. Delhi Jal Board. Command area of Nangloi water treatment plant, Delhi. URL: http://web.archive.org/web/20130411014307/http://delhi.gov.in/DoIT/DJB/projectdetail/Nangloi_DPR.zip.

Delhi Jal Board, 2012g. Schedules. Draft request for proposal Vol-III (Part A). Delhi Jal Board. Malviya Nagar UGR command area. URL: http://web.archive.org/web/20130315124145/http://delhi.gov.in/DoIT/DJB/projectdetail/Malviya_Nagar.zip.

Delhi Jal Board, 2012h. Schedules. Draft request for proposal Volume-III A. Delhi Jal Board. Mehrauli project area. URL: http://web.archive.org/web/20130315124706/http://delhi.gov.in/DoIT/DJB/projectdetail/Mehrauli.zip.

Delhi Jal Board, 2012i. Schedules. Draft request for proposal Volume-III B Part-I. Delhi Jal Board. Vasant Vihar project area. URL: http://web.archive.org/web/20130315124706/http://delhi.gov.in/DoIT/DJB/projectdetail/Mehrauli.zip.

Dinesh Rathi & Associates, 2008. 24 x 7 water supply project for Nagpur city. Draft detailed project report. Nagpur Municipal Corporation, Water Works Department. Nagpur, India. URL: http://203.129.203.8/files/Draft-DPR.pdf.

DJB, 2014. Timing of water supply in Delhi. URL: http://delhi.gov.in/wps/wcm/connect/DOIT_DJB/djb/our+services1/timing+of+water+supply+in+delhi.

Dutta, V., Tiwari, A., 2005. Sector reforms, regulation and the challenges of sustainability: demand side analysis for urban water utility of Delhi, India, New Delhi, India. URL: http://papers.ssrn.com/sol3/papers.cfm?abstract_id=1945532.

Eales, K., 2010. A review in Bangladesh, India, and Pakistan: benchmarking for performance improvement in urban utilities. Technical Report 57483. The World Bank and WSP. Bangladesh, India, and Pakistan. URL: https://openknowledge.worldbank.org/handle/10986/17270.

Ebacher, G., Besner, M.C., Clément, B., Prévost, M., 2012. Sensitivity analysis of some critical factors affecting simulated intrusion volumes during a low pressure transient event in a full-scale water distribution system. Water Research 46, 4017–4030. doi:10.1016/j.watres.2012.05.006.

Elala, D., Labhasetwar, P., Tyrrel, S.F., 2011. Deterioration in water quality from supply chain to household and appropriate storage in the context of intermittent water supplies. Water Science & Technology: Water Supply 11, 400. doi:10.2166/ws.2011.064.

Elster, 2013. Electronic water metering: North America. URL: https://www.elsteramcowater.com/assets/downloads/ELS6427_AMCO_Brochure.pdf.

Ercumen, A., Arnold, B.F., Kumpel, E., Burt, Z., Ray, I., Nelson, K., Jr, J.M.C., 2015. Upgrading a piped water supply from intermittent to continuous delivery and association with waterborne illness: a matched cohort study in urban India. PLOS Med 12, e1001892. doi:10.1371/journal.pmed.1001892.

Erickson, J.J., Smith, C.D., Goodridge, A., Nelson, K.L., 2017. Water quality effects of intermittent water supply in Arraiján, Panama. Water Research 114, 338–350. doi:10.1016/j.watres.2017.02.009.

Fan, L., Liu, G., Wang, F., Ritsema, C.J., Geissen, V., 2014. Domestic water consumption under intermittent and continuous modes of water supply. Water Resources Management 28, 853–865. doi:10.1007/s11269-014-0520-7.

Flemming, H.C., Percival, S.L., Walker, J.T., 2002. Contamination potential of biofilms in water distribution systems. Water Science and Technology: Water Supply 2, 271–280.

Flow Dynamics, 2018. How the smart water valve works. URL: http://thesmartvalve.com/how-it-works-h2o-water-bill-meter-reducer-smart-valve-flow-device-restrictor-variable-control-air-compression-pressure/.

Fontanazza, C.M., Notaro, V., Puleo, V., Freni, G., 2015. The apparent losses due to metering errors: a proactive approach to predict losses and schedule maintenance. Urban Water Journal 12, 229–239. doi:10.1080/1573062X.2014.882363.

Fox, S., Shepherd, W., Collins, R., Boxall, J., 2016. Experimental quantification of contaminant ingress into a buried leaking pipe during transient events. Journal of Hydraulic Engineering 142, 04015036. doi:10.1061/(ASCE)HY.1943-7900.0001040.

Frauendorfer, R., Liemberger, R., 2013. The issues and challenges of reducing non-revenue water. Asian Development Bank. URL: http://www.adb.org/publications/issues-and-challenges-reducing-non-revenue-water.

Galaitsi, S., Russell, R., Bishara, A., Durant, J.L., Bogle, J., Huber-Lee, A., 2016. Intermittent domestic water supply: a critical review and analysis of causal-consequential pathways. Water (Switzerland) 8. doi:10.3390/w8070274.

García, V.J., García-Bartual, R., Cabrera, E., Arregui, F., García-Serra, J., 2004. Stochastic model to evaluate residential water demands. Journal of Water Resources Planning and Management 130, 386–394. doi:10.1061/(ASCE)0733-9496(2004)130:5(386).

Ghosh, R., Kansal, A., Aghi, S., 2016. Implications of end-user behaviour in response to deficiencies in water supply for electricity consumption - a case study of Delhi. Journal of Hydrology 536, 400 – 408. doi:10.1016/j.jhydrol.2016.03.012.

Gilmartin, D., 2003. Water and waste: nature, productivity and colonialism in the Indus Basin. Economic and Political Weekly , 5057–5065URL: http://www.jstor.org/stable/4414343.

Gómez-Ibáñez, J.A., 2006. Regulating infrastructure: monopoly, contracts, and discretion. 1. paperback ed ed., Harvard Univ. Press, Cambridge, Mass. OCLC: 845129804.

Government of India, 1949. The Constitution of India. URL: http://www.pocketlawyer.com/blog/wp-content/uploads/2017/01/The-Constitution-of-India.pdf.

Government of NCT of Delhi, 2002. Water supply and sewerage, in: Economic survey of Delhi. volume 2001-2002, pp. 114–123.

Government of NCT of Delhi, 2004. Water supply and sewerage, in: Economic survey of Delhi. volume 2003-2004, pp. 157–167.

Government of NCT of Delhi, 2006. Water supply and sewerage, in: Economic survey of Delhi. 2005-2006 ed., pp. 147–162.

Government of NCT of Delhi, 2009. Water supply and sewerage, in: Economic survey of Delhi. volume 2008-2009, pp. 151–163.

Government of NCT of Delhi, 2013. Water supply and sewerage, in: Economic survey of Delhi. 2012-2013 ed., pp. 178–191.

Government of NCT of Delhi, 2015. Water supply and sewerage, in: Economic Survey of Delhi. volume 2014-2015, pp. 184–199.

Government of NCT of Delhi, 2017. Water supply and sewerage, in: Economic survey of Delhi. 2016-2017 ed., pp. 182–199.

Goyal, R.V., Patel, H.M., 2015. Analysis of residual chlorine in simple drinking water distribution system with intermittent water supply. Applied Water Science 5, 311–319. doi:10.1007/s13201-014-0193-7.

Gupta, R., Bhave, P.R., 1996. Comparison of methods for predicting deficient-network performance. Journal of Water Resources Planning and Management 122, 214–217. doi:10.1061/(ASCE)0733-9496(1996)122:3(214).

Guragai, B., Takizawa, S., Hashimoto, T., Oguma, K., 2017. Effects of inequality of supply hours on consumers' coping strategies and perceptions of intermittent water supply in Kathmandu Valley, Nepal. Science of The Total Environment 599-600, 431–441. doi:10.1016/j.scitotenv.2017.04.182.

Hall, D.J., 2004. Water finance: a discussion note, Public Services International Research Unit (PSIRU), Delhi/Mumbai.

Hamilton, S., Charalambous, B., 2015. Leak detection: technology and implementation. IWA Publishing. doi:10.26530/OAPEN_578133.

Health of Towns Association, 1846. Report of the committee to the members of the association, on Lord Lincoln's sewerage, drainage, etc., of town's bill. Technical Report. Health of Towns Association. London. URL: https://babel.hathitrust.org/cgi/pt?id=uc1.$b93318;view=1up;seq=241.

ISO 4064, 2014. Water meters for cold potable water and hot water. Standard ISO 4064-1:2014. International Organization for Standardization. URL: https://www.iso.org/obp/ui/#iso:std:iso:4064:-1:ed-4:v1:en:ref:4.

Jacobson, C., 2001. Ties that bind. 1st ed., University of Pittsburgh Press, Pittsburgh.

Jain, P., 1997. Demand management of water supply of the National Capital Territory of Delhi. Water Supply 15, 31 – 34.

Kalam, A.A., 2002. President's address to both the houses of parliament assembled together on 25th of February 2002. URL: http://164.100.47.5/rsnewjournals/sessionno/195/25022002.htm.

Khandekar, N., 2014. Delhi Jal Board installs meters Kejriwal had rejected. Hindustan Times URL: http://www.hindustantimes.com/india/delhi-jal-board-installs-meters-kejriwal-had-rejected/story-g3BKOmV7lZZHZQab6RiQ9N.html.

Kim, J.H., Kim, T.G., Kim, J.H., Yoon, Y.N., 1994. A study on the pipe network system design using non-linear programming. J. Korean Water Resour. Assoc 27, 59–67.

Kirmeyer, G.J., Martel, K., 2001. Pathogen intrusion into the distribution system. American Water Works Association.

Klingel, P., 2010. Von intermittierender zu kontinuierlicher Wasserverteilung in Entwicklungsländern (From intermittent to continuous water distribution in developing countries). Ph.D. thesis. Institute for Water and River Basin Management, Karlsruhe Institute of Technology. Karlsruhe, Germany. URL: http://digbib.ubka.uni-karlsruhe.de/volltexte/1000019357.

Klingel, P., 2012. Technical causes and impacts of intermittent water distribution. Water Science and Technology: Water Supply 12, 504–512. URL: http://ws.iwaponline.com/content/12/4/504.abstract.

Koonan, S., Sampat, P., 2012. Delhi water supply reforms: public-private partnerships or privatisation? Economic & Political Weekly 47, 32–39.

Kumar, A., 1997. Leakage control in intermittent water supplies. Water Supply 15, 55–58. URL: search.proquest.com/docview/13629959.

Kumpel, E., Nelson, K.L., 2013. Comparing microbial water quality in an intermittent and continuous piped water supply. Water Research 47, 5176–5188. doi:10.1016/j.watres.2013.05.058.

Kumpel, E., Nelson, K.L., 2014. Mechanisms affecting water quality in an intermittent piped water supply. Environmental Science & Technology 48, 2766–2775. doi:10.1021/es405054u.

Kumpel, E., Nelson, K.L., 2016. Intermittent water supply: prevalence, practice, and microbial water quality. Environmental Science & Technology 50, 542–553. doi:10.1021/acs.est.5b03973.

Kumpel, E., Woelfle-Erskine, C., Ray, I., Nelson, K.L., 2017. Measuring household consumption and waste in unmetered, intermittent piped water systems. Water Resources Research 53, 302–315. doi:10.1002/2016WR019702.

Lambert, A.O., 2002. International report: water losses management and techniques. Water Science and Technology: Water Supply 2, 1–20. URL: http://ws.iwaponline.com/content/2/4/1.

Lambert, A.O., Fantozzi, M., 2005. Recent advances in calculating economic intervention frequency for active leakage control, and implications for calculation of economic leakage levels. Water Science and Technology: Water Supply 5, 263–271. URL: http://ws.iwaponline.com/content/5/6/263.

Lambert, A.O., McKenzie, R.D., 2002. Practical experience in using the Infrastructure Leakage Index, in: Proceedings of IWA Conference–Leakage Management: A Practical Approach. Lemesos, Cyprus.

Larock, B.E., Jeppson, R.W., Watters, G.Z., 2000. Hydraulics of pipeline systems. CRC Press, Boca Raton, FL.

Laspidou, C., Spyropoulou, A., 2017. Global dimensions of IWS - number of people affected worldwide, in: Dealing with the complex interrelation of intermittent supply and water losses. IWA Publishing, London, pp. 5–16.

Lee, E., Schwab, K., 2005. Deficiencies in drinking water distribution systems in developing countries. Journal of Water and Health 3, 109–127. URL: http://www.iwaponline.com/jwh/003/jwh0030109.htm.

Legislative Assembly of the National Capital Territory of Delhi, 1998. The Delhi Jal Board Act 1998. URL: http://ielrc.org/content/e9802.pdf.

Lieb, A., Rycroft, C., Wilkening, J., 2016. Optimizing intermittent water supply in urban pipe distribution networks. SIAM Journal on Applied Mathematics 76, 1492–1514. doi:10.1137/15M1038979.

Lindley, T.R., Buchberger, S.G., 2002. Assessing intrusion susceptibility in distribution systems. Journal of American Water Works Association 94, 66. URL: http://www.awwa.org/publications/journal-awwa/abstract/articleid/14600.aspx.

Liou, C.P., Hunt, W.A., 1996. Filling of pipelines with undulating elevation profiles. Journal of Hydraulic Engineering 122, 534–539. doi:10.1061/(ASCE)0733-9429(1996)122:10(534).

London Board of Health, 1850. Report by the general board of health on the supply of water to the metropolis. Clowes and Sons, London. URL: https://books.google.com/books?id=uVQ-AQAAMAAJ.

Macke, S., Batterman, A., 2001. A strategy to reduce technical water losses for intermittent water supply systems. Ph.D. thesis. URL: http://sdteffen.de/diplom.

Mastaller, M., Klingel, P., 2017. Adapting the IWA water balance to intermittent water supply and flat-rate tariffs without customer metering. Journal of Water Sanitation and Hygiene for Development 7, 396–406. doi:10.2166/washdev.2017.116.

Mathur, M.P., Chandra, R., Singh, S., Chattopadhyay, B., 2007. Norms and standards of municipal basic services in India. National Institute of Urban Affairs (NIUA) Working Paper , 07–02URL: http://www.indiawaterportal.org/sites/indiawaterportal.org/files/Norms_standards_municipal_basic_services_in_India_NIUA.pdf.

McIntosh, A.C., 2003. Asian water supplies: reaching the urban poor: a guide and sourcebook on urban water supplies in Asia for governments, utilities, consultants, development agencies, and nongovernment organizations. Asian Development Bank; International Water Association, Manila, Philippines: London. OCLC: ocm53826577.

McIntosh, A.C., 2014. Urban water supply and sanitation in Southeast Asia: a guide to good practice. Asian Development Bank. URL: http://www.adb.org/publications/urban-water-supply-and-sanitation-southeast-asia-guide-good-practice.

Ministry of Water Resources, 2002. National water policy. URL: http://www.dowrorissa.gov.in/ActsnPolicies/NWP/2002/NationalWaterPolicy2002.pdf.

Mohapatra, S., Sargaonkar, A., Labhasetwar, P.K., 2014. Distribution network assessment using EPANET for intermittent and continuous water supply. Water Resources Management 28, 3745–3759. doi:10.1007/s11269-014-0707-y.

Morgan, P., 2002. Technical assistance: correcting the precedents. Development Policy Journal 2, 1–22. URL: http://www.pnud.org/content/dam/aplaws/publication/en/publications/capacity-development/development-policy-journal--special-issue-on-technical-cooperation/Development-Policy-Journal--SpecialIssue-TechCoop.pdf#page=9.

MoUD, 2010. Handbook of service level benchmarking. Technical Report 102619. Ministry of Urban Development. New Delhi, India.

Murray, R., Klise, K., Moriarty, D., Bynum, M., Laird, C., 2018. Water Network Tool for Resilience (WNTR). URL: http://wntr.readthedocs.io.

Mutikanga, H.E., 2012. Water loss management: tools and methods for developing countries. Ph.D.. TU Delft, Delft University of Technology. URL: http://repository.tudelft.nl/view/ir/uuid:d78a06e4-7535-4a74-bdc9-d8942cc7556c/.

Nair, R., 2013. Fire safety in India - an overview. URL: http://www.ind-safety.com/Articles/fire-safety-in-india-an-overview/242025/5254725/5250000.

New Delhi Statement, 1990. Some for all rather than all for some. Technical Report A/C.2/43/3. New Delhi, India. URL: http://www.ielrc.org/content/e9005.pdf.

Onda, K., LoBuglio, J., Bartram, J., 2012. Global access to safe water: accounting for water quality and the resulting impact on MDG progress. International Journal of Environmental Research and Public Health 9, 880–894. doi:10.3390/ijerph9030880.

Pattanayak, S.K., Yang, J.C., Whittington, D., Bal Kumar, K.C., 2005. Coping with unreliable public water supplies: averting expenditures by households in Kathmandu, Nepal. Water Resources Research 41. doi:10.1029/2003WR002443.

Reca, J., Martínez, J., 2006. Genetic algorithms for the design of looped irrigation water distribution networks. Water Resources Research 42, W05416. doi:10.1029/2005WR004383.

Reddy, L.S., Elango, K., 1989. Analysis of water distribution networks with head-dependent outlets. Civil Engineering Systems 6, 102–110. doi:10.1080/02630258908970550.

Reynolds, W.P., 1873. Committee on the means of protecting the metropolis against conflagration. Journal of the Royal Society of Arts 21, 308–312. URL: https://books.google.com/books?id=DaY9AQAAIAAJ&pg=PA308.

Rossman, L.A., 2000. EPANET 2: users manual. Users manual EPA/600/R-00/057. National Risk Management Research Lab; U.S. EPA. Cincinnati, OH. URL: ftp://84-255-254-95.static.t-2.net/Epanet%202.0/EN2manual.pdf.

Sainath, P., 1999. Everybody loves a good drought: stories from India's poorest districts. Review, London. OCLC: 488584441.

Sangameswaran, P., 2014. Neoliberalism and water: complicating the story of 'reforms' in Maharashtra. Orient Blackswan, New Delhi. OCLC: ocn879524181.

Secretary of State for India in Council, 1875. Memorandum of the Army Sanitary Commission on the report of the Calcutta Municipality for 1873, in: Report on sanitary measures in India in 1873-74; together with miscellaneous information up to June 1875. Eyre and Spottiswoode. volume VII, pp. 230–233. URL: https://books.google.com/books?id=e8AIAAAAQAAJ&pg=230.

Seetharam, K.E., Bridges, G., 2005. Helping India achieve 24x7 water supply service by 2010. Technical Note 1. Asian Development Bank. Bangalore and Delhi, India. URL: http://www.adb.org/sites/default/files/publication/29256/helping-india-24x7.pdf.

Shaheed, A., Orgill, J., Ratana, C., Montgomery, M.A., Jeuland, M.A., Brown, J., 2014. Water quality risks of 'improved' water sources: evidence from Cambodia. Tropical Medicine & International Health 19, 186–194. doi:10.1111/tmi.12229.

Siew, C., Tanyimboh, T.T., Seyoum, A.G., 2016. Penalty-free multi-objective evolutionary approach to optimization of anytown water distribution network. Water Resources Management 30, 3671–3688. doi:10.1007/s11269-016-1371-1.

Singh, A., 2008. Political economy of reforms: learning from the Delhi water sector experience, in: Odugbemi, S., Jacobson, T. (Eds.), Governance reform under real-world conditions: citizens, stakeholders, and voice. Washington, D.C.: World Bank, pp. 419–429.

Solgi, M., Bozorg-Haddad, O., Seifollahi-Aghmiuni, S., Ghasemi-Abiazani, P., Loáiciga, H.A., 2016. Optimal operation of water distribution networks under water shortage considering water quality. Journal of Pipeline Systems Engineering and Practice 7, 04016005. doi:10.1061/(ASCE)PS.1949-1204.0000233.

Solgi, M., Bozorg Haddad, O., Seifollahi-Aghmiuni, S., Loáiciga, H.A., 2015. Intermittent operation of water distribution networks considering equanimity and justice principles. Journal of Pipeline Systems Engineering and Practice doi:10.1061/(ASCE)PS.1949-1204.0000198.

Soltanjalili, M.J., Bozorg Haddad, O., Mariño, M.A., 2013. Operating water distribution networks during water shortage conditions using hedging and intermittent water supply concepts. Journal of Water Resources Planning and Management 139, 644–659. doi:10.1061/(ASCE)WR.1943-5452.0000315.

Subbaraman, R., Nolan, L., Sawant, K., Shitole, S., Shitole, T., Nanarkar, M., Patil-Deshmukh, A., Bloom, D.E., 2015. Multidimensional measurement of household water poverty in a Mumbai slum: looking beyond water quality. PLOS ONE 10, e0133241. doi:10.1371/journal.pone.0133241.

Tanyimboh, T., Tahar, B., Templeman, A., 2003. Pressure-driven modelling of water distribution systems. Water Science and Technology: Water Supply 3, 255–261. URL: http://ws.iwaponline.com/content/3/1-2/255.

Tanyimboh, T.T., Templeman, A.B., 2010. Seamless pressure-deficient water distribution system model. Proceedings of the Institution of Civil Engineers - Water Management 163, 389–396. doi:10.1680/wama.900013.

Taylor, D.D.J., 2014. Reducing booster-pump-induced contaminant intrusion in Indian water systems with a self-actuated, back-pressure regulating valve. Thesis. Massachusetts Institute of Technology. Cambridge, MA. URL: http://hdl.handle.net/1721.1/92062.

Taylor, D.D.J., Khush, R., Peletz, R., Kumpel, E., 2018a. Efficacy of microbial sampling recommendations and practices in sub-Saharan Africa. Water Research 134, 115–125. doi:10.1016/j.watres.2018.01.054.

Taylor, D.D.J., Slocum, A.H., Whittle, A.J., 2018b. Analytical scaling relations to evaluate leakage and intrusion in intermittent water supply systems. PLOS ONE 13, e0196887. doi:10.1371/journal.pone.0196887.

The World Bank, 1994. Water resources management. Technical Report 12335. The World Bank. URL: http://documents.worldbank.org/curated/en/940261468325788815/Water-resources-management.

The World Bank, 2011. Implementation, completion and results report (IBRD-47300) on a loan in the amount of US$ 39.5 million to the government of India for the Karnataka Urban Water Sector Improvement Project. Technical Report ICR00001950. World Bank.

The World Bank, 2013. Karnataka Urban Water Sector Improvement Project : three towns pilot 24/7 water supply. Technical Report 76537. The World Bank. India. URL: http://documents.worldbank.org/curated/en/198351468258299307/Karnataka-Urban-Water-Sector-Improvement-Project-three-towns-pilot-24-7-water-supply.

Thornton, J., Lambert, A., 2005. Progress in practical prediction of pressure: leakage, pressure: burst frequency and pressure: consumption relationships, in: Proceedings of IWA Special Conference 'Leakage 2005', Halifax, Canada. pp. 1–11. URL: http://env1.kangwon.ac.kr/leakage/2009/management/research/knowledge/09/na/Progress%20in%20practical%20prediction%20of%20pressure%20relationships.pdf.

ToI, 2017. Malviya Nagar reels under water woes. The Times of India URL: https://timesofindia.indiatimes.com/city/delhi/malviya-nagar-reels-under-water-woes/articleshow/59008348.cms.

Totsuka, N., Trifunovic, N., Vairavamoorthy, K., 2004. Intermittent urban water supply under water starving situations, Vientiane, Lao PDR.

Toyama, K., 2015. Geek heresy: rescuing social change from the cult of technology. PublicAffairs, New York.

UN, 1992. The Dublin statement on water and sustainable development. Technical Report. United Nations. Dublin, Ireland. URL: http://www.un-documents.net/h2o-dub.htm.

UN-HABITAT, 2004. Dialogue on urban services: making the private sector work for the urban poor, HSP, Barcelona. URL: http://mirror.unhabitat.org/downloads/docs/3079_41309_K04717807%20WUF2-9.pdf.

Vairavamoorthy, K., Elango, K., 2002. Guidelines for the design and control of intermittent water distribution systems. Waterlines 21, 19–21. doi:10.3362/0262-8104.2002.041.

Vairavamoorthy, K., Gorantiwar, S.D., Mohan, S., 2007a. Intermittent water supply under water scarcity situations. Water International 32, 121–132. doi:10.1080/02508060708691969.

Vairavamoorthy, K., Yan, J., Galgale, H.M., Gorantiwar, S.D., 2007b. IRA-WDS: A GIS-based risk analysis tool for water distribution systems. Environmental Modelling & Software 22, 951–965. doi:10.1016/j.envsoft.2006.05.027.

Vairavamoorthy, K., Yan, J., Gorantiwar, S.D., 2007c. Modelling the risk of contaminant intrusion in water mains. Proceedings of the ICE - Water Management 160, 123–132. doi:10.1680/wama.2007.160.2.123.

Van Zyl, J.E., 2011. Introduction to integrated water meter management. 1st ed., Water Research Commission, Gezina, South Africa. OCLC: 761290901.

Vernon-Harcourt, L.F., 1890. Water supply: intermittent and constant supply, in: The encyclopaedia britannica: a dictionary of arts, sciences and general literature. 9th ed.. Henry G. Allen Company, New York. volume XXIV, p. 410. URL: https://books.google.com/books?id=K6E7DDiSIrwC&pg=410.

Wagner, J.M., Shamir, U., Marks, D.H., 1988. Water distribution reliability: simulation methods. Journal of Water Resources Planning and Management 114, 276–294.

Walter, D., 2015. Experimental investigation of Accuracy of domestic water meters at intermittent water supply = Experimentelle Untersuchung der Genauigkeit von Hauswasserzählern bei intermittierender Wasserversorgung. Master's thesis. Karlsruher Institut fur Technologie (KIT). Karlsruhe.

Walter, D., Mastaller, M., Klingel, P., 2017. Accuracy of single-jet water meters during filling of the pipe network in intermittent water supply. Urban Water Journal 14, 991–998. doi:10.1080/1573062X.2017.1301505.

Walter, D., Mastaller, M., Klingel, P., 2018. Accuracy of single-jet and multi-jet water meters under the influence of the filling process in intermittently operated pipe networks. Water Science and Technology: Water Supply 18, 679–687. doi:10.2166/ws.2017.149.

Walters, V., 2013. Water, democracy and neoliberalism in India: the power to reform. Number 70 in Routledge contemporary South Asia series, Routledge, Milton Park, Abingdon, Oxon.

Wang, Q., Guidolin, M., Savic, D., Kapelan, Z., 2014. Two-objective design of benchmark problems of a water distribution system via MOEAs: towards the best-known approximation of the true Pareto front. Journal of Water Resources Planning and Management 141, 04014060. doi:10.1061/(ASCE)WR.1943-5452.0000460.

WHO, 2017a. Progress on drinking water, sanitation and hygiene: 2017 update and SDG baselines. World Health Organization (WHO) and the United Nations Children's Fund (UNICEF), Geneva. OCLC: 1010983346.

WHO, 2017b. Safely managed drinking water - thematic report on drinking water 2017. World Health Organization, Geneva, Switzerland.

Wise, M.N., Smith, C., 1989. Work and waste: political economy and natural philosophy in nineteenth century Britain (i). Hist Sci History of Science 27, 263–301. OCLC: 5825128783.

Wright, J., Gundry, S., Conroy, R., 2004. Household drinking water in developing countries: a systematic review of microbiological contamination between source and point-of-use. Tropical Medicine & International Health 9, 106–117. doi:10.1046/j.1365-3156.2003.01160.x.

Zérah, M.H., 2000. Water, unreliable supply in Delhi. Manohar Publishers.